STRUCTURAL DISCONTINUITIES IN THE WITWATERSRAND GROUP ON THE E.R.P.M. MINE: THEIR GEOLOGY, GEOCHEMISTRY AND ROCK MECHANICS BEHAVIOUR

David George Jeffery

A Dissertation Submitted to the Faculty of Science,
University of the Witwatersrand, Johannesburg
for the Degree of Master of Science

Johannesburg 1975.

Bernard Price Institute of Geophysical Research

University of the Witwatersrand, Johannesburg

1 Jan Smuts Avenue Johannesburg 2001 South Africa
Telephone 724-3659. Telegrams BPI University

DECLARATION

I, David George Jeffery do hereby declare that this Dissertation is my own work and has not been presented to any other University for the purpose of obtaining a Degree.

D G JEFFERY

February 1975

ABSTRACT

The structural discontinuities (dykes, faults, shear zones and joints) found in the E.R.P.M. are described in terms of their distribution, petrography, geochemistry and rock mechanics behaviour. Five groups of dykes have been recognised: of possible Bushveld age are a melanorite dyke/sill (The Simmer Dyke) and a swarm of ilmenite diabases, and of possible Ventersdorp age are two sets of 030° striking tholeiitic quartz dolerites and a series of east-west striking ultramylonite zones that are geochemically shown to be dykes. The geochemistry shows all the dykes to be tholeiitic and generally alkali poor.

Faulting in the mine is characterised by complex rotational movements. Rotational faulting, fault terminations, fault fills and shear zones are discussed. Three groups of faults are described: one set which dips south and strikes parallel to the sediments, probably formed during the formation of the basin but they have since been reactivated to reverse faults. The other two groups, one of which shows a sinistral strike-slip displacement and the other a dextral strike-slip displacement, form a conjugate pair.

Detailed descriptions of both original and mining induced jointing are given, the influence of structural discontinuities on jointing distribution is discussed and some mechanisms of formation are proposed. Five sets of original jointing and two main types of mining induced fracturing are recognised.

Regional lineation patterns are analysed and it is found that the main regional trends are similar to the local E.R.P.M. trends. A dynamic analysis of the structural discontinuities is described and a stress history, on both a regional and local scale, is proposed.

A detailed rock mechanic study of four large dykes in the mine is discussed; specimens have been tested in both uniaxial and triaxial compression and the uniaxial compressive strength, Young's Modulus, Poisson's Ratio, uniaxial tensile strength, intrinsic shear strength and angle and coefficient of internal friction have been determined for various specimens.

In the final chapter, the effects of structural discontinuities on the distribution of rockbursts and seismic events is discussed. The results indicate that the distribution of seismic events is not controlled by the structural discontinuities but some dykes do control the distribution of rockbursts.

ACKNOWLEDGEMENTS

I am indebted to my supervisor, Dr N C Gay, for many hours of valuable criticism, discussion and a never ending interest in the project. I would like to thank the staff of the Bernard Price Institute, especially Mr S L Fumerton and Mr F Arnott for their assistance during the past two years.

Professor J McIver of the Geology Department read Chapter 2 and Mr T S McCarthy, also of the Geology Department, assisted greatly with the geochemical analyses.

I would like to thank Mr W D Ortlepp, the Rand Mines Rock Mechanic Engineer, for his organisation and assistance in the mines and for many hours of discussion; in addition I would like to thank the General Manager and staff of the E.R.P.M., especially those of the Geology Department, for their assistance.

I am grateful to the Geological Survey, Pretoria, for crushing some of the geochemistry samples and the National Institute for Metallurgy for analysing some geochemical samples.

This work was carried out at the Bernard Price Institute of Geophysical Research under a research grant provided by the Transvaal and Orange Free State Chamber of Mines Research Organisation (Project Number 102/73); their financial support is gratefully acknowledged.

Finally, I would like to thank Mrs Rosalind Bowles for typing this dissertation.

CONTENTS

LIST OF FIGURES

On or facing page

On or facing page

LIST OF TABLES

APPENDIX TABLES (continued)

LIST OF PLATES

NOTATION

C_0	Uniaxial compressive strength
d	Diameter
E	Young's modulus
g	Acceleration of gravity
H	Height or length
K	Constant
S_0	Intrinsic shear strength
T_0	Uniaxial tensile strength
ψ	Angle between a failure plane and the maximum principal stress
ϕ	Angle of internal friction
$\varepsilon_1, \varepsilon_2, \varepsilon_3$	Principal strains
μ	Coefficient of internal friction
ν	Poisson's ratio
ρ	Density
$\sigma_1, \sigma_2, \sigma_3$	Principal stresses; $\sigma_1 > \sigma_2 > \sigma_3$
Δ	Volumetric strain

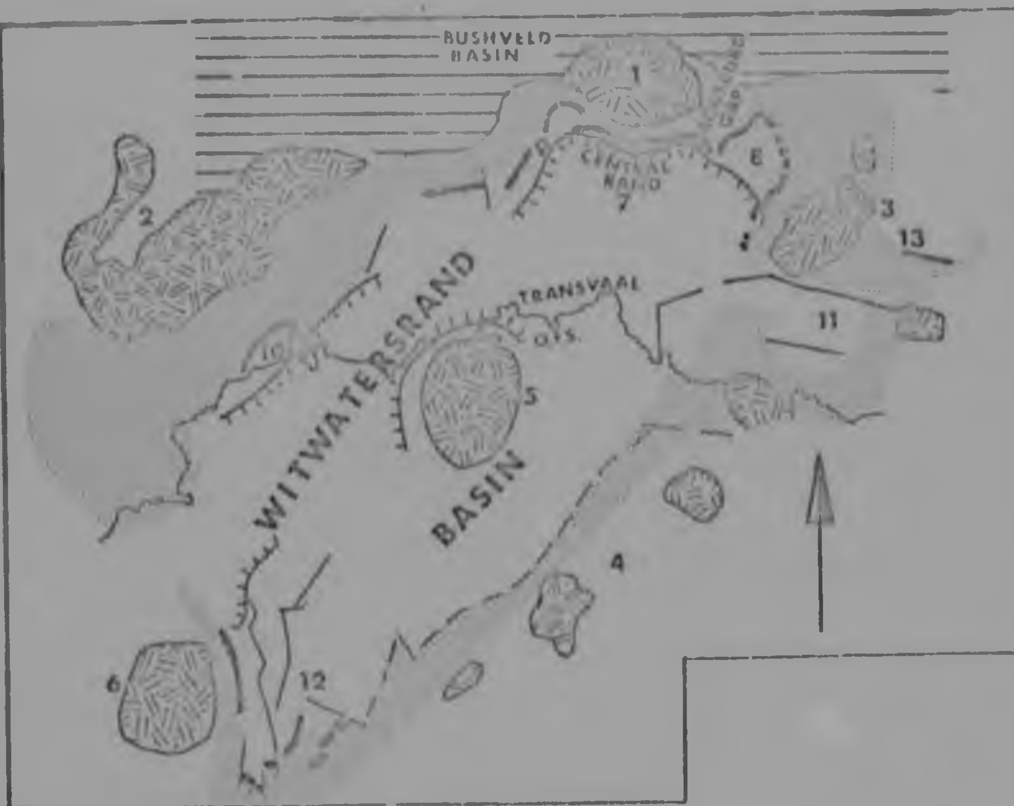

a THE WITWATERSRAND BASIN

b LOCATION OF THE E.R.P.M.

FIGURE 1-1

THE LOCATION OF THE E.R.P.M. IN THE WITWATERSRAND BASIN

a. The Witwatersrand Basin (after Brock and Pretorius, 1964b)

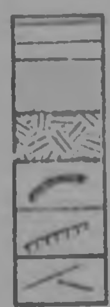

Bushveld Basin

Regressive Overlaps

Granite Domes

Payable Rim Segment

Peripheral Fault

Other major faults

1. Johannesburg-Pretoria Granite Dome
2. Granite massif
3. Devon Dome
4. Granite and schist under cover
5. Vredefort Dome
6. Wesselbron Dome (under cover)
7. Central Rand
8. East Rand Basin
9. West Rand
10. Klerksdorp Basin
11. Balfour Basin
12. Virginia area (Orange Free State)
13. Kinross area

b. Location of the E.R.P.M. in the Central Rand (after Shipway, 1972)

8. East Rand Proprietary Mine Ltd.
27. Simmer and Jack Mines Ltd.
28. City Deep Ltd.
29. Van Dyk Consolidated.

Mining properties.

INTERNATIONAL TIME SCALE		M.Y. b.p.	LOCAL TIME SCALE
CAINOZOIC	QUATERNARY	0	KALAHARI
	TERTIARY		
MESOZOIC	CRETACEOUS		
		154	KARROO McDougall(1963)
	JURASSIC		
	TRIASSIC	204	KARROO Manton(1968)
	PERMIAN		
PALAEOZOIC	CARBONIFEROUS		
	DEVONIAN		
	SILURIAN		
	ORDOVICIAN		CAPE
	CAMBRIAN	500	
PRECAMBRIAN		1000	
		1290	PILANESBERG Schreiner and Van Niekerk(1958)
		1500	
			WATERBERG
		1950	BUSHVELD Nicolaysen, *et a* (1958)
		2000	
		2330	VENTERSDORP Van Niekerk and Burger(1964)
		2500	
			WITWATERSRAND
		2800	DOMINION REEF
		3000	Van Niekerk and Burger, (1969)
		3200	BASEMENT GRANITE Halfway House Allsopp (1961)
		3500	SWAZILAND

FIGURE 1.2 INTERNATIONAL AND LOCAL TIME SCALES

CHAPTER 1

INTRODUCTION

1.1 THE EAST RAND PROPRIETARY MINE (E.R.P.M.)

The E.R.P.M., a large ultra-deep gold mine, is situated on the northern edge of the Witwatersrand Basin in the immediate vicinity of Boksburg and East Germiston, some 30 kilometres east of Johannesburg. Auriferous conglomerates are mined at seven main localities in the Witwatersrand Basin (Figure 1.1a) and the E.R.P.M. is the eastern most mine of the Central Rand district (Figure 1.1b).

Mining on the Witwatersrand commenced soon after the discovery of a gold reef on the farm "Langlaagte" in 1886. The E.R.P.M., which was registered in 1893, is an amalgamation of many small, shallow-working gold mines plus new leases added during recent years to cover the deepest portions of the mine, so that today the mine area is approximately 53 square kilometres.

The E.R.P.M. is one of the deepest mines in the world, working to depths of 3,25 km below surface, and is the only working ultra-deep mine on the Central or East Rand, thus it provides a unique opportunity to study rocks under high natural stresses.

1.2 REGIONAL GEOLOGY

The geological time scale for north-east South Africa is compared with the international time-scale in Figure 1.2.

In the Witwatersrand Basin area the basement granite is the Kaapvaal Craton, a large stable nucleus surrounded by three large mobile belts. Basement granite crops out at many localities in the eastern and northern Transvaal, and nearer to the Witwatersrand Basin it crops out between Johannesburg and Pretoria(Johannesburg-Pretoria Granite Dome) and near Parys (Vredefort Ring) and is also present as granite domes under younger cover at many localities surrounding the Basin (Figure 1.1a). The overlying sediments are derived essentially from this basement complex and more specifically from the basement highs represented by these outcrops. Allsopp (1961) has dated the Halfway House Granite, part of the Johannesburg-Pretoria Granite Dome, at 3200 ± 65 m.y., although it is now thought to be 3100 m.y. (H.L. Allsopp, personal communication, 1974).

The Witwatersrand Triad (Hamilton and Cooke, 1960) overlies the basement complex and comprises the Dominion Reef, Witwatersrand and Ventersdorp Groups. Separating the Witwatersrand System from the basement is the Dominion Reef Group lying unconformably on the basement. The Dominion Reef Group is not intersected in the E.R.P.M. but has been dated elsewhere at 2900 ± 150 m.y. by Nicolaysen et al. (1962) and at 2800 ± 60 m.y. by Van Niekerk and Burger (1969).

The Witwatersrand Group rests unconformably on the Dominion Reef Group and it is within this group that all mining in the E.R.P.M. is carried out. Unfortunately no direct age of the Witwatersrand sediments can be determined but sedimentation took place between 2800 m.y. and 2330 m.y. ago, the ages of the younger and older sediments. The character of the Witwatersrand Group will be discussed in more detail [illegible] 1.3.

The third and youngest member of the triad, the Venters[illegible]p overlies the Witwatersrand Group conformably on the Central Rand but is normally unconformable. This group, which crops out on the southern parts of E.R.P.M., consists essentially of basaltic to andesitic lavas, quartz-porphyries and felsite, with intercalated banded tuffs and sediments (Brock and Pretorius, 1964a). Ventersdorp volcanism overlaps with Witwatersrand sedimentation and took place about 2330 ± 50 m.y. (Van Niekerk and Burger, 1964); in places the Ventersdorp lavas may exceed 3500 metres in thickness.

Overlying the triad are sediments of the Transvaal and Karroo Systems, both of which crop out in the southern portions of the E.R.P.M. In addition at least four different ages of intrusive rocks cut the Witwatersrand

TABLE 1-1

STRATIGRAPHY OF THE CENTRAL WITWATERSRAND (after PRETORIUS, 1964)

SYSTEM	SERIES
KARROO 60m	ECCA 60m
TRANSVAAL 110m	PRETORIA 460m
	DOLOMITE 610m
	BLACK REEF 30m
VENTERSDORP 1520m	LAVAS 1520m
WITWATERSRAND 7347m	KIMBERLEY/ELSBURG 1860m
	MAIN-BIRD 1005m
	JEPPESTOWN 1115m
	GOVERNMENT REEF 1920m
	HOSPITAL HILL 1495m
OLD GRANITE	GRANITE AND GNEISS
SWAZILAND 215m	ONERWACHT 215m

GROUP	METRES
ELSBURG REEF	520
QUARTZITE	855
KIMBERLEY REEF	305
KIMBERLEY SHALE	180
BIRD REEF	230
QUARTZITE	580
MAIN REEF	45
QUARTZITE	150
SHALE	135
QUARTZITE	60
SHALE	105
QUARTZITE	45
SHALE	60
QUARTZITE	105
SHALE	135
QUARTZITE	135
SHALE	105
QUARTZITE	60
SHALE	170
GOVERNMENT REEF SERIES	
HOSPITAL HILL SERIES	

strata (Brock and Pretorius, 1964a). The oldest and most abundant intrusives are associated with Ventersdorp volcanism; these rocks now occur as highly altered, intermediate to basic diabases. Pyroxenites, gabbros, dolerites and quartz-dolerites of possible Bushveld age (1950 ± 30 m.y. ; Nicolaysen, et al., 1958) are also common and the third group consists of Pilanesberg age (1290 ± 180 m.y.; Schreiner and Van Niekerk, 1958; 1310 ± 80; Van Niekerk, 1962) syenites, quartz keratophyres and diorites. Finally, the Karroo (154 - 190 m.y.; McDougall, 1963; 204 ± 14 m.y.; Manton, 1968) dolerite sills and dykes are found.

Two further groups, not discussed by Brock and Pretorius (1964a), are the post-Waterberg dolerites, an example of which has been dated from the Van Dyk Mine (adjacent to the E.R.P.M.) at 1120 m.y. (McDougall, 1963) and the Ongeluk lavas of the Transvaal System which have been dated at 2224 ± 21 by Crampton (1972).

An analysis of lineation trends from Earth Resources Technical Satellite (E.R.T.S.) imagery revealed four strong regional trends averaging 032°, 290°,328° and 356°. The first of these represents the numerous Ventersdorp dykes; the second a set of shear zones; the third may represent a swarm of Bushveld age dykes, and the fourth is of unknown affiliation.

1.3 GEOLOGY OF THE CENTRAL WITWATERSRAND AND THE E.R.P.M.

The Witwatersrand sediments are situated in a structurally controlled basin of elliptical cross section with long and short axes of 300 km and 130 km. E.R.P.M. is situated on the northern edge of the basin in the Central Rand, which is the type area defined by Mellor (1917) for the stratigraphy of the Witwatersrand sediments (Table 1-1). In this type area, the sediments comprise about 7 400 m of southerly dipping shales, quartzites and conglomerates. The Hospital Hill Series (1495 m), Government Reef Series (1920 m) and the Jeppestown Series (1115 m) make up the lower Witwatersrand System. Included in the Upper Witwatersrand

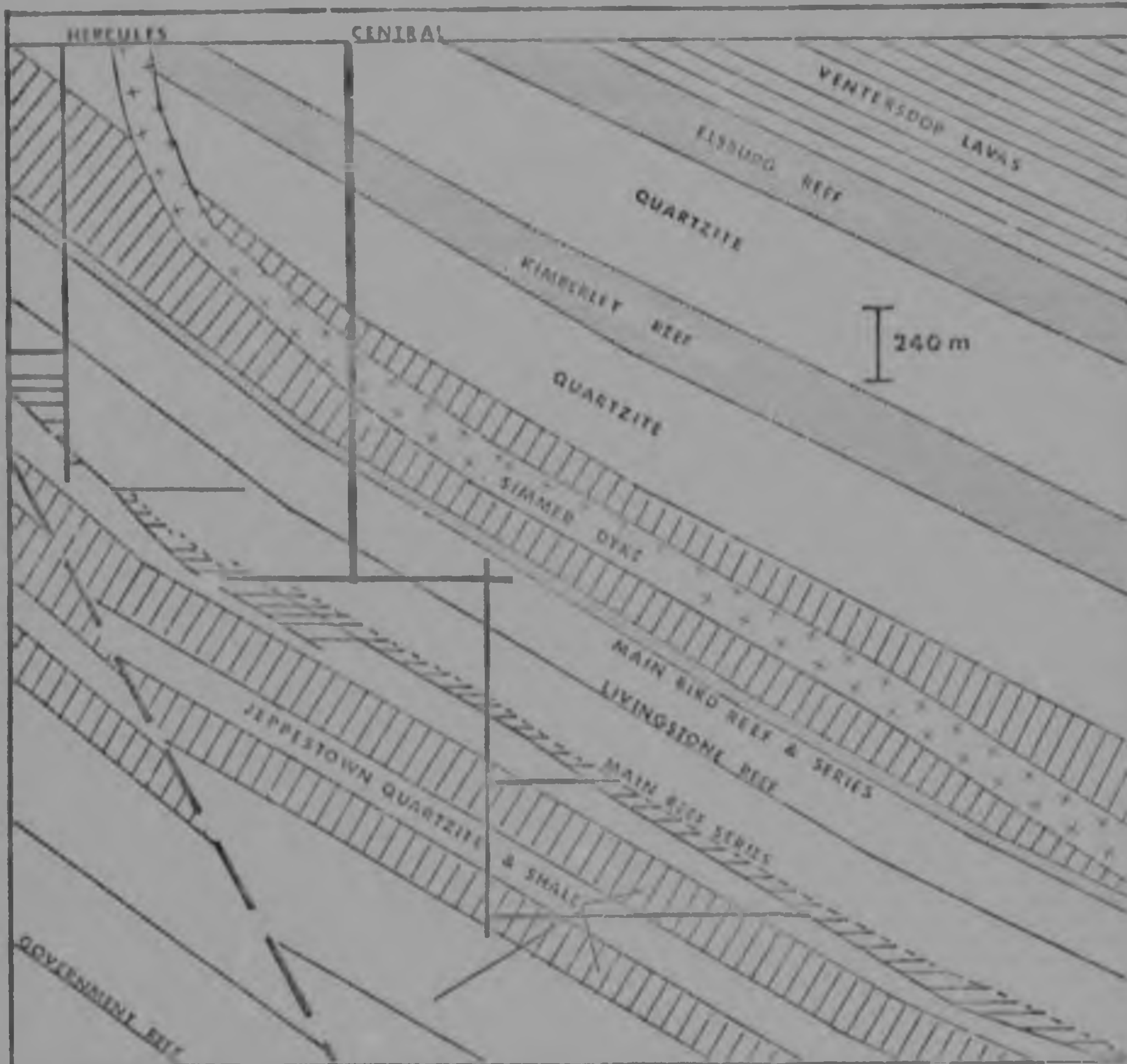

a. Stratigraphic dip section through central E.R.P.M. (after Cook et al, 1966)

b. Diagramatic strike section at about 58 level showing merging of reefs eastwards towards the Boksburg Gap. (after Shipway, 1972)

FIGURE 1-3 STRATIGRAPHIC SECTIONS OF THE E.R.P.M are the Kimberly-Elsburg (1860 m) and the Main Bird (1005 m) Series, in which most of the important gold bearing conglomeratic reefs are found.

Mining in the E.R.P.M. is confined mainly to a narrow conglomeratic horizon in the lower Main Bird Series although some accesssible development is present down into the Upper Jeppestown footwall rocks and up as far as the Livingstone Reef in the hanging-wall, a normal stratigraphic distance of about 250 metres. A geological section illustrating the stratigraphy of the sediments in the Upper Witwatersrand and Jeppestown Series is reproduced in Figure 1-3a. The distribution of the reefs in the E.R.P.M. is illustrated in Figure 1.3b.

Although the terms 'quartzite' and 'shale' are used extensively on the Witwatersrand a s dissertation, rock types corresponding to the terms in their st petrologic sense are rarely found. In fact, within the broad group encompassed by 'quartzite' is a complete spectrum ranging from quartzites sensu-strictu to meta-arkoses, and 'shales' includes shales sensu-strictu, mudstones siltstones. In general, shales are not associated with the gold ng reefs on the E.R.P , and quartzites form both the hanging and footwalls. The characteristics of hangingwall and footwall quartzites are markedly different with the footwall quartzites containing a higher proportion of argillaceous material, resulting in a dull, dirty appearance, than the hanging-wall quartzites which are much 'cleaner' and have a white or light-green glassy appearance. According to Fuller (1958) Jeppestown Series footwall quartzites are composed of quartz (50-60%), feldspar(10%), biotite (5%), calcite (5%), rock fragments plus sericite, chlorite, pyrite, leucoxene, epidote, apatite, zircon and tourmaline. Five thin sections of footwall quartzites from the E.R.P.M. were examined. One consisted of equidimensional interlocking grains of primary quartz with secondary quartz and matrix minerals similar to the Jeppestown Series quartzites filling the interstices, whilst the other four specimens were made up of isolated quartz grains in the same matrix material. All five specimens could be classified as metamorphic arenites. The hangingwall quartzites have an almost idential composition but quartz makes up more than 80% of the rock, with the volume of the other constituents proportionally reduced. Grains are invariably equidimensional and interlocked and the groundmass is distributed in the interstices. Because of the different compositions, the rocks have different compressive strengths, namely: footwall quartzites, 200-225 MPa; hangingwall quartiztes, 350 MPa; this will be discussed in detail in Chapter 5.

Metamorphism in the Witwatersrand sediments is restricted to a low grade regional greenschist facies except for slight contact metamorphic effects associated with the intrusives. The regional metamorphism probably resulted from lithostatic pressures due to the great thickness of sediments and the tectonic forces accompanying the basin development and subsequent deformations. The main effects have been the production of secondary quartz, sericite, chlorite and chloritoid, and interlocking of the grains, thus forming quartzite,and shales and slates from the arenaceous and argillaceous sediments respectively.

The structure of the basin in the Central Rand is relatively simple despite some complicated faulting, but in the nearby East Rand Basin (Figure 1-1b) several large folds and faults and severe basining have complicated the structure considerably. In the E.R.P.M. the sediments dip at 45° to 50° south near surface and at 25° in the deepest areas of active mining. Cross-bedding is well developed near the reef and sets measured in the L shaft, 74 level, exploration crosscut (Map 1) had a 25° steeper dip than bedding.

The sediments thin eastwards, cut out at the Boksburg Gap, a basement high devoid of the main auriferous conglomerates (Shipway, 1972), and then reappear further east in the East Rand Basin.

A structural interpretation of the E.R.P.M. with respect to dykes and fault appears on Map 2 and it is clear that there are several distinct sets of dykes and faults. Faulting on the Central and East Rand is abundant. Most faults strike approximately east-west but many of the dykes, which are mostly dip features, also have fault displacements across them. The strike faults normally show an oblique movement; that is, both strike-slip and dip-slip components of movement, and both reverse and normal faults are present. Often faults may have a pivotal type displacement; that is, displacement has been rotational about a point on the fault plane. This type of faulting will be discussed in detail in Chapter 3. Several particularly large faults occur on the Witwatersrand. Mellor (1921) showed that four of these, the Rietfontein, Roodepoort, Doornkop and Witpoortje Faults, are subparallel to the strike of the bedding. The Rietfontein fault, really a series of small faults, is the largest on the Central Rand and passes just north of the E.R.P.M. According to Mellor (1917) the fault zone dips northwards and the dip-slip displacement is normal. Mellor (1910) states that the fault can be recognised by a marked change in dip of the sediments across the fault. Hatch and Corstorphine's (1906) maps show the fault to have a dextral strike-slip displacement.

Folds are rare on the E.R.P.M., but on the larger scale the basin shape appears to have been modified by tectonic movements. Brock and Pretorius (1964b) have described the shape of the Central Rand sediments as monoclinal, 'draped' on the Pretoria-Johannesburg Granite dome, which has provided a stabilizing effect to the deformations affecting adjacent areas. Geological investigations in the Central and East Rand show that smaller scale folding is present trending about north-north-west. On the E.R.P.M. these folds may only be represented by a change in strike of bedding from 122° in the east to 070° in the west, but in the adjacent East Rand Basin several open to tight folds have been mapped.

1.4 AIMS AND SCOPE OF THE STUDY

In 1964, the Rock Burst Committee defined a rockburst as a 'sudden and violent rupture of rock in situ in which movements into the excavation result from forces other than, or in addition to, the dead weight of the rock that moves and are not caused intentionally by tools, explosives or other like agencies'. Recent research indicates that 'rockbursts', that is, the actual sites of damage of excavations, are a result of 'seismic events', a sudden energy release or failure that is not necessarily coincident with the 'rockburst' site.

The problem of rockbursts in the Witwatersrand gold mines is very real, and an understanding of their origin, conditions under which they occur and techniques by which they may be controlled or eliminated is of great importance when considered in the light of the number of accidents, deaths and days of lost production for which they are responsible. This is emphasised by the fact that the depth of mining will probably increase well beyond its present 3,25 kilometres in the near future.

The Chamber of Mines of South Africa has been sponsoring research into rockbursts and mining induced seismic activity for many years and a wealth of data covering the seismic, rock mechanics, mining and statistical aspects of rockbursts has been collected, but by comparison little pure geological data is available. This gap in data collection is particularly bad on the Central Rand where no systematic geological mapping has been carried out on some mines, because of the simple geological configuration and the ease of following the gold bearing reefs. However, a great deal of research into seismicity and rockbursts has been carried out on the E.R.P.M. and this dissertation forms a part of a project, concerned with investigating geological parameters which appear to be associated with rockbursts and seismic events. In particular, this work has concentrated on the influence of structural discontinuities such as dykes and faults on the occurrence of rockbursts.

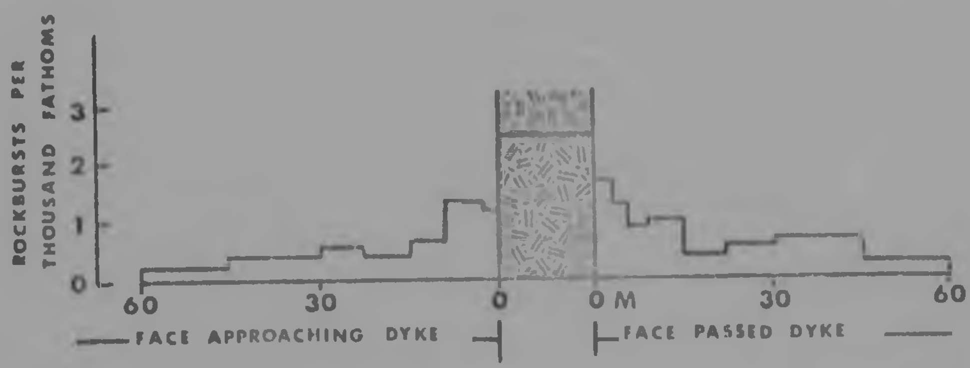

a. Large dyke in a large abutment

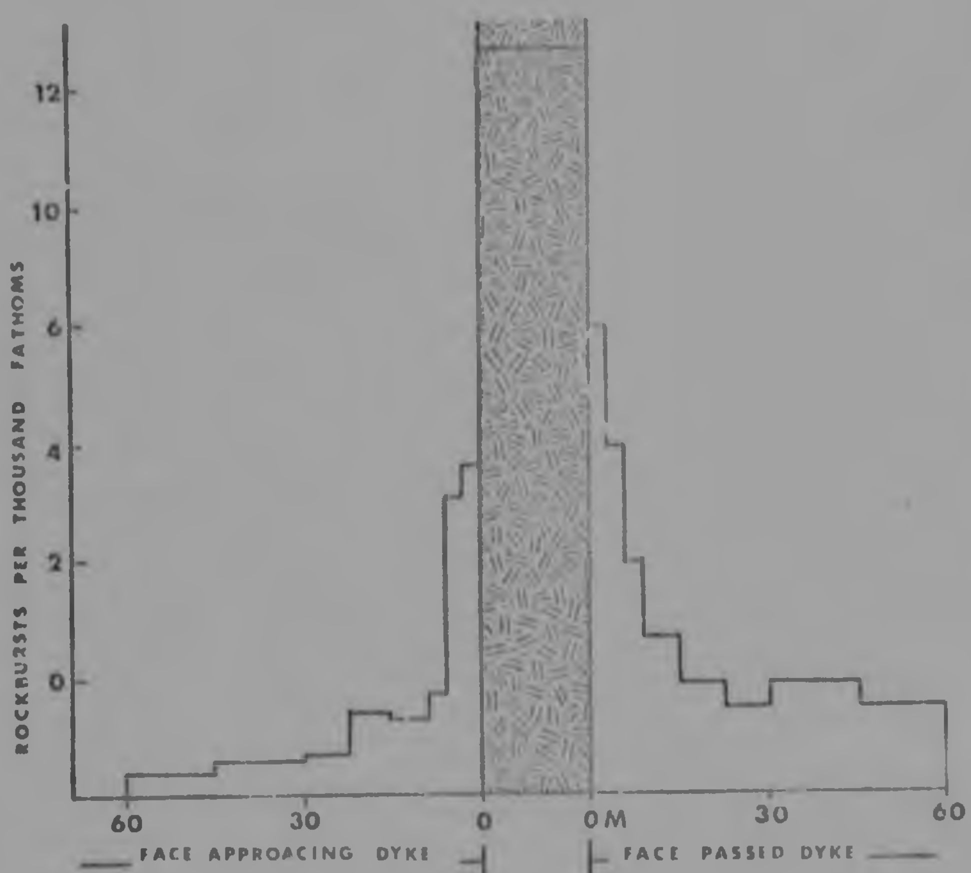

b. Large dyke in a small remnant pillar

FIGURE 1-4 EFFECT OF DYKES ON ROCKBURST INCIDENCE IN THE E.R.P.M. (after Cook et al, 1966)

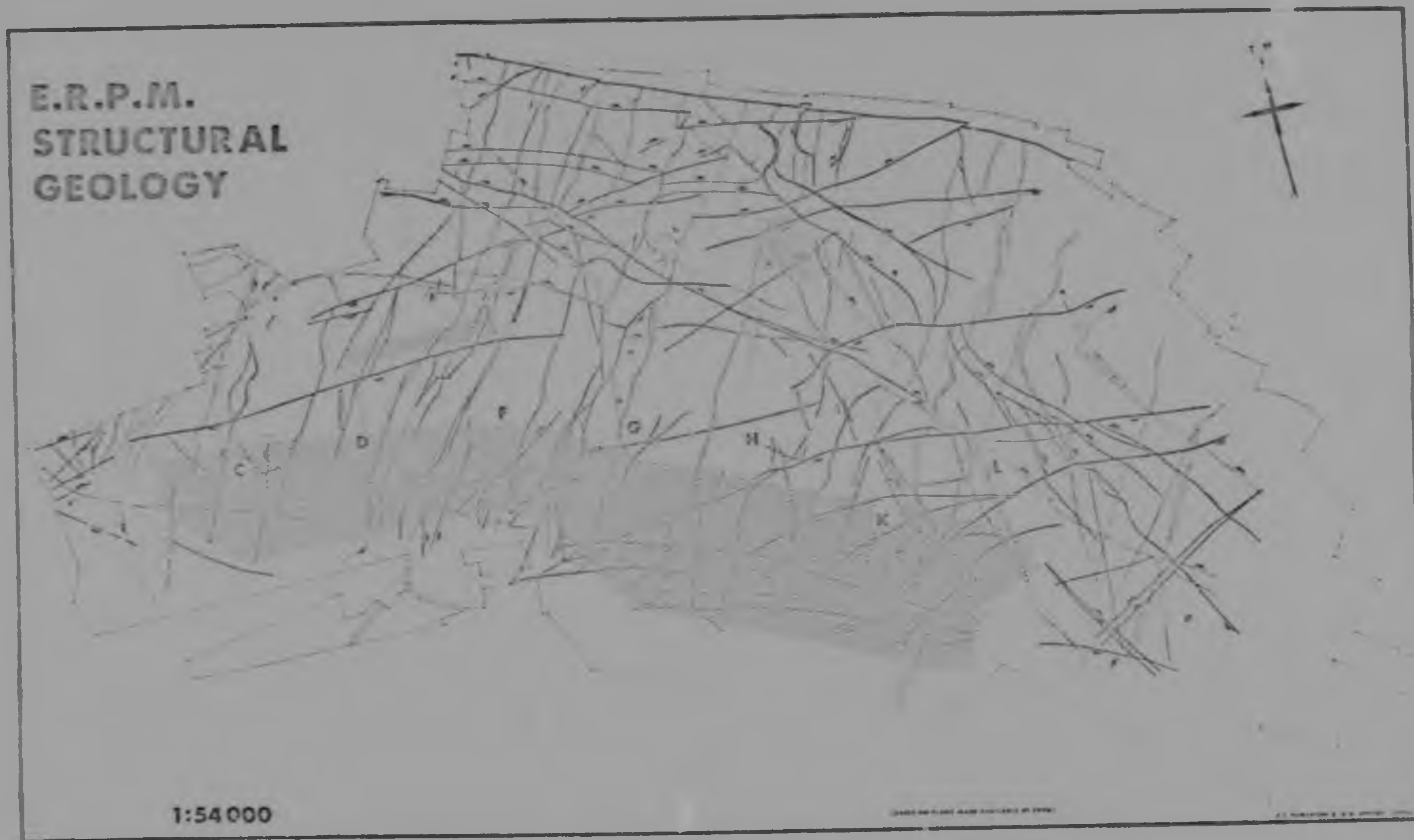
E.R.P.M.
STRUCTURAL
GEOLOGY
C
D
F
G
H
K
L
1:54000

FIGURE 1.5

Plan of the E.R.P.M. showing areas where work has been carried out.

Vertical shaft

Incline shaft

Mine boundary

Dyke

Fault showing downthrown side

Area where work has been carried out

Investigations into the problem of rockbursts on the Witwatersrand has been carried on since the turn of the century; in a historical summary Cook et al. (1966) report investigations into seismic and rockburst problems by the Ophirton Earth Tremors Committee in 1908 and the Witwatersrand Earth Tremors Committee in 1915. A considerable amount of investigation took place in the 1930's (for example: Grey, 1931; Association of Mining Managers, Transvaal, 1933; Sinclair, 1936). More recently it has been shown by Hill (1954) and confirmed by various other authors (Rock Mechanics Research Team, 1959a and 1959b; Cook et al., 1966; Pretorius, 1966) that the incidence of rockbursts increases near dykes and faults (Figure 1.4) and that some dykes are more prone to rockbursts than others. Hence, the primary aim of the present study is to investigate this behaviour by establishing the geology of many of the structural discontinuities (dykes and faults) in the lower levels of the E.R.P.M. Geological parameters considered include the general geometry, petrology, geochemistry, contact effects, rock mechanics and jointing patterns of dykes, faults and shear zones and their effects upon the adjacent quartzites. In Chapter 6 an attempt is made to establish relationships between the geological parameters and rockburst activity in H section of the mine (Map 1). Although some conclusions are drawn, difficulties prohibited the study being expanded to include more shafts. In addition, also in Chapter 6, a study of the relationship between seismic events and geological discontinuities is outlined. In Chapter 4 early stress systems as indicated by the present geology are determined and a possible structural history is proposed.

Figure 1.5 is a much reduced photograph of Map 2 illustrating the areas where work for this dissertation has been carried out. A similar photograph appears at the beginning of each chapter showing the relevant discontinuities mentioned and areas considered. From the map in Figure 1.5 one can see that the bulk of the work

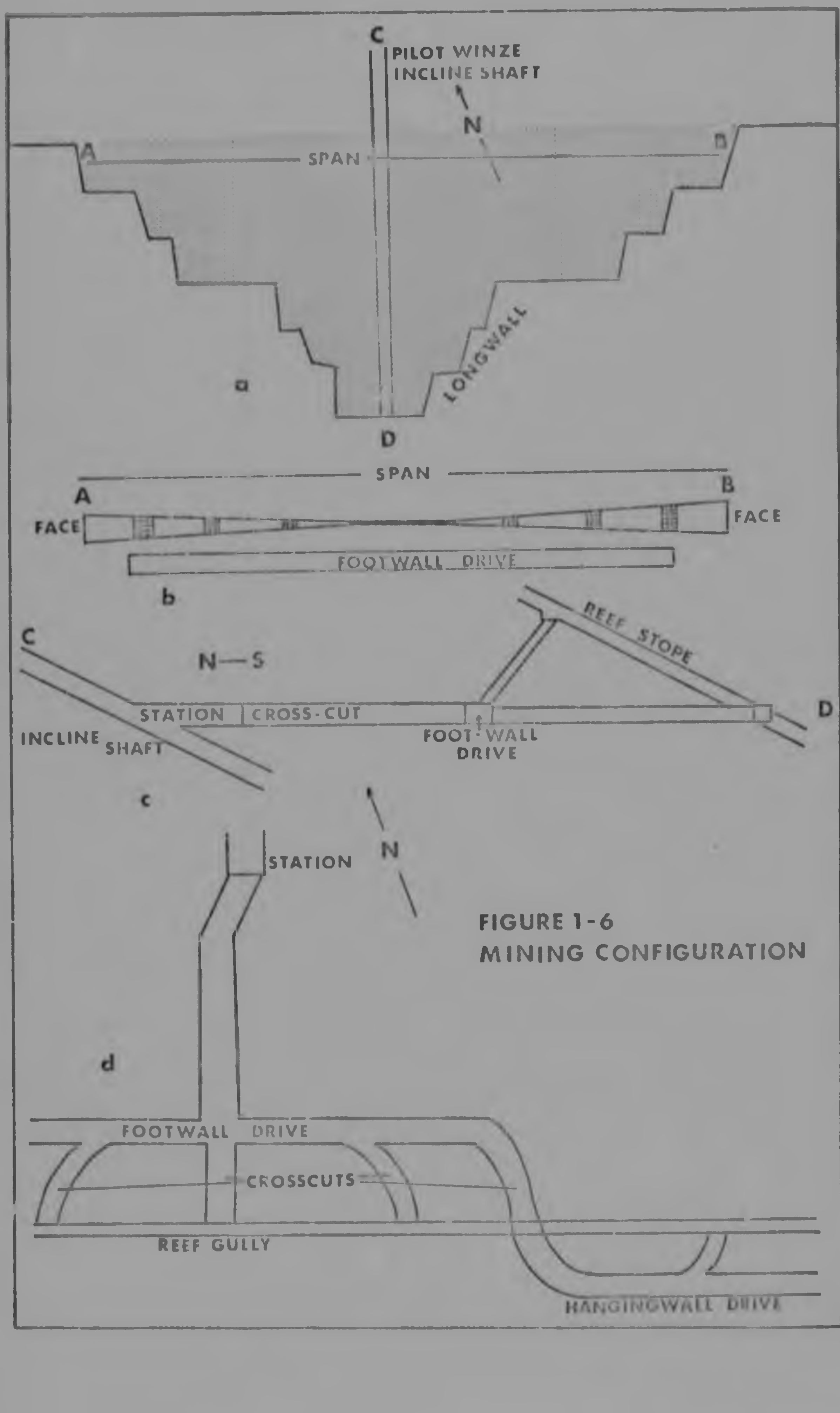

FIGURE 1-6
MINING CONFIGURATION

FIGURE 1.6

MINING CONFIGURATION

a. Plan view illustrating the meaning of the terms span and longwall. Mined-out areas are stippled.

b. East-west, vertical section along AB showing closure of the stope behind the mining face and the relative position of a footwall drive.

c. North-south, vertical section showing access from the incline shaft, which is parallel to the reef, to the area of active mining (reef stope).

d. Detailed plan-view showing the position of footwall and hangingwall drives and crosscuts with respect to the reef gully.

has been concentrated in a small area of the mine, between C and L shafts and between 68 and 78 levels. Consequently only about 60 of the estimated 240 large structural discontinuities in the mine have been visited. Accessibility into the upper levels is limited and only a few trips were made. The emphasis on the work has been between F and L shafts where the strike of the sediments is constant. The C and D sections are mined at shallower depths and the sediments vary in strike, a few dykes were also examined here.

1.5 MINING CONFIGURATION AND TERMINOLOGY

Many Witwatersrand gold mines and especially the E.R.P.M. have very simple mining configurations which can be attributed to the simple sedimentary geology and the absence of major tectonic disturbances, except for the few large fault displacements. The general mine development is illustrated on Map 1 and the configuration is illustrated in Figure 1.6.

The reef dips uniformly southwards and is mined in an underhand method of longwall stoping resulting in a thin tabular opening dipping south. Access from surface is by vertical shafts, then by incline shafts which run parallel to the reef in the footwall, and finally, access to the reef is by eastward and westward trending footwall drives and southward trending crosscuts or raises. (Figure 1.6). Most field-observations were made in footwall drives and the mining geometry is almost identical from one level to the next. Occasionally, where mining problems are encountered the footwall drives are turned southwards through the reef to become hangingwall drives. The drives are not usually on reef at deep levels but in th old areas access was always via reef-drives. In addition, the mining technique in old areas was to mine only pay zones leaving small scattered remnant pillars, whereas today stabilization pillars are left occasionally and all reef areas between are mined out resulting in the hangingwall sagging to meet the rising footwall some distance behind the working area (Figure 1.6).

In the E.R.P.M. there are at least 48 vertical and inclined shafts although only 25 are in use today (Map 1). The mine is divided into three broad sections: the West Section includes the South-west vertical and subvertical and C and D incline shafts; the Central Section includes Central vertical and subvertical, Hercules vertical and F, G, H and H1 incline shafts; and the East Section includes Southeast vertical and subvertical and K and L incline shafts. In this dissertation a reference to the , for example, 'Central Section' refers to areas described above and a reference, for example, 'H75E' implies H incline shaft, 75 level and the east side. 'H75W' is the same level but the west side. 'FWD' implies footwall drive and 'HWD' hangingwall drive. The term 'cross-cut' is abbreviated to 'x-cut'.

The notation used to describe the orientation of structural features is as follows: for a planar feature the strike, dip and a rough dip direction are given; for example, 049/60/SE implies a plane striking at 49° east of north, dipping at 60° degrees towards the south-east; and for a lineation the plunge and trend are given, for example, 62/055 implies a lineation plunging at 62° towards 055°.

0
1000
metres
N
C
D
G
H
K
L
11
16
24
26
27
32
33
34
35
38
56
58
77
79
82
100
109
110
110A
114A
117
121
144
149
157
159
162
164
165
167
182
192 in footwall

FIGURE 2.1

Plan of a section of the F.R.P.M. showing discontinuities referred to in Chapter 2.

Vertical shaft

Incline shaft

Mine boundary

Dyke

Fault showing downthrown side

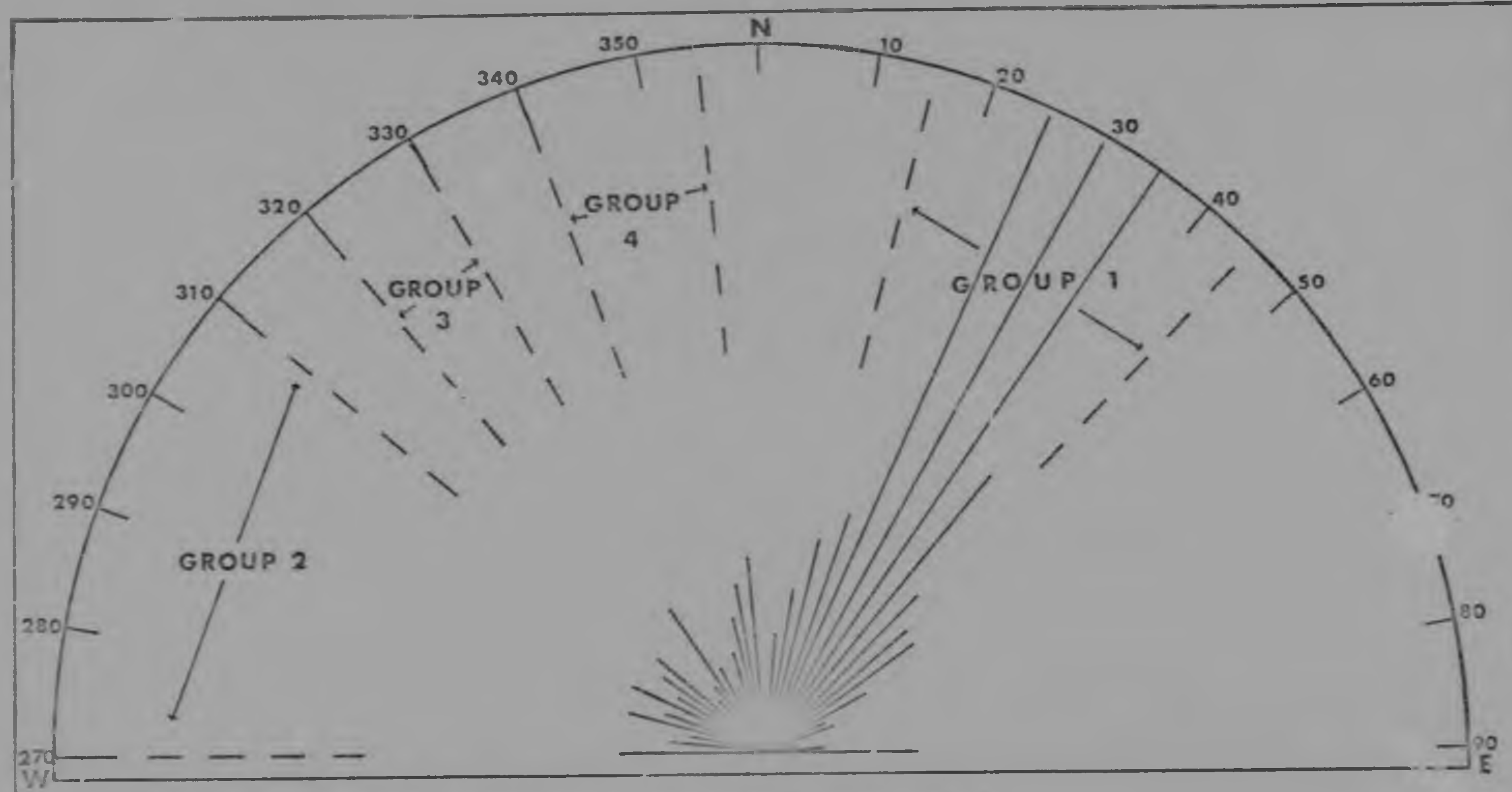

FIGURE 2-2 STRIKE-FREQUENCY DIAGRAM FOR DYKES

RADIUS = 11,4% , NUMBER OF POINTS IS 544 , BROKEN LINES REPRESENT GROUP BOUNDARIES

CHAPTER 2

INTRUSIVE ROCKS

2.1 DISTRIBUTION

Of the 232 major structural discontinuities in the E.R.P.M. considered in this dissertation, some 57% are intrusives and a further 10% are dykes with faulted contacts. The intrusives include both dykes and sills ranging in composition from acid to basic and in width from one or two centimetres to more than 100 metres. Basic intrusives are far more common than acid intrusives; the latter are only represented by a series of 'en echelon' aplite sills, which have been studied in detail by Fumerton (1975) and therefore, will not be considered here. The intrusives referred to in this chapter are plotted on the mine plan in Figure 2.1. Map 2 shows the locations of all the dykes in the mine. In this map several sets of dykes can be recognised and their strike directions have been analysed using a technique of Donath's (1962). Using this method, a square grid of 500 metres side was drawn over the structural map of the E.R.P.M. (Map 2), and the strike of every dyke passing into or through each square was measured and plotted on a dyke-strike frequency diagram (Figure 2.2). Then, areas of higher frequency were visually selected and the mean strike, standard deviation from the mean, and mean frequency for each data group were calculated. These data are summarised in Table 2.1.

TABLE 2.1

Summary of strike analysis data for dykes

NO.	GROUP BOUNDARIES	MEAN STRIKE	STANDARD DEVIATION OF THE MEAN STRIKE	AVERAGE FREQUENCY WITH EACH GROUP (No of points and frequency)
1	$015^{\circ} - 045^{\circ}$	030°	$10,0^{\circ}$	30,4 (7,2%)
2	$270^{\circ} - 310^{\circ}$	291°	$12,9^{\circ}$	10,4 (1,9%)
3	$320^{\circ} - 330^{\circ}$	325°	$4,1^{\circ}$	10,0 (1,8%)
4	$340^{\circ} - 355^{\circ}$	349°	$5,8^{\circ}$	13,0 (2,4%)

This type of analysis, which is repeated for faults in Chapter 3 and regional lineations in Chapter 4, tends to bias the results because each individual dyke may be counted several times, thus giving more weight to a large dyke than a small dyke. An alternative method of analysis not used here is to count the strike of each dyke, irrespective of its size or length, only once; this prevents two or three large dykes from swamping a swarm of smaller features. Because of the well defined trends in the E.R.P.M. this is unlikely to happen and so only the first method was used for analysis.

In addition to the four groups of dykes classified in Table 2.1 there are two sill like intrusives in the mine. The Simmer Dyke (No.26, Map 2) is an undulating intrusive which can be up to 200 metres thick; its unusual structure will be discussed in Section 2.4. The other sill, number 192, has been detected beneath K and L shafts between 77 and 78 levels in a pilot winze and a deep bore hole. These intersections show that the intrusive cuts across the sediments at a low angle and is at least 15 metres thick. Little else is known about its geometry.

Apart from the Simmer Dyke, the intrusives are regular in their shape and dimensions except where bifurcation, 'horns' or rafted-off blocks of quartzite are present. These features are discussed in Section 2.4 on the geometry of the intrusives.

2.2 PETROGRAPHY

2.2.1 Previous work

Only a few descriptions of the intrusive rocks in the Witwatersrand mines have been published by previous workers and in these very little reference is made to the Central Witwatersrand. However, in 1898 Henderson described several suites of South African intrusive rocks including data from two dykes from near the old Angelo Incline Shaft (see Map 1). He described one of these dykes as a dark-green diorite containing lath-shaped hornblende crystals, plagioclase and several accessories and the other as a highly decomposed, fine grained, greenish, schistose norite. In a detailed discussion of intrusive rocks of the Witwatersrand, McDonald (1911) reported the presence of an intermediate, pyroxene-andesite intrusive from near the Blue Sky Incline Shaft (Map 1). This rock was fine-grained and consisted of lath-shaped plagioclase (An 40-60), small black orthopyroxenes as bastite pseudomorphs and augite in a devitrifying glassy groundmass. In additic . McDonald classified the basic intrusives on the Witwatersrand into two classes: olivine-dolerites and dolerites without olivine.

The bulk of the more recent work on intrusives has been concerned with the East Rand Basin but many of the conclusions derived from these studies are applicable to the Central Witwatersrand. There appear to be two broad divisions in the type of intrusives: the complex or multiple intrusive dykes (Ralston, 1953) and the simple or single intrusion dykes (Ellis, 1946). In particular, Ellis (1946) has described two types of simple dykes, namely, fresh dolerites of Karroo age, and older, altered ilmenite diabases. Whiteside (1950) and Ralston (1953) have both recognised six categories of intrusives, not all similar to each other, covering several age periods. A combination of their work provides a division of the intrusives into seven categories:

1. Karroo dolerites: These are dykes and sills of dolerite and olivine-dolerite respectively, which are mostly unaltered and consist of clear plagioclase and augite with an ophitic texture. They strike NW-SE, are up to 100 metres thick and do not displace the reef.

2. Complex intrusives: These are multiple injections with an amphibolite composition.

3. Pilanesberg suite: These are NW-SW striking (345^o) intrusions associated with the Pilanesberg alkaline complex in the north-western Transvaal. Gelletich (1937) used a magnetometer to trace the dykes, which have a magnetic field opposite to the present one, from the Pilanesberg onto the Witwatersrand. The dyke swarm consists of simple tholeiitic basalts, andesites and complex salic dykes with more femic margins (Ferguson, 1973).

4. Bushveld suite: These are NE-SW striking ilmenite diabase dykes (Ellis, 1946) and sills containing characteristic 'boxworks' of ilmenite.

5. Major Ventersdorp Dykes: These are fine-grained, altered quartz dolerites and include large stepped intrusives described by Ellis(1940). A large displacement across them is common.

6. Minor Ventersdorp Dykes: These are numerous narrow dykes and sills that are highly altered and sheared, Generally their original constituents are unrecognisable.

7. Other problematic dykes: These include quartz-sericite dykes which may be mylonites and quartz-prophyries.

2.2.2. The E.R.P.M. intrusives

In this section the petrology, age and contact metamorphic effects of the various intrusive rocks are discussed. Using the orientation data outlined in Table 2.1 and the petrological characteristics, the intrusives can be divided into six groups. This sub-division is supported by the detailed geochemical data discussed in Section 2.3.

The petrological descriptions are often very short because the rocks are sometimes very fine grained and may be extremely altered and sheared. The degree of alteration is used as an indication of the age of an intrusive and using this criteria the groups are discussed in chronological order. All the dykes listed below have been examined in-situ and sampled for thin section work; in addition those marked with an asterisk have also been geochemically analysed.

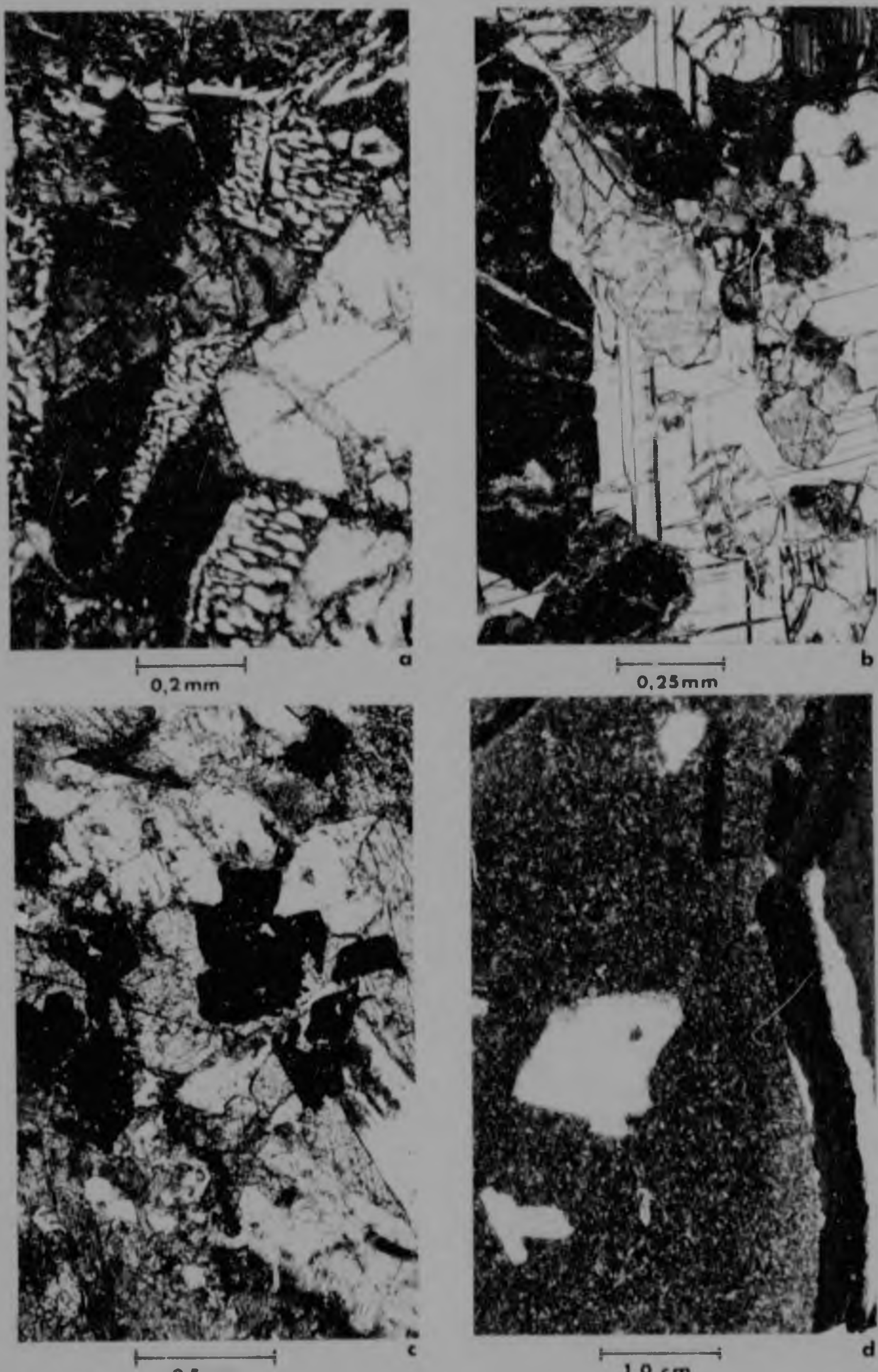
0,2 mm
a
0,25 mm
b
0,5 mm
c
1,0 cm
d

PLATE 2.1

Dykes 26, 149 and 144(groups 1, 2 and 3)

a. Photomicrograph of dyke 26 (group 1; melanorite) showing excellent quartz-alkali feldspar intergrowths.

b. Photomicrograph of dyke 26 (group 1; melanorite) showing subhedral pyroxenes in a large feldspar crystal.

c. Photomicrograph of dyke 149 (group 2; ilmenite dolerite) showing characteristic skeletal ilmenites.

d. A polished hand specimen of dyke 144 (group 3; quartz dolerite) showing characteristic feldspar phenocrysts in a very fine grained groundmass.

PLATE 2.1

Dykes 26, 149 and 144(groups 1, 2 and 3)

a. Photomicrograph of dyke 26 (group 1; melanorite) showing excellent quartz-alkali feldspar intergrowths.

b. Photomicrograph of dyke 26 (group 1; melanorite) showing subhedral pyroxenes in a large feldspar crystal.

c. Photomicrograph of dyke 149 (group 2; ilmenite dolerite) showing characteristic skeletal ilmenites.

d. A polished hand specimen of dyke 144 (group 3; quartz dolerite) showing characteristic feldspar phenocrysts in a very fine grained groundmass.

Group 1 : dyke 26*, the Simmer Dyke

melanorite (Plates 2.1 a & b)

This dyke is quite unique in the E.R.P.M. in both its geometry and composition. In hand specimen it is melanocratic having a coarse crystalline texture and breaking with a fresh conchoidal fracture.

In thin section the rock consists of almost entirely of feldspar and pyroxene with a granulitic texture (Harker, 1964, p 120). Plagioclase (An 40-60) comprises about 30% of the rock; the crystals are large, heavily twinned and mostly unaltered. Pyroxenes are present as smaller euhedral to subhedral crystals within the plagioclases (Plate 2.1b). Orthopyroxenes, which are more common than clinopyroxene are magnesium rich, probably bronzites; both cleavages are well displayed in most sections but the crystals are traversed by irregular cracks along which a chloritic or serpentine-like alteration is present. The clinopyroxene is normally augite with a pale brown colour and shows excellent herringbone structures. Small patches of quartz-orthoclase microintergrowths are also common (Plate 2.1a);these appear to be similar to granophyric intergrowths described and illustrated by Barker (1970) , although he restricts their occurrence to rocks of a 'granite' composition. In addition small quantities of brown biotite, chlorite, apatite, iron ore and secondary quartz are present.

This rock is similar to that described by Henderson (1898)(see 2.2.1 above), except that the present specimen is fresh whereas his was severely altered and weathered.

The Simmer Dyke is the freshest dyke observed in the E.R.P.M. and this may indicate that it is one of the youngest intrusives, possibly of Bushveld age,because similar intrusives of pyroxenitic and gabbroic composition elsewhere on the Witwatersrand are thought by Brock and Pretorius(1964a)to be related to the Bushveld complex.

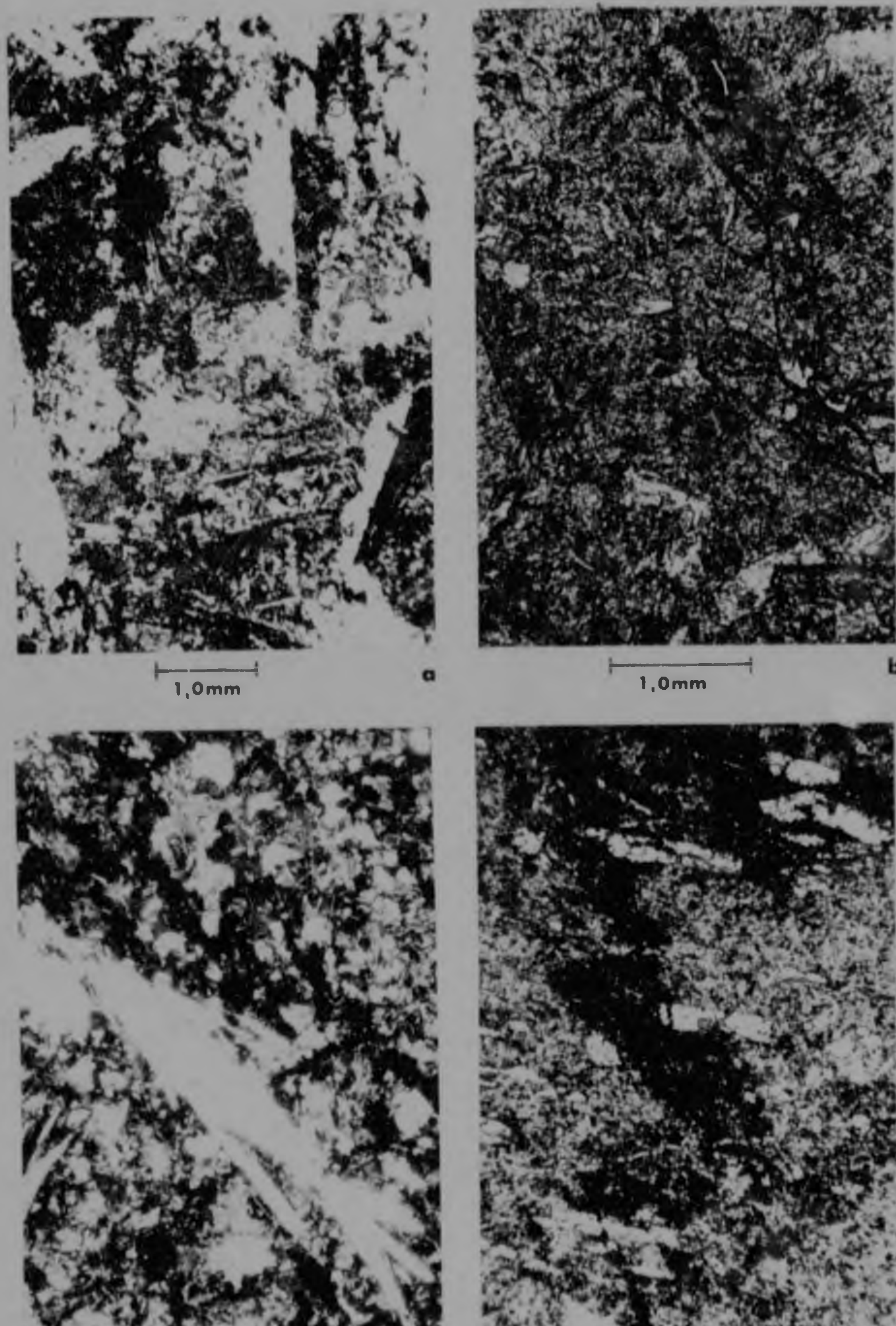
1,0mm
a
1,0mm
b
0,25mm
c
0,5mm
d

PLATE 2.2

Dyke 32(group 3) and group 5 shear zones

a. Photomicrograph of dyke 32(group 3; quartz dolerite) showing general texture, alteration and feldspar phenocrysts in a fine groundmass. Specimens from group 4 dykes are similar but finer grained and heavily altered.

b. Photomicrographs from group 5 shear zones(mylonites) chloritoid crystals in a completely altered and fine grained groundmass.

c. Large epidote needles in a fine groundmass.

d. Microfolding of a black chloritic layer by variable displacement along a strong foliation within a mylonite.

a

b

c

d

PLATE 2.3

Dyke/quartzite contacts

In each of these plates the dyke is dark and the quartzites light.

a. Dyke 149. The contact is extremely sharp and planar suggesting intrusion along a prexisting fracture plane such as a joint.

b. Dyke 117. The contact is extremely sharp but irregular in this particular diamond core. However, often the contacts for this dyke are similar to (a).

c. Dyke 100. The dyke is sharp and planar at this locality but often some shearing is present.

d. Dyke 82. At this locality the contact is sheared and irregular. A small horn is shown in the photograph.

Group 2: dykes 82*,149 ,157,164,165,167

Ilmenite dolerites (Plate 2.1c)

These dykes only occur as a swarm of at least 20 dykes between K and L shafts. They all dip vertically, strike about 140° and are between five and eight metres thick. Contacts with the quartzites are sharp without shearing (Plate 2.3a) or reef displacement; chilled margins are common and the dykes are fine grained in the centre. Horns are often present and in one place, L70E, a wedge of quartzite 1,5 metres long, which varies in thickness from two to 20 centimetres, has been rafted into dyke 149.

In hand specimen, the chilled margins are black and too fine grained to see individual crystals but the centre of the dyke comprises a dark grey, crystalline, mafic rock.

In thin section, the rocks are holocrystalline with only minor alteration; plagiocalse is subophitic with anhedral pyroxenes. Andesine, which is the most common mineral, is present as small, poorly developed but heavily twinned laths. Sericitization and some kaolinisation has clouded the crystals but in general they are quite fresh. Clinopyroxenes are quite abundant but orthopyroxene is not as common. Some pyroxenes have signs of serpentine alteration and partial bastite pseudomorphs are occasionally present. A distinguishing feature of the dyke is the presence of skeletal ilmenite (Plate 2.1c) which forms about five per cent of the rock and which may be altered to leucoxene. Brown biotite, chlorite as patches and halos around plagioclase, apatite and microintergrowths of quartz and orthoclase are minor accessories.

Pilanesberg age intrusives (see Section 2.2.1 above) strike parallel to this swarm but are otherwise completely dissimilar. Whiteside (1950) and Ralston (1953) both considered ilmenite diabases, which strike at 045°, to be of Bushveld age and although those on E.R.P.M. have a different strike, the similarity in petrology suggests a possible Bushveld age.

Group 3: dykes 32*,33*,58*,100*,144*,182*

Quartz dolerites (Plates 2.1d and 2.2a)

The most common strike of intrusives in the E.R.P.M. is 030° (see Table 2.1) and group 3 dykes form part of this trend. Their thickness varies from about 16 to 41 metres and they all have near vertical dips. They can be distinguished from other dykes of the same orientation by grain size and degree of alteration.

In hand specimen the dykes are medium grained and dark-green grey in colour; in addition dykes 33, 144 and 182 have large feldspar phenocrysts as prominent features (Plate 2.1d). All have fine-grained chilled contact zones with the sediments; the contacts may be sharp with no shearing evident (Plate 2.3c) or else varying amounts of shear movements may have taken place (Plate 2.3d).

Feldspar and pyroxene are the two most common constituents. The feldspar, normally oligoclase, occurs as large phenocrysts and laths in the groundmass (Plate 2.2a); it is always twinned and often is clouded by chlorites and kaolin. The pyroxene is normally augite; it occurs as green and brown crystals which are partly altered to chlorite and serpentine. Brown hornblende is present in all specimens in small quantitites. Accessories include sphene, which has been corroded to a rough skeletal shape, apatite, a little primary quartz intergrown with feldspar, some secondary quartz, chlorites and ilmenite or magnetite.

The age of this group is not known but by comparing the degree of alteration to that of groups 1 and 2, these dykes appear to be older. It is [illegible]t likely that they belong to one of the Ventersdorp intrusive phase[illegible]

Group 4: dykes 16*,24,27*,38*,70*,77*,79*,117*,121*

Quartz dolerites

This group is similar in both orientation and composition to group 3 but differs in that the rocks are much finer grained and heavily altered.

In hand specimen it is difficult to see individual grains and no phenocrysts were observed. The contacts are regularly sheared for distances up to several centimetres and quartz veining is common.

In thin section the most significant differences from group 3 are the secondary minerals. Group 4 dykes regularly contain calcite, epidote and abundant chlorite; the original minerals are extremely difficult to observe but when they can be seen, they are similar to those of group 3.

Dyke 117 requires special mention because of an unusual glomeroporphyritic texture in which patches of calcite and chlorite are surrounded by clinopyroxene and orthopyroxene. In addition it also differs from the rest in that it has a very sharp but irregular contact with the quartzites (Plate 2.3b).

The dykes of group 4 may correspond to the 'major Ventersdorp dykes' discussed in section 2.2.1 above; however, their advanced degree of alteration suggests that they are older than group 3.

Group 5: dykes 162, 114A*,109*,110*,110A,159*

Shear zones - mylonites (Plates 2.2b,c and d and 3.1 a, b and c)

The specimens from this group represent the numerous E-W striking shear zones in the mine in which the degree of shearing and alteration is such that the original minerals are normally unrecognisable.

In hand specimen, the rocks are dark grey and brittle with a very strong foliation (see Plate 3.1 a and b) and quartz pods ranging in size from microscopic to 20 centimetres or more are frequently visible (Plates 3.1 b and c).

Thin section examination reveals little about the original composition. The grain size is variable but all specimens are very fine-grained and in some specimens grains have a maximum diameter of 0,05 mm. The mineralogy includes abundant chlorites, chloritoid laths, calcite, minor primary quartz, pyrite, epidote and secondary quartz (Plates 2.2 b and c).

Physical deformation of the crystals including stretching, realignment and internal deformation indicated by undulose extinction is common (Plate 2.2d).

Group 6: dyke 11* and sill 192

Neither of these intrusives can be categorized in any of the above groups although they do have close similarities with some of them.

Dyke 11 is similar petrologically to dykes of group 3 but strikes about 125° and dips 60° south, whereas those of group 3 strike about 030° and dip close to vertical. It is noteworthy that dyke 11 is almost orthogonal to those of group 3.

Sill 192 differs in orientation (see 2.2.1 above) and composition from all the other groups. It is a medium grained mafic rock, consisting of abundant, large (1,5 mm long)green amphibole laths in a groundmass of chlorites, alkali feldspar, calcite, apatite, opaques and secondary quartz. Alteration is moderate. Its very mafic nature and sill-like nature suggests a possible relationship to the melanorite of group 1.

2.2.3. Ages of intrusives

All the intrusives in the E.R.P.M. are displaced by faulting, hence, no comparative age relations can be determined in this way. Also, no absolute age determinations have been made on the basic rocks of the E.R.P.M. However, Fumerton (1975) has determined the age, by Rb/Sr techniques, of the aplite sills in the E.R.P.M. to be late-Transvaal (2137 ± 13 m.y.) and a comparative age relation to some of the basic dykes has been made. Dykes 34, 35, 58, 70, 117 and 121 are intersected by the aplite sills and the intrusive relationships show that they are all older than the aplite. These dykes belong to groups 3 and 4 above and therefore, these groups, plus possibly group 5, are older than 2100 m.y., Physical deformation of the crystals including stretching, realignment and internal deformation indicated by undulose extinction is common (Plate 2.2d).

Group 6: dyke 11* and sill 192

Neither of these intrusives can be categorized in any of the above groups although they do have close similarities with some of them.

Dyke 11 is similar petrologically to dykes of group 3 but strikes about 125° and dips 60° south, whereas those of group 3 strike about 030° and dip close to vertical. It is noteworthy that dyke 11 is almost orthogonal to those of group 3.

Sill 192 differs in orientation (see 2.2.1 above) and composition from all the other groups. It is a medium grained mafic rock, consisting of abundant, large (1,5 mm long)green amphibole laths in a groundmass of chlorites, alkali feldspar, calcite, apatite, opaques and secondary quartz. Alteration is moderate. Its very mafic nature and sill-like nature suggests a possible relationship to the melanorite or group 1.

2.2.3. Ages of intrusives

All the intrusives in the E.R.P.M. are displaced by faulting, hence, no comparative age relations can be determined in this way. Also, no absolute age determinations have been made on the basic rocks of the E.R.P.M. However, Fumerton (1975) has determined the age, by Rb/Sr techniques, of the aplite sills in the E.R.P.M. to be late-Transvaal (2137 ± 13 m.y.) and a comparative age relation to some of the basic dykes has been made. Dykes 34, 35, 58, 70, 117 and 121 are intersected by the aplite sills and the intrusive relationships show that they are all older than the aplite. These dykes belong to groups 3 and 4 above and therefore, these groups, plus possibly group 5, are older than 2100 m.y., but by association to previous work and because of the small volume of basic lavas in the Transvaal System the dykes of these groups are here considered to be of Ventersdorp age.

The degree of alteration is here considered to be an indicator of the age of intrusives provided similar types of intrusives are compared. In this work, all intrusives are basic and contain abundant plagioclase feldspars and pyroxenes, hence, the comparison is probably justified. Within the Ventersdorp age intrusives (groups 3, 4 and 5) group 5 is by far the most altered, although this may be a direct result of the amount of shearing, and thus is possibly the oldest. Using the same arguments group 4 is the next oldest followed by group 3. Groups 1 and 2 are 'fresh' in comparison to groups 3, 4 and 5 and are possibly younger. The suggested Bushveld age is only by comparison to previous work. At no accessible locality could dykes of group 1 and 2 be found intersecting the aplite sills.

The age relations and rock types are summarized in section 2.5.

2.2.4. Contact metamorphic effects on the sediments

The sediments adjacent to the intrusives often show evidence of contact metamorphism although the effects are not marked because of the background regional metamorphism which was described in Chapter 1.3. In hand specimen, the main contact metamorphic effect is a slight darkening of the quartzites for distances up to two or three metres from the dykes, although often no effects are visible. In thin section some degree of recrystallisation of the quartz to produce interlocking grains and/or patches of secondary quartz has taken place. The original argillaceous material is present as concentrations of chlorites and micas but much of this is often due to regional rather than contact metamorphism.

The lack of severe contact metamorphism, even near very large dykes suggests that some of the dykes may have intruded as a partially crystalline cool mush. The dykes of group 3 contain large feldspar phenocrysts which are concentrated towards the centre of the dyke; phenocrysts were never observed near dyke margins. This may be an example of flowage differentiation (Bhattacharji and Smith, 1964; Bhattacharji, 1967; Komar, 1972), in which solid particles, suspended in a flowing fluid, concentrate in the area of greatest velocity; this is towards the centre of an intruding dyke. The presence of flow differentiated phenocrysts in dykes implies that the magma is partially solidified (and cooled) at the time of intrusion, and is, therefore, less likely to cause as severe contact metamorphism as a completely liquid magma. Flowage differentiation, as well as rapid cooling, may also account for the presence of extremely fine grained margins on many dykes.

2.3 GEOCHEMISTRY OF DYKES, SILLS AND FAULT ZONES

Detailed geochemical analyses of 22 dykes, sills and shear zones have been carried out and the C.I.P.W. norms for the rocks determined. This work was done to supplement the petrological descriptions in section 2.2 above; to elucidate whether the shear zones contain intrusive material or if they are sheared quartzites and for comparison with the rock mechanic properties, discussed in Chapter 5. With respect to this last aim, a further five samples were analysed from dyke 182 so that a geochemical trend across a dyke, notorious for rockbursts, could be compared with the rock mechanic trends.

In Appendix 1 sampling procedures, sample locations and methods of analysis are discussed, and the analysts, the 27 geochemical analyses determined for this dissertation and some previously determined geochemical analyses of sediments and intrusives are listed. In the following text, analyses are referred to by their respective dyke numbers as used above in section 2.1 and 2.2 and the number in brackets refers to the analysis number in Tables 1B, 1C or 1D in Appendix 1. These analysis numbers (i.e. Nos 1 to 27) are also used on the figures.

2.3.1. Silicate analyses

A general examination of the silicate analyses listed in Appendix 1 shows several clear features to be present, the most obvious of which is the low alkali content. Only specimen 144(9) has greater than four per cent total alkalies whilst most contain between two and three per cent. Five specimens (numbers 114A, 109, 79, 110 and 117; analyses 23-27) have less than 0,5 % total alkalies. A breakdown of the alkalies shows potassium to be the most depleted ranging from only 0,01 % to 0,95%. Thin section examinations generally revealed only small quantities of alkali-feldspar confirming the paucity of potassium. TiO_2 is unusually high for three specimens; numbers 149 (14), 82(19) and 117(27), and in dykes 149 and 82 this is reflected petrologically by abundant characteristic skeletal ilmenites (see Group 2, section 2.2.2. above). Al_2O_3 is generally similar between specimens except in dyke 70(22) where there is 20,06% compared to between 7% and 15% for the rest. Unfortunately, because of the fine grained and altered nature of the rock no particularly abundant aluminium-rich mineral was observed in thin section. Dyke 27(20) has an unusually high (17,88%) MgO content which is reflected in thin section by a high percentage of pyroxene but all other specimens have average, similar amounts of MgO (generally 5% to 8%). Finally, CaO is unusually low in three specimens, numbers 70(22), 114A(23) and 109(24). In specimens 114A and 109 this has caused complications in the norm calculations, which are discussed in Appendix 1.

It is not intended to discuss the norms in detail as they closely reflect the abnormalities in the chemistry as discussed above but rather the silicate analyses are used in conjunction with the norms for classification of the analyses into groups and rock types.

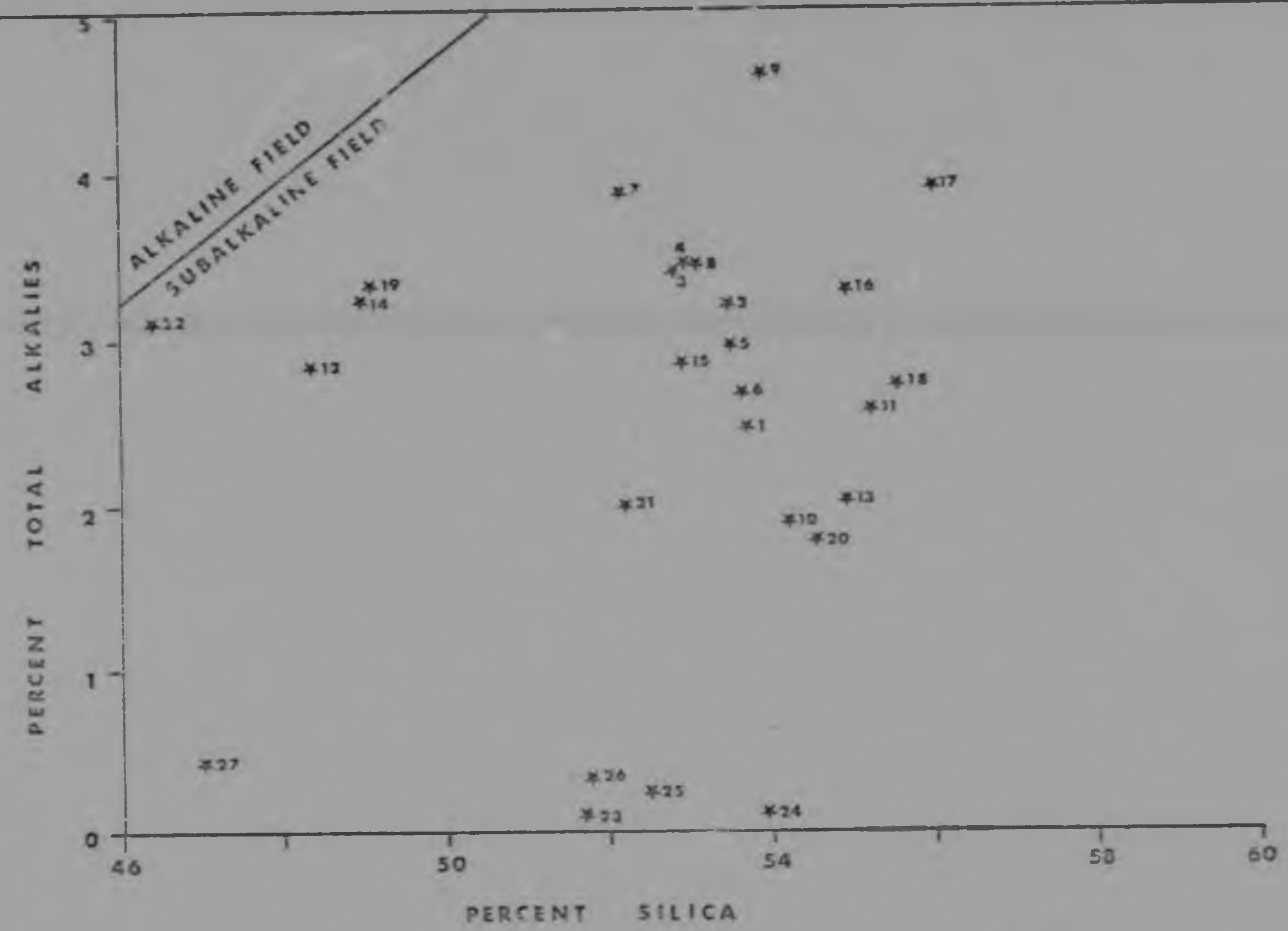

FIGURE 2-3 : ALKALIES-SILICA DIAGRAM (after Irvine and Baragar, 1971, Fig. 3)

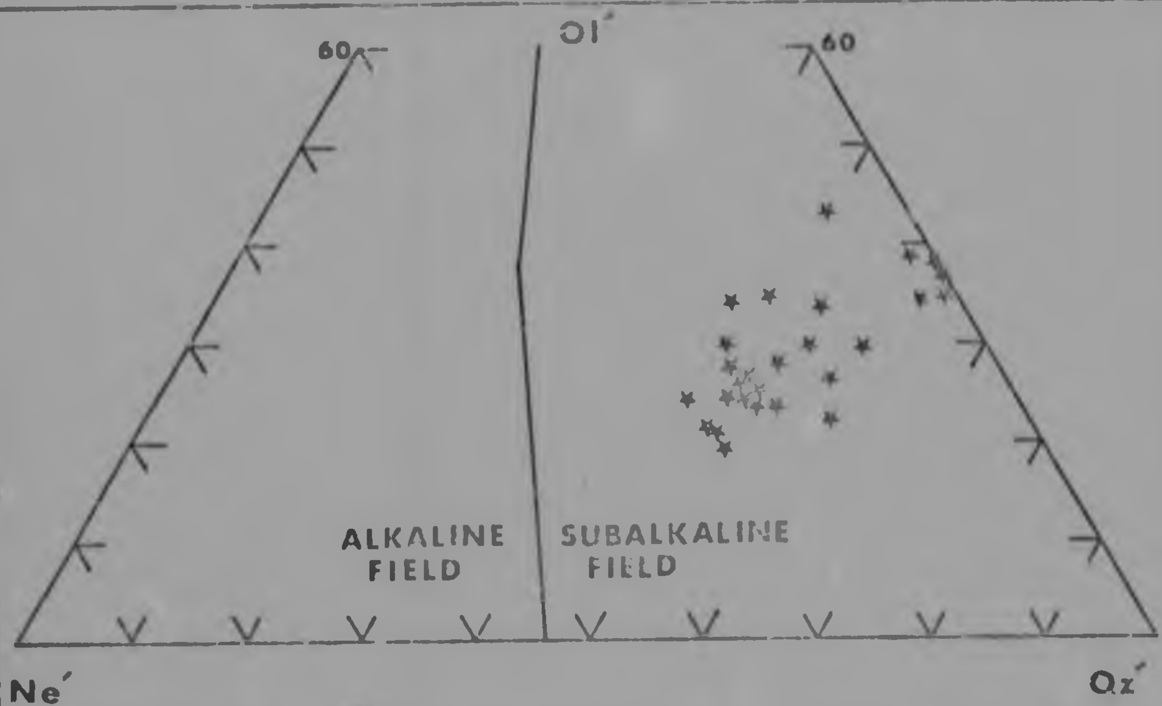

FIGURE 2-4 Ol'-Ne'-Qz' PROJECTION (after Irvine and Baragar, 1971, Fig. 4).

Ol' = OLIVINE + 0.75 . ORTHOPYROXENE

Ne' = NEPHELINE + 0.6 . ALBITE

Qz' = QUARTZ + 0.4 . ALBITE + 0.25 . ORTHOPYROXENE

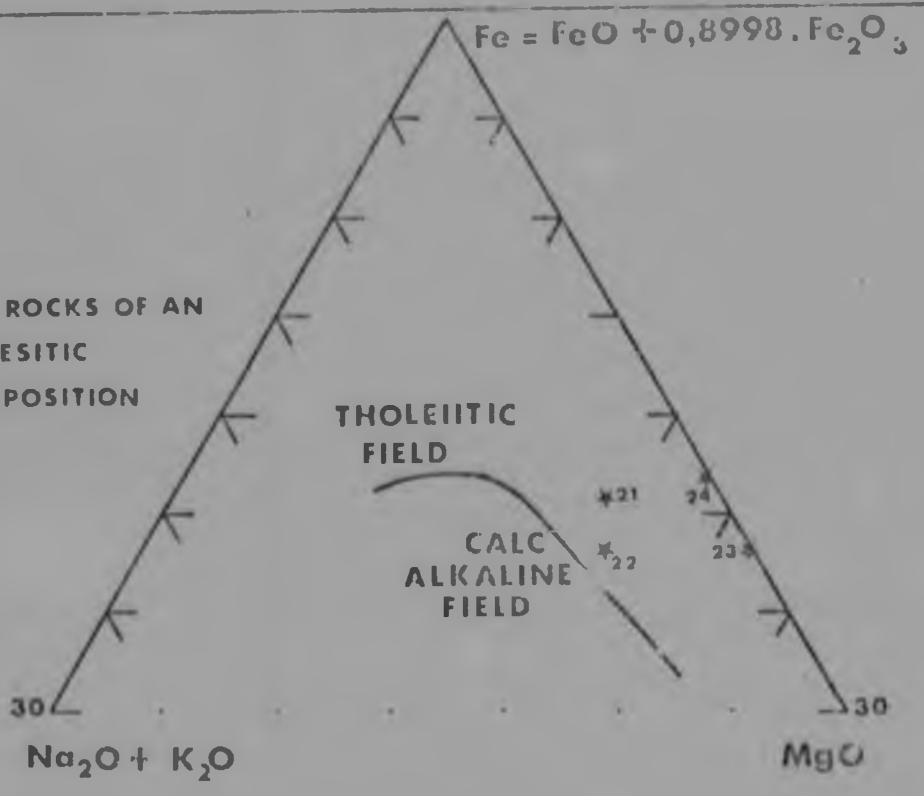

FIGURE 2-5 IRON-ALKALIES-MAGNESIA DIAGRAM (after Irvine and Baragar, 1971, Fig. 2)

2.3.2. Geochemical classification of the E.R.P.M. intrusives

The method of interpretation has closely followed Irvine and Baragar's (1971) chemical classification of common volcanic rocks, but before the results are compared and classified it is important to consider the degree of alteration of the rocks. The presence of various degrees of alteration in the samples was clearly established by thin section examination; dykes 114A (23), 109(24) and 110(26) can be considered as being affected by severe alteration and dykes 7(10), 121(12), 6(13), 27(15), 38(18), 159(21), 70(22), 79(25) and 117(27) as being moderately affected. In addition the geochemistry can be used as an indicator of alteration. Irvine and Baragar (1971) suggest that samples with a percentage Fe_2O_3 greater than TiO_2 plus 1,5% are altered; this applies to dykes 100(8), 149(14), 114A(23) and 110(26). Chayes (1966) suggests that specimens with Fe_2O_3/FeO ratios greater than 0,6 are altered; this only applies to dyke 149 (14). These analyses, which have been altered, may have unusual chemistry due to alteration and must be treated with some caution.

Peralkaline verus alkaline and subalkaline suites

No analyses contain normative acmite, which, according to Irvine and Baragar(1971) is a good indicator of a peralkaline rock. Hence, only alkaline and subalkaline rocks are included in the present suite.

Alkaline versus subalkaline suites

Descriminations between these two rock types can be done by using the boundary lines on an alkali-silica diagram (Figure 2.3),which is the simplest method, or on an olivine'- nepheline'-quartz'ternary diagram (Figure 2.4; see this figure for an explanation of the dashes) which is considered to be the most reliable. On both these diagrams it is clear that all members of the E.R.P.M. suite are sub-alkaline which supports the general observations in 2.3.1. above.

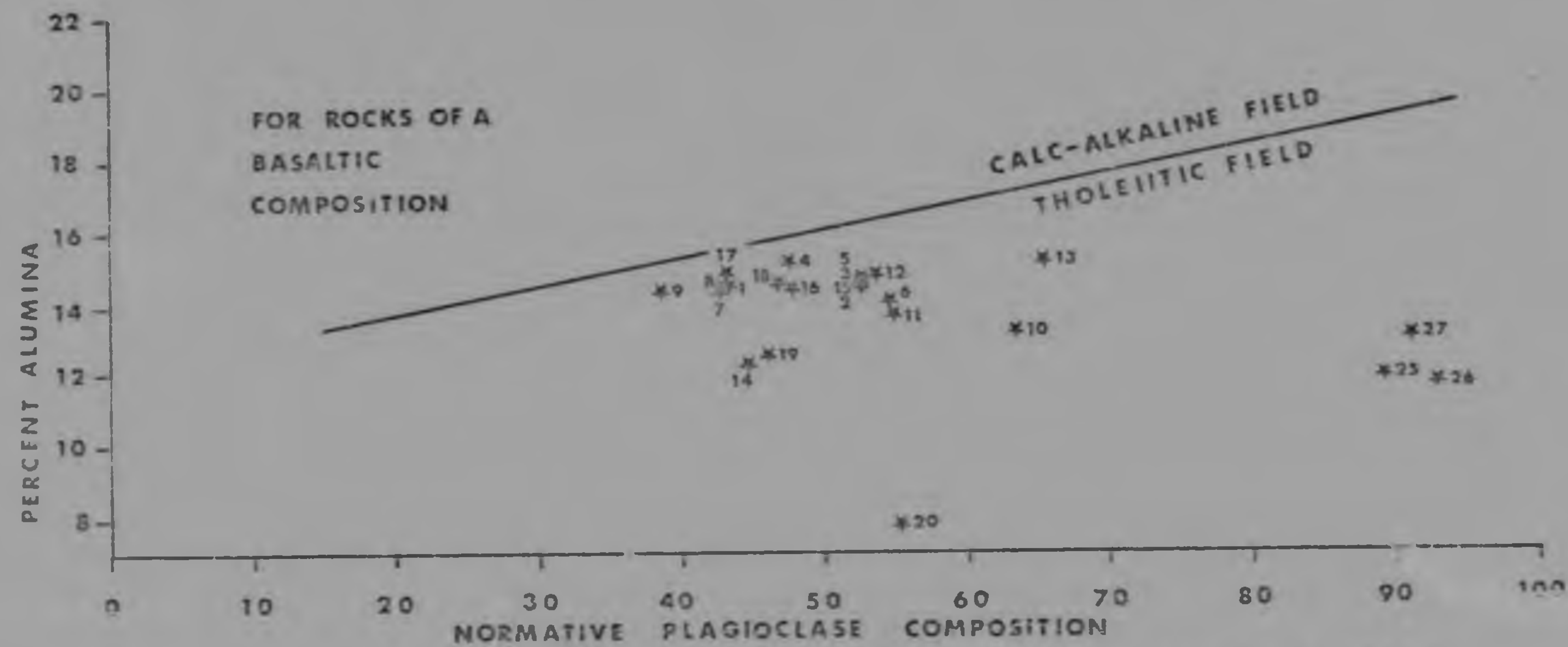

FIGURE 2-6: ALUMINA – NORMATIVE PLAGIOCLASE COMPOSITION DIAGRAM
(after Irvine and Baragar, 1971, Fig. 6)

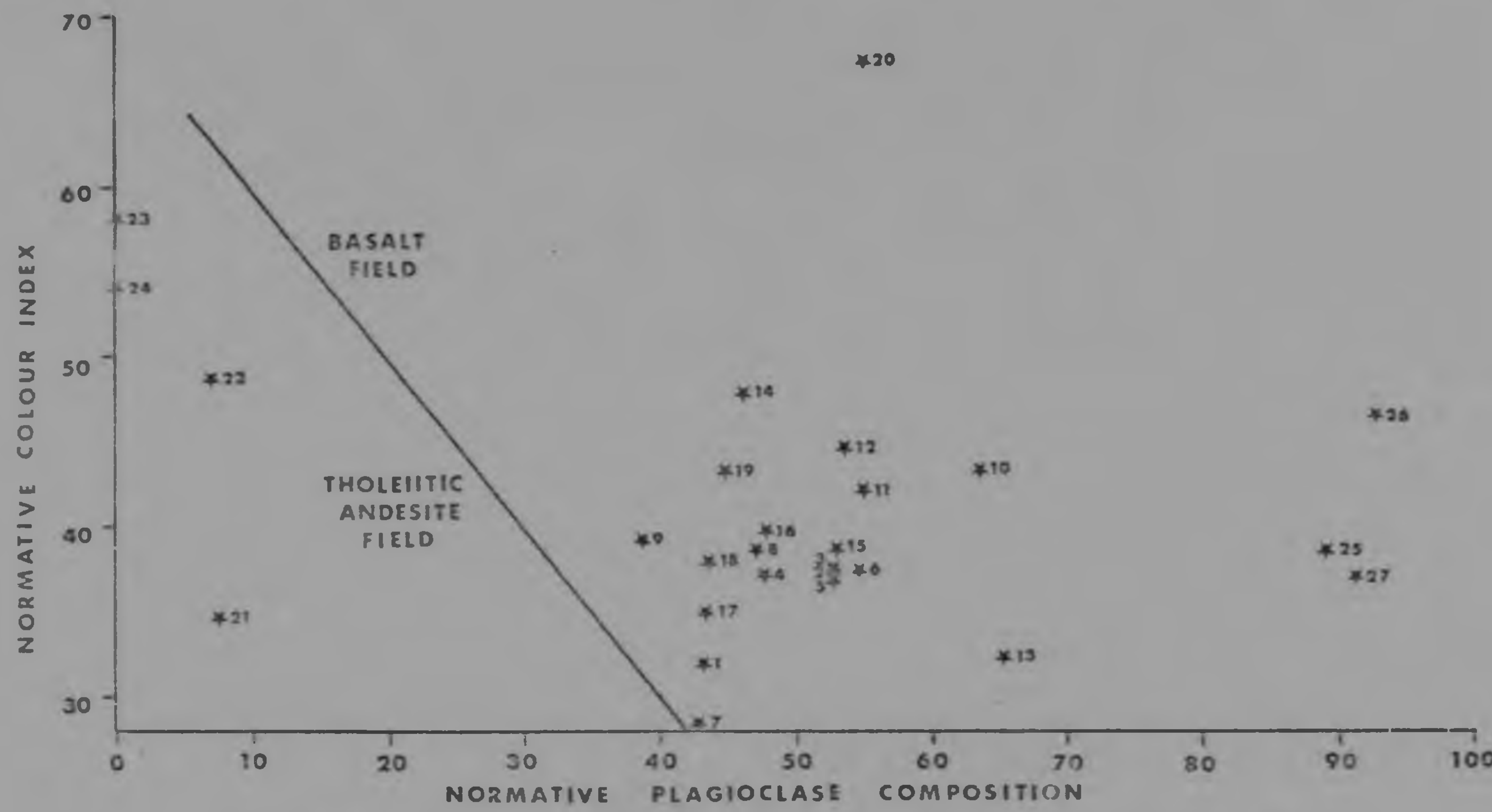

FIGURE 2-7 : NORMATIVE COLOUR INDEX – PLAGIOCLASE COMPOSITION DIAGRAM
(after Irvine and Baragar, 1971, Fig. 7)

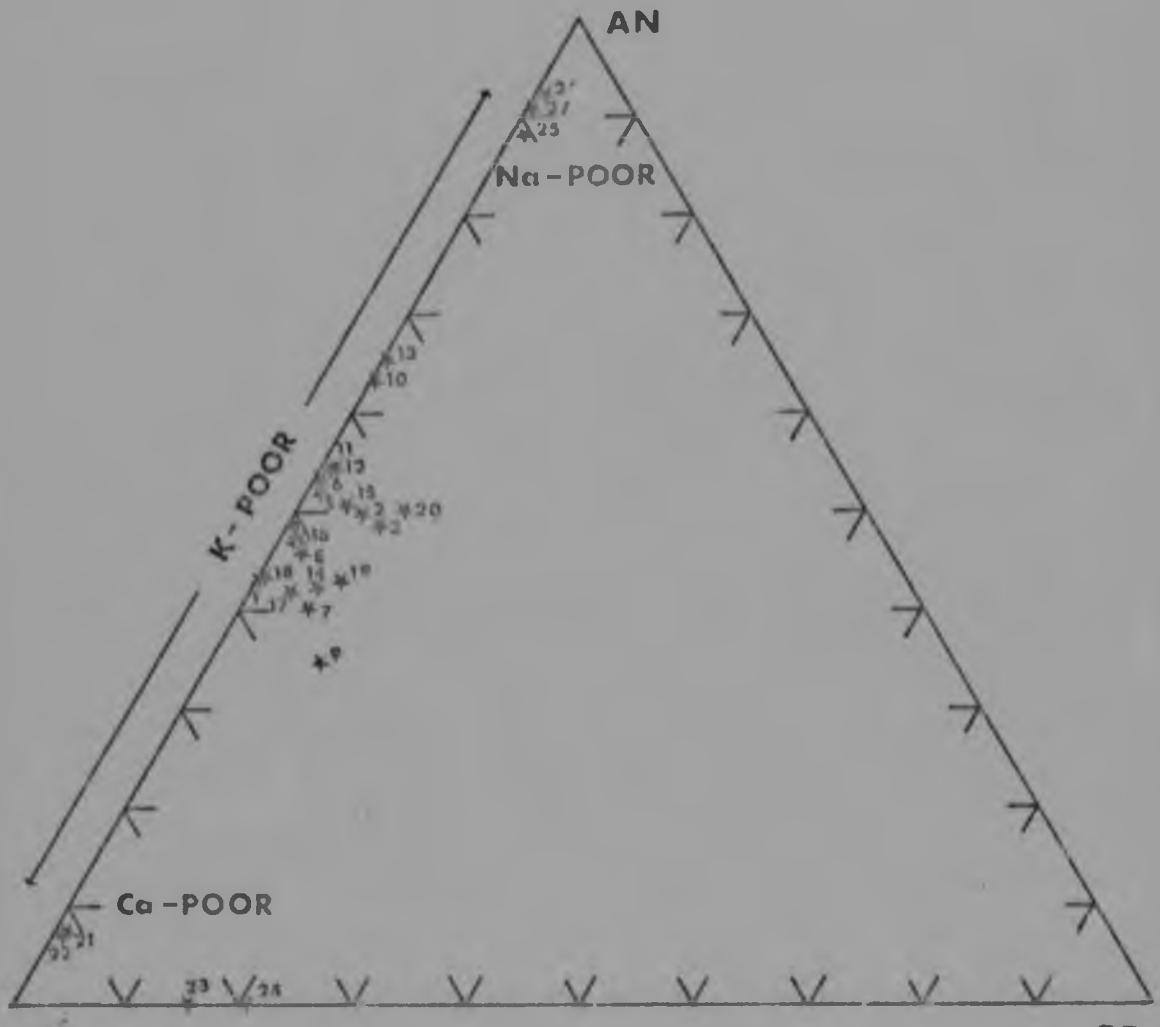

FIGURE 2-8 : ANORTHITE - ALBITE' - ORTHOCLASE PROJECTION (after Irvine and Baragar, 1971, Fig.8)

AB' = . .BITE + 1,67 . NEPHELENE

Calc-alkaline versus tholeiitic suites

Two plots are best used for discrimination between these two rock types; an iron-alkali-magnesia ternary diagram(Figure 2.5) is best for rocks of an andesitic composition and an alumina-normative plagioclase composition diagram is best for rocks of a basaltic composition(Figure 2.6) according to Irvine and Baragar (1971). Rocks with basaltic and andesitic composition can be distinguished on a normative colour index-normative plagioclase composition diagram (Figure 2.7). This plot shows that only four dykes, numbers 159(21), 70(22), 114A(23) and 109(24) to be andesitic and the rest basaltic. Similarly, Figures 2.5 and 2.6 show that all the E.R.P.M. specimens are tholeiitic.

Ca-,K-, or Na- rich or poor

To determine if the analyses are calcium-,sodium- or potassium-rich or poor an anorthite-albite-orthoclase ternary diagram (Figure 2.8) is used in conjunction with the analyses listed in Appendix 1. As was noted in section 2.3.1. all specimens are alkali poor whilst some are particularly poor in calcium. However, Figure 2.8. shows all specimens to be potassium-poor whilst numbers 79(25), 110(26) and 117(27) are distinctly sodium-poor and numbers 159(21), 70(22), 114A(23) and 109(24) are distinctly calcium poor. This figure also shows that there is very little alkali-feldspar in the E.R.P.M. suite and that the plagioclase compositions range from almost pure albite to pure anorthoclase with most compositions in the vicinity of An_{50}.

An important point made by Irvine and Baragar (1971) is that after the analyses have been classified according to the above method they should be compared with typical average analyses to rock types (see, for example, appendix II in Irvine and Baragar, 1971; Nockolds, 1954; Wedepohl, 1969) to avoid erronious classification due to alteration or an exceptional composition. Typical analyses for tholeiites, tholeiitic basalts, andesites and tholeiitic andesites are listed in Appendix Table 1E, analyses 31-34 respectively; comparison between the present analyses and this data is discussed below after a summary of the geochemical classification described above.

SUMMARY

1. No peralkaline rocks were analysed.

2. All rocks analysed are subalkaline. Figures 2.3 and 2.4.

3. All rocks analysed are tholeiitic (Figures 2.5 and 2.6). No calc-alkaline rocks are present.

4. Four dykes have an andesitic composition (Figure 2.7). These are dykes 159(21), 70(22), 114A(23) and 109(24). All other dykes are basaltic.

5. a. All rocks analysed are potassium poor. (Figure 2.8)

   b. Dykes 79(25), 110(26) and 117(27) are distinctly alkali poor. (Figure 2.8).

   c. Dykes 159(21), 70(22), 114A(23) and 109(24) are distinctly calcium poor (Figure 2.8).

2.3.3. Geochemical features of the dyke groups

In addition to the above general observations and classification it is found that the groups of dykes which were classified by petrology and orientation also have some distinctive geochemical characteristics.

Group 1: dyke 26 (Analysis 20) Appendix Table 1D

The chemistry of the dyke is exceptional in that it does not fit into the classification system outlined above. It is characterised by a high magnesium (17,88%) and a low aluminium content (7,77%) compared to the rest of the E.R.P.M. suite. This is reflected in the petrology by abundant pyroxenes and in the norms, by over 50% orthopyroxene (En_{76}) and a high colour index(67). The chemistry is very similar to that of a melanorite described by Van Zyl (1970) from the Bushveld Igneous Complex (Appendix Table 1E, Analysis 35). This similarity in composition is further support that dyke 26 is of Bushveld age.

Group 2: dykes 149(14) and 82(19)

Both of these dykes can be classified as K-poor, tholeiitic basalts and a comparison with an average tholeiitic basalt composition (Appendix Table 1E, No 32) supports this. The chemistry is characterised by a high TiO_2 content (2,59% and 2,69%) as discussed in 2.2.2. and 2.3.1. above. Compared to the rest of the E.R.P.M. suite they have a low silica content (48,97% and 49,10%).

Group 3: dykes 182(4), 58(7), 100(8), 144(9), 32(16) and 33(17)

All these dykes can be classified as K-poor, tholeiites and analyses compare well with an average tholeiite composition (Appendix Table 1E, Analysis 31). Their chemistry is generally similar to that of group 4 except that all the specimens have higher alkali concentrations than the other groups.

Group 4: dykes 77(10), 121(12), 16(13), 27(15), 38(18), 70(22), 79(25) and 117(27)

Petrologically, all the dykes of this group are similar but distinct geochemical differences are present possibly due to varying degrees of alteration. From Irvine and Baragar's classification, dykes 77(10), 121(12), 16(13), 27(15) and 38(18) are K-poor tholeiites.

However, dyke 77 differs from the rest in its relatively high normative plagioclase composition (An 64); dyke 121 in its relatively low silica content (48,26%); dyke 16 in its lower than average total alkalies (2,03%) and relatively higher normative plagioclase composition (An 66); and dyke 159 is low in total alkalies (1,99%) and has a very low normative plagioclase composition (An 7)

Dyke 70 can be classified as a calc-alkali-poor tholeiitic andesite with a very similar chemistry to a high - Al basalt. The dyke has a high aluminium content (20,06%), a low normative plagioclase composition (An 7) and a low silica content (46,4%).

Dyke 79 and 117 are classified as alkali-poor tholeiitic andesites but have a sim lar chemistry to alkali-poor tholeiites. Both analyses are characterised by very low total alkalies (0,42% and 0,23%) and unusually high normative plagioclase compositions (An 89 and An 91) but dyke 117 has a low silica content (47,04%).

In Appendix Table 1E, Analysis 30, the geochemistry of a Ventersdorp lava from Klipriviersberg is listed; unfortunately the analysis is not complete and the specimen was quite altered or weathered as indicated by the high percentage of Fe_2O_3. However, it does show similariti s to some analyses of group 4, and more specifically, to dyke 16(13); for example, the similar SiO_2 percentages the high Al_2O_3 percentages and the low total alkalies. This association may support a Ventersdorp age for the dykes of group 4.

Group 5: dykes 114A(23), 109(24), 110(26) and 159(21)

These analyses are of material collected from the E-W trending shear zones. They were carried out in order to compare their geochemistry with those of typical quartzites (Appendix Table 1E, numbers 28 and 29) and the dykes.

The maximum SiO_2 that any of these shear zones has is 53,95% which is distinctly lower than SiO_2 ncentrations for the quartzites (85% and 95%) and is very similar to the average SiO_2 concentrations in the dykes (52%). This suggests that these shear zones are probably severely sheared and altered dykes.

It is probably not meaningful to classify these sheared dykes according to their geochemistry because of the high degree of alteration but they do have a distinct geochemistry. Firstly, apart from dyke 159 (21), their total alkalies are extremely low (0,1 - 0,32%); dyke 159 has 1,99%, and secondly, dykes 114A and 109 have almost no calcium (0,11% and 0,07%). This deficiency in alkalies and calcium is possibly due to a loss of the elements during alteration. The problems in determining normative minerals with such a low CaO is discussed in Appendix 1, but it is noteworthy that the normative plagioclase composition is An_0 and there are no normative pyroxenes. By contrast dyke 110 has a very high normative plagioclase composition (An_{93}) because of the very low sodium content.

Group 6: dyke 11(11)

The geochemistry of this dyke is almost identical to that for group 3. Also it was noted that petrological similarities are also present suggesting that this dyke may well be included in group 3. The significance of the similar compositions and the orthogonal attitudes between dyke 11 and group 3 dykes will be discussed in section 2.4 below in terms of intrusion mechanisms.

2.3.4. Geochemical and petrological variations across dyke 182

Six specimens, selected at regular intervals through the dyke (see Appendix 1-A for locations) were examined in hand specimen and thin section and were geochemically analysed(Analysis numbers 1-6) to determine trends that could be compared to rock mechanic trends.

Thin section petrology reveals little difference across dyke 182 except for a distinct grain size variation. The margins are chilled and fine grained and grade towards a coarser centre which has numerous feldspar phenocrysts.

There is a distinct geochemical trend in Figure 2.3 which shows that towards the centre of the dyke, alkalies increase as silica decreases, illustrating a small but significant geochemical variation about the centre of the dyke.

Secondly, the orthogonal attitudes may be a result of similar intermediate and minimum stress magnitudes. If in this situation a suite of intrusives intrudes into the plane defined by σ_1 and σ_2 a significant volume increase by lengthening the crust will take place in the direction of σ_3. In the E.R.P.M. this increase in length is estimated to be up to 100 m/km or 10% for the 030° striking dykes. As the total thickness of the intrusives grows, the magnitude of σ_3 (in compression) increases, possibly until it is larger than σ_2. When this happens further intrusives or branches from the intrusives should form normal to the original intrusives. One would expect intrusives in the intermediate orientations also but the bulk of the intrusives would probably lie in the two dominant directions.

2.4.2. En echelon dykes, horns, steps and rafting

All these features are found at various localities within the mine and are defined by sketches in Figure 2.10.

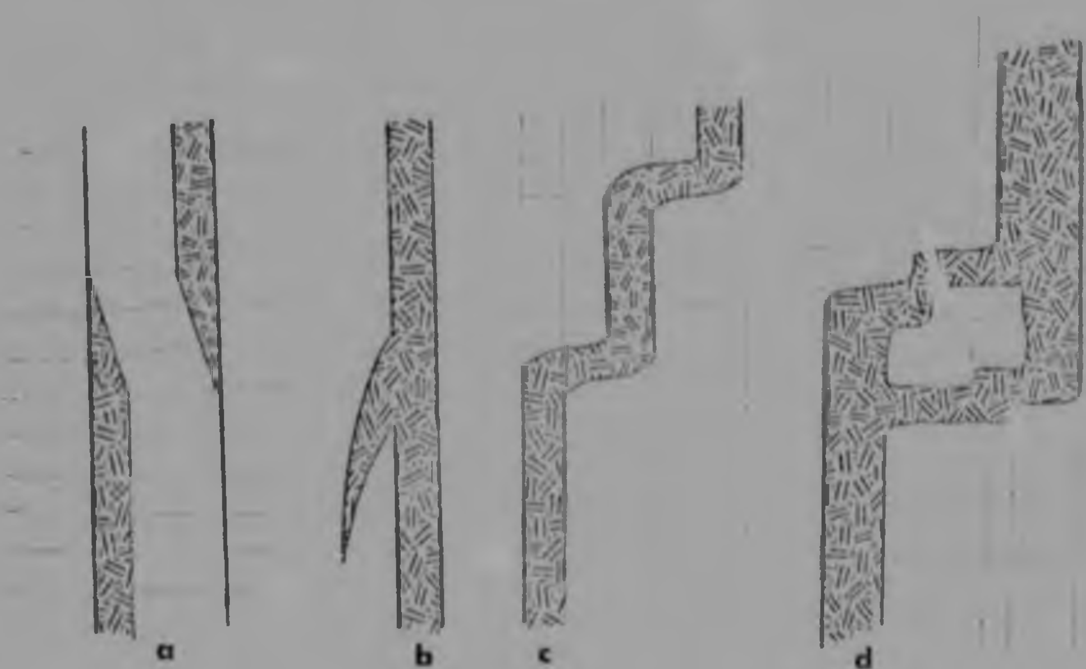

Figure 2.10. Idealised en echelon dyke (a), horn (b), step (c) and raft (d) (after Roberts and Sanderson, 1971).

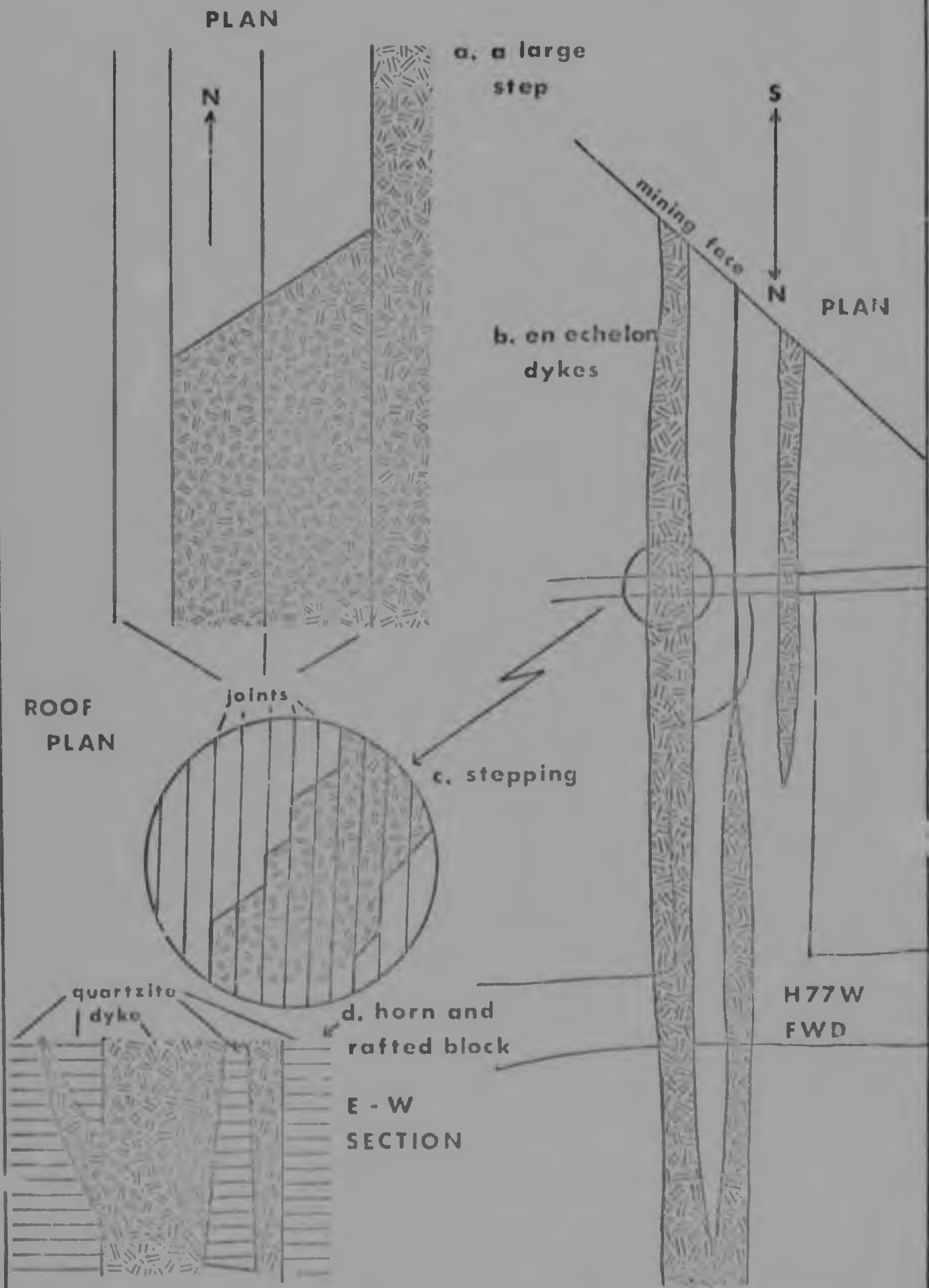

FIGURE 2.11 EXAMPLES OF STEPS, HORNS, RAFTING AND EN ECHELON DYKES IN THE E.R.P.M.

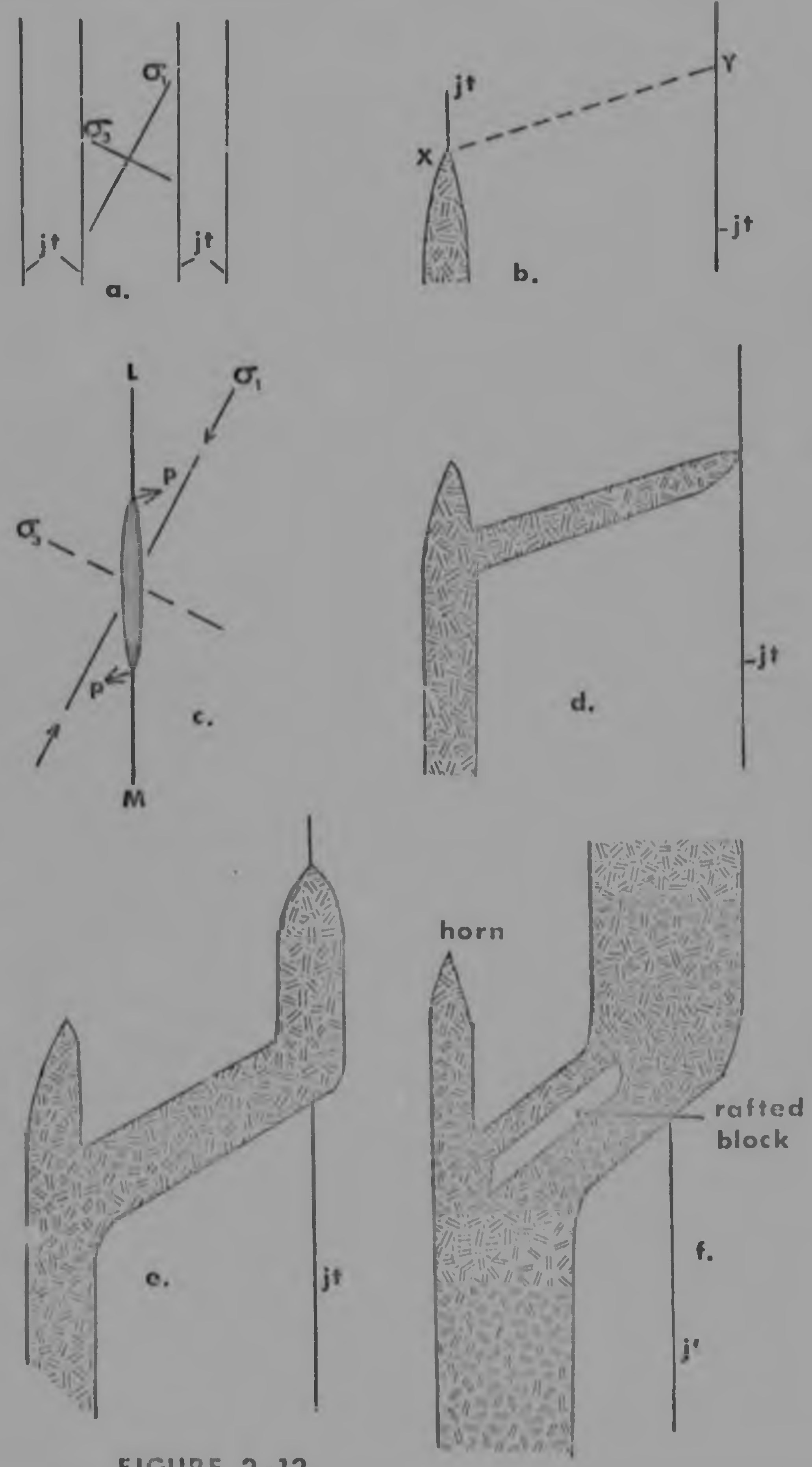

σ_1
σ_3
jt
jt
a.
jt
Y
X
-jt
b.
L
σ_1
P
σ_3
P
c.
M
-jt
d.
e.
jt
horn
rafted
block
f.
j'

FIGURE 2-12

FIGURE 2.12

Suggested method for the formation of steps, horns and rafting during dyke intrusion

a. The present stress field is inclined to an existing set of joints.

b. The intrusion path of the dyke follows a joint, which is the path requiring the least energy. However, the joint terminates and the intruding dyke must make a new crack which will lie in the direction X-Y (see c).

c. An open crack in compression showing the directions(P) in which a crack will propagate (initially) under the stress field shown (after Jaeger and Cook, 1969, p. 326, Figure 12.5).

d. Intrusion proceeds along the direction defined in (c) until a new joint is encountered and the dyke again follows the path requiring the least energy (e).

e. The final state showing a horn, where the dyke overshoots the interrupting plane X-Y for a short distance; rafting, where a block of joint bounded quartzite has been surrounded by intruding magma and a step.

En echelon dykes and step features were observed in dyke 117, a member of group 4 dykes, which appears to have intruded into previously jointed rock. Figure 2.11a is a plan view of H75 station crosscut illustrating a contact between the dyke and quartzites which closely follows a joint plane in one particular area and then cuts across at an angle of about 60° to the joints for a short distance before following another joint plane. Similarly, in H77W reef gully (Figure 2.11b), a stepped contact can be observed (Figure 2.11c) and on a larger scale, the dyke at this locality bifurcates and shows an en echelon style of intrusion (Figure 2.11b). In addition, it is noteworthy that the orientations of the joint planes in the country rock are not parallel to overall direction of t dyke.

Horns and rafting of quartzite were observed in dyke 149, a member of group 2 dykes, on L70E level (Figure 2.11d). The contacts of this dyke are extremely sharp, as if following a pre-existing fra ture, and the shape of the rafted block of quartzite is elongate and angular suggesting fracture along joint planes.

These features and their relationship to fracturing suggest that the dykes intruded into previously jointed country rock (Roberts and Sanderson, 1971; Currie and Ferguson, 1970) and that the overall direction of the intrusion was not parallel to the joint planes; in other words, the stress systems associated with the formation of the pre-existing joints and the intruding dykes did not coincide. In Figure 2.12 a mechanism of intrusion which could account for these features is presented. At the time of intrusion a pre-existing joint set is inclined to the present direction of the principal stresses(Figure 2.12a). An intrusion would preferentially lie normal to the minimum principal stress but propagation along the pre-existing fractures requires less energy than opening a new crack and so the intrusion follows a joint as in Figure 2.12b. If at some stage during the intrusion the joint terminates or the stress system alters so that the present intrusion direction is no longer possible, and if the magma pressure is sufficient to form a new crack then the direction of propagation of a new crack will tend to lie towards the direction of maximum principal stress (X-Y in Figure 2.12b). This is explained in some detail by Jaeger and Cook (1969, p. 326, Figure 12.5). Intrusion proceeds along this new crack until a new joint plane is encountered where the dyke again propagates in the dominant direction (Figure 2.12e). The overall direction of the intrusion lies normal to the minimum principal stress.

A horn may be formed, as in Figure 2.12f where the dyke overshoots the interrupting plane X-Y for a short distance. Rafting is illustrated in (f); a block of joint bounded quartzite is surrounded by intruding magma. En echelon dykes would be formed if the connecting zone X-Y between two parallel but offset dykes were closed after the intrusion without enclosing any magma; that is, the zone X-Y is only used as a feeder.

2.4.3. Bifurcation of the dykes

A common feature of the dykes on the E.R.P.M. is their splitting or bifurcation and rejoining at a later stage. The cause of such bifurcation is probably pre-existing fractures or intrusion through layers of varying mechanical properties. For example, Pollard (1973) has described experiments which show that the direction of propagation of a dyke will vary as the dyke passes through layers with different Young's Moduli. However, it is usual for the dykes to bifurcate upwards initially but in the E.R.P.M. it is common for two members of swarm to coalesce, giving the impression of a downwards bifurcation. For example dyke 117 changes from three dykes below 77 level to one dyke above; dykes 32 and 33 cross and then rejoin in F section and dykes 56 and 58 join in G section. The fact that many of the dykes are seen to combine at the reef plane may be connected with the transition from footwall to hangingwall quartzites which have significantly different strengths and Young's Moduli. In addition Pollard (1973) notes that contemporaneous sheet intrusions that are close to one another relative to their length will interfere and change propagation direction and that two parallel intrusions that are offset from one another have a tendency to curve towards one another. These observations could also apply to the intrusives described here.

2.5 SUMMARY OF THE GEOLOGICAL FEATURES OF THE INTRUSIVES

Group 1 : The Simmer Dyke - possibly Bushveld age.
Melanorite, characterised by abundant pyroxenes and a high magnesium and low aluminium content. In hand specimen it is mafic, fresh and breaks with a conchoidal fracture. The dyke is up to 200 metres thick and has a very irregular geometry.

Group 2 : Ilmenite dolerites - possibly Bushveld age.
These dykes make up a swarm striking about 140^{o} and dipping vertically. They are generally five to eight metres thick and have sharp contacts and chilled margins with the quartzites. In thin section they are characterised by skeletal ilmenite which is reflected in the chemistry by a high TiO_2 content. Chemistry also indicates that they are tholeiitic in composition.

Group 3 : Quartz dolerites - possibly late Ventersdorp age.
These dykes are large, varying in thickness from 16 to 41 metres; they strike at 030^{o} and dip vertically. They have a medium grain size, are relatively fresh and are often characterised by large feldspar phenocrysts. Their chemistry shows the group to be tholeiitic.

Group 4 : Quartz dolerites - possibly Ventersdorp age.
Similar in orientation and composition to group 3 but are finer grained, do not have large phenocrysts, are more severely altered and are generally thinner, with widths of about one to 20 metres. Their chemistry shows the group to be tholeiitic.

Group 5 : Ultramylonites - possibly early Ventersdorp age.
This group includes all the east-west striking shear zones. They vary in dip, strike and thickness but the geochemical analyses shows that they are all severely altered sheared dykes of possibly tholeiitic composition. Characteristic features include black ultramylonite fill with a well developed foliation.

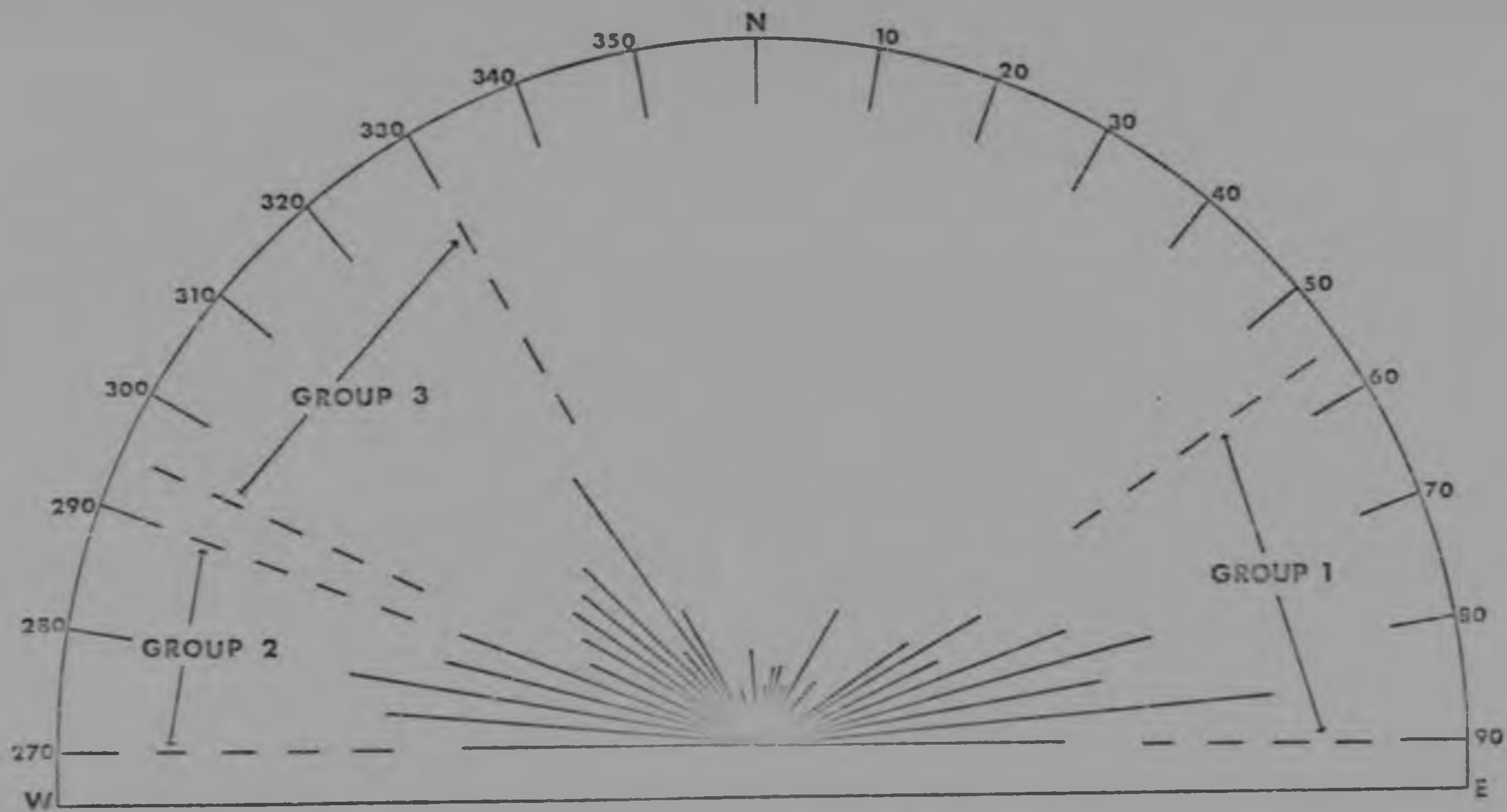

FIGURE 3-1 STR[illegible] [illegible]QUENCY DIAGRAM FOR FAULTS

RADIUS = 10.7[illegible] [illegible]INTS IS 348 , BROKEN LINES REPRESENT GROUP BOUND[illegible]ES

CHAPTER 3

FAULTING AND JOINTING

A. FAULTING

3.1 INTRODUCTION AND DISTRIBUTION OF FAULTS

The faults in the E.R.P.M. are numerous and vary in nature from normal to reverse, strike-slip to dip-slip and translational to rotational, with movement ranging from less than one centimetre to 400 metres or more (Map 2). Many are associated with dyke intrusions and most contain gouge material of varying thickness. Of the 234 macroscopic structural discontinuities considered in this dissertation, some 33% are faults and at least 10% are dykes along which some displacement has occurred.

In general, the geometry of the faults is poorly known because strikes and dips are not normally recorded during mining; nevertheless, many dip directions and angles of dip have been calculated from shaft-section plans and senses of movement ascertained from dislocated planar features and irregularities in mining configuration on mine plans.

Faulting trends were determined by the method described in Chapter 2; these are illustrated in a strike-frequency diagram (Figure 3-1) and the areas of high frequency, means and standard deviation are listed in Table 3.1.

TABLE 3.1

SUMMARY OF STRIKE ANALYSIS DATA FOR FAULTS

NO.	GROUP BOUNDARIES	MEAN STRIKE	STANDARD DEVIATION OF THE MEAN STRIKE	AVERAGE FREQUENCY WITHIN EACH GROUP (No of points and percentage)
1	055^{o}- 090^{o}	075^{o}	11.8^{o}	16.4(4.7%)
2	270^{o}- 290^{o}	280^{o}	7.1^{o}	18.4(5.3%)
3	295^{o}- 330^{o}	313^{o}	6.4^{o}	11.1(3.2%)

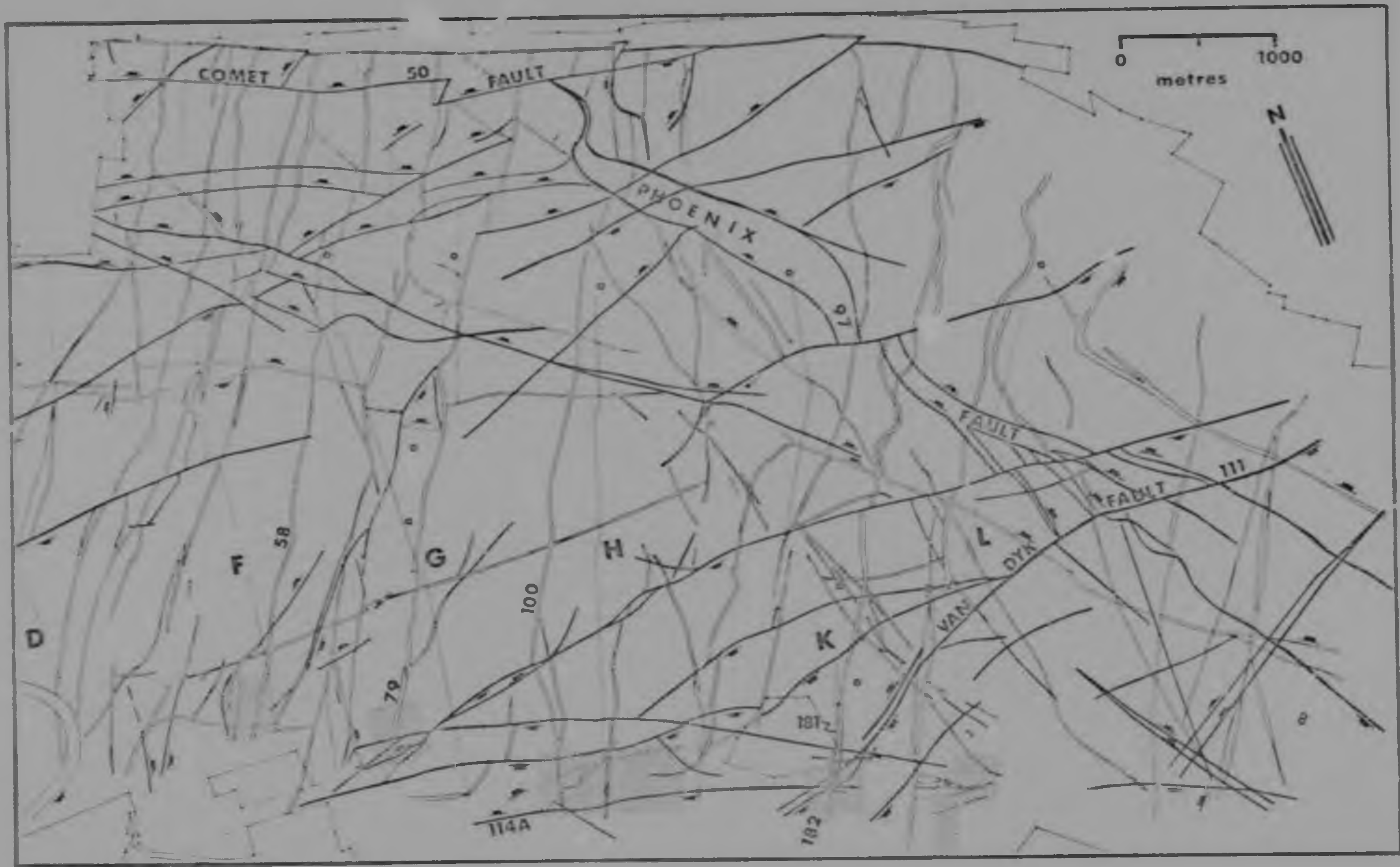

0
1000
metres
N
COMET
50
FAULT
PHOENIX
97
FAULT
111
FAULT
VAN
DYK
D
F
58
G
79
100
H
K
L
181
182
114A
8

FIGURE 3.2

Plan of a section of the E.R.P.M. showing discontinuities referred to in Chapter 3 and areas where joints were measured (stippled).

Vertical shaft

Incline shaft

Mine boundary

Dyke

Fault showing downthrown side

Apart from the three groups listed in the table a strong 030° trend is present (see Figure 3.1) but has not been included because (1) it represents only a small proportion of the points plotted and (2) it is coincident with the strongest trend for dykes (*cf.* Table 2.1) and hence is probably due to movement on the dykes. Group number 2, with a mean strike of about 280°, is subparallel to the sediment strike in the mine and Groups 1 and 3 form a possible conjugate pair about Group 2.

3.2 FAULTING STYLES

Figure 3.2 is an annotated reduction of Map 2 and shows all the faults referred to in this chapter as well as the three groups listed in Table 3.1. Generally the dip of the faults is close to 90° with displacements less than 10 metres, but in some cases dips are as low as 40° and some faults show displacements greater than 200 metres. It is difficult to classify the faults into the categories normal and reverse because of the paucity of dip-direction data but a strong correlation between sense of movement and strike could be made. Group 1 faults, with a mean strike of about 07[illegible]°, invariably have a downthrow to the south and a dextral strike-slip displacement. Group 3 faults, with a mean strike of about 133°, invariably have a downthrow to the north and a sinistral strike-slip displacement. Finally, Group 2 faults, striking at about 100° are not as regular but the downthrow is generally to the north near the surface and south at depth, with both sinistral and dextral displacements.

3.2.1. Rotational Faulting

Many faults have a rotational component associated with their movement but rarely is the geometry sufficiently well understood for it to be described in detail. Rotational faults, in contrast to translational faults, involve a rotational movement about an axis normal

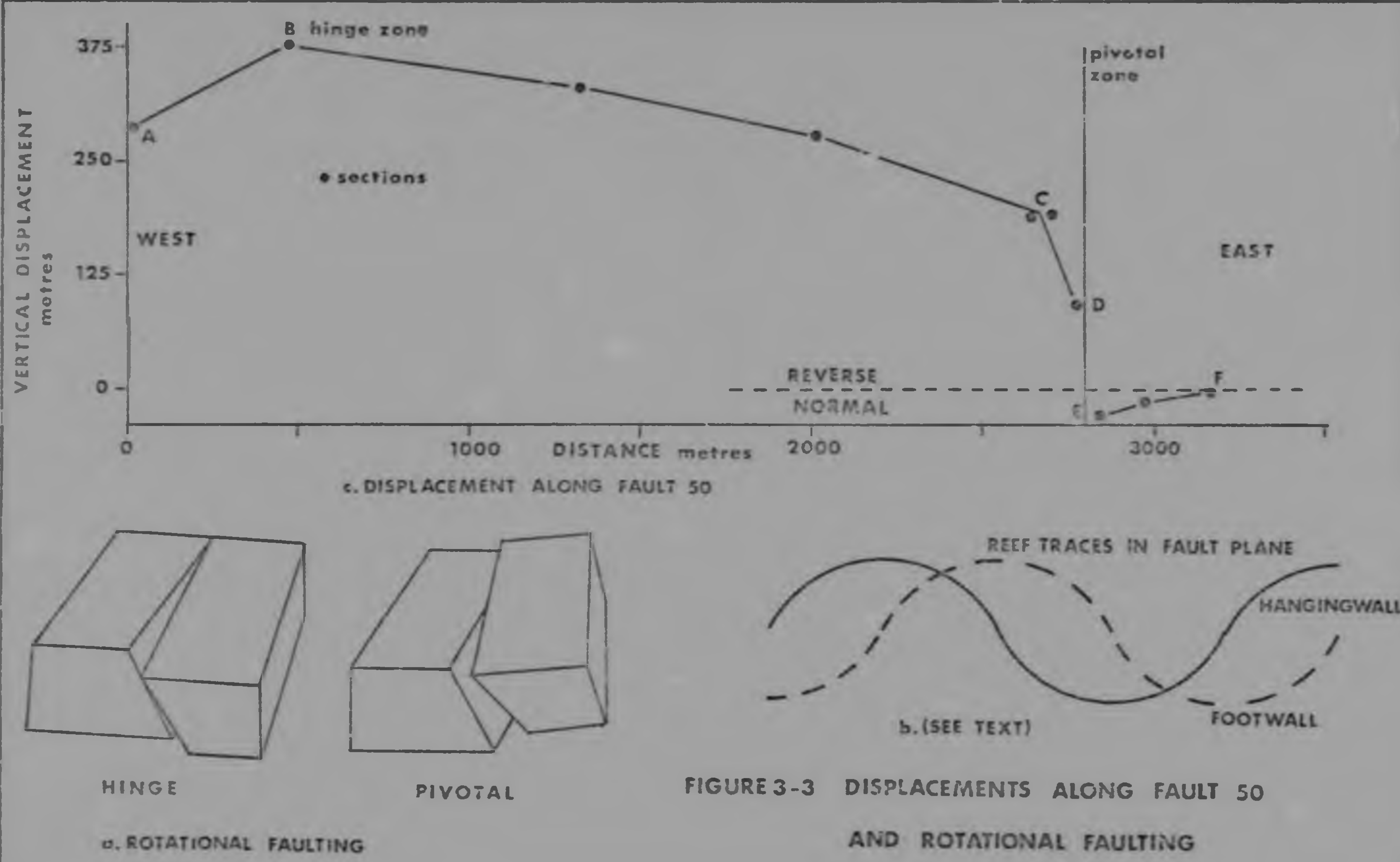

FIGURE 3-3 DISPLACEMENTS ALONG FAULT 50 AND ROTATIONAL FAULTING

to the fault plane; the two possible types, pivotal and hinge, are illustrated in Figure 3.3a. In pivotal faults the vertical displacement decreases at a regular rate to zero at the pivotal point and then increases in the opposite sense. Thus, an inclined fault will have at one end a normal and at the other end a reverse dip-slip displacement. In a hinge fault the vertical movement increases regularly away from the hinge zone on one side only. The fault may be normal or reverse but movement is in the same sense throughout its length. In addition, hinge faulting involves the flexuring of one half of the fault into an angular monocline, whereas pure pivotal faulting requires no internal deformation of the two fault blocks. Generally, the apparent strike-slip displacements due to rotational faulting are irregular because the sense of displacement depends on (1) the apparent dip of the planar body cut by the fault plane, (2) the amount of rotation and (3) the position in space of the reference plane, (e.g. plane of the reef) compared to the pivotal point.

The interpretation of rotational faulting is also further complicated by any later translational or rotational movement, which tends to move the pivotal point to a different place.

An example of the difficulties in interpreting rotational faulting is provided by Ellis (1943) describes a major strike-slip fault in the East Rand Basin. Ellis noted that the fault had previously been called a scissor (or pivotal) fault because it had been thrown down on both sides alternatively, but closer examination revealed that the vertical displacements were apparently due to a non-planar reference plane, in this case a folded conglomeratic reef, and the only displacement was strike-slip. In Figure 3.3b this is represented diagrammatically by two identical, but slightly out of phase, wave trains which represent the hangingwall and footwall intersections of the reef(reference) plane with the fault plane. It is clear that in places the hangingwall trace

TABLE 3-2

SUMMARY OF DISPLACEMENTS ALONG FAULT 50

SECTION	DISTANCE* (metres)	TYPE**	VERTICAL DISPLACEMENT (metres)	DIP(°)
DRIEFONTEIN No 2	0	R , S	294	79 S
DRIEFONTEIN No 1	450	R , S	381	81 S
ANGELO MAIN	1300	R , D	334	76 S
COMET	2000	R , D	280	80 S
-	2624	R , D	192	68 S
MUNRO	2695	R , D	196	69 S
-	2760	R , D	89	70 S
-	2826	N , D	33	72 S
-	2973	N , ?	19	65 S
CASON	3170	N , ?	8	64 S

* Distance measured along strike east from Driefontein No 2 shaft

** R = Reverse dip-slip displacement

N = Normal dip-slip displacement

S = Sinistral strike-slip displacement

D = Dextral strike-slip displacement

(solid line) is 'upthrown' compared to the footwall (broken line) but elsewhere the opposite applies.

Unfortunately such a simple explanation is not applicable to the E.R.P.M. rotational faults because their strike is often approximately parallel to bedding.

The best known example of a rotational fault on the E.R.P.M. is fault 50 which is exposed close to surface over a distance of four kilometres. This typical E.R.P.M. fault does not appear to have been given a particular name previously and is here called the Comet Fault because of its proximity to Comet Inclined Shaft (Map 1). It is a large, complex, rotational fault which strikes parallel to bedding and dips between 64^{o} and 81^{o} south. However, the sense of movement along it changes over its strike length. At its western end the dip-slip movement is reverse, the strike -slip movement is sinistral and a large dyke has intruded into the fault plane, but at the eastern end the fault is normal, dextral and has only a small companion dyke.

A detailed description of the Comet Fault has been obtained from ten vertical dip sections, spread over a strike distance of 3170 metres. The information, which is summarized in Table 3.2, suggests that the fault is rotational, because of variations in the vertical displacement along the fault, and more specifically, pivotal because of the presence of both normal and reverse dip-slip displacements. In Figure 3.3c. the change in vertical displacement along the fault, from Driefontein No 2 shaft eastwards, is plotted, illustrating the complexity of the fault. The pivotal point of the fault must lie along D-E because of the change from normal to reverse faulting but there must also be a dislocation in the pivotal zone because of the sudden decrease in vertical displacement between C and E. In addition, between points E and F, the displacement increases <u>towards</u> the pivotal zone and not <u>away</u> as would be expected in ideal pivotal faulting; this is probably due to the dislocation.

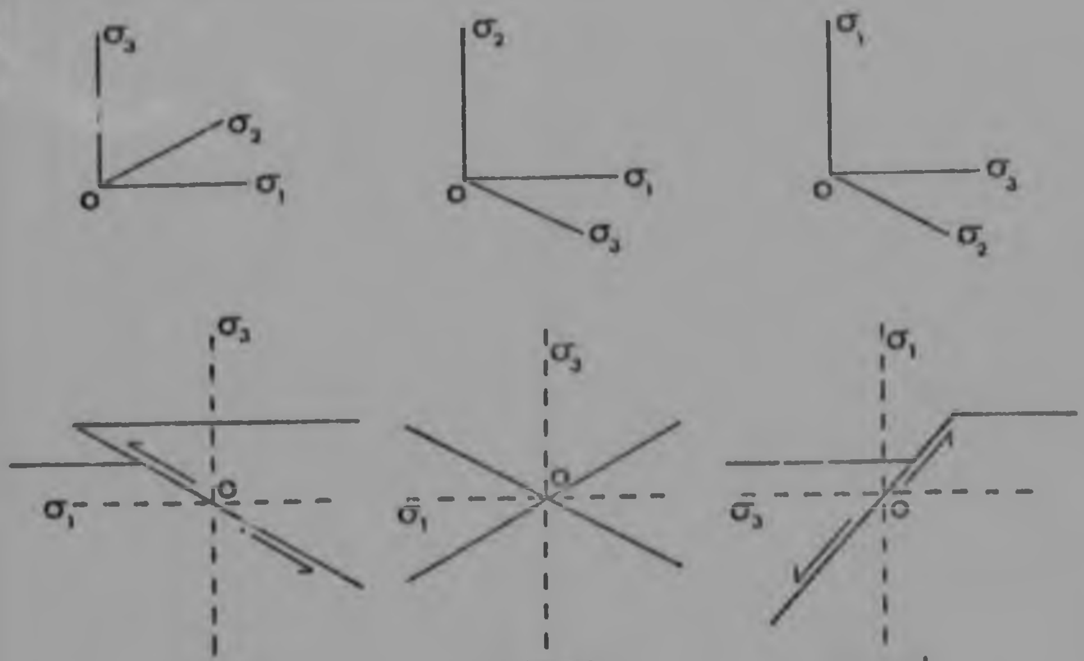

a. Faulting stress systems (after Jaeger and Cook, 1969)

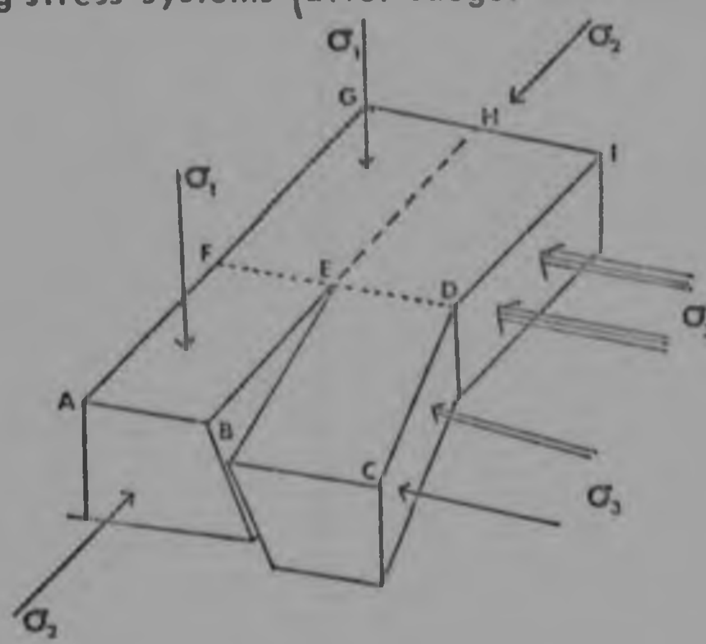

b. Formation of a rotational fault - see text

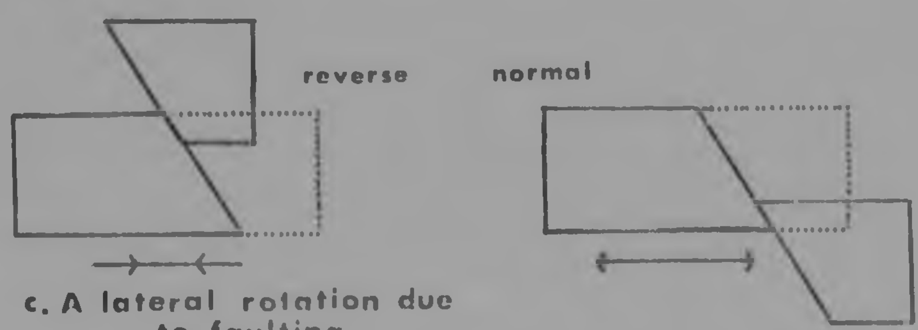

c. A lateral rotation due to faulting

FIGURE 3-4 FAULTING

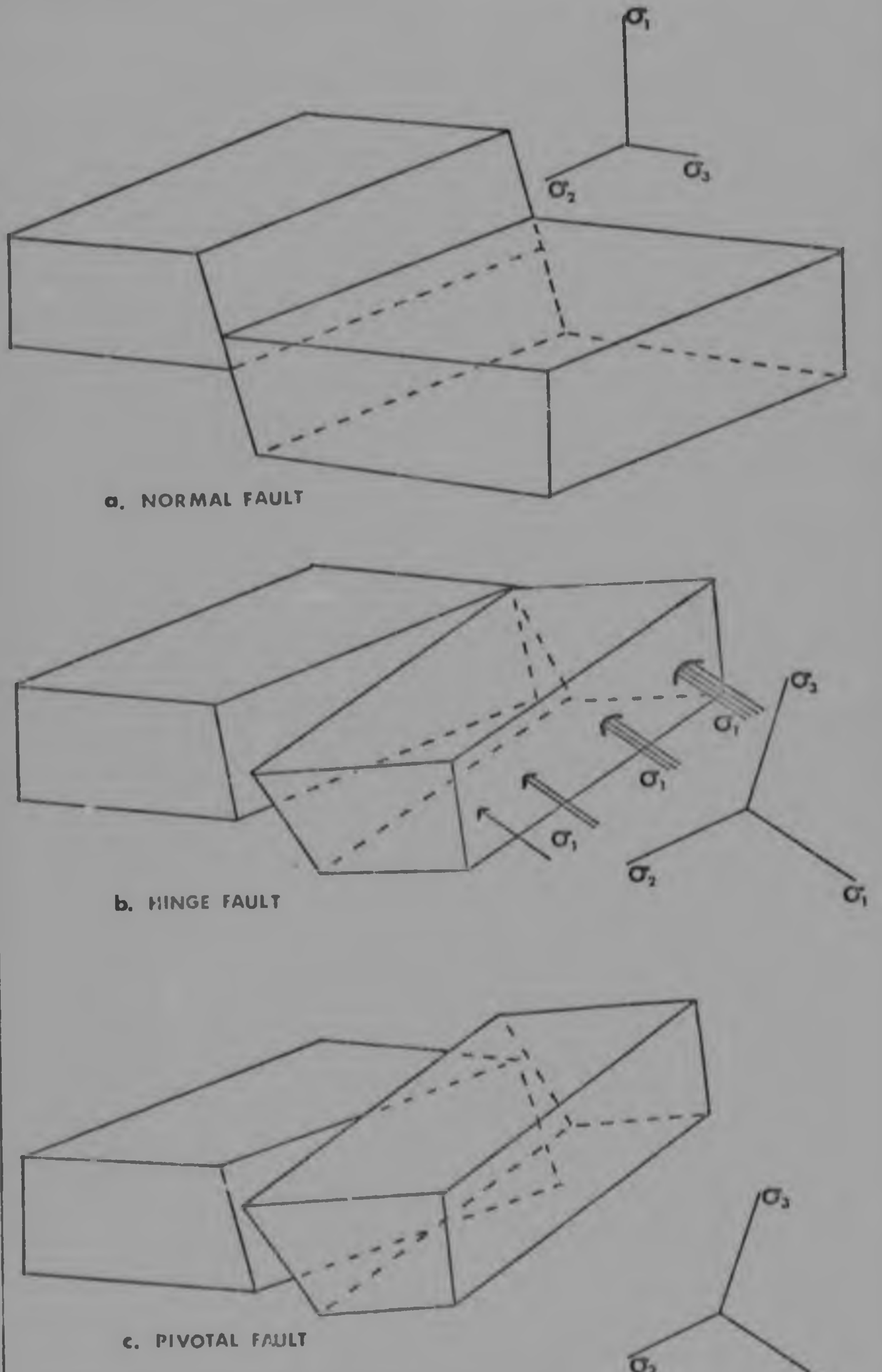

FIGURE 3-5 PROPOSED METHOD OF FORMATION OF ROTATIONAL FAULTS – see text for explanation

Finally, in Figure 3.3c, the displacement decreases towards both the east and from point B, thus there are two hinge faults about point B with opposite senses of displacement.

Figure 3.4b outlines a possible mechanism for the formation of faults with variable displacement, such as the Comet Fault, in relation to the forces operating at the time of faulting. In Figure 3.4a the stress environments outlined by Anderson (1951) for the formation of normal, reverse and strike-slip faults are illustrated. Clearly none of these will permit variable, or rotational displacement along the fault plane. However, a possible modification which would allow rotational faulting is an inhomogeneous stress system, similar to that proposed by Ramsay (1967, Figure 7-105, p. 436) for producing folds. Such a system is illustrated in Figure 3.4b where the vertical maximum principal stress (σ_1) has a constant magnitude over the length of the block but the horizontal minimum (σ_3) stress varies in magnitude. In parts of the block the stress difference (σ_1 - σ_3) is large enough to cause failure and initiate faulting in a normal sense. If cohesion is to be maintained between the faulted and unfaulted segments of the block, the resultant fault must be rotational. Stress concentrations at the point E, due to the lengthening of the faulted block compared to the unfaulted block, (Figure 3.4c) are likely to cause propagation of the fault to the point H. If this occurs the hinge point is translated to H rather than the fault pivoting about the point E.

Another perhaps more feasible method for development of pivotal faulting involves differential movement on a pre-existing fault (Figure 3.5). For example, a normal fault with a large consistent vertical displacement (Figure 3.5a) is later subjected to a different stress system in which the magnitudes of the principal stresses vary along the block, which causes the downthrown hangingwall block to ride back up the footwall block. If the block only travels part of the way back to its original position and if the amount of movement has been variable along the fault plane a hinge fault is defined (Figure 3.5b); if, in places, it rides back past its original position a pivotal fault is formed (Figure 3.5c).

Complications must arise at the end of a pivotal fault because the vertical displacement cannot increase indefinitely. The most logical way of termination is for either the pivotal fault to become a hinge fault or for a cross fault to be present. Fault terminations are discussed in more detail in Section 3.2.2.

The second mechanism seems to be the most applicable to the Comet Fault and a possible scenario for its formation follows. The fault dips southwards and strikes parallel to the basin edge, suggesting that it formed as a normal type fault during the formation of the basin. Then, it was intruded by a dyke from the west (the dyke is considerably thicker at its western end) during Ventersdorp times. Later, when the maximum principal stress was plunging southwards at less than 45^{o} to the fault plane and the stress difference varied in magnitude along the fault plane, failure occurred along the zone D-E (Figure 3.3c), resulting in the west side being moved back past its original undeformed position to form a reverse fault.

3.2.2. Fault Terminations

Faults can terminate by branching or splay faulting, transform faulting, a gradual reduction in displacement towards the fault margins (rotational faulting as described in 3.2.1 above), folding and faulting, but well-documented examples of terminations are rare.

The Phoenix Fault (No. 97) is a large oblique-slip reverse fault which strikes at an average angle of 143^{o} (Group 3 in Table 3.1), dips at approximately 56^{o} south (in K section) and has a dextral strike slip displacement. Control on the fault geometry is poor as only two sections

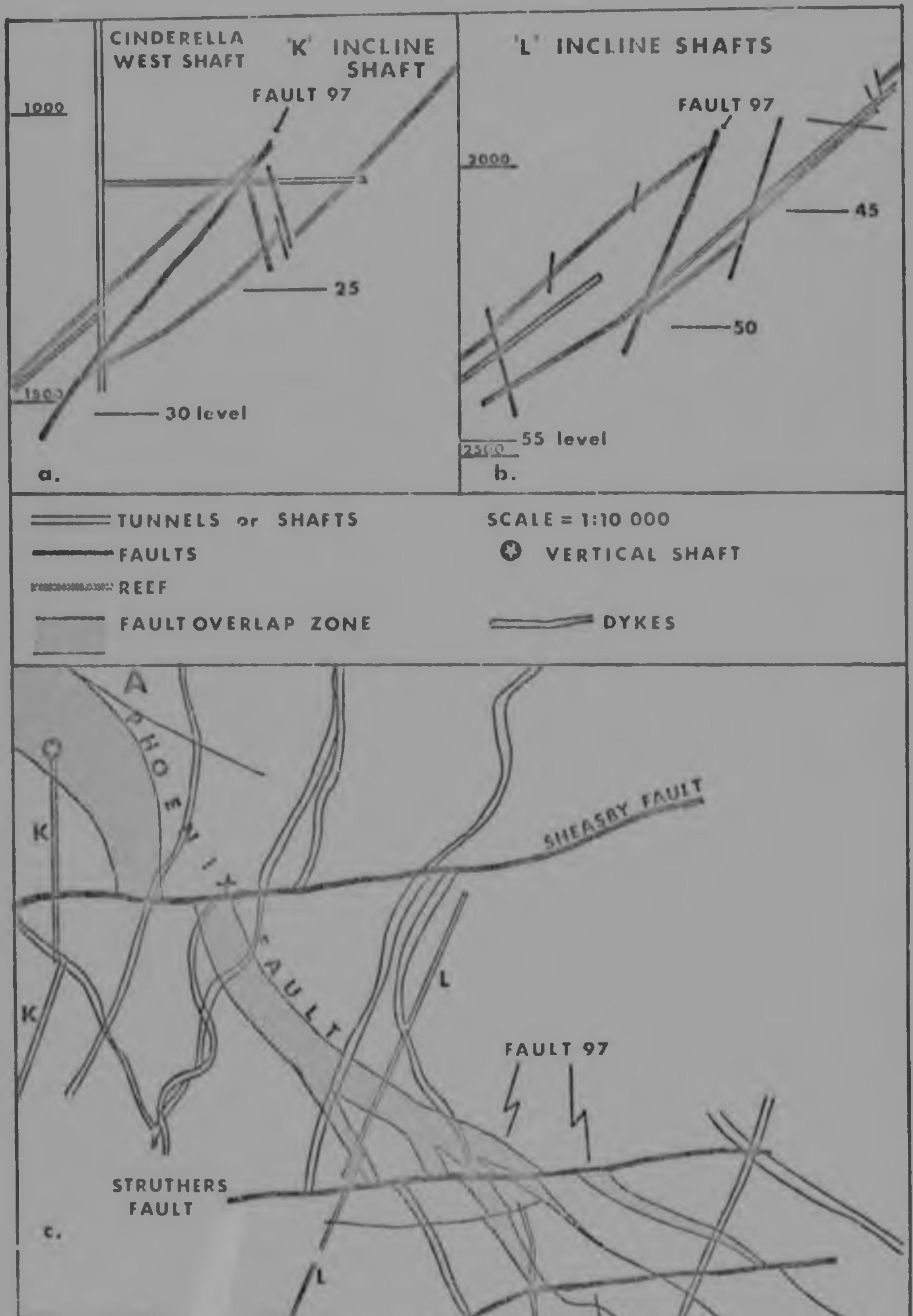

FIGURE 3-6

VERTICAL SECTIONS IN K(a) and L(b) SHAFTS and a REEF PROJECTION(c) SHOWING the GEOMETRY of FAULT 97 through the fault could be obtained (Figure 3.6 a and b) but the fault-reef intersection trace clearly shows the fault to have a minor displacement near surface (Map 2), a 300 metre overlap or gain of ground at a depth of 1300 metres (point A, Figure 3.6c) and then finally to disappear some 6.5 km on the reef trace from surface, after branching to form splay-faults (point B). The important feature of the Phoenix Fault is its method of termination - in this case the splay-faulting interpretation was suggested by Mr C Duke of the E.R.P.M. Geology Department. Hinge faulting has also been important. Between K and L shafts, the main fault is rotational with the vertical displacement decreasing towards the south-east. Then, in the vicinity of L section the fault splays into four smaller faults, the displacement across which disappears near the Far East section.

3.2.3. Gouge filled faults and shear zones

The cataclastic material present in the faults and shear zones in the E.R.P.M. varies from a solid, hard, coherent mass to soft gritty infillings to dry white powder. These three end members can be classified as follows using Higgins' (1971) classification of cataclastic rocks.

(i) Those where primary cohesion and fluxion structures (a foliation or fabric due to cataclastic processes) are present, where cataclasis is dominant over new mineral formation and recrystallisation, and the size of the porphyroblasts is less than about 0,2 mm, are classified as ultramylonites. Members of this group in the E.R.P.M. are hard and brittle and can usually be identified by chemical analysis as highly deformed, but unrecognisable dykes. The internal fabric of these fault fills is usually a compositional layering consisting of quartz-feldspathic layers and platy-mineral layers.

The Van Dyk Fault strikes at an average of 067° (Group 1 in Table 3.1), dips near to vertical, has a downthrow to the south and a dextral strike-

a

b

c

d

PLATE 3.1

Underground photographs of shear zones

Photographs of shear zone 114A(group 5) on H77W level.

a. The strong foliation which is curved and inclined at an angle to the shear zone.

b. A close up of the sheared area showing a strong foliation and a large elongate quartz pod in the foliation plane.

c. Similar to (b) but at another locality.

d. Photograph of a large bedding plane shear on H22 level. Note the bedding plane joints above the sheared area.

slip displacement. It is not unusual in its geometry but is a typical example of faults and shear zones with gouge zones of cataclastically deformed and mylonitic material. The width of the gouge zone may exceed several metres (Van der Berg, 1973) but it is normally a little over a metre thick. Such large variations in distance between the fault walls suggest an irregular initial fracture plane along which pod like gaps were filled with cataclastic rock during movement. The formation of these pods may be analogous to step structures which are commonly found on a smaller scale on both naturally and experimentally produced fault planes. Norris and Barron (1968) consider steps to be formed by either accretion of gouge material or secondary fracture. Accretionary stepping is common on the Van Dyk Fault, being usually formed in areas of [illegible] irregularities in the fault walls by the gouge plastered on [illegible] the rock surface in the lee of irregularities.

An excellent example of an ultramylonite type shear zone in which the catacla[illegible] material is of a constant thickness was observed section. The shear zone (Plates 3.1a, b and c) strikes approximately parallel to the reef and dips between 40° and 85° north; displacement across the shear is oblique in a reverse sense at the east end of the exposure (H76E) but appears to be purely strike-slip at the west end (H7/W). Within the 1.5 metre wide shear is a highly foliated ultramylonite with a dyke like composition (c.f. Appendix Table 1d, Analysis 23) in which are large pods of quartz. The sheared area is very well defined and does not extend into the adjacent quartzites; the foliation within the shear is also very well defined (Plate 3.1a) curving as it is traced from the margin to the centre. It is never parallel to the contacts of the shear zone and the angle of the foliation to the contact

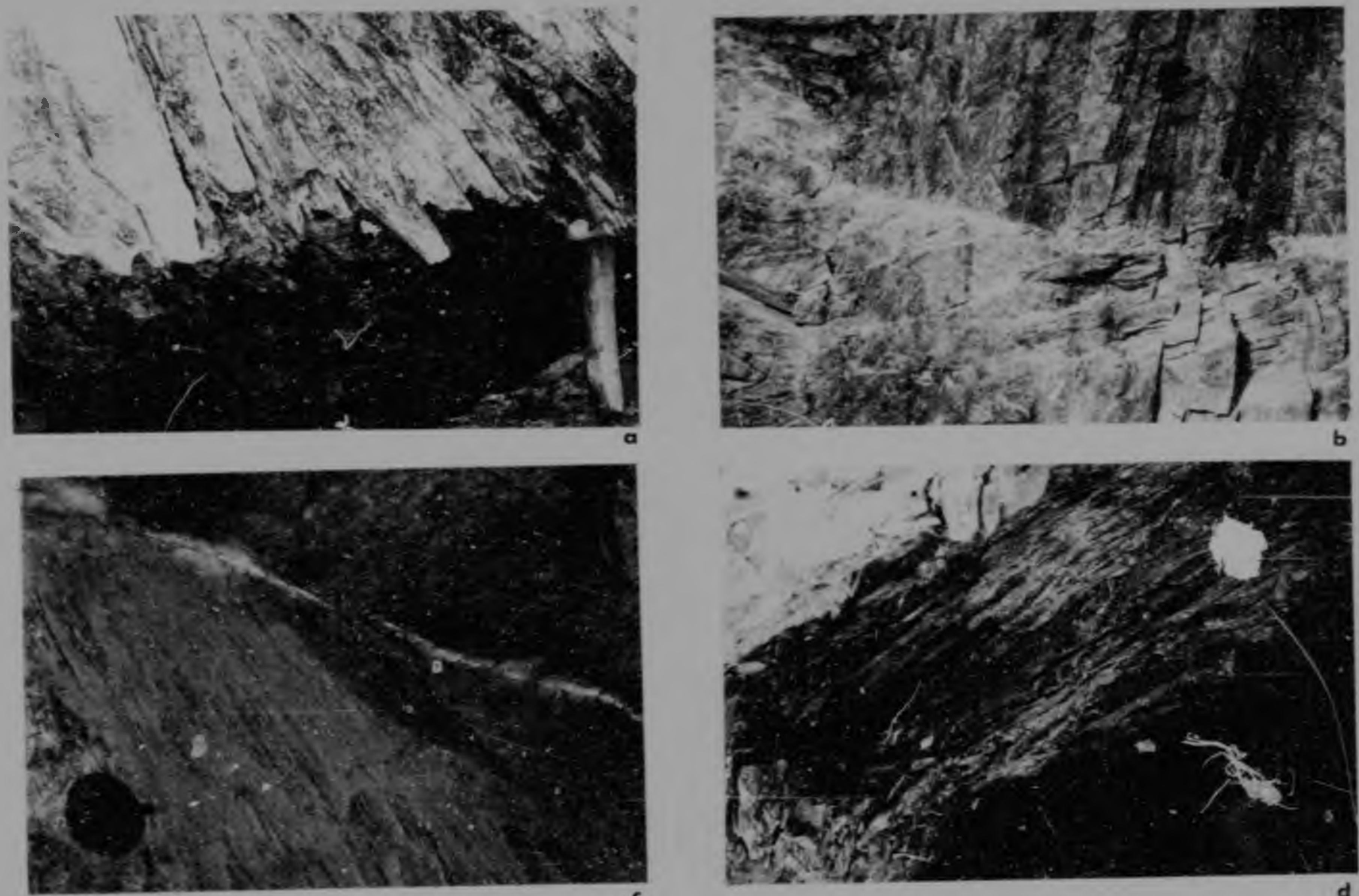

a b c d

PLATE 3.2

Mining-induced fractures

a. Type 1 fractures in a stope. The unusually high density has been caused by an irregular mining configuration. The fractures dip towards the mining face; that is, the face advance is to the right. (Photo by W.D. Ortlepp).

b. Type 2 fracture in a footwall drive. Note the high degree of comminution in the fracture plane and the feathering of the fracture zone downwards (Photo by W.D. Ortlepp).

c. Embryonic zone of high comminution (white line) from which wall spalling initiates. Photo taken in the L74 exploration crosscut.

d. Severe wall spalling and 'self-mining' in the L74 exploration crosscut.

is about 20°. Ramsay and Graham (1970) have discussed the production of these foliations in some detail. They, conclude that shear zones, similar to the one described above are a product of hetrogeneous simple shear; the schistosity is dependent on the finite strain state of the rock and forms parallel to the XY plane of the finite strain ellipsoid.

Similar shearing has also been observed parallel to the bedding planes on H23E (Plate 3.1d) in zones up to 20 cm wide.

(ii) Higgins (1971) defined fault breccia and fault gouge as a rock formed by crushing and grinding in which any coherence is secondary. Fault breccia particles are visible to the unaided eye and fault gouge particles are not. The soft, gritty infillings often found in the E.R.P.M. can be classified as fault gouge, although many particles are of fault breccia size. Water is regularly associated with these zones.

(iii) The dry white powdery substance is strictly a fault breccia but requires special attention because it is the end product of mining-induced fracturing. Two types of mining-induced fractures are commonly found in the Witwatersrand deep-level gold mines and have been called Type 1 and Type 2 fractures by McGarr (1971) (Plate 3.2). Type 1 fractures exhibit characteristics fundamental to the definition of a joint and will be discussed in detail in Section B of this chapter. However, observations of Type 2 fractures suggest violent failure and an association with rockbursts. Their distribution is irregular and underground observations reveal that they are up to 20 cm wide and that displacements across them are in the order of two to three centimetres.
Within these Type 2 shear zones the cataclastic material is mostly a very fine, white powder (less than 0.1 mm in diameter) in which particles several centimetres long are embedded. Thin sections of sheared quartzites

show that severe fracturing and comminution of the individual quartz grains has taken place. Kersten (1964) noted the characteristic surface features of Type 2 fractures to be slickensiding, mylonitic powdered material, a smooth fracture plane and an absence of visible grain boundaries. These fractures rarely terminate on bedding planes.

3.2.4. Ages of faulting

The latest movement on the faults displaces most intrusives but some faulting took place even before the intrusion of the Ventersdorp dykes; that is, during deposition of the Witwatersrand sediments. Group 2 faults (Table 3.1), in particular, are sub-parallel to the sedimentary basin edge and may have formed as normal faults during basin subsidence. These faults now have a strike-slip displacement indicating later movement along them. Groups 1 and 3 faults appear to be more recent than Group 2 and are probably associated with some later stress field with the maximum principal stress oriented approximately east-west. This may be a conjugate pair as indicated by their opposing strike-slip displacements and the fact that they displace each other in an irregular fashion implies a similar age. The stress systems indicated by faulting will be discussed in Chapter 4.

B. JOINTING

3.3 INTRODUCTION

A detailed analysis of jointing patterns is essential for an understanding of the effects of larger discontinuities (i.e. dykes and faults) on the adjacent rocks and mining excavations, as well as to establish the early stress fields. The aim of this section is to establish the patterns of both the original geological joints and the mining induced fractures; the different response of quartzites and dykes during brittle failure to mining induced stresses, and the differences

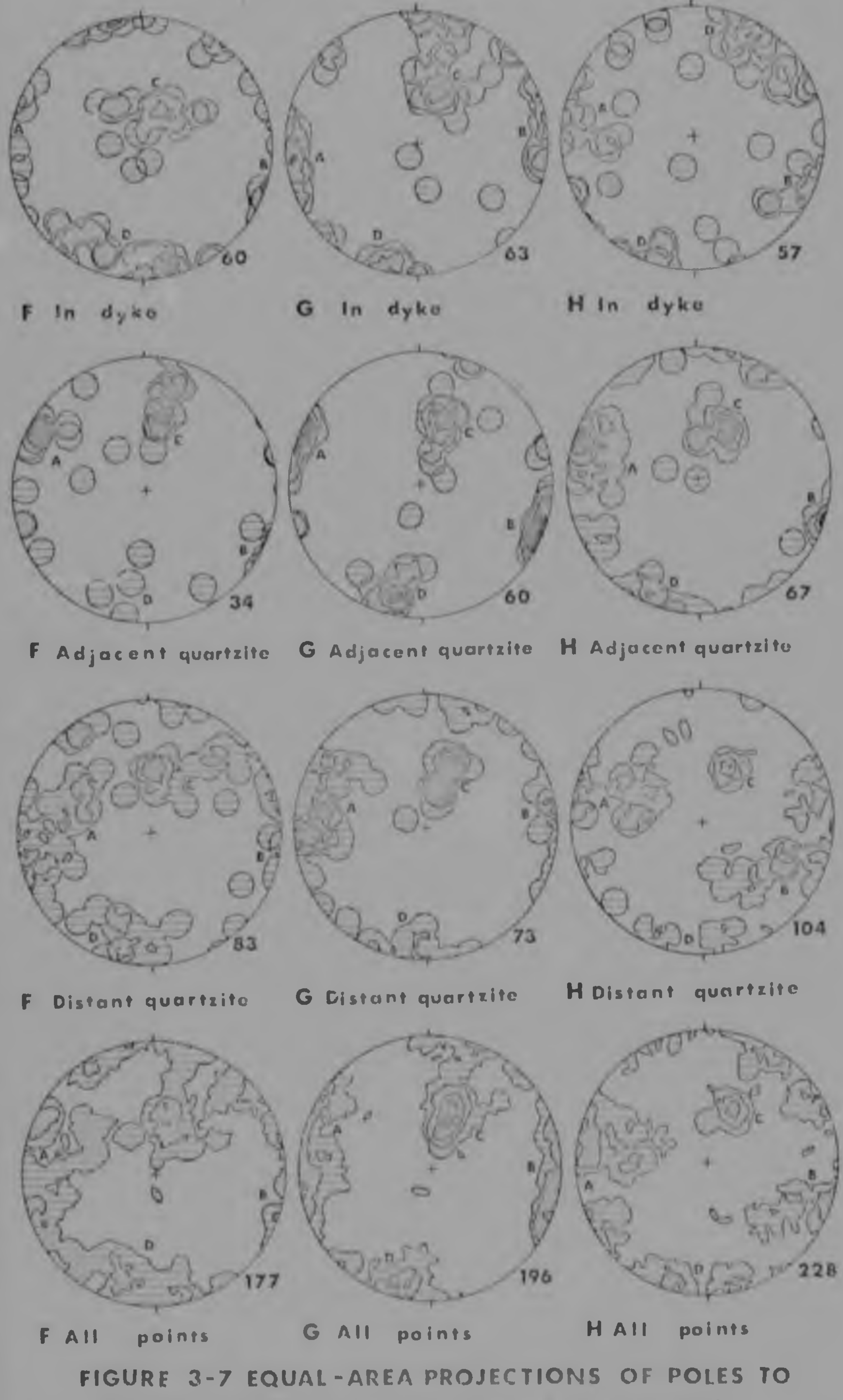

FIGURE 3-7 EQUAL-AREA PROJECTIONS OF POLES TO JOINT PLANES; see text and Table 3-3 for details.

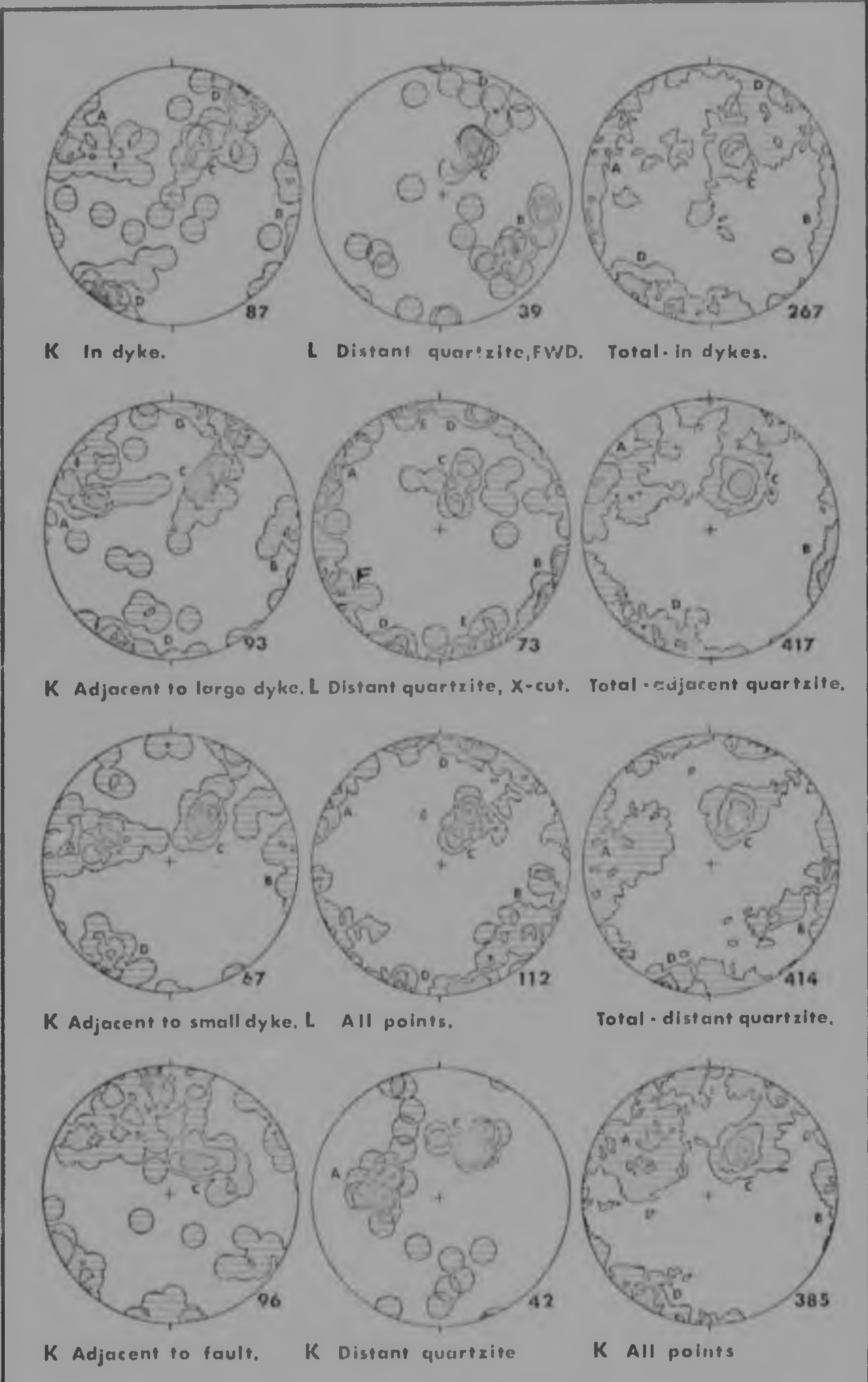

CONTOURS EQUAL 1%, 3%, 6% and 10% per 1% area
NUMBERS REFER TO THE NUMBER OF POINTS

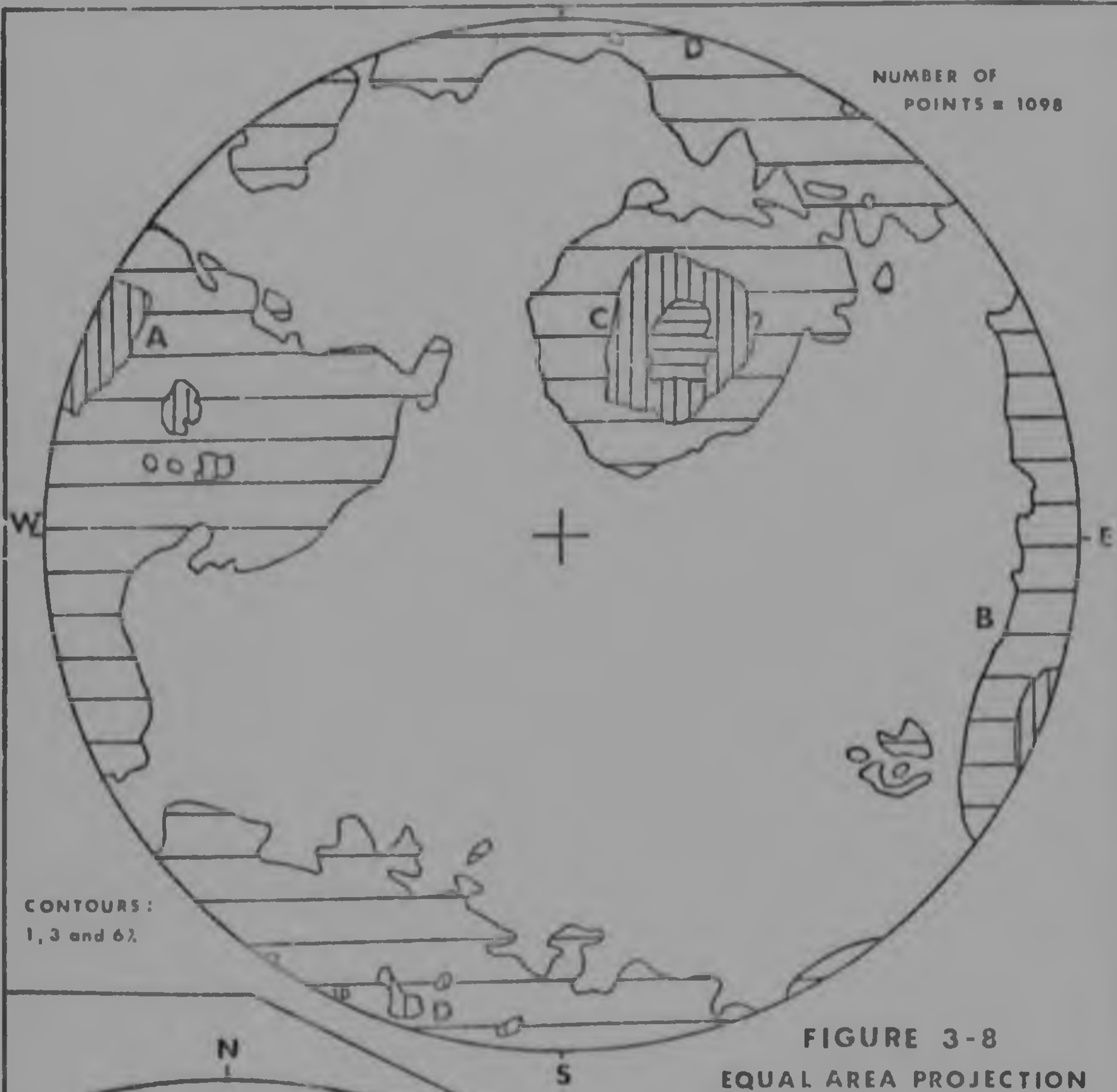

FIGURE 3-8
EQUAL AREA PROJECTION OF POLES TO ALL JOINTS MEASURED IN THE E.R.P.M.

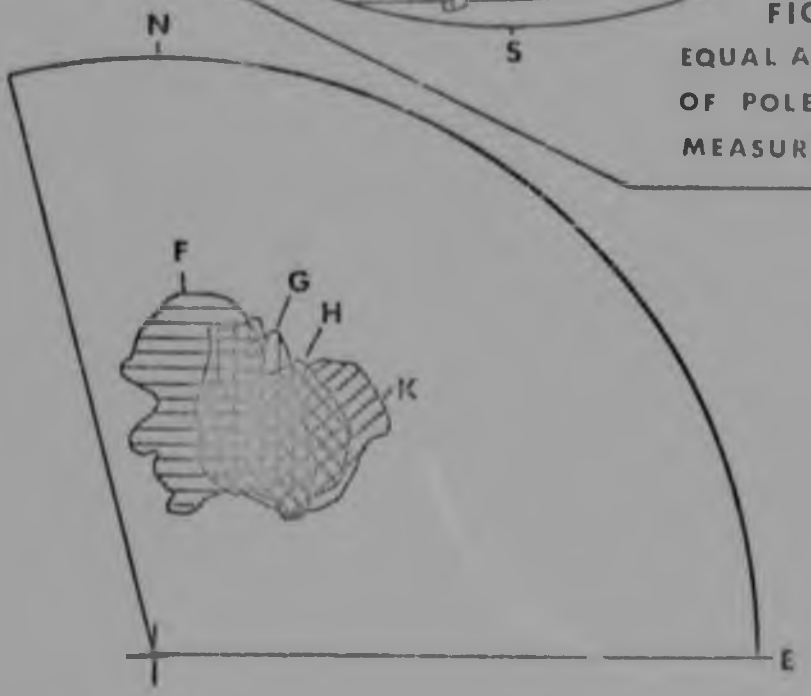

FIGURE 3-9
EQUAL AREA PROJECTION OF POLES TO SOME BEDDING PLANE JOINTS IN F,G,H and K SHAFTS

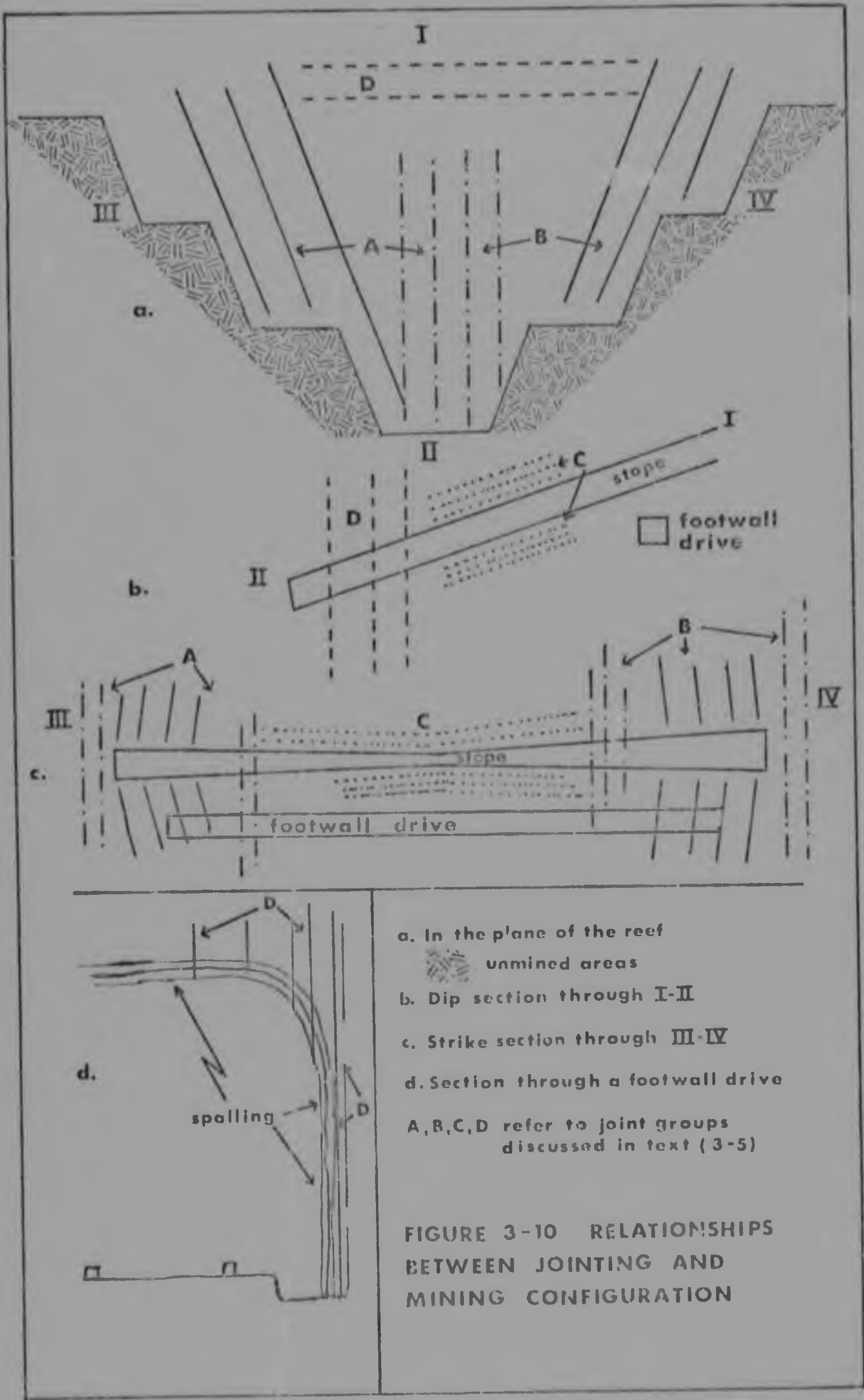

FIGURE 3-10 RELATIONSHIPS BETWEEN JOINTING AND MINING CONFIGURATION

TABLE 3-3

LOCATIONS OF JOINT READINGS

IN DYKES			IN QUARTZITES ADJACENT TO DYKES AND FAULTS			IN DISTANT QUARTZITES		TOTALS	
LOCATION	DYKE NO	NO*	LOCATION	FAULT NO or DYKE NO	NO*	LOCATION	NO*		
F68W	58	60	F68W	58	34	F68W	83		177
G73W	79	63	G73W	79	60	G73,75W	73		196
H76W	100	57	H76W	100	67	H75,76,77E,77W	104		228
K69C	182	87	K69C	182	93	K69W	42	289	
			K69W	181	67				385
			K69E	Van Dyk Ft(111)	1			96	
			K70E	Van Dyk Ft(111)	45				
						L74,71E	39		112
						L74 Ex,Xcut	73		
TOTAL		267	TOTAL		417	TOTAL	414		1098

NO* Number of measurements taken

in fracture patterns in quartzites adjacent to small dykes, large dykes and faults. Of the five dykes in and near which measurements were made, four are 'large'(Dykes 58, 79,100,182) ranging in thickness from 15,5 metres to 21 metres and one is 'small' (Dyke 181) being only 1,7 metres thick. The fault considered is the Van Dyk Fault (No 111). These dykes and the fault have been marked on Figure 3.2.

Joints are extremely well developed in all parts of the E.R.P.M. particularly those that are mining induced. However, there are at least three important geological sets present with a possible two further poorly developed sets. A total of 1098 joint plane orientations have been measured in F,G,H, K and L shaft areas, between 68 and 78 levels, concentrating on three locations within each shaft, namely: in the dykes, in the quartzites adjacent to dykes and faults to an arbitrary distance of ten metres, and in quartzites distant from any discontinuities. In Figure 3.2 the areas where joints were measured are marked and in Table 3.3 the locations and number of readings at each location are listed.

No detailed joint analyses have previously been attempted on the E.R.P.M. but in 1964 Kersten analysed the orientations of mining induced joints in the immediate hangingwall rocks on three Witwatersrand gold mines. He described three classes of fractures basing his division on surface features and dip direction. (He observed that the strike varied little and concentrated on dip measurement). Since then, McGarr (1971) has reclassified Kersten's three classes of fractures into Type 1 and Type 2 fractures. Type 1 fractures (Groups A and B, solid lines, in Figure 3.10c) dip towards the direction of stope face advance in the hangingwall and away from this direction in the footwall; Type 2 fractures dip in the opposite sense. The characteristics of Type 2 fractures, which as previously noted, cannot be considered as joints, have been discussed in 3.2.3. above and the characteristics of Type 1 joints will be discussed below (see Plates 3.2a and b).

3.4 METHOD OF ANALYSIS

The method used to determine the orientation of the joints was as follows: because of the abundance of ferromagnetic mining materials a clinorule was used for orientation measurements instead of a magnetic compass. Strike was measured with respect to the tunnel orientation and then recalculated to true north from mine-survey plans; dip could usually be measured in the normal way on individual joint planes.

The measured orientations were statistically analysed by constructing contoured, lower-hemisphere, equal-area, stereographic projections of poles to joint planes. A computer programme (Starkey, 1970), adapted for the University of the Witwatersrand computer by Mr S L Fumerton has been used for this purpose. Stereographic projections have been constructed for each group of data, namely: in dykes; in adjacent quartzites and in distant quartzites, as well as for all data in each shaft and all data measured in the E.R.P.M. These projections are reproduced in Figure 3.7 and Figure 3.8.

Joint orientations were mostly measured in footwall drives, but some were measured in hangingwall drives and the L74 exploration cross-cut (Map 1, Table 3.3). Development areas rather than stopes were used because of difficulties in determining strikes in a stope.

Measurement of joint orientations in a restricted environment such as footwall drives does bias the results. Spalling on the side walls of the drives masks any steeply dipping-joints striking parallel to the tunnel (i.e. parallel to bedding strike) (see Figure 3.10d). Further, both footwall and hangingwall drives are associated with mining disturbances which mask original joints. Type 1 joints, for example, often obscure a vertically dipping set striking down the dip of the sediments; this can be seen in Figure 3.10a and c, where two members of groups A and B have similar strikes and dips. For these reasons joints were also measured in the L74 exploration crosscut which runs orthogonally to the footwall drives, is in the hangingwall and has no mining above or below it.

Moreover, bias in the measured Type 1 joint distribution is present; most major dykes in the E.R.P.M. are or were associated with westward-advancing stope-faces, hence, in these footwall drives Type 1 joints dip steeply eastwards. However, in the H shaft area, joints were measured on both sides of the shaft and the stereographic projection for joints in distant quartzites (Figure 3.7) shows a symmetrical distribution pattern - that is, Type 1 joints dipping both east and west.

Also, the strike of the bedding and hence the trend of the footwall and hangingwall drives varies from 099° in F shaft to 121° in L shaft resulting in a spread of the orientations of bedding joints and induced spalling joints on the stereographic projections. A composite projection of bedding joints in each shaft clearly shows the strike variation (Figure 3.9) from F shaft in the west to L shaft in the east. Further the orientation of stope-mining induced joints is solely dependent on the orientation of the mining face which varies considerably and hence, one cannot expect a very regular pattern for these joints.

Although there are limitations to the analysis as outlined above, the descriptions of the results below clearly establishes two prominent sets of mining induced joints, three sets of well developed geologically derived joints and two other poorly developed joint sets.

3.5 RESULTS

The various stereographic projections for each group of data are illustrated in Figure 3.7 except for the projection for all joints measured in the E.R.P.M which is shown in Figure 3.8. Each projection has, at a maximum, four contours representing concentration levels of 1%, 3%,6% and 10% per 1% area.

All projections have several areas of high concentration, but there are four of these areas that are common to the majority of the projections. These four groups can initially be described as:

(a) Group A : Strike = 030^{o}, dip = 60^{o} - 90^{o} east

Joints present : Type 1 and a geologic set.

(b) Group B : Strike = 030^{o}, dip = 60^{o} - 90^{o} west

Joints present : Type 1 and a geologic set.

(c) Group C : Strike 120^{o}, dip = 20^{o} - 50^{o} south

Joints present : bedding and cross-bedding parting planes plus parallel joints in the dykes.

(d) Group D : Strike = 120^{o}, dip = 90^{o}

Joints present : Spalling on tunnel walls and a geologic set.

These groups are indicated on the stereographic projects in Figures 3.7 and 3.8 by their respective letters.

3.5.1. Groups A and B joints

These joints are well developed in all areas of the mine, especially where stoping has occurred. They are best developed in the distant and adjacent quartzites where they dip at 60^{o} - 90^{o}. Within the dykes, however, they are poorly developed and are essentially parallel to the near vertical dyke walls. This suggests that a dyke is a sufficiently large enough structural discontinuity to affect the orientation of mining induced jointing near it and partly resist mining induced jointing within it.

This conclusion can be added to by introducing a dyke thickness factor. Dykes 58, 79, 100 and 182 are 'large dykes' and affect the orientation and density of joints in the adjacent quartzites but the distribution of the joints adjacent to the 'small' dyke .81 is more similar to that for distant quartzites implying that only large dykes can

3%,6% and 10% per 1% area.

All projections have several areas of high concentration, but there are four of these areas that are common to the majority of the projections. These four groups can initially be described as:

(a) Group A : Strike = 030°, dip = 60° - 90° east

Joints present : Type 1 and a geologic set.

(b) Group B : Strike = 030°, dip = 60° - 90° west

Joints present : Type 1 and a geologic set.

(c) Group C : Strike 120°, dip = 20° - 50° south

Joints present : bedding and cross-bedding parting planes plus parallel joints in the dykes.

(d) Group D : Strike = 120°, dip = 90°

Joints present : Spalling on tunnel walls and a geologic set.

These groups are indicated on the stereographic projects in Figures 3.7 and 3.8 by their respective letters.

3.5.1. Groups A and B joints

These joints are well developed in all areas of the mine, especially where stoping has occurred. They are best developed in the distant and adjacent quartzites where they dip at 60° - 90°. Within the dykes, however, they are poorly developed and are essentially parallel to the near vertical dyke walls. This suggests that a dyke is a sufficiently large enough structural discontinuity to affect the orientation of mining induced jointing near it and partly resist mining induced jointing within it.

This conclusion can be added to by introducing a dyke thickness factor. Dykes 58, 79, 100 and 182 are 'large dykes' and affect the orientation and density of joints in the adjacent quartzites but the distribution of the joints adjacent to the 'small' dyke 181 is more similar to that for distant quartzites implying that only large dykes can alter the stress field significantly enough to reorient mining induced fractures.

Two types of joints, Type 1's and a geological set, were defined above as making up Groups A and B, both of which can be recognised on some stereographic projections. The projection for distant quartzites in H shaft shows Groups A and B to cover three concentrations, one lying on the primitive great circle and the other two dipping steeply east and west. The first of these concentrations represents a geological set and the latter two, Type 1 joints. This subdivision is also present, although not as clearly defined, in F and G shafts, but in K shaft the geological set is completely absent.

Near the Van Dyk Fault, groups A and B are hard to identify and are disrupted to such an extent that Group A joints coalesce with Groups D and C. This indicates that large faults, like large dykes, can affect the orientation of mining induced joints.

3.5.2. Group C Joints

These joints are always represented by good point maxima on the stereographic projections for distant quartzites but often these maxima are elongated in the dip direction because of the difference in the angle of dip for bedding and cross-bedding. In the projections for adjacent quartzites, the maxima may join to that for Group D to form a weak great circle distribution. This suggests that the regularly oriented bedding is slightly disrupted near to dykes, and presumably also near faults.

One of the most unusual features of the jointing in the mine, is the presence of 'bedding joints' in dykes 58, 79 and 182. Group C jointing in dykes is not as well defined as in adjacent quartzites but nevertheless it is prominent enough in places for the dykes to be mistaken for bedded sediments underground. However, this set is absent in Dyke 100.

3.5.3. Group D Joints

These joints appear to be all but absent in the distant quartzites but they may be masked by spalling on the tunnel walls. However, in the adjacent quartzites and within the dykes the group is clearly visible (except in the quartzites adjacent to Dyke 58). This may be due to a better development of the geological joints near the dykes or to less spalling. The latter seems the most likely because some of the best examples of geologic Group D joints were observed in distant quartzites.

3.5.4. Joints away from active mining areas

All the above descriptions and associated stereographic projections referred to joints in areas near stope mining. To check the validity of this data and to identify the groups more precisely 73 joints were measured in a section along the south-trending L74 exploration crosscut, well away from active mining. Group C joints are, as expected, well developed although abundant cross-beds have caused an elongated point maxima. All other joints dip vertically forming a weak primitive great circle with four areas of concentration. Two of these correspond to Groups A and B and Group D but the other two cannot be correlated with any previously described groups. In the crosscut, spalling joints strike at 030^{o} and do not form part of Group D; this confirms the presence of a geological set of joints in Group D.

The two new maxima which appear in the projections (Figure 3.7) correlate with two further sets of vertically dipping joints, one strong set striking at about 075^{o} (Group E) and one weak set striking at about 165^{o} (Group F). As will be shown in Chapter 4 these correspond to weak regional lineation trends and further, a reinvestigation of the stereographic projections for other areas reveal a few joints striking at these orientations. Thus, these maxima probably represent weak geological joint sets which are present throughout the mine.

a


b


c

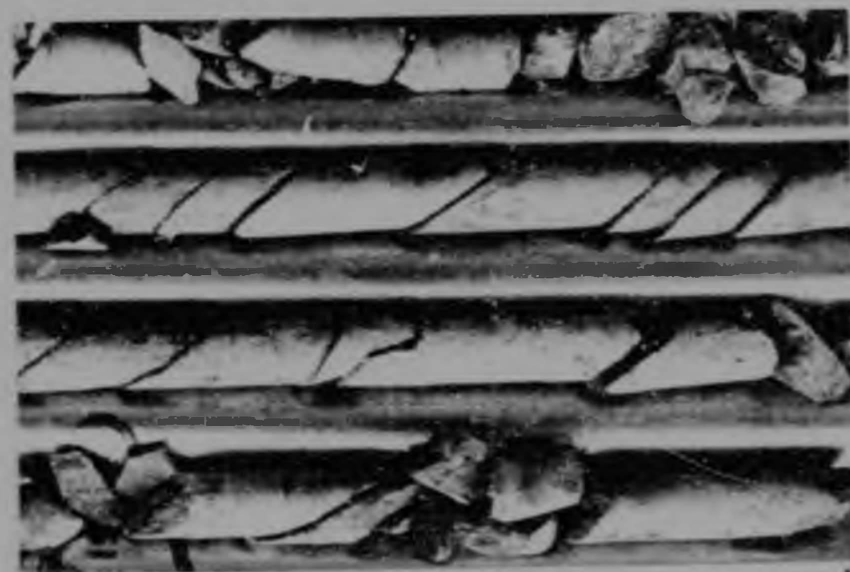
d

PLATE 3.3

Original jointing (bedding planes; group C and east-west joints; group D).

a. A section of diamond drill core showing open bedding plane joints (ends of the core) and inherent bedding plane weaknesses (lighter lines within the core).

b. Bedding plane joints (horizontal fractures) and well developed type 1 fractures (dipping to the left) in a footwall drive (Photo by W.D. Ortlepp).

c. Well developed bedding plane jointing forming lineations on an extremely planar vertical joint striking east-west. (Photo by W.D. Ortlepp).

d. Diamond drill core showing regular bedding plane fractures.

a

b

c

PLATE 3.4

Original and mining induced jointing

a. A planar bedding plane joint (roof) on which traces of type 1 fractures can be seen which extend down the back wall. (Photograph by W.D. Ortlepp).

b. Diamond drill core showing regular cross fractures (X) which are evidence for groups A and B original jointing.

c. Dyke/quartzite contact in a north-south striking station crosscut showing original group A and B jointing (Y) and curved spalling fracturing (Z).

These joints, like the geological joints in Groups A and B and Group D, are oriented at 90° to each other.

3.6 DESCRIPTION OF JOINTS

3.6.1. Mining induced joints (Plate 3.2 and Plate 3.4a and c)

The general orientation of Type 1 joints and their relationship to mining configuration have already been discussed. Kersten (1964) noted the surface features of Type 1 fractures to include plumose structure, clearly visible grain boundaries, an absence of slickensiding and an irregular surface. They usually terminate on bedding planes (cf. Type 2 fractures in 3.2.3.).

A further feature demonstrated by Kersten is that the angle of dip increases with the span of the stope. Dip increases from about 40° to 75° as the half-span width increases from 10 to 50 metres but beyond 50 metres the increase is minimal; this change in dip is restricted to a small portion of a section because half-span distances range up to 1000 metres. The frequency of these joints should vary with lithology but this is rarely observed becuase mining is confined to one sedimentary horizon. However, for no apparent reason, the frequency varies within the quartzites and also, as demonstrated above, there is a degrease in frequency within dykes compared to quartzites.

Kersten concluded that Type 1 joints are probably tension features. His description of the surface characteristics outlined above tends to support this, apart from one feature; the presence of plume structures. Price (1966 pp. 122-155) suggests that plume structures are probably a result of shear failure but notes that because plume structures are developed during Brazilian tests there is doubt as to whether they are a conclusive indicator of shear failure. However, McGarr (1971) using dislocation theory and Gay (1973) using a combined theoretical and experimental approach, have both considered Type 1 joints to be shear structures which form between five and ten metres ahead of the working face. It may prove that Type 1 joints form by both extension and shear mechanisms depending on their proximity to the stope. In the stope face these features are clearly vertical and immediately in front of this the stress system is oriented with the maximum principal stress vertical; that is,it lies in the plane of the fracture. This suggests that an extesnion mechanism at this point is more likely than a shear one. However, this situation may vary away from the stope. The principal stresses are reoriented about a stope as mining proceeds such that the maximum principal stress is oriented parallel to the excavation (see for example, Gay, 1973, Fig. 3a). The observed Type 1 fracture patterns do not show any signs of becoming parallel to the excavation and hence they are probably formed by a shear mechanism away from the stope face.

Spalling or slabbing on the tunnel walls is a common feature at depth due to the large stresses induced around the openings. It was best observed in the L74 exploration crosscut (Map 1); a tunnel which was initially about 2,5 metres wide and 3,0 metres high and which has not been stress relieved by overstoping. In this crosscut, slabs appear to initiate from a highly-stressed zone of comminution formed at the intersection of two planar features: a geological feature such as a fault or a prominent bedding plane and the tunnel walls or the tunnel roof and a wall. This 'embryonic zone' (Plate 3.2c) is concave in section and is usually near the top of the tunnel walls but often migrates down to waist height as spalling proceeds. Slabs with thicknesses ranging from a centimetre to 15 centimetres or more form parallel to the tunnel walls thus widening the tunnel by 'self-mining'. (Plate 3.2d). Individual slabs collected are mostly curviplanar but towards them embryonic zones they are tapered and even hooked.

In footwall and hangingwall drives, which have been destressed by a stope above or below, the spalling is mild by comparison to that in the cross-cut, obvious self-mining is rar and spalling joints are vertical and do not tilt over.

Comminution of material is confined mainly to embryonic zones and the smooth and curviplanar joint surfaces are similar in most respects to Type 1 fractures. Many of the slabs contain plume structures possibly suggesting a shear mechanism and Gay (1970) concluded that spalling surrounding slits in sandstone cylinders under hydrostatic compression took place by shear.

3.6.2. Geological joints (Plates 3.3 and 3.4)

(a) Possible extension joints

Two of the original joint sets, part ps A and B and part of group have been recorded in drill cores (Plates 3.4b) and occasionally in underground excavations Plates 3.3c and 3.4c) where they are not often identified because of the masking effects of mining induced jointing. Where observed, they are quite planar and show no displacement across the joint plane. The surface of the joints is usually coated with chloritic material unless small quartz veins are present. In at least one location the 030° trending joints have controlled the intrusion of a small dyke of Ventersdorp age (Plate 3.4c) indicating that they formed early in post-Witwatersrand times.

The fre ncy of Groups A,B and D geologic joints is not well known although in shaft, the observed joints were spaced about 0,25 me res apart.

The joint sets are orthogonal to each other and are oriented at high angles to the sediments which suggests that they may be related to the basining processes. North-south and east-west vertical sections through the basin at the E.R.P.M. show the sediments to be concave upwards and the joints may be tensional features associated with this flexuring. Alternatively they may be extension joints formed during uplift as suggested by Price (1959).

Groups E and F joints were too poorly developed to be studied but are presumed to be of a geological origin.

(b) Bedding plane joints

The most consistently developed joints in the mine are bedding joints (Plate 3.3 and 3.4a), the dip of which varies from about 45° at surface to 25° at the deepest mining levels, but as demonstrated above local variations are common especially near faults and dykes. In addition, bedding is occasionally disrupted by ancient gullies and wash-aways and by cross-bedding which dips at angles which are up to 25° greater than the dip of the main bedding planes. Bedding plane joints seem to have developed where there is an inherent weakness such as a fine layer of shale in the quartzites and hence, they are usually more frequent in 'dirtier' quartzites where the shale content is abundant. The distance between them ranges from about five centimetres to more than a metre.

The joints are either planar (main-bedding) or curviplanar(cross-bedding) and they are usually covered by a fine coating of chloritic or clay material; comminution is rare but the surface is often striated. Movement across them has caused the displacement of small veins and joints for distances of up to one centimetre; shear zones parallel to bedding as discussed in Part A of this chapter also imply movement along bedding.

From a comparison of the bedding plane fractures in the L74 exploration crosscut and footwall drives it is clear that the frequency of the joints is higher in the footwall drives where they are also more open. This better development of the joints in mining areas is probably related to the closure of the stopes, which occurs some tens of metres behind the position of the active mining face.

(c) Mechanism of formation of bedding plane joint

On the Witwatersrand the measured vertical stresse are in go d agreement with the calculated stress from the weight the overburden (Gay, 1972, 1975), hence, at the deepest mining lev. ls the vertical stress, which should approximate to the maximum principal stress, is about 90 MPa if one assumes the density of the overburden to be 2700 Kg/m^3 (Grobbelaar, 1957), depth to be 3,3 kilometres and acceleration due to gravity to be 980 cm/sec^2. In addition, Gay (1975) has shown that at depth in Southern Africa the vertical stresses are almost twice as large as the horizontal so in the E.R.P.M. it is reasonable to assume a horizontal stress of 50 MPa, which will approximate to the minimum and intermediate principal stresses.

The mechanism of formation of the bedding joints is undoubtedly geological but the opening up of the joints, the higher frequency near active mining areas, and possibly the formation of those in the dykes, is obviously related to the mining activity. When the reef is removed by mining, the underlying footwall rocks are subjected to an almost instantaneous removal of three kilometres of overburden with a concomitant reduction in the vertical stress and a reorientation of the prinicipal stresses, so that the maximum principal stress becomes horizontal and the minimum vertical. Under these conditions parting across the bedding planes could easily occur in a manner similar to valley bulging or the formation of sheet joints during erosion. Sheet jointing has been discussed in detail by Johnson (1970) in terms of removal of material by erosion and Ferguson (1967) has discussed valley bulging in terms of stress relief during erosion. In the examples cited by Ferguson the centre of the valley arches up a few degrees and vertical tension fractures and bedding plane partings are formed. In a series of experiments simulating mining conditions under stress (N.C. Gay, personal communication, 1975) has produced vertical tension fractures in the centre of a tabular 'mined -out' area as well as near horizontal fractures along bedding planes.

Following Johnson's (1970) suggestion that sheeting joints may be due to buckling, a similar model has been developed for the opening-up of bedding joints in the sediments, where, because of the sudden removal of the vertical stress, the horizontal stress is large enough to deform the beds.

The problem is to determine if the horizontal stress is large enough to buckle a series of quartzite sheets which are separated by pre-existing but closed bedding joints, with no vertical stress acting on the surface of the upper layer; that is, to see whether the horizontal stress will be large enough to open up the bedding plane joints.

Cobbold et al. (1971) have shown that the resistance of a layered body to a deforming force acting parallel to the layers is dependent on the resistance to deformation of the individual layers. Therefore, in the simple analysis given here, the behaviour of a single layer will only be discussed. Also important, is the resistance to layer parallel shear between the sheet being buckled and the surrounding sheets, which depends on the ease of slip between the layers. In the E.R.P.M. the strength across the bedding planes is probably minimal because of the presence of an initial weakness, coatings of chloritic or clay material which provide lubrication and an absence of a large vertical confining stress once the rock have been overstoped.

The critical value of the compressive stress required to buckle a free rectangular plate can be determined from the Euler Equation:

$$\sigma_{crit} = (\pi^2 E.t^2)/(12.L^2.(1-\nu^2)) \quad \text{(Johnson, 1970, page 385)}$$

where E is Young's modulus, ν is Poisson's Ratio, t is thickness and L is the length of the plate. In the E.R.P.M. reasonable values for E and ν for footwall quartzites are 0.75×10^5 MPa and 0.2 respectively (McGarr et al, 1975). Also, underground observations reveal the bedding frequency to vary from less than one to 20 joints per metre. Assume that the layers are one metre thick and that the length of the sheet, which is defined by the mining span is,500 metres.

Under these conditions the critical stress for buckling is only 2,5 MPa which is very much smaller than the predicted horizontal stress of 50 MPa. Of course, the critical stress will be higher in the mine because of the resistance to buckling imparted by the stope supports but still will be very small.

This brief analysis suggests that there is sufficient horizontal stress at depth to buckle some or all of the beds between the stope and the footwall drive resulting in an opening of the bedding joints and at least partial closure of the stope.

The 'bedding-joints' in the dykes are most probably geological because they are parallel with bedding and their surfaces are coated with chloritic material. Their origin is obscure but it seems as though they form by the propagation of parting planes from the sediments into the dykes. Hence,one would expect a much higher frequency of joints nearer the contact than in the centre but this is not obvious underground. The jointing in the centre of the dyke may form by propagation of these joints, particularly after removal of the overburden by mining.

Alternatively, the 'bedding joints' in the dykes may be extension joints (N.C. Gay, personal communication, 1975): as the dykes are overstoped they are subjected to a high horizontal confining pressure, with little or no vertical load, which would cause them to fail in extension

(Figure 3.11). In Chapter 5, the uniaxial tensile strength of a large dyke is calculated to be about 30 MPa which is significantly lower than the 50 MPa horizontal stress estimated to be present in the mine.

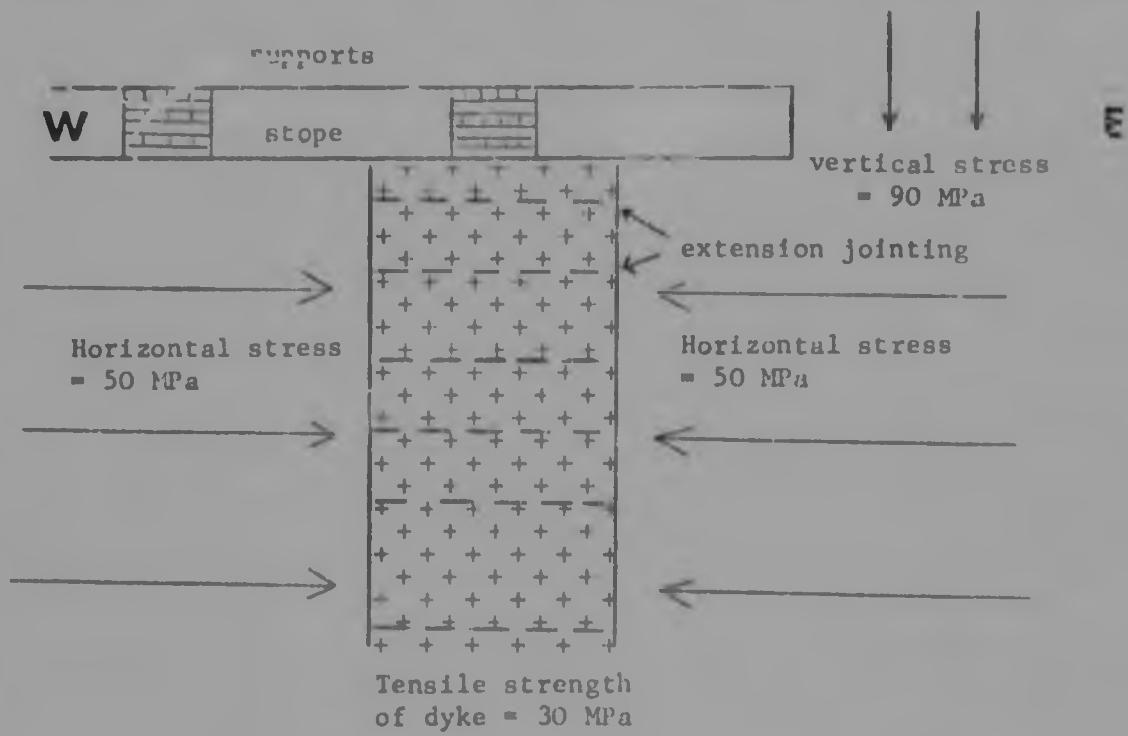

Figure 3.11 Explanation of formation of extension jointing in dykes.

FIGURE 4-1 MAP OF REGIONAL LINEATIONS (from E.R.T.S. imagery and the 1:1 000 000 map of South Africa)

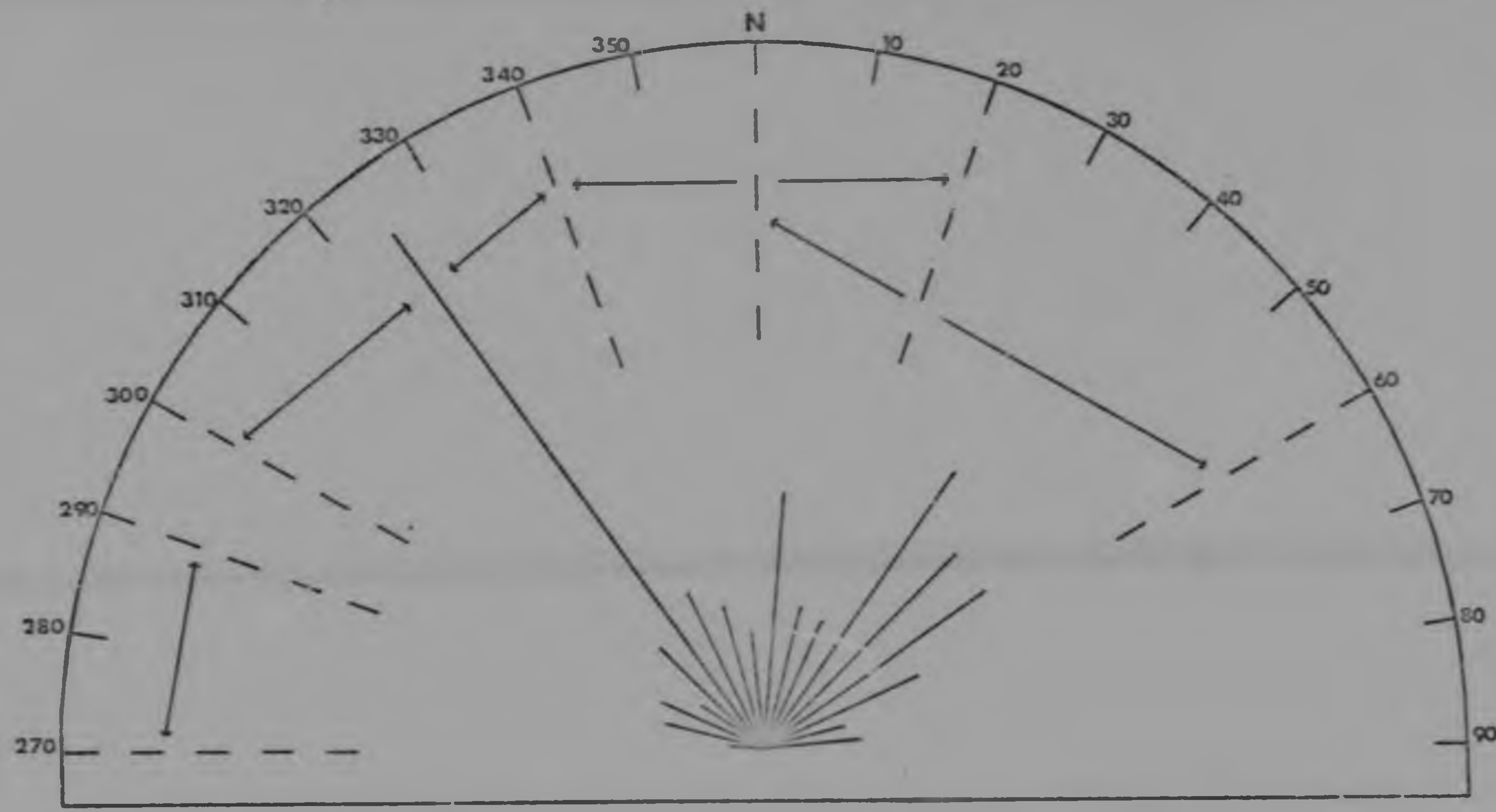

FIGURE 4-2 STRIKE-FREQUENCY DIAGRAM FOR REGIONAL LINEATIONS

RADIUS = 21.4 %, NUMBER OF POINTS IS 414, BROKEN LINES REPRESENT GROUP BOUNDARIES

CHAPTER 4

REGIONAL STRUCTURAL PATTERNS AND EARLY STRESS SYSTEMS

4.1 REGIONAL STRUCTURAL PATTERNS

In this section the regional lineation patterns, as determined from Earth Resources Technical Satellite (E.R.T.S.) imagery are compared with regional geology and the local lineation patterns in the E.R.P.M., which were described in Chapters 2 and 3 above, so as to establish how representative the lineations in the mine area are of the region as a whole and to determine the regional and local early stress systems.

Regional lineation patterns were determined from 1 : 500 000 scale E.R.T.S. imageries (supplied by Spectral Africa, Pty Ltd) for about 14 000 square kilometres of the Central Transvaal (Figure 4.1). Only lineations were recorded on the imagery; obvious cultural artefacts (e.g. roads) and stratigraphy, which is very clear on E.R.T.S. imagery, were ignored. The resultant lineation map is shown in Figure 4.1 together with some regional geological features as determined from the 1 : 1 000 000 geological map of South Africa. The lineation trends are analysed in a strike frequency diagram (Figure 4.2) which was produced from Figure 4.1 using the method described in Chapter 2. The limits of the chosen sets, their mean values, standard deviations and mean frequencies are listed in Table 4.1.

TABLE 4.1

SUMMARY OF STRIKE FREQUENCY DATA FOR REGIONAL LINEATIONS

LIMITS	MEAN STRIKE	STANDARD DEVIATION OF THE MEAN STRIKE	AVERAGE FREQUENCY WITHIN EACH GROUP (No of points and percentage)
0° - 060°	32°	$17,2^{\circ}$	27,6(6,7%)
270° - 290°	290°	$5,0^{\circ}$	13,5(3,3%)
300° - 340°	328°	$11,4^{\circ}$	36,7(8,4%)
340° - 020°	356°	$10,0^{\circ}$	20,4(4,9%)

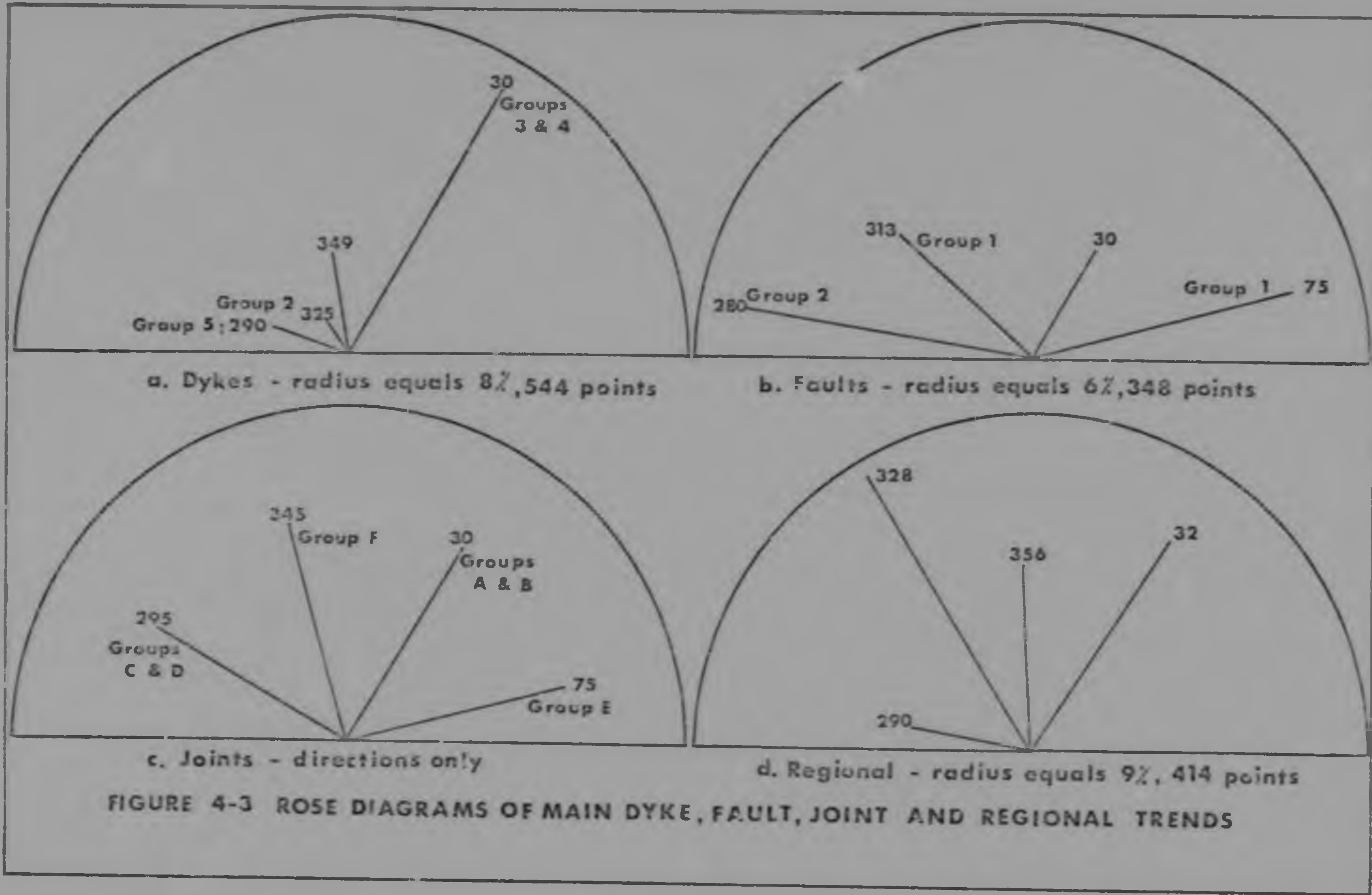

a. Dykes - radius equals 8%, 544 points

b. Faults - radius equals 6%, 348 points

c. Joints - directions only

d. Regional - radius equals 9%, 414 points

FIGURE 4-3 ROSE DIAGRAMS OF MAIN DYKE, FAULT, JOINT AND REGIONAL TRENDS

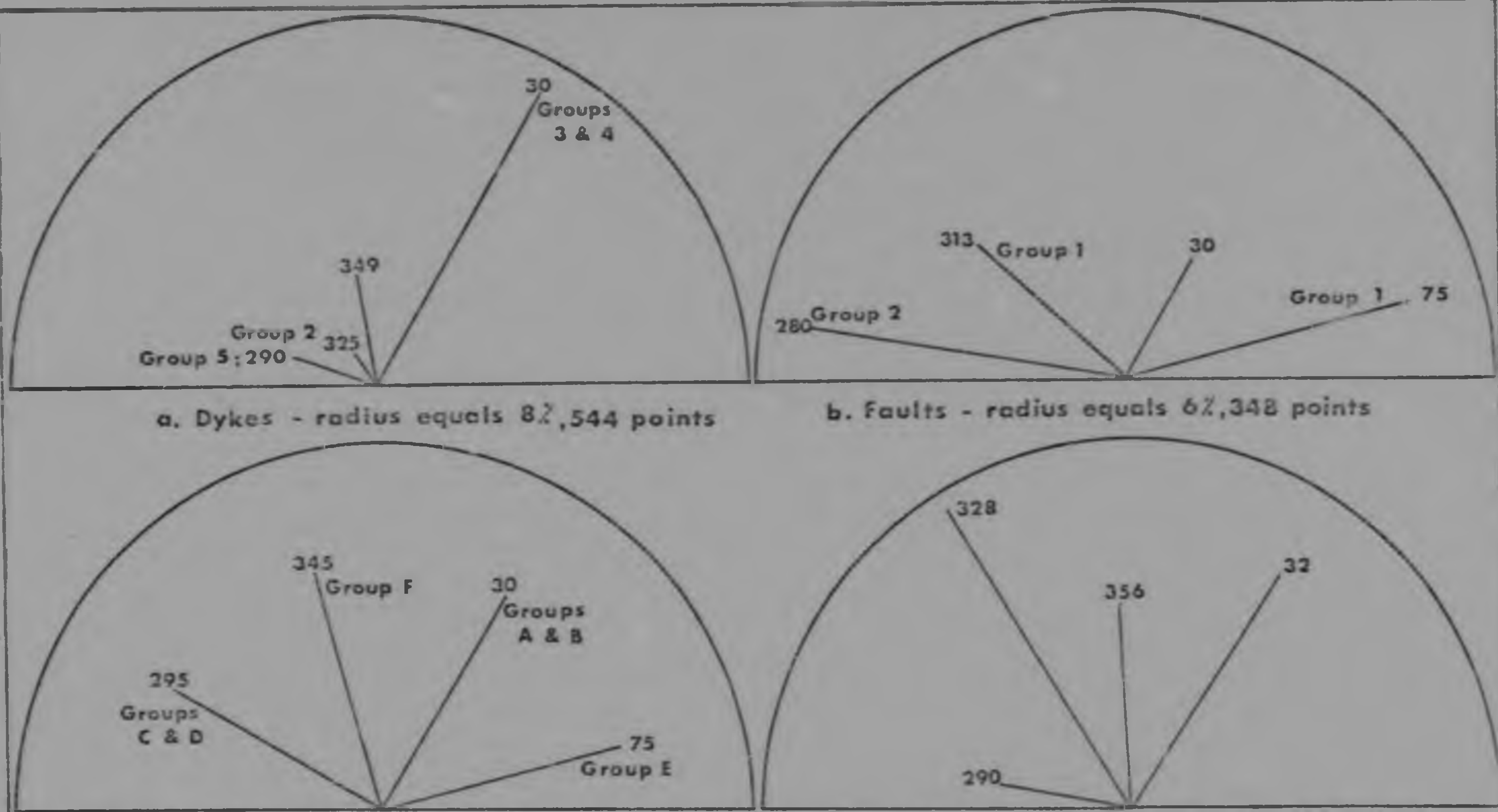

a. Dykes - radius equals 8%,544 points

b. Faults - radius equals 6%,348 points

c. Joints - directions only

d. Regional - radius equals [illegible]%, 414 points

FIGURE 4-3 ROSE DIAGRAMS OF MAIN DYKE, FAULT, JOINT AND REGIONAL TRENDS

With E.R.T.S. imagery it is difficult to know exactly what each lineation represents. Stratigraphy is the most easily recognisable feature due to vegetation variations, topography and curvilinear traces, but most lineations cut across stratigraphy and it is not clear whether they represent dykes, faults for man-made artefacts. In fact, many of the geological faults and dykes plotted in Figure 4.1 do not correlate with the E.R.T.S. lineations but a few do and others run parallel to them.

A much better idea of what lineations represent is obtained by comparing the local E.R.P.M. and regional lineation patterns. In Table 4.2 and Figure 4.3 the strike-frequency data for dykes, faults and joints on the E.R.P.M. are compared with the regional data and it is clear that three out of four regional trends are present in the local E.R.P.M. data. However, the very strong regional lineation at 328° is weak in the E.R.P.M. where it is represented by the Group 2 and Pilanesberg dykes: the 030° regional trend is present in the E.R.P.M. and is comprised of dykes, faults and joints; the faults, joints and dykes oriented about 110° are not strongly represented on the regional scale and finally, the faults and joints oriented along 075° do not show up on the E.R.T.S. lineation analysis. However, it appears that in general the E.R.P.M. structures form a part of the regional lineation pattern and probably reflect the regional stress fields operating at the times the structures were formed.

TABLE 4.2

SUMMARY OF STRIKE FREQUENCY DATA FOR DYKES, FAULTS, JOINTS AND REGIONAL LINEATIONS

	MAIN TRENDS						
Dykes**	-	030°	-	290°	325°	-	349°
Faults**	-	(030°)	075°	280°	-	313°	-
Joints†	-	030°	(075°)	295°	-	-	(345°)*
Regional** lineations	356°	032°	-	(290°)	328°	-	-

* In L74 exploration crosscut only
() Implies a weak concentration
** Mean values
† Strongest trends

4.2 EARLY STRESS SYSTEMS

4.2.1. Introduction

A great deal of experimental and theoretical work has been done on the failure of rock under various stress regimes which shows that the failure patterns of rock can be predicted for a particular stress system. Conversely it is possible to estimate what the stress systems are from the resultant fracture patterns.

Faulting in brittle rocks takes place one one or both of a pair of conjugate failure planes which are inclined at an angle(ψ) of less than 45° to the principal stress direction. This theory is based on the Coulomb and Mohr theories of shear failure and from it the stress systems surrounding reverse, normal and strike-slip faults can be predicted (Jaeger and Cook, 1969, p. 401) as in Figure 3.4. Commonly only one member of the conjugate pair develops preferentially.

The angle (ψ) between the fault plane and the direction of maximum principal stress is given by,

$$\psi = \pi/4 - \phi/2 \qquad (1)$$

where ϕ is the angle of internal friction for rocks. (Jaeger and Cook, 1969, p. 90); if $\phi = 0^{\circ}$ then $\psi = 45^{\circ}$. Jaeger and Cook (1969, p. 402) quote results from several sources which suggest that ψ is between 25° and 30° for normal faults, 20° and 25° for reverse faults and about 30° for strike-slip faults and hence, the angle of internal friction (ϕ) varies between 30° and 40°.

The above discussion assumes that failure is accompanied by a significant displacement of one block past another, that is, faulting. The alternative situation is where no displacement occurs across the fracture zone; that is, jointing and some dyke intrusions. These structures are thought to form parallel to the plane normal to the minimum

TABLE 4-3

ATTITUDES OF EARLY PRINCIPAL STRESSES DEDUCED FROM DYKES, FAULTS AND JOINTS IN THE E.R.P.M.

STRUCTURE	σ_1	σ_2	σ_3	AGE
DYKES:				
GROUP 2	vertical	0/145*	0/055*	BUSHVELD
3	vertical	0/030	0/120	VENTERSDORP
4	vertical	0/030	0/120	VENTERSDORP
5	vertical	0/110	0/020	VENTERSDORP
	vertical	0/165	0/075	PILANESBERG
JOINTS				
GROUPS A, B	vertical	0/030	0/120	VENTERSDORP
C	?	?	?	?
D	vertical	0/120	0/030	VENTERSDORP
E	vertical	0/075	0/165	VENTERSDORP
F	vertical	0/165	0/075	PILANESBERG
FAULTS				
GROUP				
2 normal	vertical	0/100	0/010	LATE WITWATERSRAND
2 reverse	0/010	0/100	vertical	?
1, 3	0/104	80/194	12/014	?

* 0/145 implies a lineation plunging [illegible] towards 145°

principal stress direction, that is, in the plane containing the maximum and intermediate principal stress directions (Anderson, 1951, p. 42; Friedman, 1964). This is the only indication of the principal stress directions that a dyke or a joint gives unless there is also a displacement present. It is common in the E.R.P.M. for vertical displacements to occur across vertical dykes; in these cases it can be assumed that the maximum principal stress is approximately vertical.

Using these principles the orientations of pre-existing stress systems that have operated in the E.R.P.M. and the surrounding districts can be estimated from the orientations and geometry of dykes, faults, joints and the regional lineation patterns. This is done in the following sections for each group of structural discontinuities, from which a stress history for the mine is deduced.

4.2.2. Dykes

The orientations of the dyke groups found in the mine are plotted on a rose diagram in Figure 4.2a, excluding Group 1 (a single dyke/sill) and Group 6(dykes and sills that do not fit into any other group).

In Table 4.3 the attitudes of the early principal stresses as deduced from these sets of dykes are listed assuming that the minimum principal stress lies normal to the plane of the intrusion and the maximum principal stress is vertical; this latter assumption is reasonably valid considering the vertical displacement across many of the vertical dykes and that a stress system due to gravity will have the maximum principal stress vertical. The intermediate and minimum principal stresses are horizontal but as discussed in Chapter 2, the orthogonal geometry of the intrusives indicates that the orientations of these principal stresses may be transposed during a particular period.

4.2.3. Joints

In Chapter 3B six groups of joints, termed A to F were recognised. These six sets have been marked on a rose diagram (Figure 4.2c) and are listed in Table 4.3 with their possible times of formation and the orientations of the minimum principal stress direction. The maximum principal stress has been assumed to be approximately vertical in Table 4.3 because of the probable correlation to dykes of a similar age. However, no conclusive evidence is available for defining the intermediate and maximum principal stress directions.

Group A and B joints are comprised of Type 1 mining induced joints and a vertically dipping geological set. The latter group is possibly pre-Ventersdorp or penecontemparaneous with Ventersdorp intrusives because the intrusion of a dyke in H shaft is distinctly controlled by joints of these sets (see Chapters 2 or 3B). No age control is available on Group C joints, which are parallel to bedding. Group D joints are subparallel to Group 5 dykes and Group 2 faults and by association with the dykes are Ventersdorp or older. Group E joints are subparallel to Group 1 faults and are possibly of a similar age and finally Group F joints are subparallel to the Pilanesberg age dykes and hence may be of a similar age or older. The joints of groups A or B and D may have formed contemporaneously because of their association with Ventersdorp intrusives but groups E and F are likely to be of different ages.

4.2.4. Faulting

Three main faulting trends and a minor one were established in Chapter 3A; these are illustrated in Figure 4.2b and the associated stress systems are listed in Table 4.3. No dynamic analysis was carried out for the weakest group of faults which strikes at 030°. Movements on these faults probably accompanied the intrusion of the Ventersdorp dykes in the same orientation.

Group 2 faults, which strike subparallel to bedding, have been discussed in some detail in Chapter 2A in terms of fault 50. They appear to have

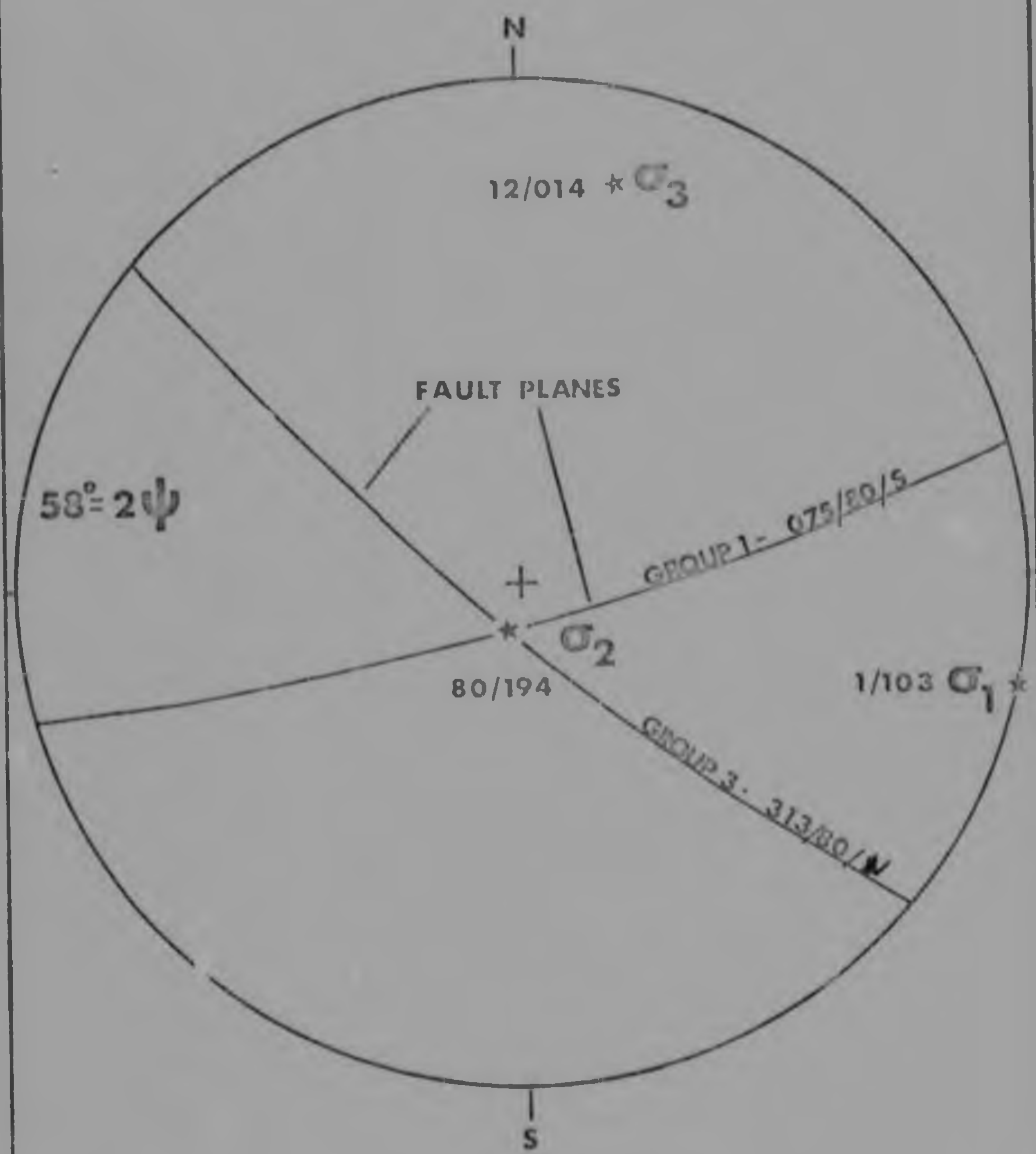

FIGURE 4-4 DETERMINATION OF PRINCIPAL STRESS DIRECTIONS FOR THE CONJUGATE FAULTS

formed as normal faults as a response to the lengthening of the basin floor during sedimentation but those near surface were later modified into reverse faults; the deeper faults were not modified because of a much larger vertical stress, due to overburden, than at surface. Near surface these faults have a downthrow to the north and at depth to the south; all faults dip south or are vertical. The determined stress field at the time of their formation as normal faults has the maximum principal stress vertical, the intermediate horizontal, trending at 100^{o}, and the minimum principal stress horizontal trending at 010^{o}. To reactivate the fault into a reverse fault the maximum principal stress must be inclined to the existing fault plane at less than 45^{o}, so that on the relatively steeply dipping faults seen in the mine it should plunge steeply southwards. However, at deeper levels in the basin, these faults can have shallower dips and the maximum principal stress can be near horizontal. This orientation is assumed in fixing the positions of the principal stresses as given in Table 4.3.

The other two groups of faults, numbers 1 and 3 represent a pair of conjugate fractures with group 1 faults better developed than those of group 3.

Both groups have significant strike slip movements, the sense of displacement being dextral for group 1 and sinistral for group 3, while group 1 has a downthrow to the south and group 3, a downthrow to the north. The two sets of faults displace each other at several localities but the derived age relationships are not constant, which suggests a contemporaneous age. In Figure 4.4 the stress system associated with the formation of the conjugate faults is illustrated. In deriving these principal stress directions the maximum principal stress

TABLE 4-4

GEOLOGICAL AND STRESS HISTORY OF THE E.R.P.M.

EVENT	DESCRIPTION	AGE	σ_1	σ_2	σ_3
1	Sedimentation of the Witwatersrand Basin;deposition of the gold bearing reefs. Basining processes started causing tension in basin floor	Witwatersrand			
2	Normal faulting around basin edges caused by lengthening of b[illegible] floor. Group 2 faults.	late-Witwatersrand	90°	0°/100°	0°/010°
3	Formation of an orthogonal joint set; one parallel to sediment strike (Group D) and one parallel to sediment dip (Groups A,B) - possibly on a regional scale	probably early Ventersdorp	90°	0°/120°**	0°/030°
4	Intrusion of Ventersdorp dykes and ceposition of the Ventersdorp lava piles - on a regional scale.				
a.	Group 5 dykes	during Ventersdorp times	90°	0°/110°	0°/020°
b.	Group 4 dykes - fine grained, altered		90°	0°/030°	0°/120°
c.	Group 3 dykes - coarser and fresher		90°	0°/030°	0°/120°
5	Formation of the conjugate pairs of faults (Groups 1 and 3) and mild closure of the basin about north-south axis	probably between Ventersdorp	0°/104°	80°/194°	12°/014°
6	Formation of the rever[illegible] movement on Group 2 faults and mild close of the basin about an east-west axis	and Bushveld times	0°/010°	0°/100°	90°
7	Intrusion of Bushveld dykes and sills				
a.	Simmer dyke	Bushveld			
b.	Group 2 dykes	Bushveld	90°	0°/145°	0°/055°

8	Formation of joint groups E and F	may be contemporaneous	90°	$0^{\circ}/075^{\circ}$ **	$0^{\circ}/165^{\circ}$
9	Intrusion of Pilanesberg age intrusives- also on a regional scale	Pilanesberg	90°	$0^{\circ}/165^{\circ}$	$0^{\circ}/075^{\circ}$

* '$0^{\circ}/110^{\circ}$' implies a lineation plunging 0° towards 110° and '90°' implies that the lineation is vertical

** implies that the stress directions are interchangeable.

has been set so that it bisects the acute angle between the faulting planes:this maximum principal stress is horizontal trending at 104^{o}; the intermediate principal stress plunges at 80^{o} towards 194^{o} and the minimum principal stress plunges at 12^{o} towards 014^{o}. The angle, 2ψ, between the fault planes equals 58^{o} and from equation (1) the associated angle of friction (ϕ) is 32^{o} which agrees well with the reported values given above.

Possible ages of the faults are also listed in Table 4.3. The initial development of Group 2 faults probably took place in late-Witwatersrand or early Ventersdorp times with reactivation to form reverse faults at a later stage. The age of group 1 and 3 faults is not clear.

4.3 BRIEF GEOLOGICAL AND STRESS HISTORY OF THE E.R.P.M.

Based on the discussions in Chapters 1, 2,3 and the first parts of this chapter a geological and stress history of the mine area can be built up. In addition an indication of some of the ancient regional stresses is given by extrapolation of local stress fields to a regional scale where similar lineation patterns are present. These histories are summarized in chronological order, starting with the sedimentation of the Witwatersrand Basin, in Table 4.4.

TABLE 5-1

MECHANICAL PROPERTIES OF SOME ROCKS FROM THE E.R.P.M.
AND THE WITWATERSRAND

ROCK TYPE	LOCATION	Co (MPa)	E (MPa x 10^5)	ν	No. of Specimens	Reference
Non-decomposed diabase	G shaft, Dyke 79	432	1,01	0,25	ns	1
decomposed diabase	G shaft, Dyke 79	230	0,73	0,24	ns	1
diabase dyke						
- chill phase	G64W Dyke 79	446	1,05	0,27	ns	2
- decomposing	G64W Dyke 79	215	0,77	0,25	ns	2
- slightly decomposed	G64W Dyke 79	237	0,69	0,23	ns	2
- slightly decomposed	G64W Dyke 79	419	0,96	0,24	ns	2
Karroo dolerite	?	331	0,84	ns	ns	3
Aplite sill ("chert dyke")	H73 & 77E	457	0,78	0,28	12	4
Quartzite						
-hangingwall	H75E	352	0,86	0,14	10	5*
-footwall	H75E	212	0,75	0,20	10	5*
-hangingwall	F,G,H;67	288	0,83	0,14	152	6**
-footwall	and 68 levels	237	0,83	0,20	37	6**

1 The Rock Mechanics Research Team (1959b)

2 The Rock Mechanics Research Team (1959a)

3 Wiebols et al. (1968)

4 Fumerton (1975)

5 McGarr et al (1975)

6 Grobbelaar (1957)

* Specimens with a 3:1, length: diameter ratio; strain-gauges used.

** Specimens with a 1:1, length; diameter ratio; extensometer used.

NOTE: Specimens with a 3:1, length: diameter ratio and strain gauges were used in this dissertation

ns means not stated in the original reference.

CHAPTER 5

ROCK MECHANICS

5.1 INTRODUCTION AND METHODS

The notation used in this chapter is listed at the beginning of the dissertation.

An understanding into the problem of rockbursts when mining near or within dykes and the association between seismic events and dykes requires an understanding of the physical properties of the dykes and their host rocks. Previous determinations of the mechanical properties of rocks from the Witwatersrand, and, in particular from the E.R.P.M., have been concentrated on the host rocks; that is, the quartzites, shales and conglomeratic reefs (see for example: Grobbelaar, 1957; Rock Mechanics Research Team, 1957, 1959a; McGarr et al., 1975). Two important conclusions from this work are: (1) the hanging-wall rocks have a higher Young's Modulus than the footwall quartzites (see Table 5.1), implying that because of their ability to store a greater amount of elastic energy, they are more prone to seismic events (McGarr et al., 1975) and (2) the hanging-wall quartzites are considerably stronger than footwall quartzites.

Far le[illegible] data on the mechanical properties of the intrusive rocks are available; the results of a few tests by previous workers are listed in Table 5.1. These results show (1) a marked variation in the mechanical properties as a result of various degrees of decomposition and (2) that a chill phase on the dyke contact with the quartzites is stronger than a normal non-decomposed diabase.

The aim of the present study is to determine if the mechanical properties vary in a systematic manner across a dyke, if they can be correlated with the geological features established in Chapter 2 and if

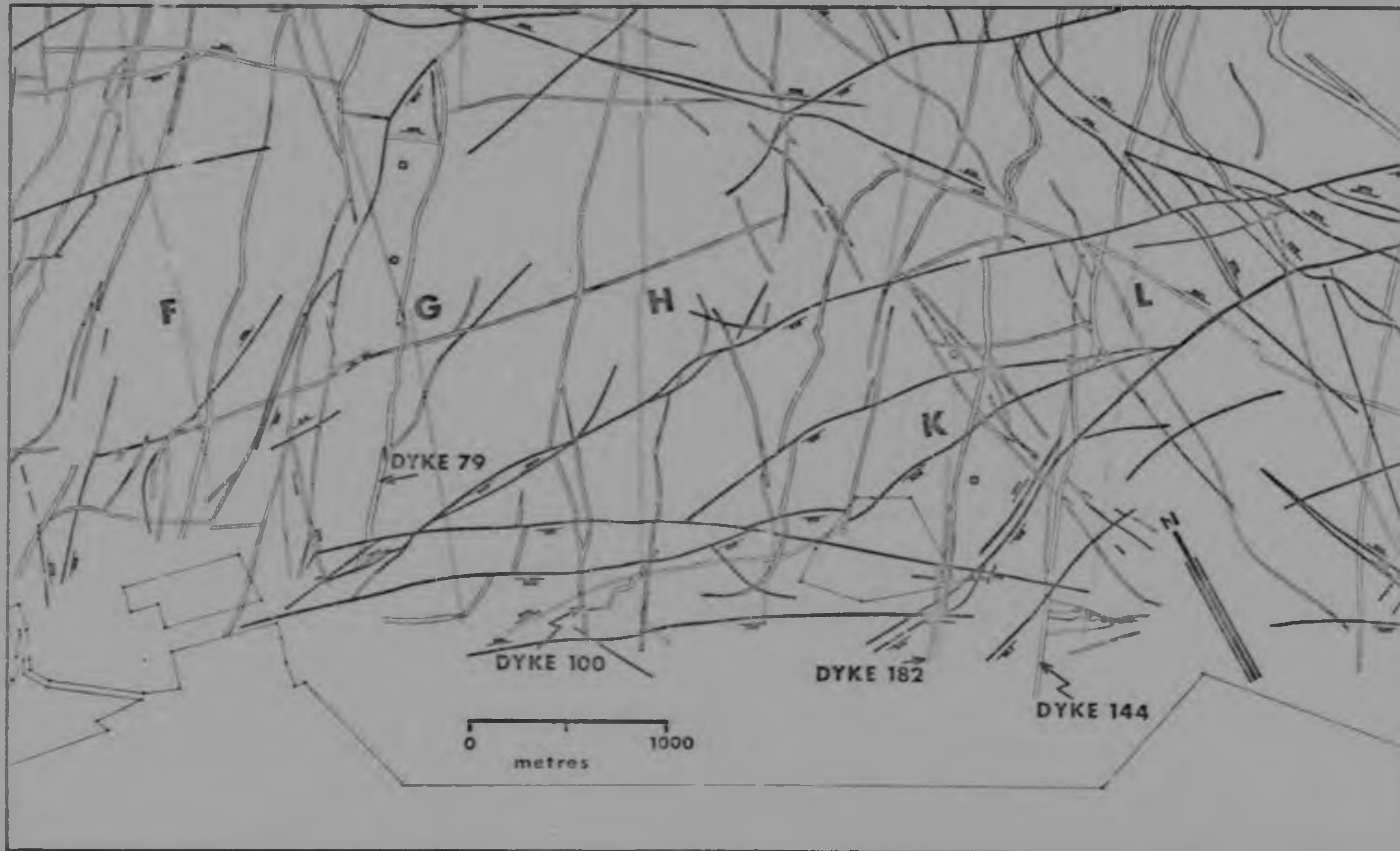
F
G
H
K
L
N
DYKE 79
DYKE 100
DYKE 182
DYKE 144
0
1000
metres

FIGURE 5.1

Plan of a section of the E.R.P.M. showing the locations of dykes used for rock mechanics.

Vertical shaft

Incline sh

Mine boun

Dyke

Fault showing downthrown side

there is any correlation between them and rockburst incidence. Four dykes, the locations of which are marked on Figure 5.1, have been studied, and the uniaxial compressive strength, static Young's modulus and Poisson's Ratio have been determined for a total of 76 specimens. In addition, a suite of 10 specimens from dyke 144 have been tested to failure under various triaxial stress conditions and six Brazilian tests have been done to obtain an estimate of the uniaxial tensile strength.

Densities have not been determined but previous determinations by the Rock Mechanics Research Team (1959a, 1959b) indicate a density range of 2770-2950 kg/m^3 for the basic dykes compared to 2670-2720 kg/m^3 for the quartzites.

All specimens were prepared from borehole cores of either AXT (32,5 mm diameter) or EX(21,6 mm) size which were drilled through each dyke. Groups of two or three specimens were selected at regular intervals along each hole. Geological inhomogeneities were avoided as much as possible but specimens often contained closed joints and cleavage zones that only became apparent during testing and also the numerous quartz-chloritic veins present in the dykes were often unavoidable. The effects of such inhomogeneities will be discussed in section 3.1 of this chapter.

Each specimen was turned on a lathe into a right-circular cylinder with a diameter of about 24 mm and a length to diameter ratio of approximately three for the uniaxial compressive strength tests; a diameter of about 30 mm and a length of 60 mm for the triaxial tests and a diameter of about 32 mm and a length to diameter ratio of approximately one third for the Brazilian tests.

The length to diameter ratio of three was chosen for the uniaxial tests because it allows a large area of uniform stress distribution in the centre of the specimens, even allowing for contact effects with the end platens (Hallbauer et al.,1973). Two vertical and two horizontal 10 mm long strain gauges were attached with Hottinger X-60 cement onto each specimen except for those from dyke 182 where only two vertical strain gauges were attached.

For the triaxial strength tests the specimen size was governed by the size of the Hoek triaxial cell used and for the Brazilian tests the specimen size was not crucial provided all specimens are of a similar size because specimen dimensions are included in the formula for tensile strength. Strain gauges were not used in these tests.

For the uniaxial compression tests, specimens were loaded at an average rate of approximately one megapascal per second with interruptions at intervals of approximately 30 MPa to read the horizontal and vertical strain increments on the Huggenberger strain meters. Because the testing machine used is not stiff very few readings were obtained after specimen failure had commenced. For the triaxial tests an axial load of about 75 MPa was applied before the confining pressure and the specimen was loaded without interruption until failure. Similarly, Brazilian test specimens were loaded at a slow uniform rate until failure. For the triaxial and Brazilian tests only the load at failure and specimen dimensions were recorded.

5.2 RESULTS

5.2.1. Uniaxial Tests

After testing, the raw data for each specimen consisted of the distance of the specimen from the contact, the diameter, length, load at failure and the axial and lateral strain increment readings. A computer programme, written in conjunction with Mr S L Fumerton, was used to determine the uniaxial compressive strength, the incremental Poisson's ratio for each load increment and to produce graphs of stress against strain, axial strain against lateral strain and stress against volume strain for each specimen. It was considered necessary to compute the incremental Poisson's ratio because it varies markedly during testing and is linked to both the volume changes and failure of the specimen. For comparison purposes, the value of Poisson's ratio for each dyke was determined in a consistent manner: on the curve of axial strain plotted against lateral strain, a tangent was drawn to the point where the rate of change of curvature is least (in all tests this was near to the corresponding load of 100 MPa). The slope of this tangent is the Poisson's ratio. Uniaxial compressive strength, Poisson's ratio, Young's modulus and volume changes were calculated using the following formulae. The uniaxial compressive strength(C_0) is given by:

$$C_0 = (4.L/\pi d^2).10^3$$

where L is the load in kilonewtons and d is the diameter of the specimen in millimetres. In uniaxial stress (that is, $\sigma_1 \neq \sigma_2 = \sigma_3 = 0$) the fractional change in volume (Δ) is given by:

$$\Delta = \varepsilon_1 + 2\varepsilon_2$$

(after, Jaeger and Cook, 1969; p. 106). The Poisson's ratio(ν) is defined as the ratio of lateral strain to axial strain ($-\varepsilon_2/\varepsilon_1$) and Young's Modulus (E) as the ratio of stress to strain(σ_1/ε_1). (Jaeger and Cook, 1969; p. 103). Note that the value of ε_2, being expansion, is reckoned negative.

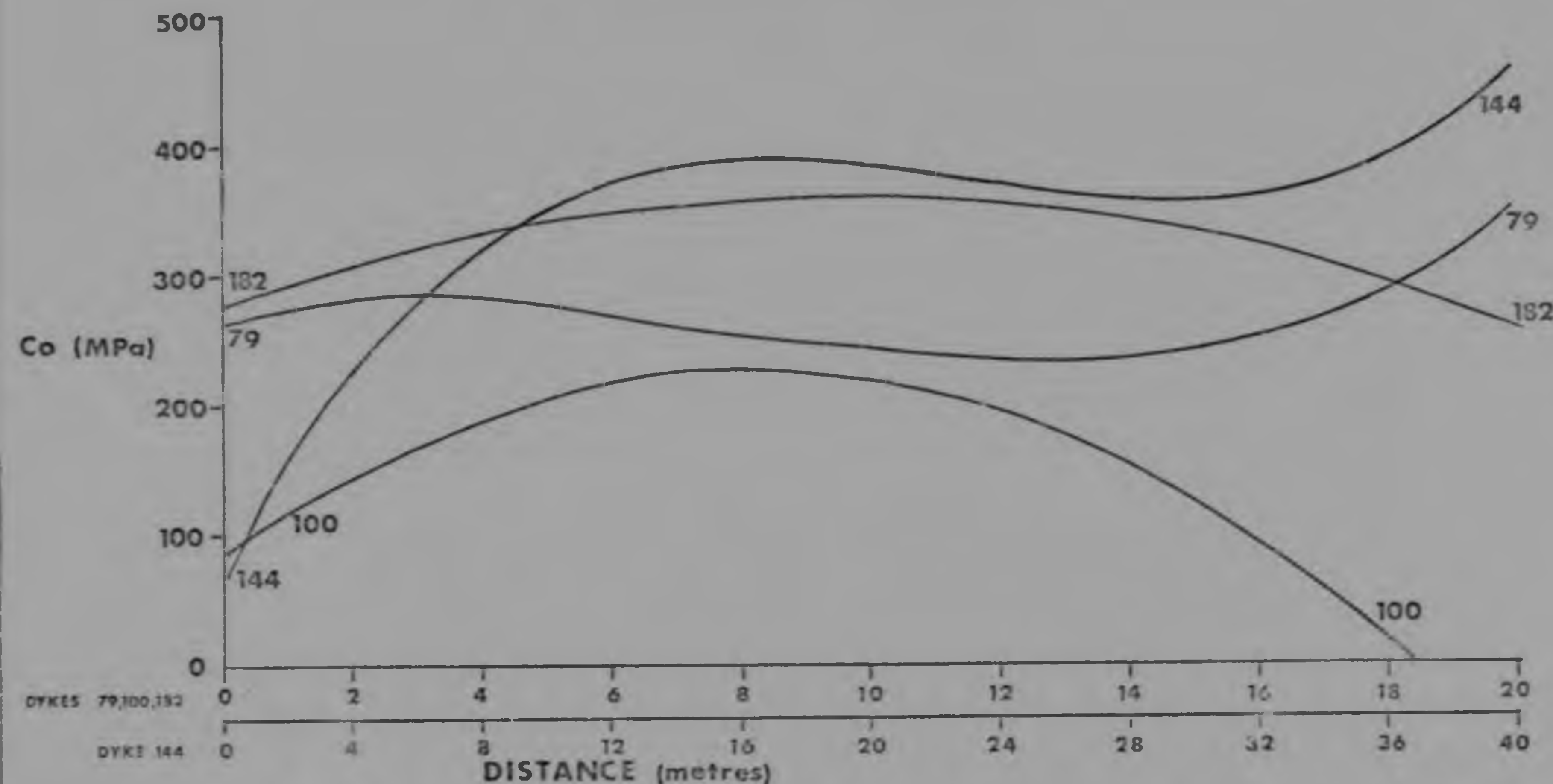

FIGURE 5-2 CURVES OF BEST FIT FOR UNIAXIAL COMPRESSIVE STRENGTH(Co) PLOTTED AGAINST DISTANCE

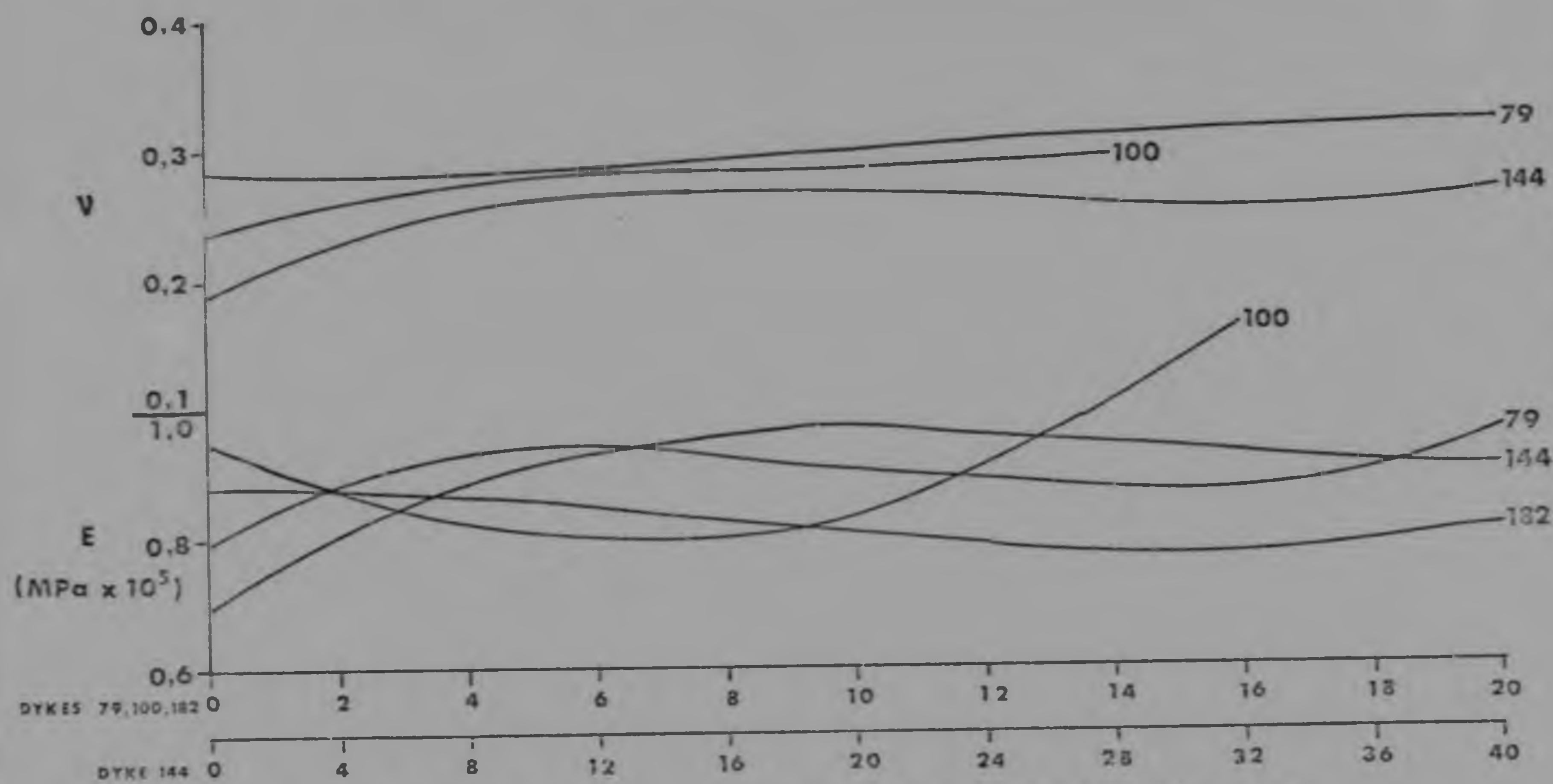

FIGURE 5-3 CURVES OF BEST FIT FOR YOUNG'S MODULUS(E) AND POISSON'S RATIO(V)

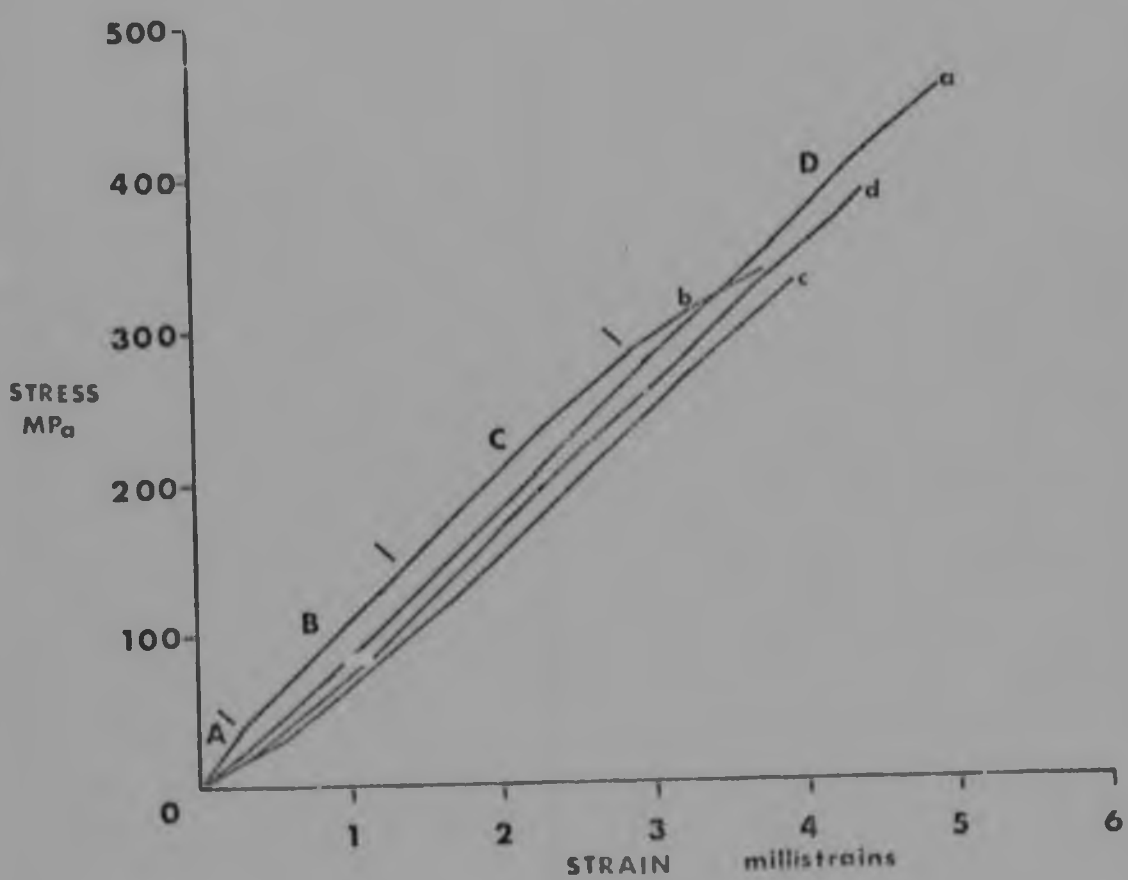

FIGURE 5-4 TYPICAL STRESS-STRAIN CURVES

SAMPLE NUMERS

a. Dyke 144 - 78,0 m

b. Dyke 100 - 28,0 m

c. Dyke 100 - 19,1 m

d. Dyke 79 - 48,2 m

e. Dyke 144 - 49,1 m

f. Dyke 79 - 28,3 m

Letters refer to curves on Figures 5-4 and 5-5.

A, B, C and D are explained in the text

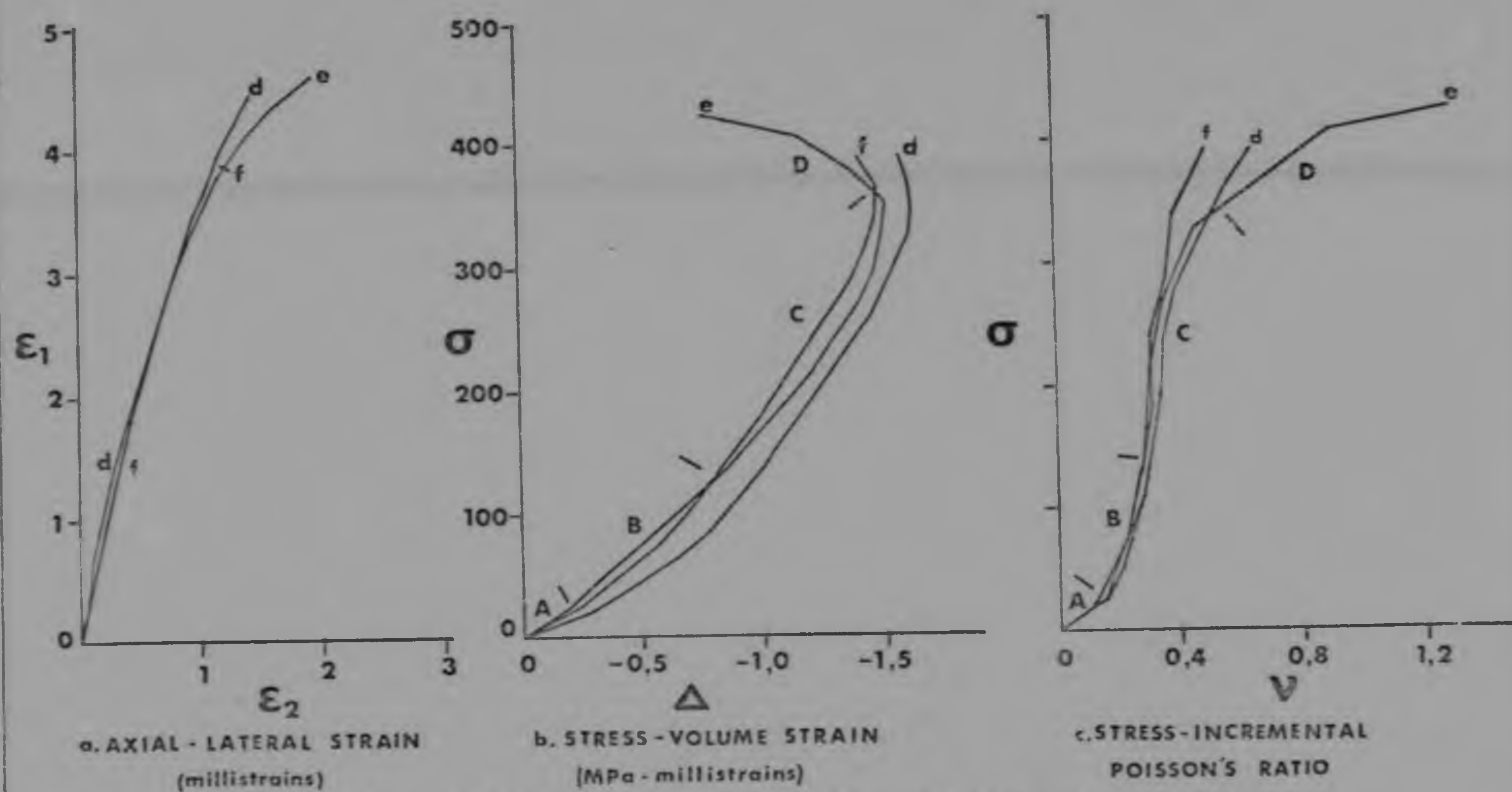

FIGURE 5-5 RELATIONSHIP BETWEEN STRESS(σ), STRAIN(ε), VOLUME STRAIN(Δ) AND POISSON'S RATIO(ν). A, B, C and D are explained in the text

TABLE 5-2

AVERAGE ELASTIC PROPERTIES FOR DYKES 79,100,144
AND 182 IN UNIAXIAL COMPRESSION*

DYKE NUMBER	C_0 (MPa)			E (MPa x 10^5)			ν		
	m	s	n	m	s	n	m	s	n
79	277	62,9	15	0,90	0,10	15	0,29	0,03	15
100	281	66,2	17	0,87	0,12	17	0,28	0,03	17
182	331	52,2	20	0,83	0,07	19	n.d.	-	-
144	361	82,4	15	0,91	0,06	15	0,26	0,02	15
ALL SPECIMENS	313	74,1	67	0,87	0,10	66	0,28	0,03	47

* Specimens considered to be seriously affected by geological inhomogeneities or uneven loading have been excluded.

C_0 : uniaxial compressive strength

E : Young's Modulus

ν : Poissons ratio

m : average value

s : standard deviation

n : number of samples

n.d.: not determined

TABLE 5.3

TRIAXIAL TEST CONDITIONS AND RESULTS FOR DYKE 144

SPECIMEN NUMBER	DIAMETER (mm)	LENGTH (mm)	RATIO d/H	σ_1 at failure (MPa)	$\sigma_2=\sigma_3$ at failure (MPa)	$A=\sigma_1/C_0$	$B=\sigma_3/C_0$	μ	ϕ	S_0 (MPa)
1	30,25	60,00	1,98	550	10	1,429	0,026	1,9	62°	49
2	29,95	60,05	2,01	518	10	1,345	0,026	1,7	60°	50
3	30,25	59,40	1,96	605	20	1,571	0,052	1,5	56°	61
4	29,95	59,95	2,00	603	20	1,566	0,052	1,5	56°	60
5	30,00	60,55	2,02	637	30	1,655	0,078	1,3	52°	67
6	30,05	60,95	2,03	705	40	1,831	0,104	1,2	50°	74
7	30,25	59,55	1,97	717	40	1,862	0,104	1,3	52°	65
8	29,90	59,10	1,98	755	50	1,961	0,130	1,2	50°	69
9	29,90	60,55	2,03	855	70	2,221	0,182	1,1	48°	72
AVERAGE VALUES								1,4	54°	63,2

d= diameter

H= length

$\sigma_1, \sigma_2, \sigma_3$ = maximum, intermediate and minimum principal stresses.

S_0= intrinsic shear strength; C_0= uniaxial compressive strength.

μ = coefficient of internal friction; ϕ= angle of internal friction.

The results are presented in tabular and diagrammatic form and are discussed in Section 5.3. The figures, tables and their whereabouts are:

A: Figures: 5.1 Location of drill holes and dykes used for specimen collection

5.2 Best-fit curves of C_0 plotted against distance

5.3 Best-fit curves E and ν plotted against distance

5.4 Graphs of stress plotted against strain

5.5 Graphs of axial strain plotted against lateral strain, stress against volume strain and stress against Poisson's ratio.

B: Tables: 5.2 Average elastic properties for all dykes.

C: Appendix Figures: 2A, Plots of actual determined values of ν, E and C_0 against distance for dyke 79.

2B, Plots of actual determined values of ν, E and C_0 against distance for dyke 100.

2C, Plots of actual determined values of ν, E and C_0 against distance for dyke 182.

2D, Plots of actual determined values of ν, E and C_0 against distance for dyke 144.

D: Appendix Tests: 2A, Mechanical Properties of dyke 79

2B, Mechanical Properties of dyke 100

2C, Mechanical Properties of dyke 182

2D, Mechanical Properties of dyke 144

5.2.2. Triaxial tests

Nine specimens chosen from near the centre of dyke 144, have been tested to failure in triaxial compression such that, $\sigma_1 \neq 0$ and $\sigma_2 = \sigma_3 \neq 0$. Tests were done for various confining pressures in the range 10 MPa to 70 MPa. The specimen dimensions, testing conditions and results are listed in Table 5.3.

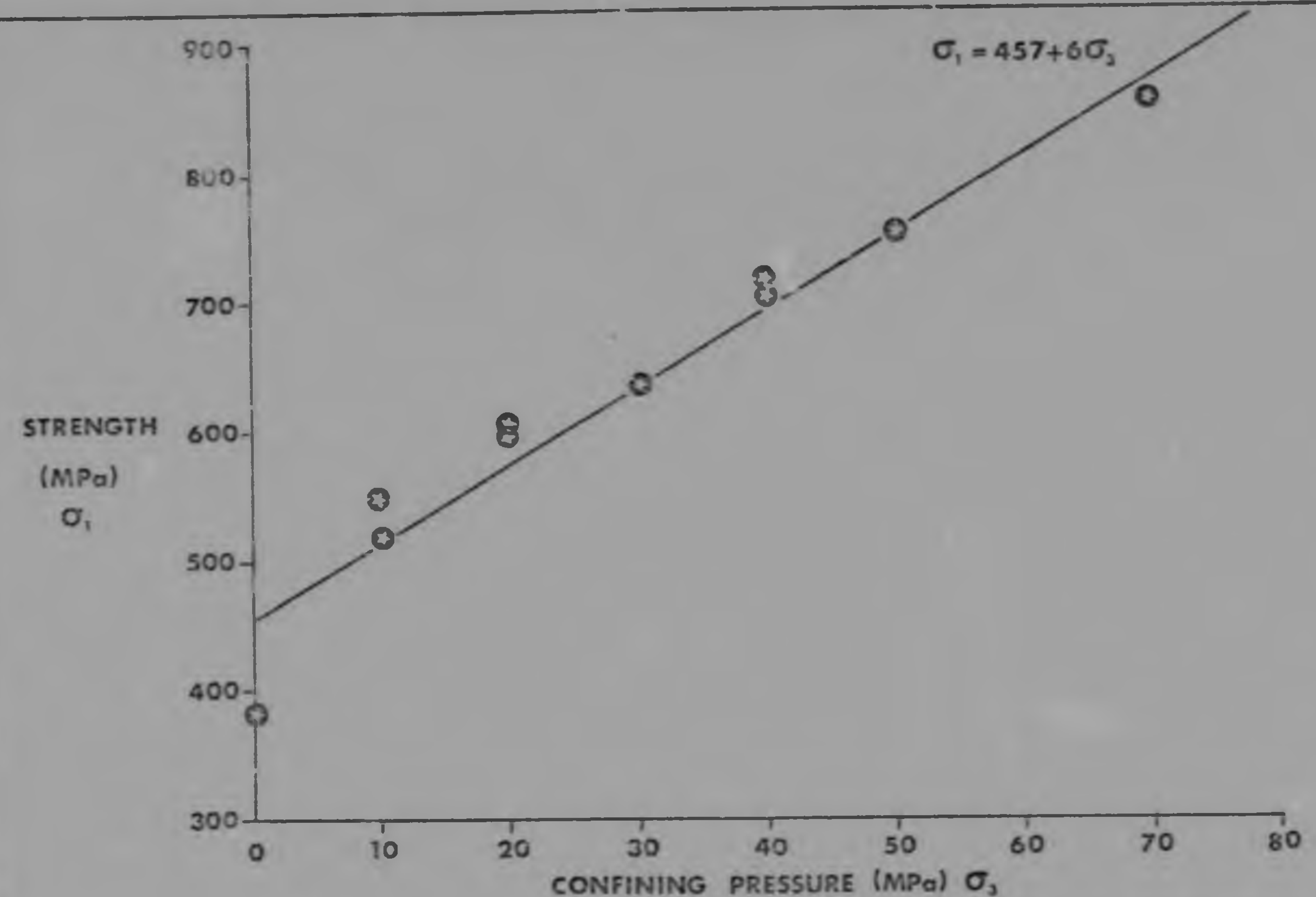

FIGURE 5-6 VARIATIONS IN STRENGTH WITH CONFINING PRESSURE

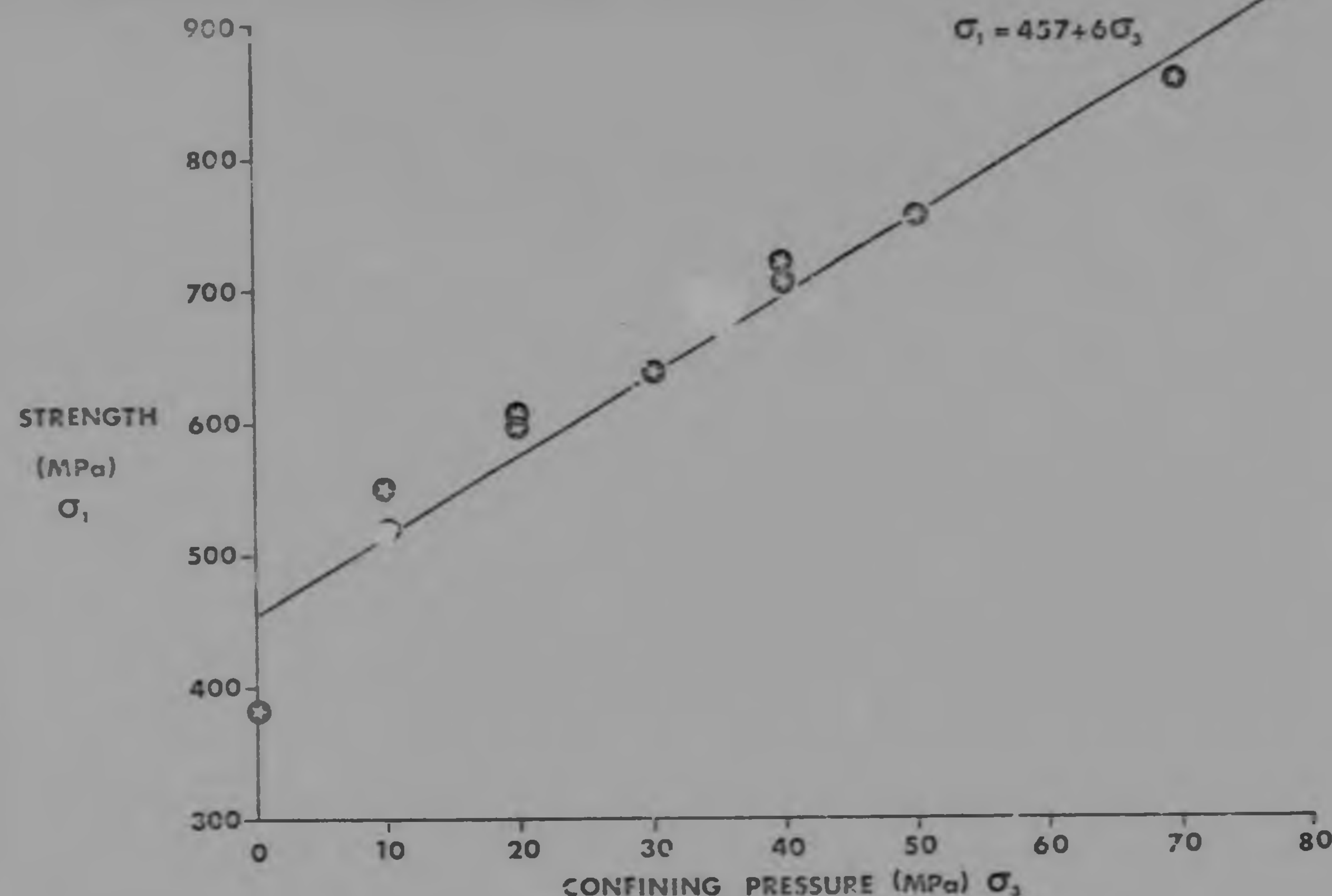

FIGURE 5-6 VARIATIONS IN STRENGTH WITH CONFINING PRESSURE

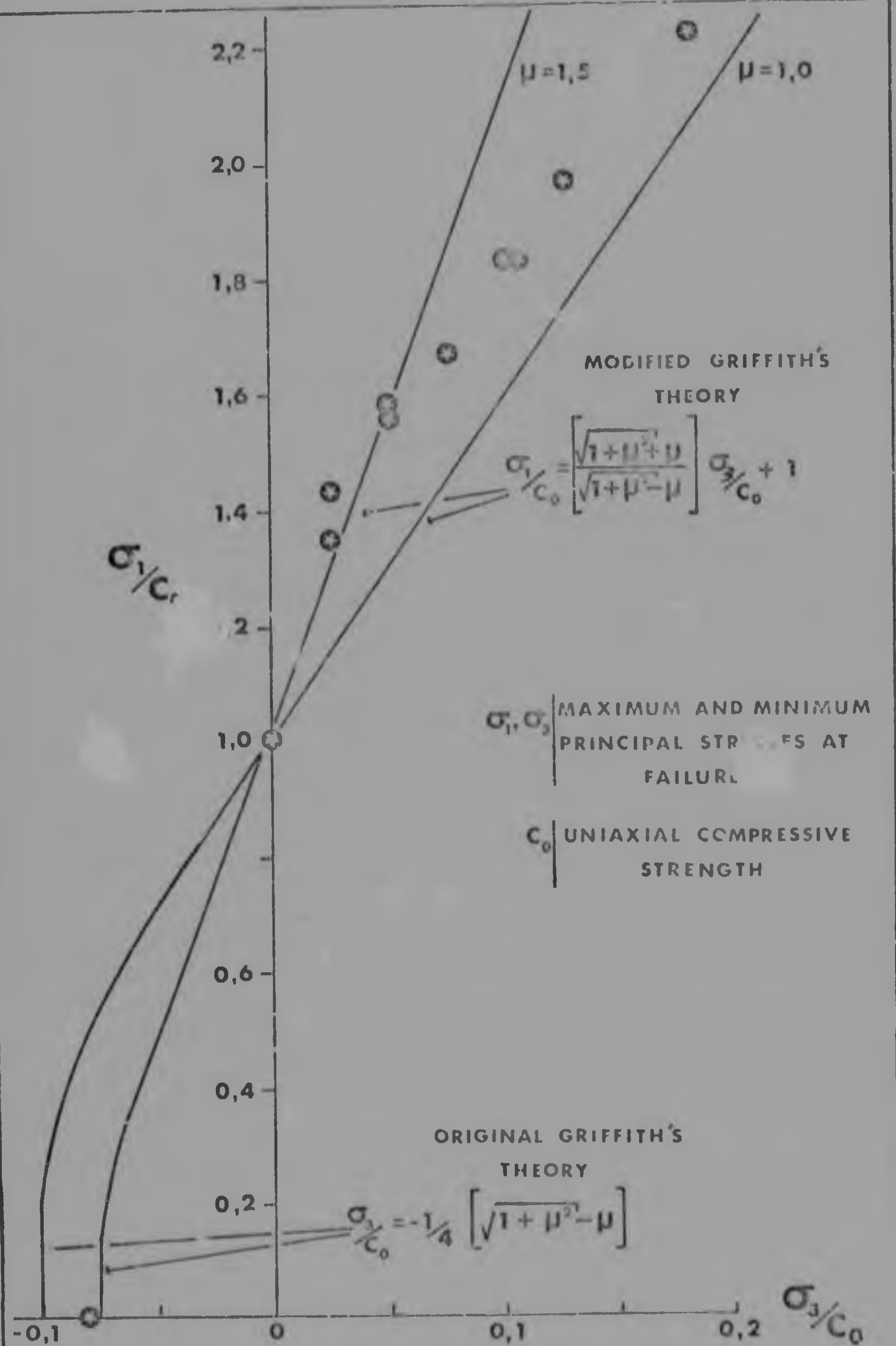

FIGURE 5-7 COMPARISON BETWEEN MEASURED STRENGTHS AND FAILURE CRITERIA

There are several ways of representing triaxial data graphically. The simplest method is to plot axial stress at failure against confining pressure. This has been done in Figure 5.6 for the data in Table 5.3., together with an average value for the uniaxial compression strength, 385 MPa, determined from specimens taken in the same part of the dyke.

Another convenient method of representing triaxial testing results is to reduce the maximum principal stress (σ_1) and the confining stress(σ_3) to a dimensionless form by dividing them by the uniaxial compressive strength (C_0) and then plotting together as in Figure 5.7. (Hoek, 1965). On this figure are also plotted the curves for the original and the modified Griffith fracture criteria for coefficients of friction (μ) of 1,0 and 1,5. In addition the value of μ has been determined for each of the test specimens using the following formulae. The modified Griffith criterion is given as,

$$\sigma_1/C_0 = ((1+\mu^2)^{1/2} + \mu)/(1+\mu^2)^{1/2} - \mu)).\ (\sigma_3/C_0) + 1$$

Hoek, 1965, p. 52)

which can be rearranged to

$$\mu = (A - B - 1)/2(AB - B)^{1/2}),$$

where $A = \sigma_1/C_0$ and $B = \sigma_3/C_0$.

The angle of internal friction (ϕ) can be determined using the formula,

$$\mu = \tan \phi \text{ (Jaeger and Cook, 1969, p. 90)},$$

assuming a Mohr-Coulomb criteria.

In addition, the intrinsic shear strength (S_0) can be determined for each specimen; it is defined in Figure 5.8 in terms of a Mohr circle. It is common for the value of S_0 to be measured from a Mohr circle diagram, however, it can be calculated using the following equations which are derived, using basic trigonometry, from Figure 5.8.(inset)

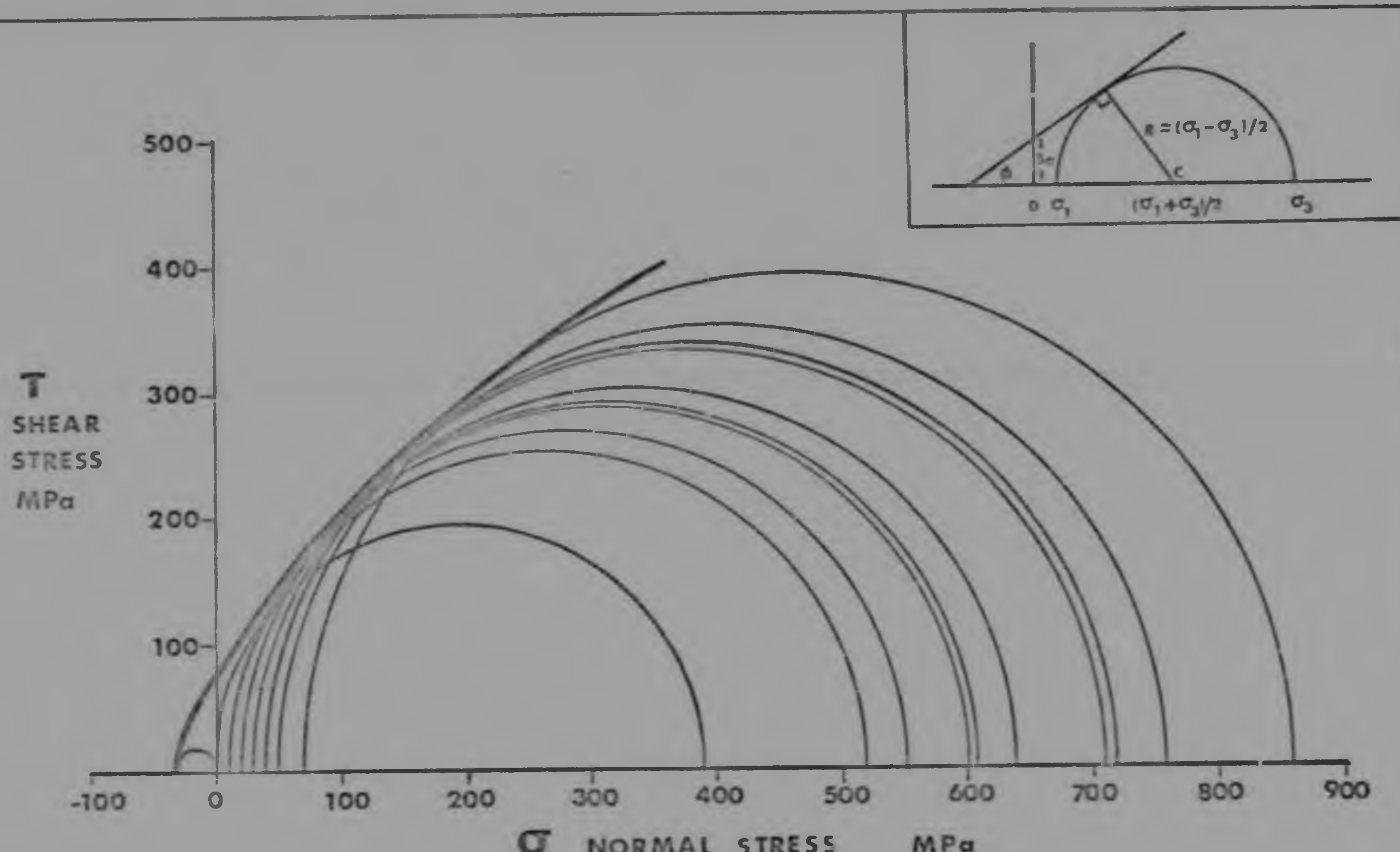

FIGURE 5-8 MOHR ENVELOPE FOR DYKE 144

TABLE 5-4

BRAZILIAN TEST RESULTS

SAMPLE NUMBER	HEIGHT (mm)	DIAMETER (mm)	RATIO	LOAD kN	TENSILE STRENGTH MPa
1	11,8	32,35	2,74	19,2	32
2	11,5	32,35	2,81	17,6	30
3	11,2	32,35	2,89	20,0	35
4	11,6	32,35	3,05	14,2	26
5	11,2	32,35	2,89	17,2	30
6	11,8	32,35	3,00	17,8	32

MEAN TENSILE STRENGTH = 31 MPa

$S_0 = ((R/\mathrm{Sin}\ \phi) - C)\ \mathrm{Tan}\ \phi$

where $R = (\sigma_1 - \sigma_3)/2$ = radius of the Mohr circle,

and $C = (\sigma_1 + \sigma_3)/2$ = centre of the Mohr circle.

Values of μ , ϕ and S_0 for each test specimen are listed in Table 5.3; normally the results are averaged out graphically; that is, one value of each parameter for a series of tests are given but the present tests show a regular variation in the parameters, hence, a value for each specimen is given. The mathematical calculation of S_0 assumes a failure envelope conforming to the Mohr-Coulomb criterion.

5.2.3. Brazilian Tests

Six discs were compressed, using the Brazilian technique (Jaegar and Cook, 1969, p. 160) to obtain an estimate of the uniaxial tensile strength (T_0). The tensile strength is determined using the relationship,

$T_0 = (2.L/\pi.d.H).10^3$ (Obert and Duval, 1967),

where L is the load in kilonewtons, d is the diameter and H is the length. The specimen dimensions and values of T_0 for each specimen listed in Table 5.4.

The average tensile strength has been plotted with the triaxial test results discussed in 5.2.3. above as a series of Mohr circles from which the Mohr envelope for the rock was obtained (Figure 5.8).

5.3 DISCUSSION OF RESULTS

5.3.1. General

One of the most noteable features of the results is the great difference in behaviour of the individual dykes, as well as in the absolute values of the mechanical properties within each dyke. It is clear from the curves of best fit in Figures 5.2, 3 and 4(see also Appendix Figures 2A, 2B, 2C and 2D) that there is a variation in mechanical properties across each dyke which may, perhaps be explained in terms of geological parameters such as alteration, coarseness, composition, etc. However, the differences in properties between adjacent specimens requires discussion. These can partly be explained by the presence of inherent weaknesses that only become apparent during loading (i.e. that are reactivated by loading), by obvious and unavoidable geological discontinuities such as veining and, occasionally by uneven loading. As regards to the first point, in some tests, closed joints and minor shear zones were opened during testing thus inducing premature failure. Secondly, the diamond drill cores were often locally permeated with veins of calcite, quartz or quartz-chlorite composition. This was especially so for dyke 100 and although calcitic veining was always avoided, quartz and chloritic veins, which ranged in thickness up to two or three millimetres, were regularly present in test specimens. Surprisingly, the failure planes were never coincident with these veins. Although the presence of geological discontinuities means that the physical properties of pure dyke plus veining are being measured, it also means that a more realistic picture of the properties of the dyke are being obtained. With respect to the third point, b far the most detrimental effect on the specimens was uneven loading caused by the sticking of a spherical seat. This causes spalling of the over-loaded side and crushing of the top of the specimen thus reducing the area onto which the load is transmitted resulting in premature failure. Those specimens considered to have been seriously affected by shearing, jointing or uneven loading have not been included in the best-fit curves and in Appendix 3, Tables 1 to 4, they are marked with an asterisk.

5.3.2. Uniaxial Compressive Strength (Figure 5.2)

In this section the quoted uniaxial compressive strengths and means do not include those specimens marked with an asterisk in Appendix Tables 2A, B, C and D.

The uniaxial compressive strengths vary between 159 MPa and 480 MPa, with an average strength of 311 MPa. This value is similar to those reported by previous workers (Table 5.1). The dykes are invariably stronger than footwall quartzites and appear to be stronger than the hangingwall quartzites tested by Grobbelaar (1957) but are weaker than those tested by McGarr et al. (1975). The discrepancies between the resu'ts of McGarr et al. and Grobbelaar are at least partly due to the different stratigraphic horizons of the samples, namely: immediately adjacent to the reef(Grobbelaar) and at distances up to 50 or 60 metres from the reef into the hanging and footwalls (McGarr et al.). Comparing the average strengths given in Table 5.1 and the different sample localities, it appears that hangingwall quartzites get stronger and footwall quartzites weaker away from the reef, although this is contrary to a statement by the Rock Mechanics Research Team (1959a, p.6). The differences may also be due to the different specimen geometry (see footnotes for Table 5.1).

It is clear from the curves of best fit for each dyke (Figure 5.2) that the dykes fall into two distinct groups. Dykes 100 and 182 are strongest towards their centre and weakest towards their contact regions and have a parabolic curve of best fit symmetrical about the centre of the dyke. On the other hand, dykes 79 and 144 are weak on one contact, stronger towards the centre, a little weaker towards the other contact and strongest at this other contact, and thus have asymmetrical cubic curves of best fit. Within each of these two groups the members can be distinguished by strength differences. Dykes 79 and 100 are the weakest on average and dykes 144 and 182 the strongest (see Appendix 3, Tables and Figures 2A, 2B, 2C and 2D.

5.3.3. Young's Modulus (Figure 5.3)

Young's Modulus varies considerably within each dyke and the average values range from 0,83 to 0,91 x 10^5 MPa, with an overall average of 0,87 x 10^5 MPa(see Table 5.2 for standard deviations)

The results compare well with previous work listed in Table 5.1 but a comparison with the quartzite results reveal that the mean modulus for all dykes is higher than that for both hangingwall and footwall quartzites.

In Appendix Figures 2A, 2B, 2C and 2D Young's Modulus is compared to the uniaxial compressive strength across each dyke. The two parameters vary sympathetically in dyke 79 but they are distinctly non-sympathetic in dyke 100. In dykes 144 and 182 the relations are not regular.

5.3.4. Real Poisson's Ratio (Figure 5.3)

Poisson's ratios reported here are a little higher than those found by previous workers (Table 5.1) and are significantly higher than the value for the quartzites, being almost double that for hangingwall quartzites. In general, Poisson's ratio does not vary significantly across the dykes; the mean values for the dykes lie between 0,26 and 0,29 and the mean for all specimens tested is 0,28.

5.3.5. Stress-strain curves, volume changes and mechanisms of brittle fracture (Figures 5.5)

In this section the results of the tests are related to the mechanisms of brittle fracture of rock, as described by Bieniawski (1967). He described five stages in the behaviour of rock during compression, namely,

A. Closing of cracks

B. Linear elastic deformation

C. Stable fracture propagation

D. Unstable fracture propagation

E. Forking or coalescence of cracks.

It is rare in uniaxial compression for stage D to be present and stage E is always absent. According to Bieniawski (1967) stage C starts at about 35% of the maximum stress and D at about 80%. In the figures referred to below, these stages are indicated by their respective letters.

Four typical stress-strain curves are plotted in Figure 5.4. Apart from curve 'b', the curves are almost linear indicating only elastic deformation (stages A, B and C). Failure in all specimens was sudden and violent with little or no tendency to behave inelastically (stage D). Curve 'b' in Figure 5.4 is an example of one of the few specimens that showed signs of unstable fracture propagation(stage D).

Three graphs, all related to volume changes, can be constructed. These are a graph of axial against lateral strain from which the incremental and tangential Poisson's ratio can be calculated(Figure 5.5a); a graph of stress against volume strain(Figure 5.5b) and a graph of stress against incremental Poisson's ratio (Figure 5.5c) as determined from Figure 5.5a). In Figure 5.5a Poisson's ratio is given by the slope of the tangent to the curve, this slope should be constant for elastic material, but because of fracturing within the specimen during testing, the material becomes inelastic and the curve becomes non-linear. Ideally, Poisson's ratio is less than 0,5 (which corresponds to a negative volume change) but when greater than 0,5 the material becomes discontinuous as the volume increases. In most of the test specimens failure occurred as soon as the volume started to increase (curves 'f' and 'd' in Figure 5.5b) but occasionally quite large volume increases were measured (curve 'e'). The point where the incremental Poisson's


148
a
b
c
d
e

PLATE 5.1

Typical failure patterns of the dykes in uniaxial compression

a. Dyke 79. Classical conjugate failure planes. Most of the fragments are large and fine comminution is rare.

b. Dyke 79. Failure by two or three clean fractures. Comminution is absent.

c. Dyke 100. An unusual failure by the bottom of the specimen 'kicking-out'.

d. Dyke 100. Failure by several parallel shear planes. Comminution is rare.

e. Typical failure of specimens from dykes 144 and 182. A large volume of finely comminuted material is present.

ratio passes through a value of 0,5; that is, when volume change becomes positive, is equivalent to the transition from stable to unstable fracture propagation (stage C to D). In Figures 5.5b and c, regions A to C represent decreasing volume change and region D is one of increasing volume change.

Although inelastic behaviour was present in many specimens only brittle failure was observed. All specimens failed violently but the behaviour during testing and the appearance of the failed specimens differed from dyke to dyke (Plate 5.1). Specimens from dyke 144 and 182 'talked' (i.e. displayed microseismic activity) from about 75% of their failure strength but those from dykes 79 and 100 either 'talked' just at failure or not at all. Dyke 79 specimens did not fail as violently as the others tested but went with a large 'bang' across thin shear planes with only a minor volume of comminuted material. Specimens from dyke 100 usually failed with a dull, sudden thud and the failure zone consisted of many fractures with little comminuted material. For several specimens of dyke 100 the bottom 'kicked out' (Plate 5.1), which was a feature not noticed on other specimens. Dykes 144 and 182 failed comparatively slowly, gradually crumbling away until a final, violent failure. The failure plane consisted of a thick zone of highly comminuted material.

5.3.6. Triaxial tests on dyke 144

In Figure 5.6 the load at failure has been plotted against confining pressure. The most noteable features of this plot are (1) the large jump in compressive strength between confining pressures of 0 and 10 MPa, and (2) the linear relationship between strength and confining pressure at confining pressures greater than 10 MPa. With respect to the first point, the initial increase may be due to closing of inherent cracks in the rock by the confining pressure with a resultant increase in strength. The relationship between σ_1 and σ_3 at failure is represented by the empirical equation,

$\sigma_1 = C_0 + K\sigma_3$ (Price, 1966, p. 24)

In Figure 5.6, the equation of the straight line of best fit is,

$\sigma_1 = 457 + 6\sigma_3$,

but the value of C_0 as indicated by this equation is significantly greater than the average value for C_0 of 385 MPa which was determined above. Possible reasons for this discrepancy have been discussed above. Values for the constant K are commonly between 2,0 and 15,0 for rocks and more specifically, between 2,0 and 5,0 for competent argillaceous rocks, between 5,0 and 10,0 for competent arenaceous rock and greater than 10,0 for igneous rocks (Price, 1966, p. 24-25). A value of 6,0 for the present work is a little lower than is common for igneous rocks. Cook(1963) has determined the value of K for E.R.P.M. quartzites to be about six also, therefore, the strengths of quartzites and dykes in the E.R.P.M. respond to increasing confining pressure in a similar fashion. In Figure 5.7 a plot of normalized axial stress against normalized confining pressure, the present data is compared with the modified and original Griffith criterion using values for the coefficient of internal friction (μ) of 1,0 and 1,5. For the experimental results, μ is not constant but tends to decrease with increasing confining pressure as does the related angle of friction (ϕ). The significance of this unusual feature is not clear. Average values of 1,4 for μ and 54^o for ϕ are probably representative for the rock.

In Figure 5.8, Mohr circles for the triaxial, uniaxial and tensile results are plotted together with the derived Mohr envelope. The envelope is concave inwards and does not conform to the envelopes for either of the Griffith or modified Griffith criteria. However,

TABLE 5-5

SUMMARY OF THE MECHANICAL AND MAIN GEOLOGICAL PROPERTIES OF THE DYKES

	DYKE 79	DYKE 100	DYKE 144	DYKE 182
Average Co(MPa)	277(271)	282(274)	361(354)	331(278)
Shape of curve of best fit	Cubic(East is strongest contact)	Parabolic	Cubic(West is strongest contact)	Parabolic
Average E (MPa x 10^5)	0,90	0,87	0,83	0,91
Average	0,29	0,28	-	0,26
Thickness	21,1m	15,5m	41,4m	19,8m
Location	G-west	H-west	L-west	K-central
Dyke group from Chapter 2	4	3	3	3
Main petrographic features	finegrained, altered	medium grained	large feldspar phenocrysts abundant, medium grained	
Contacts-EAST	chilled, sharp	chilled but 1-8cm of shearing on both	small, mylonite zones	chilled, small sheared area
WEST	small mylonite zones		chilled, sharp	thick mylonite zone

it does predict a cohesive shear strength of about 75 MPa which agrees roughly with the average value of the calculated shear strengths (S_0) listed in Table 5.3. This value of S_0 is slightly larger than twice the uniaxial tensile strength which is predicted by the modified Griffith criterion.

5.4 COMPARISON OF THE ROCK MECHANIC PROPERTIES WITH GEOLOGICAL OBSERVATIONS AND GENERAL CONCLUSIONS

Several distinct differences between the rock mechanic properties of the four dykes are present. These are summarized in Table 5.5 together with some geological features of the dykes.

Dykes 144 and 182 are by far the strongest two dykes and these two are the coarsest grained, both containing large feldspar phenocrysts. Of the other two dykes, number 79 is the weakest, has the finest grain size and is the most altered. Dyke 100 is finer grained than dykes 144 and 182 even though it has been categorized as similar to them in Chapter 2. No association can be made between Young's modulus or Poisson's ratio and geological parameters.

Possibly the most important correlation is between strength variations across the dykes and contact relationships. The two different patterns, namely parabolic for dykes 100 and 182 and cubic for 79 and 144, can be correlated with the amount of shearing on the contacts. Alteration in the rocks adjacent to sheared zones occurs easily and hence the dykes are weakened. In other words, one would expect dykes with sheared contacts to be stronger in their central regions than they are near the contacts. Conversely, chilled contacts between dykes and quartzites are impervious to alteration and the strength of dyke rocks at these contacts would be expected to be higher. A study of the contact relationships supports these ideas. Dyke 100 has well developed sheared mylonitic contacts and corresponding low strengths in these regions. Dyke 182 also has mylonite on both contacts but that on the east contact is poorly developed compared to the thick mylonite zone on the west contact. The strength of the east contact averages 272 MPa whilst on the west contact three specimens averaged only 59 MPa. Similar relationships can be constructed for the other two dykes but in both cases, and especially for dyke 144, a chilled and welded contact appears to have caused considerable increases in strength near one contact. These are the east contact of dyke 79 and the west contact of dyke 144 (from borehole observations only).

The strength of the dykes may also be related to their tendency to fail violently as rockbursts. For example it is known that the seismicity in the hangingwall is much greater than in the footwall quartzites of the E.R.P.M. (McGarr et al.,1975) and that the hangingwall rocks are stronger and have a higher Young's modulus than the footwall rocks. McGarr et al. concluded that this implied that the hangingwall rocks could store much more elastic strain energy and were therefore more prone to seismicity. A similar conclusion can be drawn for dykes 79 and 144, both of which have a higher Young's Modulus than the hangingwall quartzites and are stronger than them, particularly at the welded contacts. The validity of this conclusion is supported by the burst history of dyke 144 which has proved impossible to mine through or to keep open a tunnel in, for the 16 levels below 58 level.

In Chapter 2, section 2.3.4., the geochemical and petrological variations across dyke 182 were discussed in order to compare them with the rock mechanic trends. The main petrological variations have been discussed above in terms of strengths and a correlation was made. Although the geochemistry varies in a similar manner about the centre of the dyke, albeit in a mild fashion, it seems more likely that the strength changes are due to grain size variations and contact relationships rather than slight chemical variations in the minerals.

CHAPTER 6

STUDIES OF THE EFFECTS OF STRUCTURAL DISCONTINUITIES ON THE DISTRIBUTION OF ROCKBURSTS AND SEISMIC EVENTS

6.1 STUDY OF THE EFFECTS OF STRUCTURAL DISCONTINUITIES ON THE DISTRIBUTION OF ROCKBURSTS

A rockburst can be simply defined as a sudden and violent rupture of rock into a mining excavation that causes damage to that excavation. A more rigid definition of a rockburst can be found in Chapter 1.

The aims of this study are to establish: (1) if the structural discontinuities (that is, dykes and faults) significantly control the distribution of rockbursts; (2) which discontinuities during a period of time have controlled the distribution of rockbursts and (3) which geological aspects of the disconuities can be considered as important in controlling the distribution of rockbursts. In section 6.2 a similar study, relating to seismic foci and structural discontinuities is discussed.

In the introductory chapter of this dissertation (section 1.4) some previous work was described which illustrated that the incidence of rockbursts increases when an active mining face is near a dyke or a fault. In addition, much statistical work, relating the distribution of seismic events and rockbursts with such parameters as dykes, faults, raises, angles of working face, abutment types, rate of face advance, stoping width excavation size etc. has been carried out (see reference list in Pretorius, 1966), but there has been no previous attempt to categorize individual structural discontinuities and the geological features of these discontinuities by their association with rockbursts.

6.1.1. Data used

Rockburst location data was obtained from an E.R.P.M. map drawn

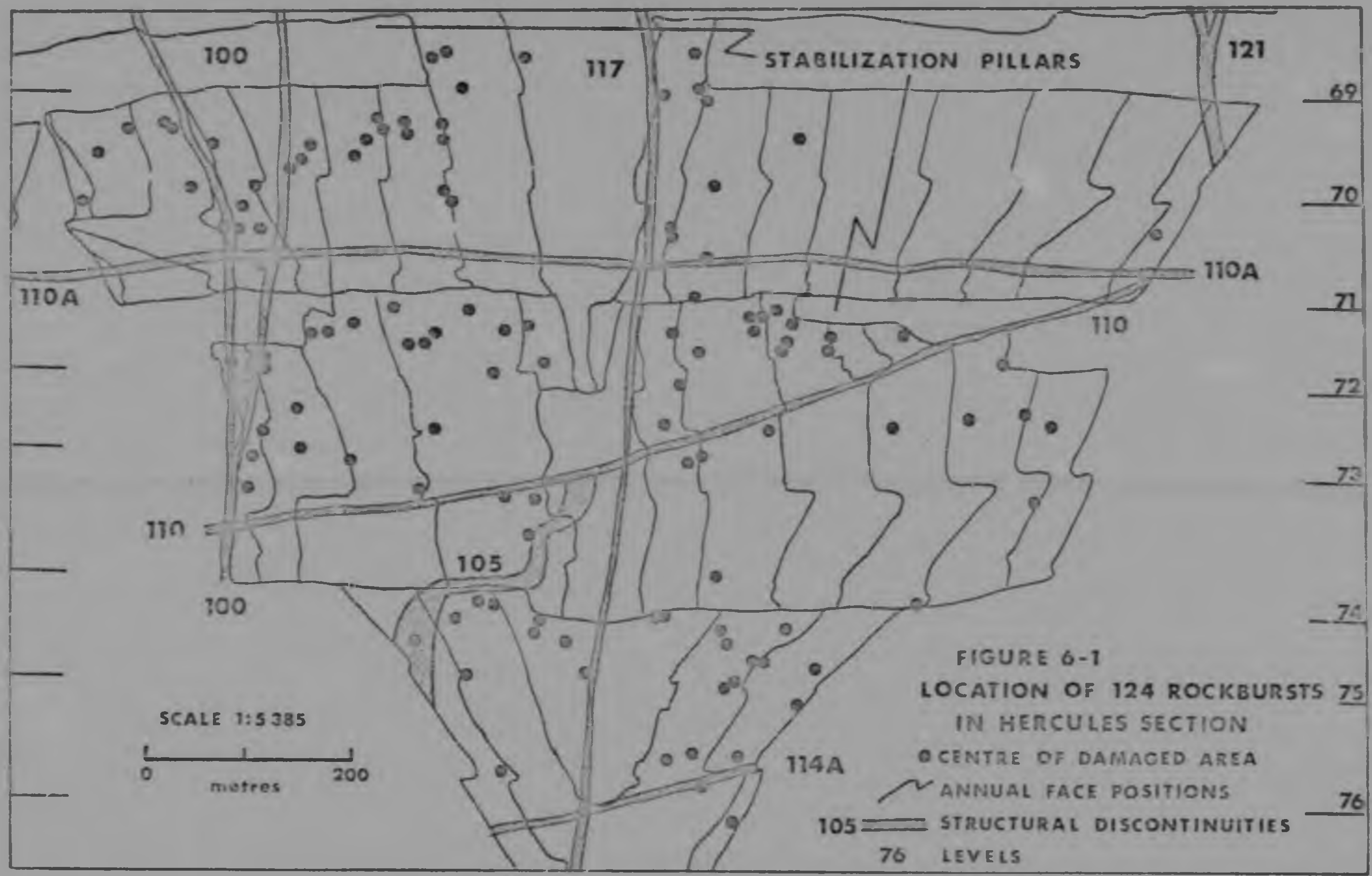

FIGURE 6-1
LOCATION OF 124 ROCKBURSTS
IN HERCULES SECTION

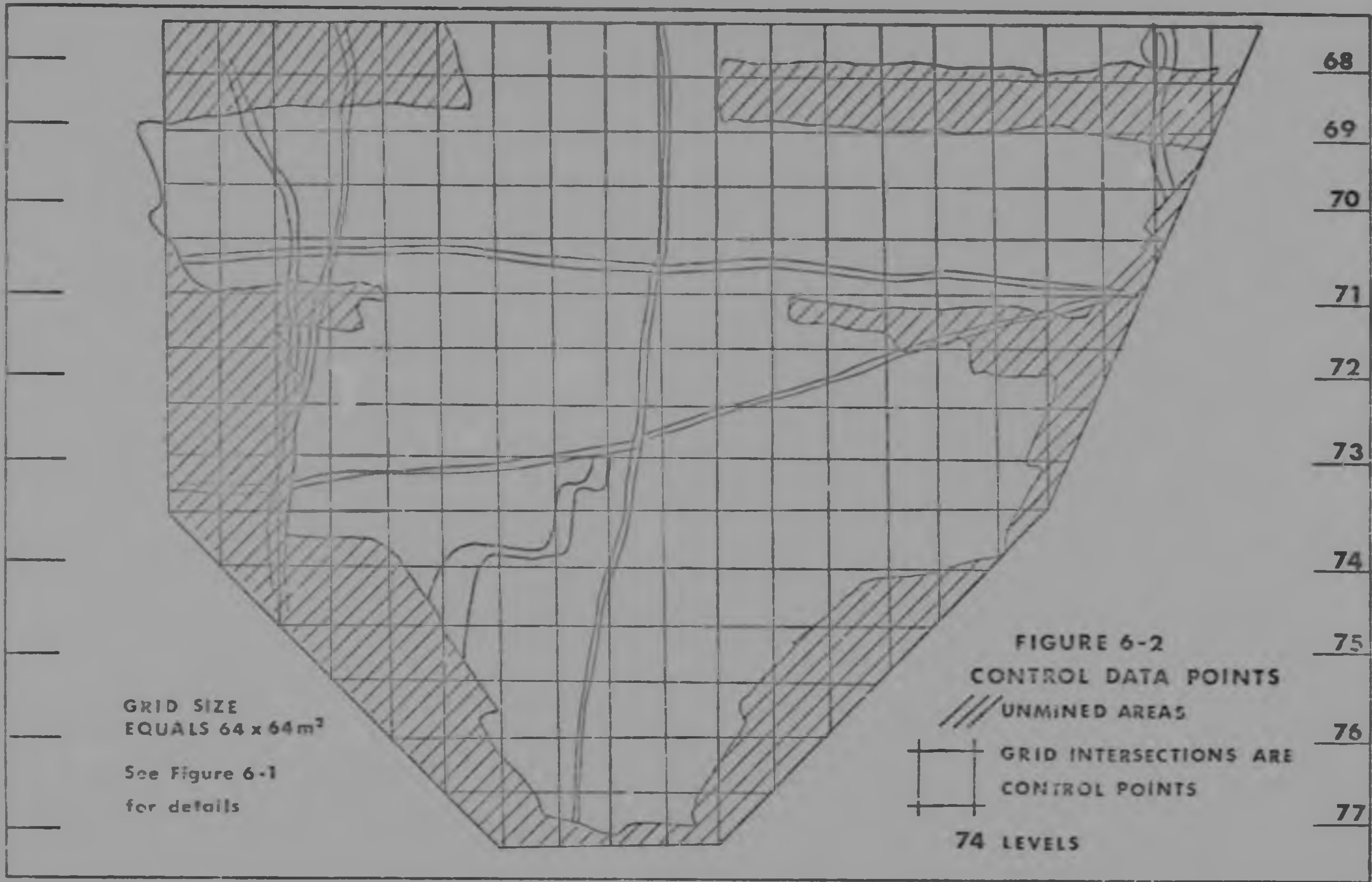

FIGURE 6-2
CONTROL DATA POINTS

during a study of the effects of stablisation pillars on the incidence of rockbursts in Hercules section, levels 69 to 77, from 30.6.62 to 31.12.69. During this 7,5 year period 124 bursts were recorded and approximately 516 500 m^2 of reef were mined, an average burst incidence of 0,24 per 10^3 m^2 mined. A m^2 implies a volume one metre by one metre by the height of the stope. The rockburst sites and the geological discontinuities considered are illustrated in Figure 6.1.

A control set of data was also derived so that a comparison could be obtained between what could be expected without constraints on rockburst locations and what actually happened. A square grid was placed over the area mined and each grid intersection was used as a control point. The locations of the control points are indicated in Figure 6.2.

6.1.2. Method of analysis

The analysis of control and rockburst points was identical. Each point was allocated a unique number and the location, depth, percentage excavation within a radius of 50 metres at the time of the burst, and the number of dykes and faults within a radius of 100 metres were recorded. In addition the strikes and distances of the two closest dykes and two closest faults to the particular burst were recorded.

This data has been analysed using a simple computer program which lists for each discontinuity a summary of distance to rockburst sites, percentage of excavated area, and the number of dykes and faults within 100 metres of each rockburst site.

In the analysis each rockburst or control point can be counted as many times as there are discontinuities within 100 m. Hence, although there are only 124 burst and 151 control points, they have been counted 169 and 206 times respectively. Two further points should

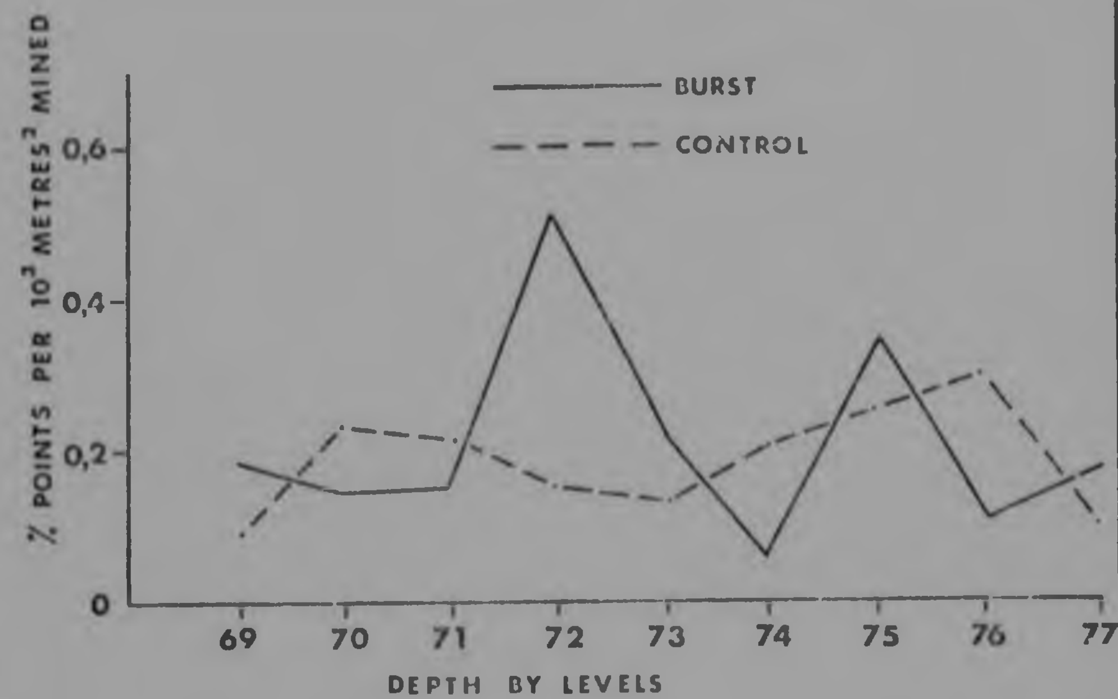

FIGURE 6-3 VARIATION IN FREQUENCY OF POINTS PER AREA MINED WITH DEPTH

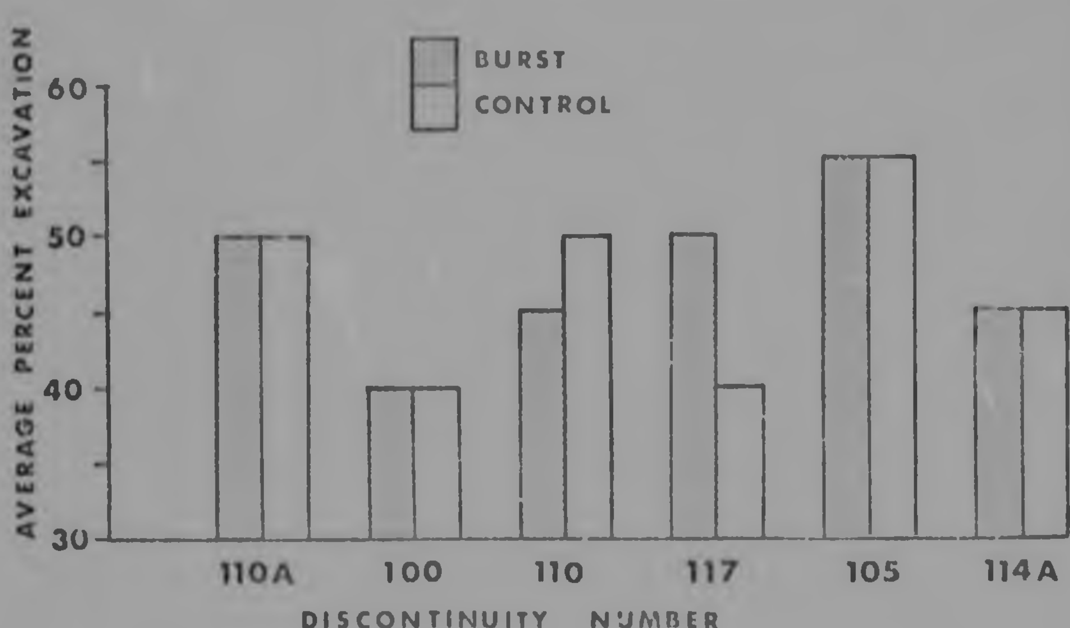

FIGURE 6-4 AVERAGE AREA MINED-OUT (PERCENT EXCAVATION) FOR BURST AND CONTROL POINTS FOR EACH DISCONTINUITY

be noted with respect to the discussions below. Firstly, the number of rockbursts and area mined near dyke 121 are considered to be too small for firm conclusions to be made for this dyke and secondly, unusual mining configuration has not been considered in the analysis although areas where a significant control on the rockburst distribution by mining geometry seems apparent are discussed.

6.1.3. Results

Two parameters appear to be good indicators of the influence of a discontinuity on the number of rockbursts in a specific area; these are the number of rockbursts per area mined and the frequency of rockbursts for various distance intervals from the discontinuity. However, before examining these, other parameters that may effect the rockburst distribution must be considered, including depth, relative size of excavation, and the number of other discontinuities that were within 100 metres of the rockburst.

(a) Depth

Table 3A, Appendix 3, lists the results of the analysis showing the variation in control points and rockbursts with depth and these data are plotted in Figure 6.3. This figure shows that the number of rockbursts varies considerably on each level and it appears that over the small depth increment considered (347 metres) depth is not an important parameter in controlling rockburst distribution. However, the large differences between the number of rockbursts and control points on several levels and the very high rockburst frequency on 72 level suggests that some other factor, which varies from level to level, is affecting rockburst distribution. This factor may be the mining configuration; an examination of the shaft plans (Figures 6.1 and 6.2) shows a large stablisation pillar at the top of the 72 level

TABLE 6.1

THE INFLUENCE ON THE OCCURRENCE OF ROCKBURSTS OF THE EXCAVATION SIZE AND THE NUMBER OF OTHER DISCONTINUITIES WITHIN 100 METRES OF A ROCKBURST

DISCONTINUITY NUMBER	AVERAGE EXCAVATION* SIZE (%)		AVERAGE NUMBER OF OTHER DISCONTINUITIES**			
			BURSTS		CONTROL	
	BURSTS	CONTROL	DYKES	FAULTS	DYKES	FAULTS
110A	50	50	1,0	0,0	0,7	0,0
100	40	40	1,0	0,0	1,0	0,0
110	45	50	0,8	0,0	1,1	0,0
117	50	40	0,7	0,1	0,8	0,0
105	55	55	0,7	0,0	1,2	0,1
114A	45	45	0,2	0,0	0,1	0,0

* These figures represent the percentage area mined-out at the time of the rockbursts.

** These figures represent the average number of other discontinuities that may have been responsible for the rockburst besides the one that it has been allocated to.

stope. In Figure 6.1 only the centres of each rockburst zone are indicated but the original plans showed the extent of the damage area and invariably the rockbursts on 72 level extend from the pillar down the stope. This suggests that the presence of the pillar may cause the anomalous rockburst incidence on 72 level.

(b) Percentage excavation

Percentage excavation is a measure of the size of the excavation at the time of the rockburst. It is determined by drawing a circle of radius 50 metres, centred on the rockburst and calculating the percentage area mined at the time of the rockburst. Pretorius (1966) considered it to be an important factor in his analysis because as the area mined increases the rockburst incidence increases. However, the data for all control and rockburst points which is listed in Table 6.1 and illustrated in Figure 6.4 shows no significant difference in the percentage area.

(c) Number of discontinuities within 100 metres of the rockburst

This information is required to see whether another dyke or fault could have been responsible for initiating the rockburst rather than the one considered, or if more than one discontinuity was responsible. The detailed results are listed in Table 3B in the Appendix. These data show that it was rare for rockbursts to have occurred within 100 metres of only one discontinuity. In fact, most bursts occurred within 100 metres of one other discontinuity although for dyke 100 the frequency of rockbursts is almost independent of the number of other dykes in the vicinity.

Table 6.1 compares the results for control points and actual rockburst sites. The number of faults is too small to be significant. However, the number of other dykes near to dykes 100, 114A and 117 is similar for control and rockburst points. For dykes 110 and 105

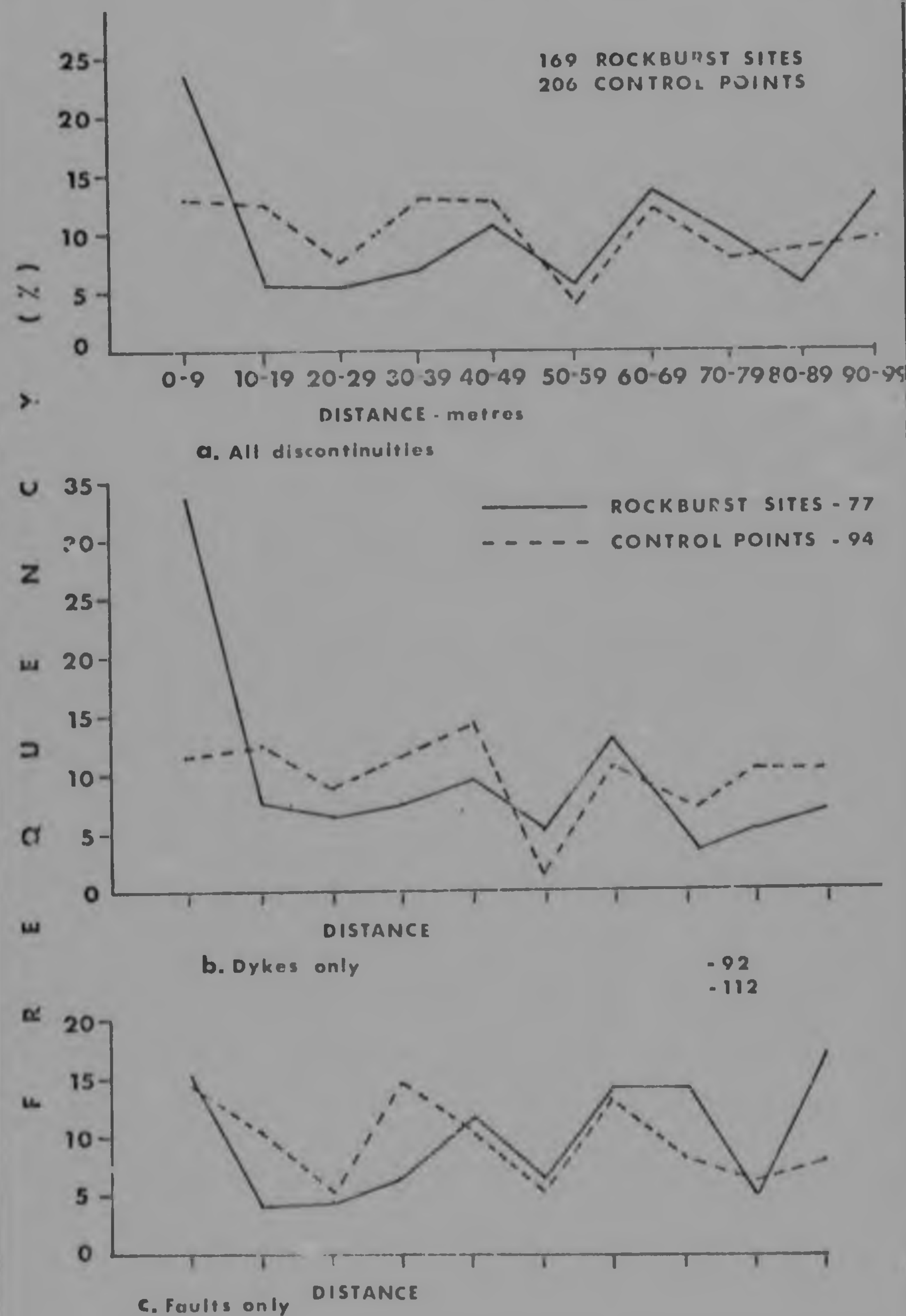

FIGURE 6-5 VARIATIONS IN FREQUENCY OF ROCKBURST SITES AND CONTROL POINTS WITH DISTANCE FROM A DISCONTINUITY

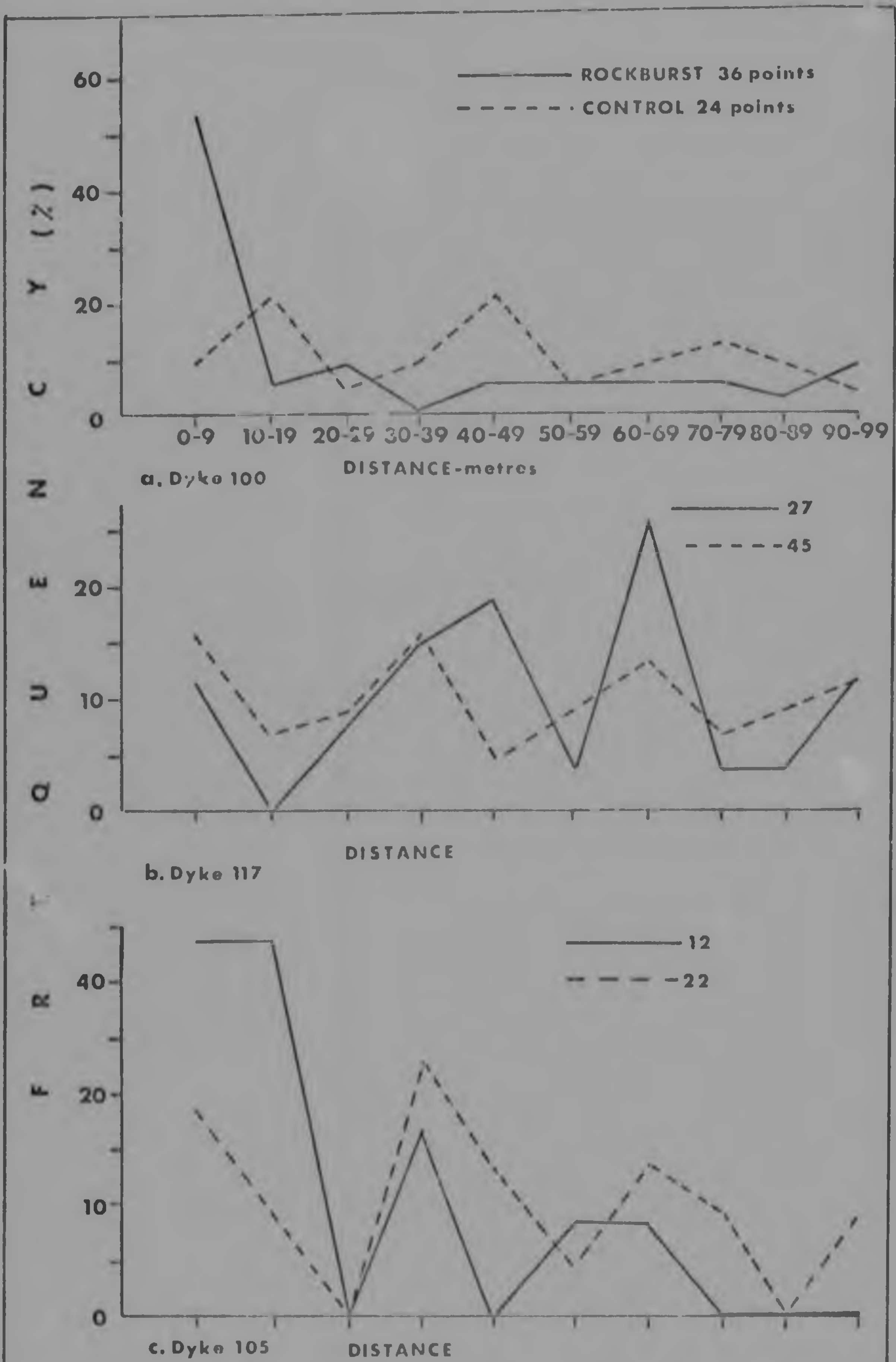

FIGURE 6-6 PLOTS OF FREQUENCY AGAINST DISTANCE FOR DYKES

TABLE 6-2

A COMPARISON BETWEEN THE NUMBER OF ROCKBURSTS AND THE SIZE OF THE MINED-OUT AREA FOR EACH DISCONTINUITY

DISCONTINUITY NUMBER	AREA MINED(m^2)	%	NO.OF BURSTS	%	NO.OF CONTROLS	%	%BURSTS/ 10^3m^2mined	%CONTROL/ 10^3m^2mined
110A	173 340	23,5	51	30,2	53	25,7	0,7	0,15
100	74 340	10,1	36	21,3	24	11,7	0,29	0,16
110	168 120	22,8	32	18,9	44	21,4	0,11	0,13
117	158 940	21,6	27	16,0	45	21,8	0,10,	0,14
121	27 000	3,7	2	1,2	3	1,5	0,04	0,06
105	90 180	12,3	12	7,2	22	10,7	0,08	0,12
114A	44 280	6,0	9	5,3	15	7,3	0,12	0,16
TOTALS	736 200	99,9	169	100,0	206	100,1	-	-

there are fewer additional dykes near the burst sites than control points; this suggests that these dykes may be responsible for the bursts. By contrast, dyke 110A has more additional dykes near to burst sites than control points, which implies that the additional dykes may be associated with the bursts.

(d) <u>Distance of the rockburst sites from discontinuities</u>

In Figure 6.5 the frequency of rockbursts is plotted against distance for (a) all discontinuities (b) dykes and (c) faults. The plot for all discontinuities differs between the control and rockburst data to a distance of 50 metres but the curves are similar beyond that distance. In addition the frequency of rockburst points is only larger than the frequency of control points from 0 to about 20 metres. This may indicate that discontinuities may only influence rockburst distribution for a distance 50 metres from the contact but within this 50 metres, the area beyond about 20 metres is a shadow zone less susceptible to rockbursts than areas further from the dyke. The area between 0 and 20 metres of the contact has the highest susceptibility. To determine whether dykes or faults are responsible for these patterns the data has been separated and plotted in Figures 6.5b and c. The diagram for faults shows very little difference between the frequency of control and burst points suggesting minimal control by faults on rockburst distribution. By contrast, the dyke-frequency plot shows strong control on bursts within 20 m of the dyke. The effect of individual dykes is shown in similar frequency-distance plots in Figure 6.6. From the curves, it appears that dyke 117 has little effect on the rockburst distribution, dyke 105 has some effect and dyke 100 has a significant effect.

(e) <u>Rockburst frequency within 100 metres of each discontinuity</u>

In Table 6.2 the size of the mined out area and the number of burst and control points within 100 metres of a discontinuity and the percentage burst and control points per area mined are listed for each discontinuity. This data shows that apart from dyke 121 the control point frequency is quite similar for each discontinuity. However, the burst frequency is significantly lower than the control for discontinuities 114A, 105 and 117; is a little lower for number 110; is a little higher for number 110A and is significantly higher for dyke 100. This suggests that dykes 100 and 110A are more liable to be associated with rockbursts than other dykes.

(f) Summary

Depth: No significant changes in the frequency of rockbursts with increasing depth could be found. However, a stabilisation pillar near the top of 72 level has possibly caused a large increase in rockburst frequency at this depth.

Size of excavation: No significant difference in the size of the excavated area around each rockburst or control point could be found for the discontinuities; hence its influence on the rockburst-dyke relationship can be ignored.

Other discontinuities: Most discontinuities which can be correlated with rockbursts have another discontinuity nearby which makes allocation of a particular burst to the discontinuity difficult. In particular dyke 110A cannot be correlated with most nearby bursts because of the other discontinuities near it. However, dykes 110 and 105 are thought to be responsible for most of the bursts near it.

Distance: Most bursts which can be correlated with dykes occur within 20 metres of the dyke. A shadow zone of lower than average burst frequency is present between 20 and 50 metres and beyond 50 metres the influence of the dykes is insignificant. In general, faults do not appear to have controlled rockburst distribution. Of the dykes

TABLE 6.3

SOME GEOLOGICAL FEATURES OF DISCONTINUITIES WHICH MAY INFLUENCE THE INCIDENCE OF ROCKBURSTS

DISCONT-INUITY	THICKNESS (m)	ORIENTATION	LOCATION	CONTACTS	PETROGRAPHY*	GEOCHEMISTRY	AGE**
110a	1	Strike shear/ dyke $110^{\circ}/65^{\circ}/S$	H71 level	Sharp but dyke is sheared	Severely altered mylonite(group 5)	-	1
100	15,5	Dip dyke $000^{\circ}-025^{\circ}/80^{\circ}/W$	H shaft far west	Both contacts have 1-8cm of shearing and chilled margins	Quartz-dolerite, medium grained, not severely altered (group 3)	K-poor tholeiite	3
110	2	Strike shear/ dyke $110^{\circ}-115^{\circ}/80^{\circ}/N$	H71-74	Sharp but dyke is sheared	Severely altered mylonite (group 5)	Alkali-poor tholeiite	1
117	1,0-3,5	Dip dyke $028^{\circ}/80^{\circ}/W$	central H	Very sharp	Quartz-dolerite, heavily altered, fine grained(group 4)	Alkali-poor tholeiite	2
105	3	Sill $090^{\circ}/30^{\circ}/S$	H73-76	Sharp	Aplite, fresh	-	4
114A	1,5	Strike shear/ dyke $110^{\circ}/40^{\circ}-90^{\circ}/N$	H76-77	Very sharp but dyke is sheared	Severely altered mylonite (group 5)	Low calc-alkaline tholeiite	1

* Group numbers refer to the groups of dykes discussed in Chapter 2.

** Relative ages; 1 is the oldest and 4 is the youngest, see Chapter 2 for more specific ages.

analysed, dyke 100 has significantly controlled the distribution of bursts, dyke 105 has to a lesser extent influenced them but dyke 117 has had no effect at all.

Rockburst frequency: The discontinuities analysed show a variation in tendency to cause rockbursts. This tendency decreases in the following order: discontinuity 100, 110A, 110 and 105, 114A and 117. Dyke 100 has a significantly larger influence than the others.

6.1.4. Geological features of the discontinuities

Geological features which may be important in controlling the tendency for discontinuities to be prone to bursting include the position of the discontinuity in space, its thickness, contact relations with quartzites, petrology, geochemistry and age. These data are summarized for the discontinuities considered in this chapter in Table 6.3.

Discontinuities 110,110A and 114A are similar in all respects except for thickness. However, the other three discontinuities are different in most aspects. Of the two dip dykes (numbers 100 and 117) only number 100 has significantly controlled the rockburst distribution. It differs from dyke 117 significantly in size and alteration and also differs in contact relationships, which suggests that a large fresh dyke is more rockburst prone than a small, altered one. The strike-shear zones, numbers 110A, 110 and 114A have had no apparent control on the rockburst distribution, which suggests that a sheared area may be associated with less rockburst activity. This conclusion may also be applicable to dykes with sheared contacts.

6.1.5. Conclusions

1. The most important conclusion from this study is that not all

discontinuities increase the frequency of rockbursts. In fact, only two of the six discontinuities considered here have affected the rockburst distribution; dyke 100 significantly and dyke 110A slightly.

2. The results show that a discontinuity most likely to be associated with bursts will be a large, fresh dip dyke with sharp and unsheared contacts with the quartzites.

3. This analysis has been conducted using the reef-discontinuity intersection traces as reference lines. However, at no place in the area considered is the stope more than 100 metres from an aplite sill (Fumerton, 1975) and this may cast some doubt on the reliability of the results.

4. Underground observations in other sections of the mine and discussions with mining personnel seem to indicate that rockburst activity is associated with the major basic dip dykes and areas of aplite sill-reef intersection. It is noteworthy that dyke 144, a large porphyritic dip dyke has not been mined through for many years because of rockbursts and the aplite sill has caused whole stopes to be closed down. The relative absence of activity near the aplite sill in this study is anomalous.

6.2 STUDIES OF THE EFFECTS OF STRUCTURAL DISCONTINUITIES ON THE DISTRIBUTION OF SEISMIC EVENTS

Two separate studies are described here; the aims of which are identical to those of the preceding section, except that here they are applied to seismic events. The term 'seismic event' and its relation to a 'rockburst' were defined in Section 1.4. Tabular mining at great depth, as in the E.R.P.M., subjects the rock around an excavation to large stress differences, causing it to fail and release energy in the form of seismic waves which can be picked up by geophones and recorded

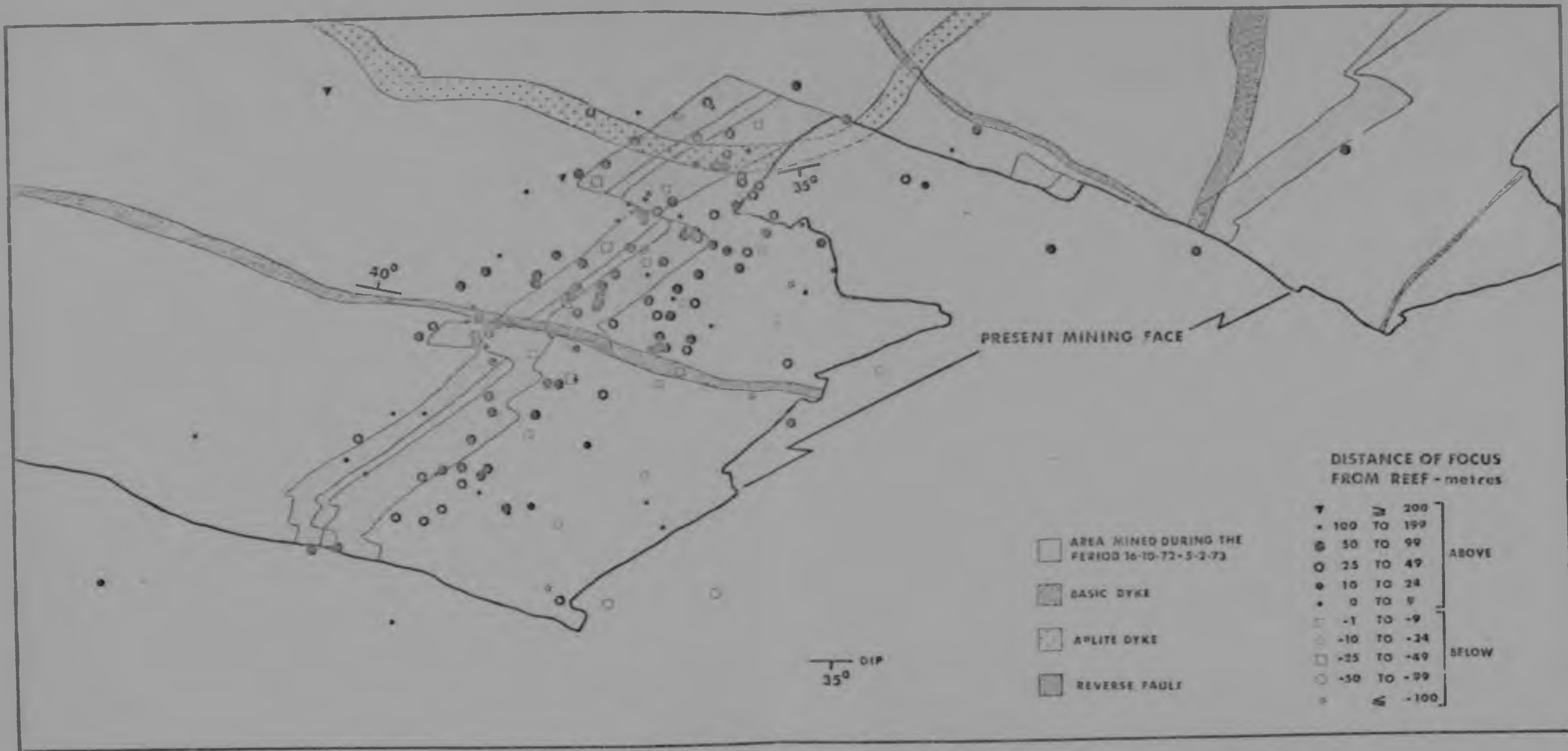

FIGURE 6.7 LOCATIONS AND DISTANCE FROM REEF OF 162 SEISMIC EVENTS IN LOWER EAST HERCULES SECTION (LEVELS 74 to 77)

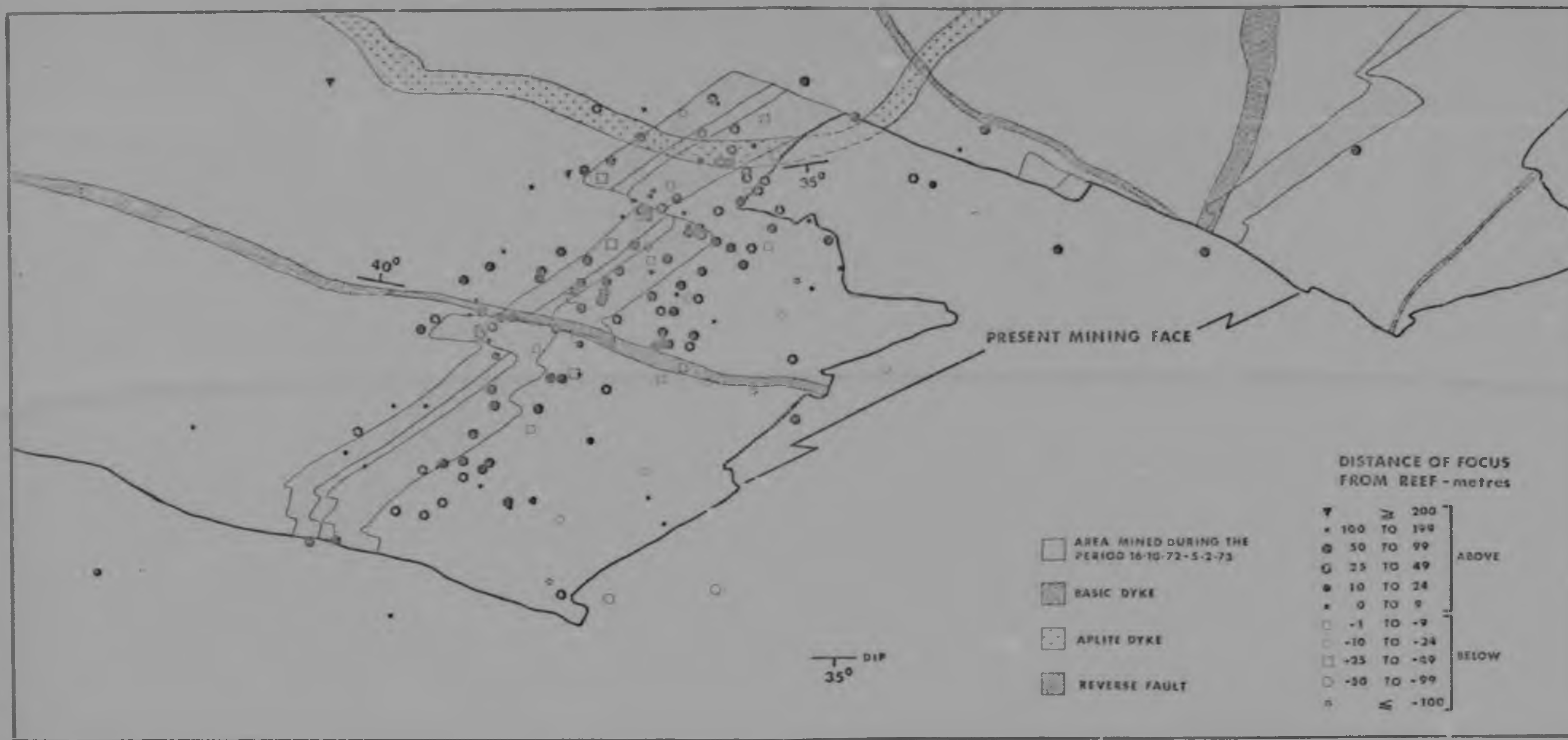

FIGURE 6.7 LOCATIONS AND DISTANCE FROM REEF OF 162 SEISMIC EVENTS IN LOWER EAST HERCULES SECTION (LEVELS 74 to 77)

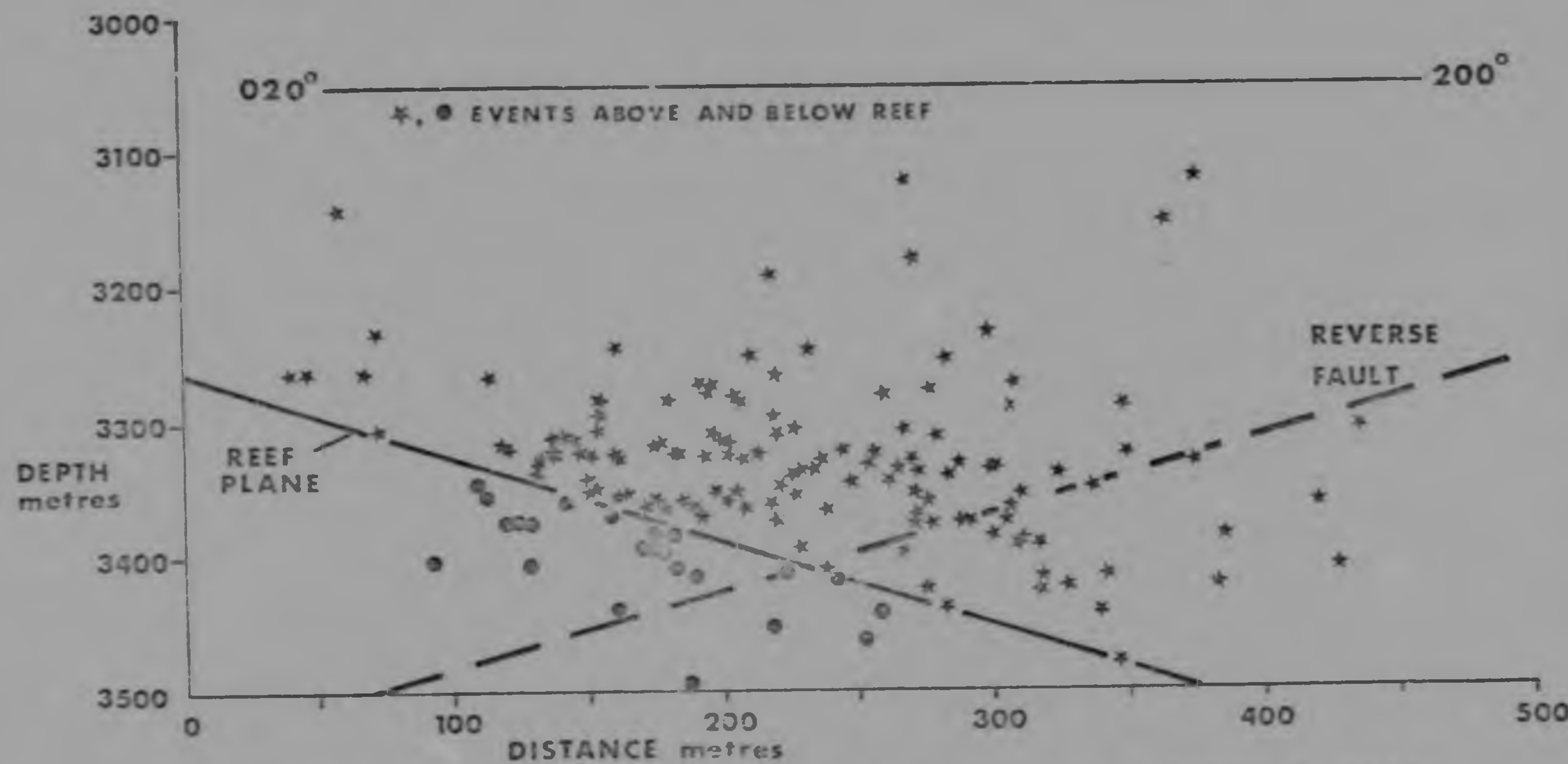

FIGURE 6-8 PROJECTION OF THE SEISMIC DATA IN FIGURE 6-7 ONTO A VERTICAL PLANE STRIKING 020°

APLITE SILL CANNOT BE DISTINGUISHED FROM THE REEF PLANE ON THIS SCALE on magnetic tapes. The times of arrival of the seismic waves from several geophones are used to calculate the focus of the seismic event. Three points related to the present analysis should be made: firstly, the accuracy to which the focus of an event is positioned varies up to 30 metres (A. McGarr, personal communication, 1974); secondly, the source area for a large event can have a diameter up to 100 metres (S.M. Spottiswoode, personal communication, 1974) and finally, it is difficult to distinguish between these seismic events caused solely by mining induced stresses from those which have been partly due to mining activity and partly due to some other parameter such as a geological discontinuity.

The procedure followed for these studies has been to project the foci and geology onto various planes in space and then to examine these projections for concentrations of foci about the geological discontinuities.

6.2.1. <u>Study in lower-east Hercules section</u>

The locations of 162 seismic events recorded in east H section, between 74 and 77 levels for the period 16.10.72 to 5.2.73 have been obtained from A. McGarr (personal communication,1974). In Figure 6.7 the events have been projected onto the plane of the reef where the geological features considered and areas mined during the period are also plotted. In addition, the seismic foci and some of the geology has been projected onto a vertical dip plane (Figure 6.8).

In the area concerned (Figure 6.7) there are five geological discontinuities; of these only two are closely associated with the main concentrations of seismicity. These are (1) an aplite sill which dips south at about 35° passing through the reef plane near the north of the area and is always within 30 metres of the reef and a reverse fault which dips at 40° northwards (see Figures 6.7 and 6.8).

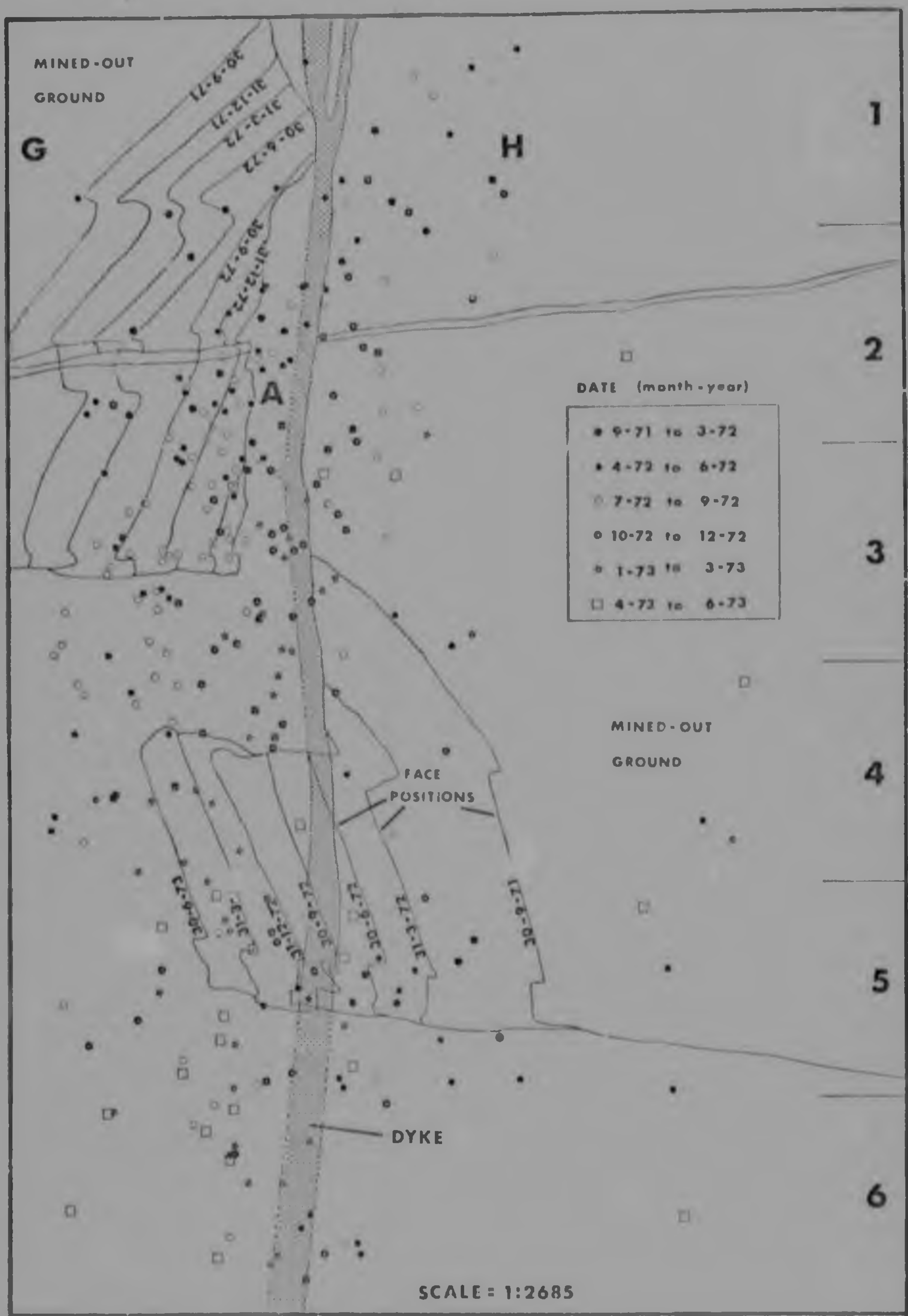

FIGURE 6-9 LOCATIONS OF 293 SEISMIC EVENTS IN LOWER WEST HERCULES AND LOWER EAST CENTRAL SECTIONS(LEVELS 72 to 79)
(large numbers refer to groups in Appendix Table 3C)

It is clear from the two projections of the data(Figures 6.7 and 6.8) that there are no obvious concentrations of seismic events near the geological discontinuities but in Figure 6.7 there is an association between the area mined and seismic activity and in Figure 6.8 a weak concentration between the reef plane and seismic activity is present. This correlation between events and mining activity is to be expected because of the large mining induced stresses. By contrast, a negative correlation with geological features may be due to the absence of any major geological features in the area except for the aplite sill, which is very close to the plane of the reef and so events due to it cannot be distinguished from those due to mining.

6.2.2. Study in lower-west Hercules section

One of the main reasons why the previous study, in the east side of Hercules section proved negative may have been the absence of a large basic dyke. These dykes are known to be rockburst prone (see Figures 1.4 and Section 6.1) and they may also induce sufficiently large stress differences to initiate seismic events. Therefore, a study was done in lower-west Hercules section, in the region where dyke 100 was mined through during the period 30.9.71 to 30.6.73. The locations of 293 seismic events in west H section and far-east G section between 72 and about 79 levels during this time were obtained from G.A. Weibols (personal communication, 1974). These events have been projected onto the reef plane in Figure 6.9.

Three noteworthy features appear in this plot. It can be calculated from Figure 6.9 that, firstly, just over half of the events (53%) occurred above or below ground which was mined out before June, 1973, with the rest being in either the remnant pillar (A) or ahead of the mining faces; secondly, only eight per cent of the events occurred in

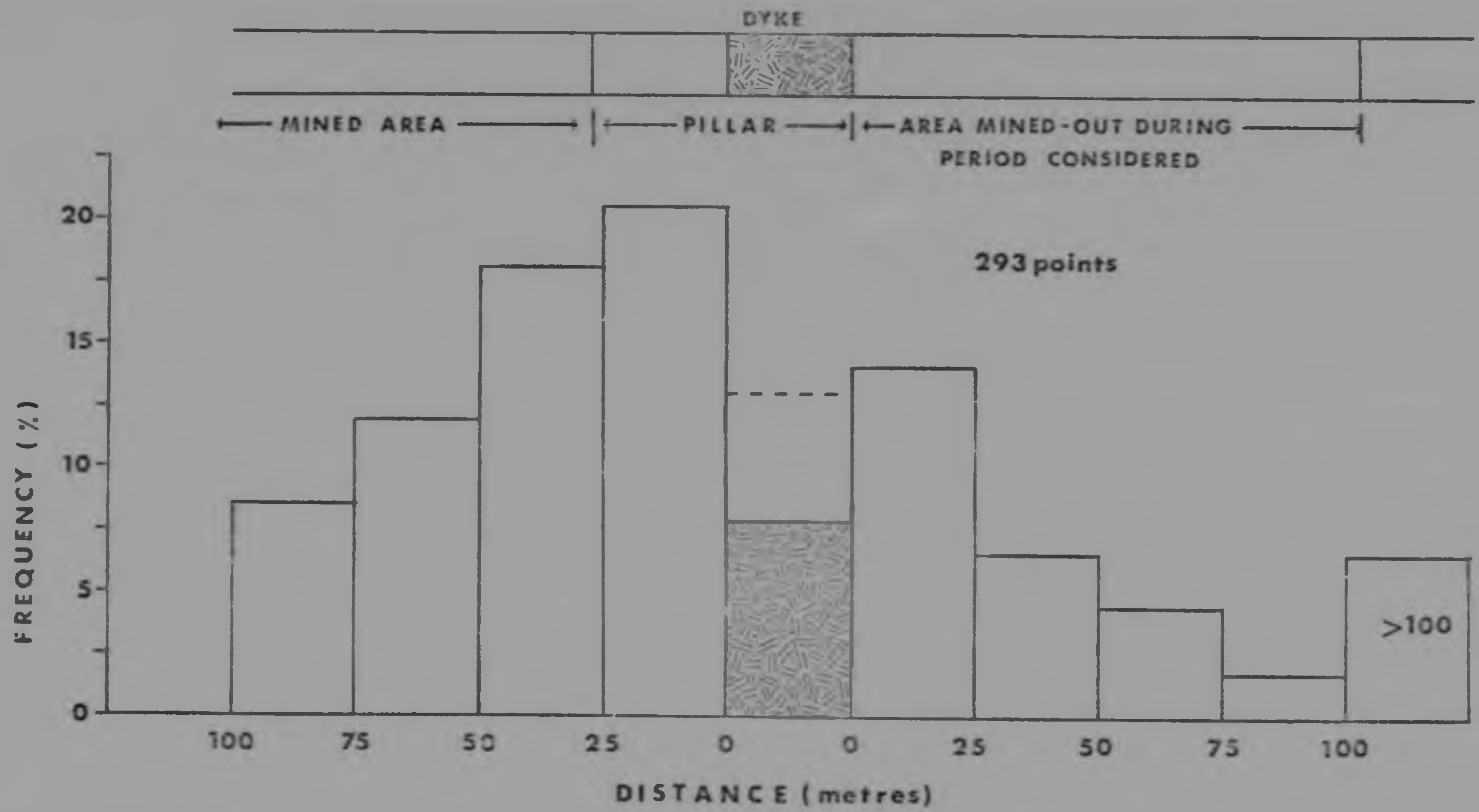

FIGURE 6-10 FREQUENCY OF SEISMIC EVENTS AROUND DYKE 100

the dyke and thirdly, the density of events is much greater for the upper mining faces than for the lower mining faces which may be related to the presence of the thin remnant pillar (A) in the upper areas (see Figure 6.9 and Appendix Table 3C).

In Figure 6.10 the frequency of seismic events is plotted against distance from dyke 100, using data listed in Appendix Table 3C. This figure clearly shows a marked increase in the frequency near to the dyke, a low frequency within the dyke and a much higher frequency of events on the west side of the dyke than the east. The very low frequency within the dyke can be explained by the fact that the distance interval chosen is 25 metres whilst the dyke is only about 15 metres thick. In Figure 6.10, the dotted line above the dyke interval represents the frequency of events proportionally increased for a dyke 25 metres thick. The greater frequency of events on the west side of the dyke than the east side of the dyke is probably due to the large area mined on the west side and the fact that the west side was mining up to a thin remnant pillar. It is also important to note that the highest frequency of events occurred within the remnant pillar.

From this study, one can conclude that firstly, an irregular mining configuration such as a thin remnant pillar has an overwhelming influence on the distribution of seismicity (upper face in Figure 6.9), and secondly, where there is a regular mining configuration such as the lower mining face in Figure 6.9, the seismicity does not appear to concentrate around the dyke even when mined through. However, the overall maxima on each side of the dyke may be significant because they correlate with rockburst distribution about a dyke (Figures 1.4, 6.5 and 6.6).

CHAPTER 7

SUMMARY AND CONCLUSIONS

7.1 INTRODUCTION

The aim of this dissertation was to determine those geological parameters of the structural discontinuities which may be associated with rockbursts and seismic events. The following is a summary of the geology of the structural discontinuities and of those parameters that may be important in controlling the distribution of seismic events and rockbursts. In addition recommendations for further study are given.

7.2 DYKES

Five groups of dykes have been recognised, based on orientation, petrography and geochemistry:

Group 1 is made up of one dyke/sill, the Simmer Dyke, which is a large undulating intrusive. It can be classified as a melanorite. By association to previous work it appears to be of Bushveld age.

Group 2 dykes form a swarm of ilmenite dolerites, striking at about 140°. They are between five and eight metres thick and are characterised in thin section by skeletal ilmenites. Geochemically they are shown to be tholeiitic, characterised by a high TiO_2 content. By association to previous work they are probably of Bushveld age.

Groups 3 and 4 dykes both strike at 030° and both have a similar geochemistry which indicates that they are tholeiitic quartz-dolerites. Group 3 dykes are characterised by large feldspar phenocrysts and are fresher and coarser than Group 4 dykes, which are fine grained and heavily altered. By association with previous work they are of Ventersdorp age.

Group 5 dykes are a series of east-west striking shear zones, which are altered and sheared such that the original minerals are unrecognisable.

They can be classified as mylonites or ultramylonites.

7.3 FAULTS

Three groups of faults have been recognised. Groups 1 and 3 faults form a conjugate pair; group 1 faults strike at 075°, have a downthrow to the south and a dextral strike-slip displacement, and group 3 faults strike at 313°, have a downthrow to the north and a sinistral strike slip displacement. Group 2 faults strike at 100° and generally the downthrow is to the north for those near surface and south for those at depth.

The faults are characterised by (1) rotational movements which are possibly a result of an inhomogeneous stress field reactivating existing normal faults; (2) gouge material which ranges from ultramylonite to fault breccia and fault gouge, and (3) terminations by splay and rotational faulting.

7.4 JOINTS

Six groups of joints have been recognised. Mining included Type 1 joints and wall spalling make up parts of groups A, B and D. In addition, vertically dipping geological joints which strike at 030°, 075°, 120° and 165 (parts of groups A, B,D,E and F) have been recognised. Of these, two groups (075° and 165°; groups E and F) could only be recognised in the L74 exploration crosscut, which is well away from active stope mining. Group C joints, which are parallel to the bedding planes, are most probably of geological origin but have been opened up during mining by buckling of the quartzite layers into the stope.

Large dykes and faults effect the orientation and density of mining induced jointing; 'bedding plane' joints could be found within the dykes and spalling and slabbing in drives initiates from an 'embryonic zone' of high comminution at the intersection of two planar features.

7.5 EARLY STRESS SYSTEMS

Regional lineation patterns, as determined from E.R.T.S. imagery reveal four strong trends, most of which can be correlated with the local E.R.P.M. patterns.

A dynamic analysis of the structural discontinuties and the regional lineations shows that the maximum principal stress has been oriented near vertical through time since the formation of the Witwatersrand Basin, becoming horizontal to produce the conjugate pair of faults (groups 1 and 3) and the reverse movements on group 2 faults.

7.6 ROCK MECHANICS

Detailed uniaxial compressive test of three dykes and both uniaxial and triaxial compressive tests of another dyke show distinct characteristics and trends across the dykes. Two of the dykes are stronger than hangingwall quartzites whilst two are a little weaker on average; all dykes are stronger than footwall quartzites. Dykes 100 and 182 are strongest towards their centre and weakest towards their contact regions whilst dykes 79 and 144 are weakest on one contact, stronger towards the centre and strongest on the other contact. Strength could be correlated with coarseness and chilled margins and weakness could be correlated with contact shearing.

Young's Modulus is generally higher than that for quartzites, averaging $0{,}87 \times 10^5$ MPa, and Poisson's Ratio is significantly higher averaging 0,28.

The triaxial testing on dyke 144 showed a linear increase in strength with increasing confining pressure beyond a confining pressure of 10 MPa, an average coefficient of internal friction of 1,4 and a cohesive shear strength of about 75 MPa. The average tensile strength determined by the Brazilian tests is 31 MPa.

One unusual feature of the dyke is the decrease in the coefficient of internal friction with increasing confining pressure.

7.7 THE EFFECTS OF STRUCTURAL DISCONTINUITIES ON THE DISTRIBUTION OF ROCKBURSTS AND SEISMIC EVENTS

The rockburst study revealed several important conclusions. There does appear to be some control by structural discontinuities but not all discontinuities effect the distribution. Noteably, faults and small dykes have no effect but large dykes, such as dyke 100, do have a significant effect. It was concluded that a large, fresh, coarse, dip dyke with sharp, welded contacts with the quartzites is the most rockburst prone. No correlation between dykes or faults and seismic events could be made but a strong correlation to mining activity is present and it appears as if seismic events have concentrated in a thin remnant pillar.

7.8 RECOMMENDATIONS FOR FURTHER STUDY

There is little doubt that the incidence of rockbursts increases near some structural discontinuities, whether they be natural(dykes) or manmade (raises). This dissertation has, unfortunately, only just touched on the association between geological parameters and rockburst distribution because it has been necessary to describe the geology of the structural discontinuities in some detail. This has not previously been done for the E.R.P.M. In addition the past records of the locations, extent of damage, time and mining configuration at the time of the rockbursts are extremely poor; it is insufficient to only record that a rockburst has occurred in a particular stope. Accurate details of the location are essential because the effect of a discontinuity on rockburst distribution probably extends less than half a stope length from the discontinuity.

A fruitful study could well be implemented to determine the geological parameters causing rockbursts, but it will necessitate accurate and detailed recording of rockburst data over several years; these records should include a geological description of each site together with details of the mining configuration. Interpretation of the data collected must be done in a rigid statistical manner.

APPENDIX 1

1.A. SAMPLE COLLECTION

Each specimen was collected as close as possible to the centre of the dyke so as to avoid host rock contamination, chilled margins and alteration which is common near the contacts. All specimens were collected below two kilometres below surface and can be considered as free from weathering; specimens were usually larger than five kilograms to avoid inhomogenieties due to large phenocrysts.

For dyke number 182, six specimens, numbered 182 - 1, 182 - 3, 182 - 5, 182 - 7, 182 - 9 and 182 - 11 were collected at 0,0m , 2,5m, 11,2m, 17,3m, 21,9m and 24,1m respectively from the east contact. The respective analyses are numbers 1 to 6 in Table 1B, of this Appendix. Specimen 182 - 5 (Analysis 4) has been chosen as the representative analysis for dyke 182.

1.B. METHOD OF ANALYSIS

A detailed account of the procedure of X-ray spectrographic analysis of geological samples on the University of the Witwatersrand X-ray spectrometer is in the process of being compiled (McCarthy,1975) and therefore only a brief description of the technique is given here. The Norrish Fusion technique has been closely followed (Norrish and Hutton, 1969).

SAMPLE PREPARATION

- Each specimen was scrubbed and broken into fist-sized pieces.
- Any piece containing veins or showing surface alteration was either discarded or broken further so that areas of contamination could be removed.
- All specimens were crushed into chip size particles in a carbon-steel jaw crusher.
- After halving the particles, specimens were crushed to a fine powder in either an agate, nickel-chrome or tungsten-carbide

concentric-ring mill. Specimens 182 - 1, 5, 7, 9 and 11 (Analyses 1 to 6) were crushed with the agate mill; numbers 27 (Analysis 15), 32(16), 33(17), 36(18), 58(7), 79(25), 100(8), 110(26), 117(27) and 144(9) with a nickel-chrome mill and the rest with a tungsten-carbide mill.

- A sample of $\pm$ 5 grams of powder from each specimen was weighed into a crucible and heated at 120°C for 24 hours to remove free water. After reweighing, all samples were heated to 1000°C for 24 hours to remove volatiles and weighed again.
- The preparation of glass fusion discs (two for each sample) has closely followed the description by Norrish and Hutton (1969), and the preparation of one pressed powder pellet for each sample has closely followed the description of Norrish and Chappel (1967).

EXPERIMENTAL CONDITIONS

Analyses for specimens 182 - 1, 3, 5, 7, 9 and 11 (Analyses 1 to 6)were performed by General Superintendence Co. Ltd, Johannesburg at the National Institute for Metallurgy on samples submitted and prepared to powder size by the author. All other specimens were analysed by the author in the Geology Department of the University of the Witwatersrand.

For this work a Phillips PW 1410 X-ray spectrometer has been used and Table 1A shows the operating conditions for the various elements. Details of the procedure have been discussed by Norrish and Hutton (1969). Note that in Table 1A the counting times are half times and each sample was counted twice and summed to avoid anomalous counts. The percentage Fe_2O_3, MnO, TiO_2, K_2O, P_2O_5, SiO_2, Al_2O_3, MgO and Na_2O have been determined in this manner in conjunction with an unpublished computer programme written by J.P. Willis, as modified by T.S. McCarthy (personal communication, 1974). All samples were done in duplicate.

FeO, CO_2 and C.I.P.W. Norms

Determination of FeO has exactly followed the descriptions by Schafer (1966).

All CO_2 determinations were by General Superintendence Co.Ltd from samples submitted to the National Institute for Metallurgy.

C.I.P.W. weight norms have been calculated for each analysis using a computer programme written by T.S. McCarthy (personal communication, 1974). A problem occurred with two analyses whilst determining C.I.P.W. norms that required some adjustment of the programme. The initial two steps of a C.I.P.W. norm calculation are:

1. All CO_2 is used with some CaO to form calcite, and
2. All P_2O_5 is used with some CaO to form apatite.

The chemistry of dykes 114A and 109 is unusual in that there is insufficient CaO to combine with CO_2 to form calcite which results in a negative normative anorthite determination. The problem was overcome by allowing apatite to form first using all the CaO necessary, then increasing the remaining CaO percentage, at the expense of MgO, until there was sufficient to combine with CO_2 and finally determining normative dolomite instead of calcite.

I-C RESULTS

The determined silicate analyses and their respective C.I.P.W. weight norms are listed in Tables 1B, 1C and 1D. In Table 1E are listed some previous analyses and typical compositions of rocks referred to in the main text.

TABLE 1A

X-RAY SPECTROMETER OPERATING CONDITIONS

ELEMENT	ANALYSING CRYSTAL	ANGLE	FILTER[2]	COLLIMATOR[3]	COUNTING TIME (SECS)	X-RAY TARGET[2]	TUBE KV	mA
Fe	LiF220	85,90	IN	COARSE	20	Cr	50	50
Mn	LiF220	95,35	IN	FINE	100	Cr	50	50
Ti	LiF200	86,2[illegible]	OUT	FINE	10	Cr	50	50
Ca	LiF200	113,20	OUT	FINE	10	Cr	50	50
K	PE	50,77	OUT	FINE	10	Cr	50	50
P	PE	89,69	OUT	COARSE	40	Cr	50	50
Si	PE	109,32	OUT	COARSE	10	Cr	50	50
Al	PE	144,92	OUT	COARSE	40	Cr	50	50
Mg	ADP	136,92	OUT	COARSE	100	Cr	50	50
Na[1]	GYPSUM	103,35	OUT	COARSE	100	Cr	50	50
Na[1]	GYPSUM	97,00	OUT	COARSE	100	Cr	50	50

1. Sodium was counted twice for each run: the first is a count of sodium plus background and the second is just background. The average of the differences for the duplicate samples was used for calculations.

2. The X-ray tube target was always Cr. This differs from Norrish and Hutton (1969) where a W target was used for Mn and Fe determinations. The present work was done on a modified machine which incorporates a filter enabling Mn and Fe to be analysed with a Cr target.

3. The collimator sizes are : fine, 150 microns and coarse, 550 microns.

APPENDIX 1 (Continued) - Table 1B

ANAL.NO.	1	2	3	4	5	6	7	8	9
Wt%									
SiO_2	53,72	53,53	52,87	52,98	53,53	53,69	52,19	53,12	53,98
TiO_2	1,00	1,01	1,03	0,95	0,98	0,95	0,85	0,79	1,15
Al_2O_3	14,32	14,39	14,61	15,07	14,65	13,98	14,25	14,46	14,33
Fe_2O_3	1,47	2,23	2,58	1,68	2,34	2,64	1,72	3.19	1,71
FeO	9,45	8,71	8,21	8,67	8,23	8,15	7.25	6,18	9,20
MnO	0,27	0,17	0,15	0,18	0,18	0,19	0,16	0,14	0,16
MgO	4,88	4,76	5,04	6,01	4,97	5,14	5,65	6,24	5,21
CaO	5,82	8,54	8,62	7,03	8,68	8,82	8,16	9,03	7,82
Na_2O	2,46	2,71	2.70	3,34	2,85	2,58	3,37	3,23	3,69
K_2O	0,01	0,51	0,73	0,14	0,13	0,10	0,54	0,24	0,95
H_2O^+	3,98	2,55	2,57	2,95	2,76	2,54	3,00	2,31	2,06
H_2O^-	0,11	0,12	0,10	0,14	0,09	0,14	0,06	0,07	0,03
P_2O_5	0,19	0,25	0,24	0,19	0,24	0,24	0,18	0,17	0,25
CO_2	1,87	0,12	0,11	0,14	0,12	0,24	2.85	0,08	0,16
Total	99,55	99,60	99,56	99,47	99,75	99,40	100,23	99,25	100,70

C.I.P.W.NORMS	1	2	3	4	5	6	7	8	9
CALCITE	8,45	0,56	0,51	0,65	0,56	1,12	12,43	0,37	0,73
ILMENITE	1,89	1,96	2,00	1,85	1,90	1,85	1,55	1,54	2,19
MAGNETITE	2,12	3,31	3,83	2,50	3,47	3,91	2,39	4,75	2,49
FERROSILITE	15,80	10,55	9,36	13,01	9,88	9,53	10,97	5,68	11,06
APATITE	0,44	0,59	0,57	0,45	0,57	0,57	0,40	0,41	0,58
ORTHOCLASE	0,06	3,08	4,42	0,85	0,79	0,61	3,06	1,46	5,64
DIOPSIDE	0,0	6,28	6,99	3,35	6,41	6,79	0,0	11,00	7,07
ANORTHITE	15,71	26,17	26,20	26,39	27,42	26,86	20,41	24,90	19,81
HEDENBERGITE	0,0	5,91	5,60	2,60	5,37	5,35	0,0	4,73	6,60
ALBITE	20,69	23,46	23,40	29,02	24,69	22,33	27,35	28,08	31,36
CORUNDUM	4,44	0,0	0,0	0,0	0,0	0,0	0,31	0,0	0,0
ENSTATITE	12,08	9,21	9,61	13,81	9,69	9,94	13,49	10,86	9,75
QUARTZ	18,33	8,93	7,51	5,52	9,25	11,16	7,66	6,22	2,73
DYKE NO	182-1	182-3	182-5	182-7	182-9	182-11	58	100	144
LOCALITY	K69C	K69C	K69C	K69C	K69C	K69C	F68W	H76W	L73W

APPENDIX 1 (Continued) - Table 1C

ANAL.NO.	10	11	12	13	14	15	16	17	18
Wt%									
SiO_2	54,24	55,25	48,36	54,95	48,97	52,94	54,95	56,05	55,59
TiO_2	0,50	0,51	1,58	0,90	2,59	0,88	0,81	0,82	0,76
Al_2O_3	13,16	13,64	14,74	15,11	12,21	14,54	14,35	14,79	14,45
Fe_2O_3	0,99	1,15	1,95	3,17	6,91	1,83	1,32	1,61	0,86
FeO	8,41	7,61	10,66	6,63	9,50	7,98	7,95	7,26	8,78
MnO	0,18	0,15	0,17	0,16	0,22	0,18	0,17	0,15	0,18
MgO	8,79	7,32	7,37	4,96	4,94	6,24	6,03	5,16	7,70
CaO	8,23	9,13	8,18	9,00	8,96	9,37	9,09	8,16	4,41
Na_2O	1,86	2,50	2,81	2,00	2,81	2,82	3,17	3,59	2,70
K_2O	0,03	0,08	0,04	0,03	0,[illegible]	0,05	0,15	0,36	0,04
H_2O^+	3,65	2,76	4,09	3,27	1,30	2,65	2,44	2,36	4,25
H_2O^-	0,05	0,03	0,06	0,05	0,08	0,08	0,04	0,04	0,05
P_2O_5	0,10	0,10	0,23	0,20	0,32	0,20	0,19	0,18	0,18
CO_2	0,61	0,13	0,56	0,15	0,64	0,61	0,09	0,12	0,49
Total	100,80	100,36	100,80	100,58	99,91	100,37	100,75	100,65	100,44

C.I.P.W.NORMS	10	11	12	13	14	15	16	17	18
CALCITE	2,80	0,60	2,58	0,70	2,90	2,79	0,41	0,55	2,27
ILMENITE	0,96	0,98	3,04	1,74	4,90	1,69	1,55	1,57	1,47
MAGNETITE	1,45	1,69	2,86	4,69	9,99	2,66	1,93	2,36	1,27
FERROSILITE	13,63	10,27	15,21	7,27	5,21	10,10	9,67	8,64	15,66
APATITE	0,23	0,24	0,54	0,47	0,74	0,47	0,45	0,42	0,43
ORTHOCLASE	0,18	0,48	0,24	0,18	2,71	2,30	0,90	2,15	0,24
DIOPSIDE	4,65	9,39	3,84	5,36	9,90	7,11	9,05	7,33	0,0
ANORTHITE	27,68	26,16	27,83	32,82	19,29	26,97	24,72	23,41	17,94
HEDENBERGITE	2,62	5,60	2,86	3,17	5,52	4,79	6,56	5,44	0,0
ALBITE	15,86	21,50	24,08	17,27	23,72	23,97	27,10	30,69	23,29
CORUNDUM	0,0	0,0	0,0	0,0	0,0	0,0	0,0	0,0	3,58
ENSTATITE	19,89	14,16	16,80	10,12	7,68	12,30	10,97	9,58	19,54
QUARTZ	10,07	8,93	0,13	16,22	7,44	6,87	6,69	7,87	14,32
DYKE NO.	77	11	121	16	149	27	32	33	38
LOCALITY	G73W	C61E	H72W	C61E	L70E	D49E	D49E	F49W	F49W

APPENDIX I (Continued) - Table 1D

ANAL. NO.	19	20	21	22	23	24	25	26	27
Wt%									
SiO_2	49,10	54,56	52,22	46,40	51,69	53,95	52,52	51,76	47,04
TiO_2	2,69	0,32	0,63	0,58	0,54	0,53	0,63	0,47	2,10
Al_2O_3	17,50	7,77	13,16	20,06	13,38	13,34	11,90	11,67	13,04
Fe_2O_3	2,47	1,47	0,70	0,88	3,41	1,55	0,89	2,59	4,73
FeO	13,59	8,13	9,30	10,41	9,10	12,05	8,15	6,51	9,69
MnO	0,23	0,18	0,21	0,27	0,25	0,19	0,25	0,19	0,25
MgO	4,91	17,88	7,27	9,75	13,94	11,54	9,34	10,94	6,06
CaO	8,96	5,34	6,12	0,74	0,11	0,07	7,66	9,98	10,40
Na_2O	2,75	1,33	1,96	3,09	0,08	0,08	0,20	0,28	0,39
K_2O	0,59	0,45	0,03	0,04	0,02	0,03	0,03	0,04	0,03
H_2O^+	1,62	2,44	4,28	6,06	7,56	6,83	5,37	4,30	4,03
H_2O^-	0,10	0,04	0,04	0,07	0,07	0,03	0,13	0,03	0,04
P_2O_5	0,33	0,08	0,11	0,11	0,09	0,08	0,18	0,10	0,47
CO_2	0,65	0,11	4,48	0,16	0,15	0,47	3,63	1,26	2,18
Total	100,49	100,10	100,51	98,62	100,39	100,74	100,88	100,12	100,45

C.I.P.W.NORMS	19	20	21	22	23	24	25	26	27
CALCITE	2,92	0,51	18,98	0,78	0,0	0,0	15,81	5,78	9,72
DOLOMITE	0,0	0,0	0,0	0,0	0,73	2,22	0,0	0,0	0,0
ILMENITE	5,05	0,62	1,12	1,17	1,09	1,05	1,15	0,90	3,91
MAGNETITE	3,54	2,16	0,95	1,36	5,26	2,34	1,24	3,79	6,72
FERROSILITE	14,94	13,45	15,66	20,24	15,21	22,41	13,86	8,95	11,14
APATITE	0,76	0,19	0,24	0,27	0,22	0,19	0,40	0,23	1,07
ORTHOCLASE	3,45	2,70	0,17	0,25	0,13	0,18	0,17	0,24	0,17
DIOPSIDE	6,42	7,29	0,0	0,0	0,0	0,0	0,0	6,48	0,49
ANORTHITE	19,80	14,09	1,23	2,06	0,0	0,0	13,28	30,73	33,03
HEDENBERGITE	8,66	1,93	0,0	0,0	0,0	0,0	0,0	1,95	0,31
ALBITE	23,02	11,42	15,46	27,84	0,72	0,70	1,62	2,39	3,24
CORUNDUM	0,0	0,0	8,78	15,14	14,08	13,70	6,18	C,0	0,0
ENSTATITE	9,11	41,76	16,87	25,84	36,43	28,22	22,27	24,47	14,57
QUARTZ	2,32	3,89	20,57	5,04	26,13	28,96	24,04	14,10	15,57
DYKE NO.	82	26	159	70	114A	109	79	110	117
LOCALITY	H23E	C58FANS	L72E	G74W	H77W	G74W	G73W	H72E	H77W

APPENDIX 1 (continued). TABLE 1E

ANAL.NO.	28	29	30	31	32	33	34	35
Wt%								
SiO_2	96,57	87,60	53,00	53,8	50,83	54,20	58,31	52,18
TiO_2	-	-	-	2,0	2,03	1,31	1,71	0,55
Al_2O_3	trace	8,20	19,70	13,9	14,07	17,17	13,77	7,31
Fe_2O_3	1,72	0,99	10,93	2,6	2,88	3.48	3,37	3,31
FeO	-	-	2,88	9,3	9,00	5,49	6,48	6,79
MnO	-	-	trace	0,2	0,18	0,15	0.23	0,23
MgO	trace	1,00	4,00	4,1	6,34	4,36	2,27	21,96
CaO	-	trace	7.20	7,9	10,42	7,92	5,58	5,24
Na_2O	0,82	1,10	0,82	3,0	2,23	3,67	3,91	0,65
K_2O	0,67	0,98	0,79	1,5	0,82	1,11	1,88	1,49
H_2O^+	-	-		-	0,91	0,86	-	0,15
H_2O^-	-	-	0,25	-	-	-	-	0,01
P_2O_5	-	-		0,4	0,23	0,28	0,46	0,12
CO_2	-	-		-	-	-	-	0,41
TOTAL	99,78	99,87	99,57	98,7	99,54	100,00	97,97	100,40

TABLE 1F(Continued)

Analysis 28:	Horwood(1910) - Analyses I, p. 44; Sericite quartzite or quartz-schist, Upper Witwatersrand, Far East Rand.
Analysis 29:	Horwood(1910) - p. 36; Upper Witwatersrand quartzite, Far East Rand.
Analysis 30:	Pretorius (1964) - Analysis M, Table 8; Ventersdorp Lava, Klipriviersberg.
Analysis 31:	Waters(1962) Table 2; Average Yakima-type tholeiite, Columbia River basalts.
Analysis 32:	Wedepohl (1969), Table 7.4; Average of 137 tholeiitic basalts.
Analysis 33:	Wedepohl(1969), Table 7.3; Average of 49 andesites.
Analysis 34:	McBirney (1969), Table 2; Average iron-rich tholeiitic andesites from oceanic and non-orogenic regions.
Analysis 35:	Van Zyl(1970), Analysis 2280, Table 2: Porphyritic melanorite, 5 m above the Merensky Reef, Northern Transvaal.

APPENDIX 2

2A EXPLANATORY NOTES TO ACCOMPANY TABLES 2A, 2B, 2C AND 2D AND FIGURES 2A, 2B, 2C AND 2D

(a) 'DISTANCE IN CORE' : This is the actual distance from the start of the drill-hole. The drill-holes were not always oriented normal to the dyke-contacts.

(b) 'TRUE DISTANCE' : This is the distance through the dyke measured orthogonally from the first contact which is the east contact for dykes 144 and 182, and the west contact for dykes 79 and 100. The true thickness is the orthogonal thickness of the dyke,

(c) Uniaxial compressive strength (C_0). Young's modulus(E) and Poisson's ratio (ν) are as explained in Chapter 5.2.

(d) An asterisk or a circled point on the figures means that the specimen was considered to have been seriously affected by geological inhomogenieties or uneven loading as discussed in Chapter 5.3.1.

(e) 'MEAN VALUES' are for all specimens and those in brackets do not include specimens marked with an asterisk.

(f) 'RATIO' is length/diameter of the specimen cylinders.

(g) 'n.d.' means not determined.

(h) C_0 = uniaxial compressive strength.

(i) E = Young's Modulus.

(j) ν = Poisson's ratio.

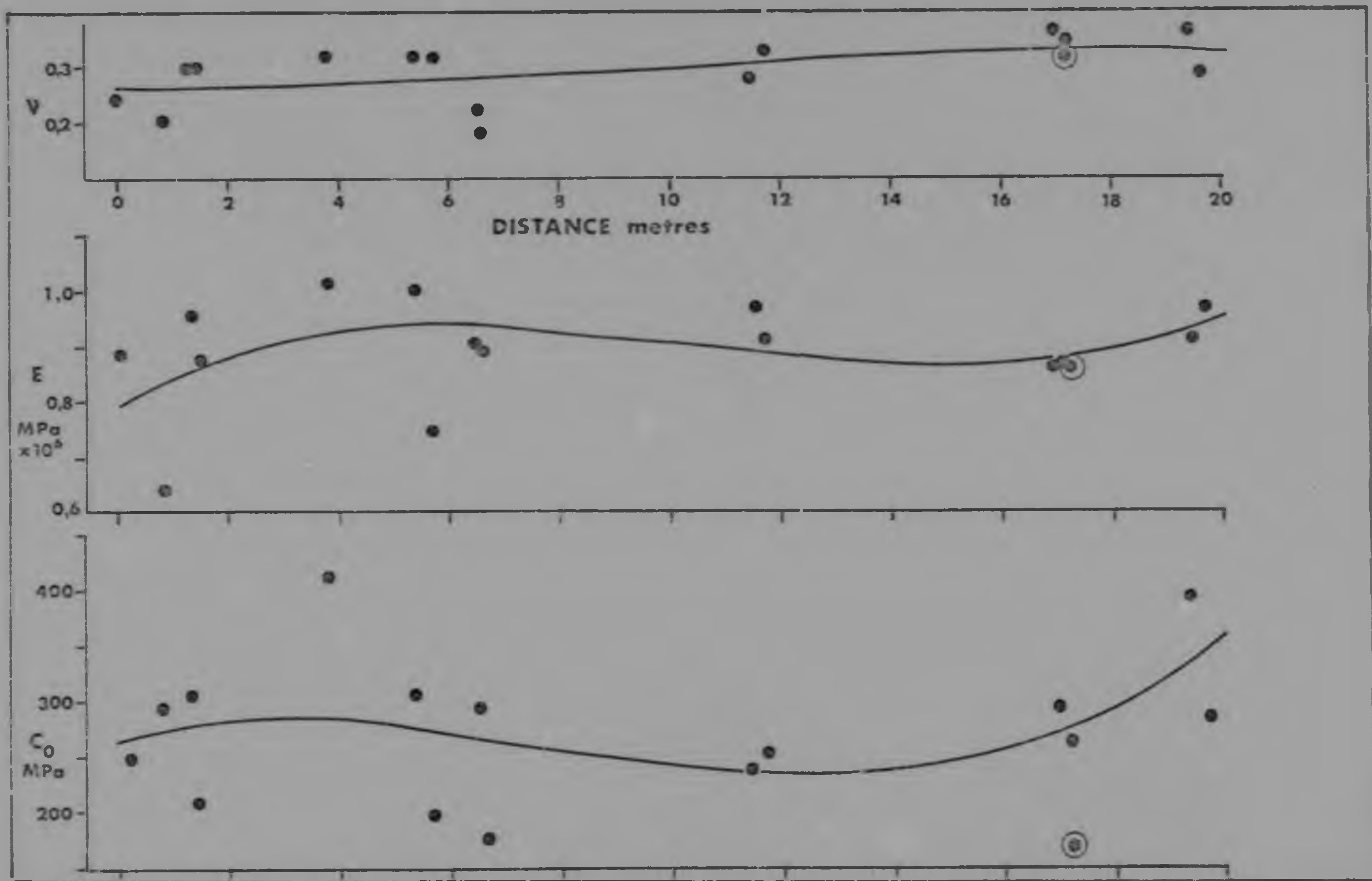

0,3
V
0,2
0
2
4
6
8
10
12
14
16
18
20
DISTANCE metres
1,0
E
0,8
MPa
x10⁵
0,6
400
300
C_0
MPa
200

APPENDIX TABLE 2A

MECHANICAL PROPERTIES OF DYKE 79

DISTANCE IN CORE (m)	TRUE DISTANCE (m)	Co (MPa)	E (MPa x 10^5)	ν	RATIO
23,8	0,2	248	0,88	0,27	3,08
24,5	0,8	294	0,64	0,25	3,03
25,1	1,3	307	0,95	0,30	2,75
25,3	1,4	207	0,87	0,30	2,91
28,3	3,8	413	1,04	0,31	2,84
30,3	5,4	305	1,00	0,31	2,83
30,8	5,7	196	0,75	0,31	2,87
31,7	6,5	297	0,90	0,26	2,96
31,9	6,6	174	0,96	0,24	2,84
38,1	11,5	240	0,96	0,29	3,00
38,3	11,7	252	0,91	0,31	2,[illegible]
45,1	17,0	290	0,85	0,33	3,00
45,3	17,2	261	0,85	0,32	2,99
45,4	17,2*	168	0,85	0,31	3,05
[illegible]8,2	19,4	391	0,95	0,33	2,99
48,5	19,7	285	0,96	0,29	3,02
MEA[illegible] VALUES		277,3	0,90	0,29	
		(270,5)	(0,90)	(0,30)	

DYKE CONTACTS WEST = 23,5 m; EAST 50,3 m

TRUE THICKNESS = 21,1 m.

FIGURE 2A POINTS AND CURVES OF BEST FIT FOR UNIAXIAL COMPRESSIVE STRENGTH(Co), YOUNG'S MODULUS(E) AND POISSON'S RATIO(ν) PLOTTED AGAINST DISTANCE.

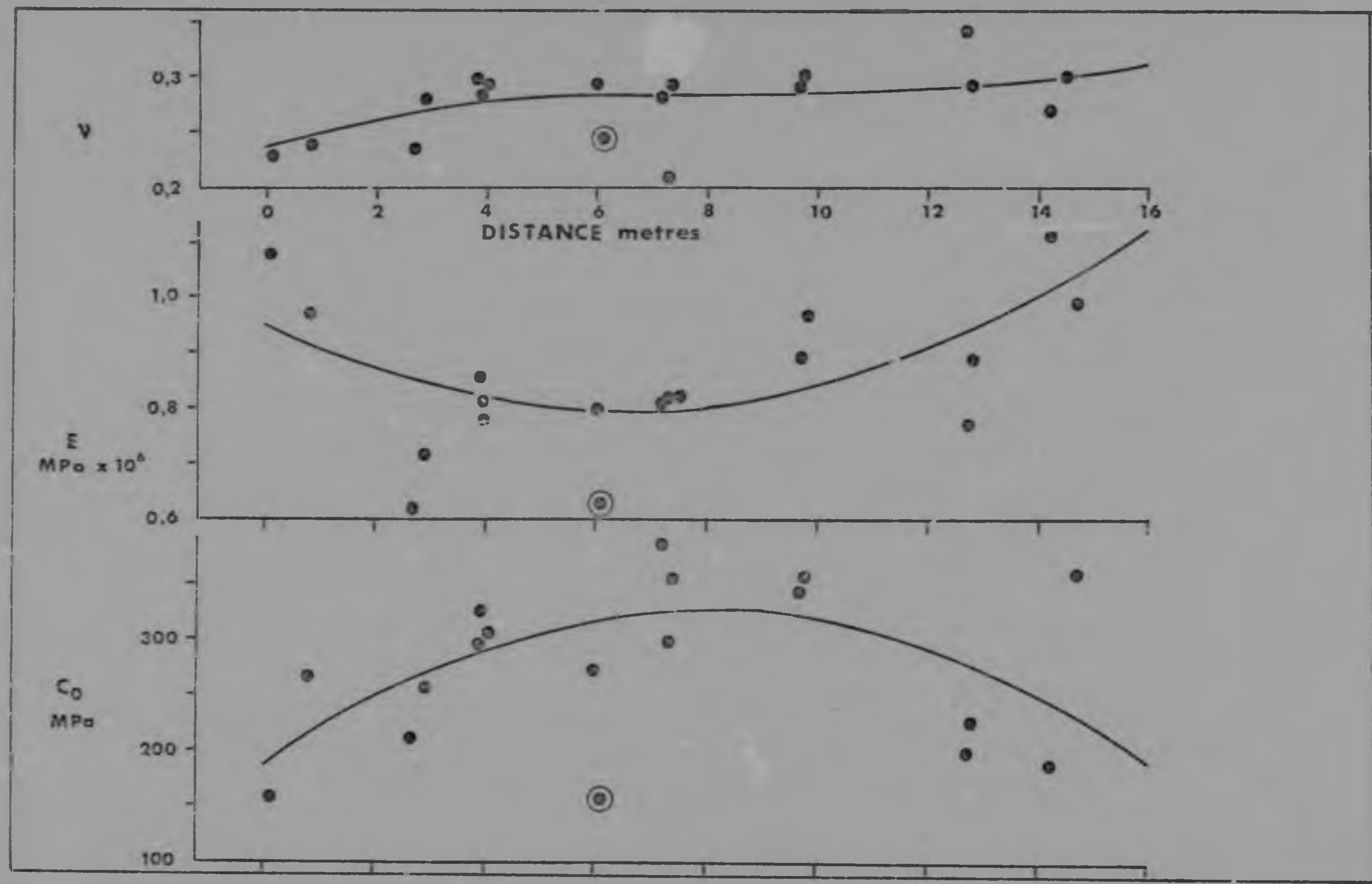

ν
0,3
0,2
0
2
4
6
8
10
12
14
16
DISTANCE metres
E
MPa x 10⁶
1,0
0,8
0,6
C₀
MPa
300
200
100

<u>APPENDIX TABLE 2B</u>

<u>MECHANICAL PROPERTIES OF DYKE 100</u>

DISTANCE IN CORE (m)	TRUE DISTANCE (m)	Co (MPa)	E (MPa × 10^5)	ν	RATIO
10,2	0,1	157	1,08	0,23	2,97
11,1	0,8	262	0,97	0,24	3,09
13,4	2,7	207	0,62	0,27	3,04
13,6	2,9	256	0,72	0,28	3,01
14,8	3,9	295	0,81	0,29	3,08
14,9	3,9	322	0,86	0,28	3,07
15,0	4,0	300	0,78	0,29	3,02
17,4	6,0	271	0,80	0,29	3,07
17,5	6,1*	154	0,63	0,24	[illegible]
18,9	7,2	386	0,81	0,28	2,98
19,0	7,3	297	0,82	0,21	2,89
19,1	7,4	358	0,82	0,29	2,86
21,9	9,7	341	0,93	0,29	3,48
22,0	9,8	356	0,97	0,30	3,45
25,6	12,7	192	0,77	0,34	2,97
25,7	12,8	227	0,89	0,29	3,07
27,4	14,2	189	1,11	0,27	3,04
28,0	14,7	362	0,99	0,30	3,12
MEAN VALUES		281,5	0,87	0,28	
		(274,4)	(0,88)	(0,28)	

DYKE CONTACTS - WEST = 10,1 m; EAST = 29,0m

TRUE THICKNESS = 15,5 m.

FIGURE 2B POINTS AND CURVES OF BEST FIT FOR UNIAXIAL COMPRESSIVE STRENGTH(C_0) YOUNG'S MODULUS(E) AND POISSON'S RATIO(ν) PLOTTED AGAINST DISTANCE FOR DYKE 100.

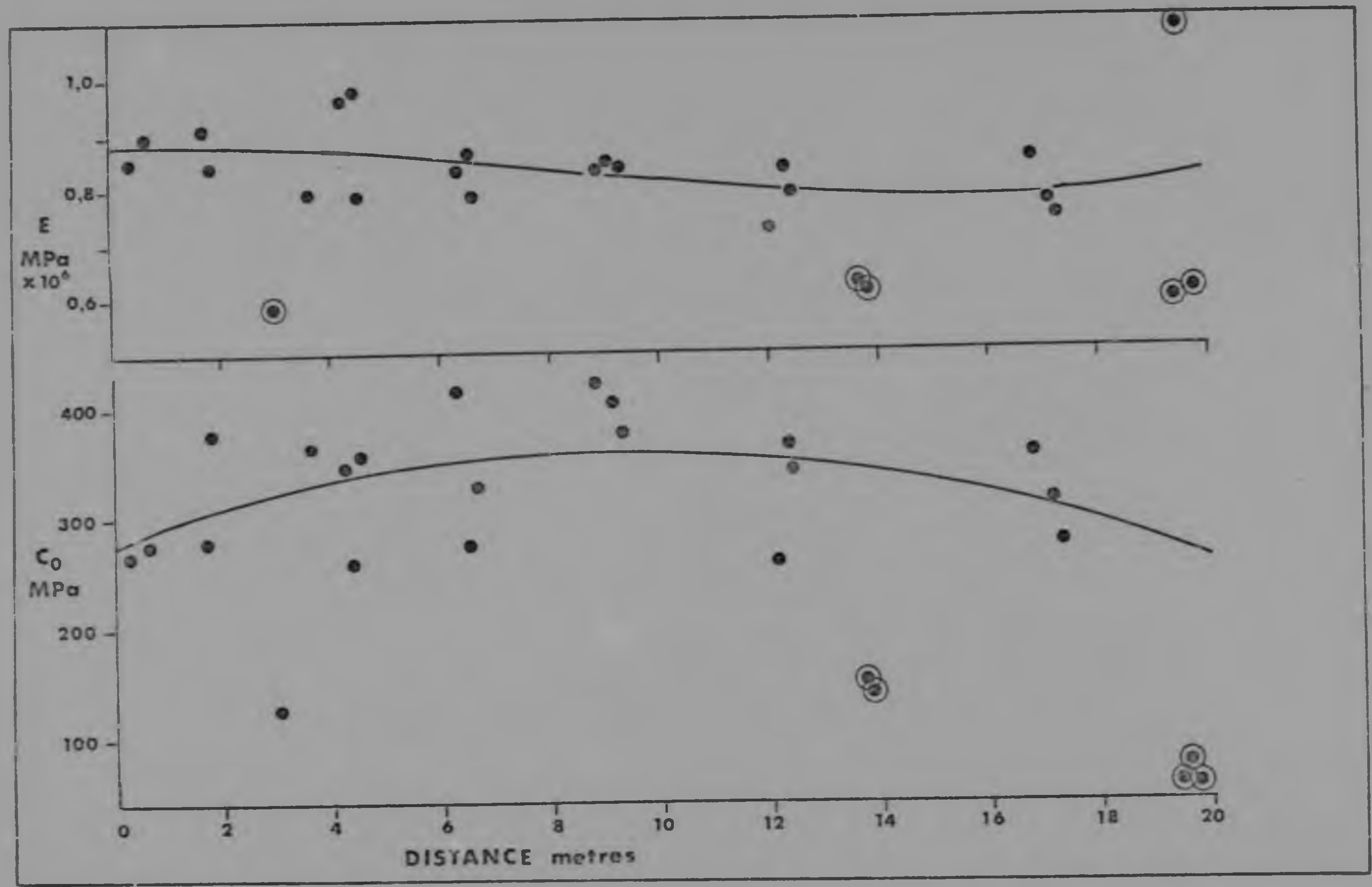
1,0
0,8
0,6
E
MPa
x 10⁶
400
300
200
100
C0
MPa
0
2
4
6
8
10
12
14
16
18
20
DISTANCE metres

APPENDIX TABLE 2C

MECHANICAL PROPERTIES OF DYKE 182

DISTANCE IN CORE (m)	TRUE DISTANCE (m)	Co (MPa)	E (MPa x 10^5)
55,8	0,3	268	0,85
56,1	0,6	275	0,89
57,3	1,7	279	0,91
57,4	1,8	374	0,84
58,7	3,0*	125	0,58
58,8	3,6	363	0,79
60,0	4,2	346	0,96
60,2	4,4	255	0,97
60,3	4,5	335	0,78
62,2	6,3	416	0,83
62,4	6,5	274	0,86
62,5	6,6	326	0,78
64,9	8,8	420	n.d.
65,2	9,1	404	0,84
65,4	9,3	378	0,83
68,3	12,0	260	0,72
68,6	12,3	361	0,83
68,7	12,4	343	0,79
70,1	13,7*	142	0,62
70,2	13,8*	138	0,61
73,4	16,8	359	0,85
73,7	17,1	313	0,77
73,9	17,3	279	0,73
76,2	19,4*	53	0,59
76,4	19,6*	71	1,08
76,5	19,7*	53	0,61

Poisson's Ratio was not determined

Dyke Contacts - EAST = 55,5m
WEST = 76,6m

True thickness = 19,8m

ON OPPOSITE PAGE

FIGURE 2C POINTS AND CURVES OF BEST FIT FOR UNIAXIAL COMPRESSIVE STRENGTH(C_0), YOUNG'S MODULUS(E) AND POISSON'S RATIO(ν) PLOTTED AGAINST DISTANCE FOR DYKE 182.

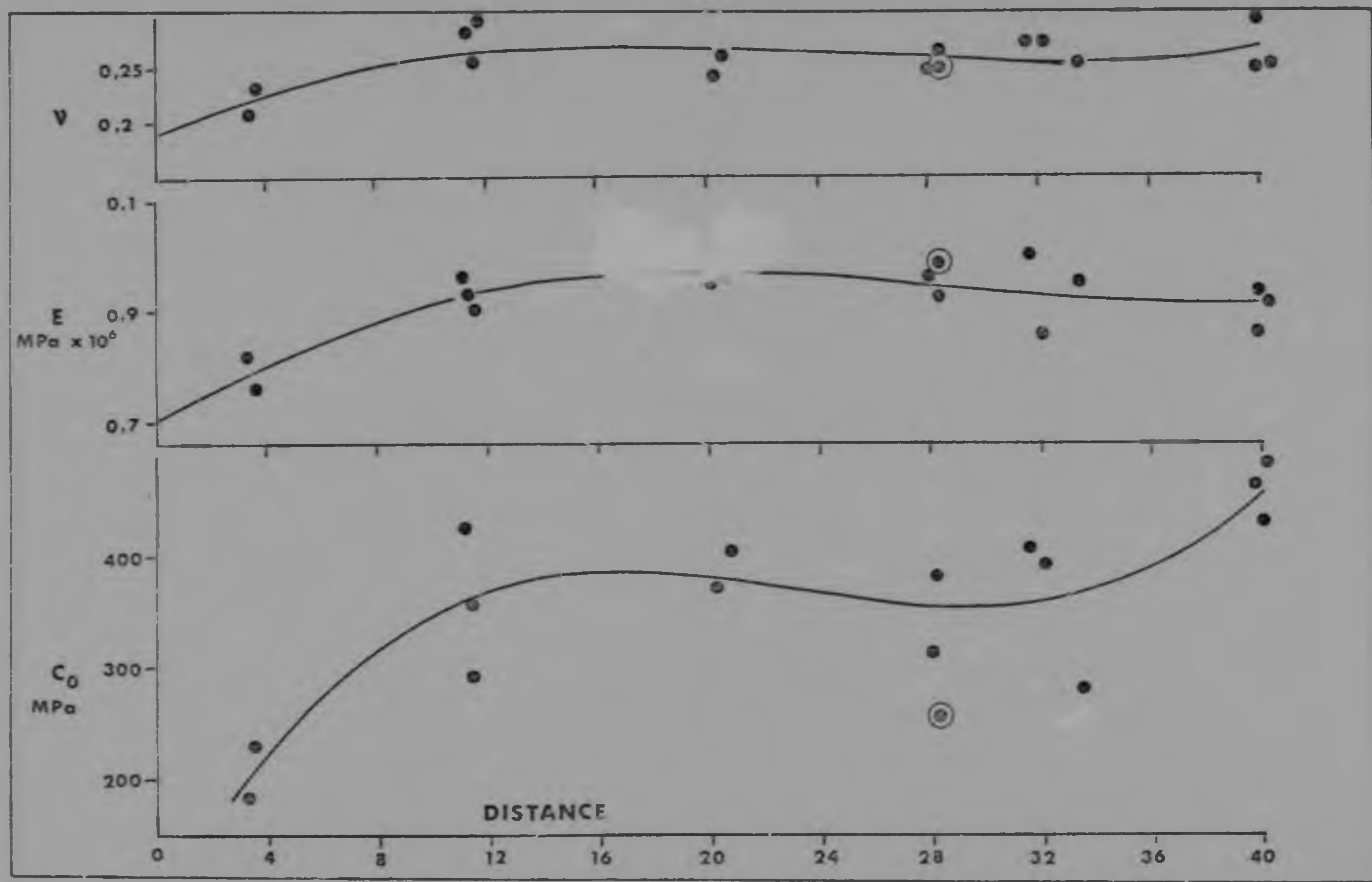

ν
0,25
0,2
0.1
E
0.9
MPa x 10⁶
0.7
C₀
MPa
400
300
200
DISTANCE
0
4
8
12
16
20
24
28
32
36
40

APPENDIX TABLE 2D

MECHANICAL PROPERTIES OF DYKE 144

DISTANCE IN CORE (m)	TRUE DISTANCE (m)	Co (MPa)	E (MPa x 10^5)		RATIO
41,1	3,3	182	0,82	0,21	2,91
41,4	3,6	230	0,76	0,23	2,86
49,0	11,2	425	0,96	0,28	2,97
49,1	11,3	292	0,93	0,25	2,95
49,2	11,4	358	0,90	0,29	3,07
58,0	20,2	372	0,96	0,26	2,98
58,5	20,7	406	0,95	0,24	2,93
65,8	28,0	314	0,96	0,25	2,99
65,9	28,1*	258*	0,98	0.25	2,99
66,1	28,3	383	0,92	0,26	2,94
69,5	31,7	403	1,00	0,27	3,13
69,6	32,1	392	0,85	0,27	2,81
69,8	33,3	280	0,85	0,25	2,93
77,6	39,8	463	0,86	0,29	3,03
77,7	39,9	432	0,93	0,25	2,79
78,0	40,2	480	0,92	0,25	2,99
MEAN VALUES		360,9	0,91	0,26	
		(354,4)	(0,92)	(0,26)	

DYKE CONTACTS - EAST = 37,8 m; WEST = 78,9m.

TRUE THICKNESS = 41,1m.

FIGURE 2D POINTS AND CURVES OF BEST FIT FOR UNIAXIAL COMPRESSIVE STRENGTH (C_0), YOUNG'S MODULUS (E) AND POISSON'S RATIO (ν) PLOTTED AGAINST DISTANCE FOR DYKE 144.

APPENDIX 3

TABLE 3A

THE INFLUENCE OF DEPTH AND THE SIZE OF THE MINED-OUT AREA ON THE NUMBER OF ROCKBURSTS

-DATA FOR LEVELS 69 - 77.

LEVEL	69	70	71	72	73	74	75	76	77	TOTALS
DEPTH(m)	[illegible]28	3160	3206	3251	3297	3343	3388	3431	3475	-
AREA MINED (m^2)	30400	103500	97200	52400	66700	82300	42800	21950	19250	316500
%	5,9	20,0	18,8	10,2	12,9	15,9	8,3	4,3	3,7	100,0
No.BURSTS	7	18	18	33	17	6	18	3	4	125
%	5,6	14,5	14,5	26,6	13,7	4,8	14,5	2,4	3,2	99,8
NO.CONTROLS	4	36	31	12	13	26	16	10	3	151
%	2,7	23,8	20,6	8,0	8,6	17,2	10,6	6,6	2,0	100,1
% BURSTS/ $10^3 m^2$ mined	0,18	0,14	0,15	0,51	0,21	0,06	0,34	0,11	0,17	-
% CONTROL/ $10^3 m^2$ mined	0,09	0,23	0,21	0,15	0,13	0,21	0,25	0,30	0,10	-

TABLE 3B

THE NUMBER OF DYKES AND FAULTS WITHIN 100 METRES OF ROCKBURSTS

		NUMBER OF OTHER DYKES AND FAULTS WITHIN 100 m OF A ROCKBURST OTHER THAN THE GIVEN DISCONTINUITY				
		DYKES			FAULTS	
Number of dykes and faults		0	1	2	0	1
		(percentage)				
Discontinuity Number	Number of Rockbursts					
110A	51	19,6*	58,8*	21,6*	100*	0*
100	36	30,6	38,9	30,6	100	0
110	32	28,1	68,8	3,1	100	0
117	27	29,6	66,6	3,7	92,6	7,4
121	2	0	100	0	0	0
105	12	33,3	66,7	0	0	0
114A	9	77,8	22,2	0	0	100

* Percentage of the number of rockbursts within 100 metres of the given number of discontinuities; i.e., 19,6% of the rockbursts within 100m of discontinuity 110A were associated with no other discontinuities, 58,8% were associated with one discontinuity other than 110A and 21,6% were associated with two discontinuities other than 110A.

APPENDIX TABLE

TABLE 3C

DISTRIBUTION OF SEISMIC EVENTS BY DEPTH AND DISTANCE FROM DYKE 100

GROUP	75 to 100m	50 to 75m	25 to 50m	0 to 25m	IN DYKE	0 to 25m	25 to 50m	50 to 75m	75 to 100m	>100m	TOTALS
1	0	1	1	1	4	5	5	3	3	1	24(8,2%)
2	6	6	18	23	3	12	6	3	0	1	78(26,6)
3	7	15	13	15	7	7	2	2	0	3	71(24,2)
4	6	8	6	9	0	2	2	1	0	10	44(15,0)
5	3	5	10	7	3	10	4	4	2	3	51(17,4)
6	3	0	5	5	6	5	0	0	0	1	25(8,5)
TOTALS	25(8,5%)	35(11,9%)	53(18,1%)	60(20,5%)	23(7,8%)	41(14,0%)	19(6,5%)	13(4,4%)	5(1,7%)	19(6,5%)	293(99,9%)

* For group locations see Figure 6-9. Groups 1,2 and 3 include the upper mining faces and Groups 4,5 and 6 the lower mining faces as referred to in the main text.

REFERENCES

Allsopp, H.L., 1961 : Rb/Sr age measurements on total rock and separated-mineral fractions from the Old Granite of the Central Transvaal, J. Geophys. Res., 66,pp. 1499-1508.

Anderson, E.M., 1937: The dynamics of sheet intrusion; Proc. Roy. Soc. Edinb., 58, pp. 242-51.

Anderson, E.M., 1951: The Dynamics of Faulting and Dyke Formation with Applications to Britain, 2nd edn., Edinburgh, Oliver and Boyd, 206 pp.

Association of Mining Managers, Transvaal, 1933: Some aspects of deep level mining on the Witwatersrand gold mines with special reference to rockbursts; J. Ass. Min. Mngrs. Transv., June, pp. 117-158.

Barker, D.S., 1970: Compositions of granophyre, myrmekite and graphic granite; Geol. Soc. Amer. Bull., 81, pp.3339-3350.

Bhattacharji, S., 1967: Mechanics of flow differentiation in ultramafic and mafic sills; J. Geol., 75, pp. 101-112.

Bhattacharji, S. and Smith, C.H., 1964: Flowage differentiation; Science, 145, pp. 150-153.

Bieniawski, Z.T., 1967: Mechanism of brittle failure of rock, Part 1: Theory of the fracture process; Int. J. Rock Mech.Min.Sci., 4, pp. 395-406.

Brandt, R.T., 1950: The geology of certain igneous intrusive rocks in the Far East Rand, Transvaal, South Africa; Unpubl. M.Sc. thesis, University of the Witwatersrand.

Brock, B.B., and Pretorius, D.A., 1964a: An introduction to the stratigraphy and structure of the Rand Goldfield. In Haughton, S.H., Ed., The geology of some ore deposits in Southern Africa. I, Geol. Soc. S. Afr., 625 pp.

Brock, B.B., and Pretorius, D.A., 1964b: Rand basin sedimentation and tectonics. In Haughton, S.H., Ed., The geology of some ore deposits in Southern Africa. I, Geol. Soc.S.Afr. 625 pp.

Chayes, F., 1966: Alkaline and subalkaline basalts; Amer. J. Sci., 264, pp. 128-145.

Cobbold, P.R., Cosgrove, J.W., and Summers, J.M., 1971: Development of internal structures in deformed anistropic rocks; Tectonophysics, 12, pp. 23-25.

Cook, N.G.W., 1963: The seismic location of rockbursts; Proceedings of the Fifth Rock Mechanics Symposium, Pergamon Press, Oxford, pp. 493-516.

Cook, N.G.W., Hoek, E., Pretorius, J.P.G., Ortlepp, W.D., and Salamon, M.D.G., 1966: Rock mechanics applied to the study of rockbursts; Jl.S.Afr.Inst.Min.Metall., 66, pp.435-528.

Crampton, D.G.V., 1972: The geochronology of the acid igneous rocks of the Derdepoort Area, N.W. Transvaal; Unpubl. B.Sc.(Hons) thesis, University of the Witwatersrand.

Currie, K.L., and Ferguson, J., 1970: The mechanism of intrusion of lamprophyre dykes indicated by 'offsetting' of dykes, Tectonophysics, 9, pp. 525-535.

Donath, F.A., 1962: Analysis of Basin-Range Structure, South-Central Oregon; Geol. Soc. Amer. Bull., 73, pp. 1-16.

Durney, D.W., and Ramsay, J.G., 1973: Incremental strains measured by syntectonic crystal growths. In De Jong, K.A., and Schotton, R., Gravity and Tectonics, Wiley, 502 pp.

Ellis, J., 1940: An intrusion of quartz dolerite occurring on the Far East Rand, Transvaal; Proc.geol.Soc.S.Afr., 43, pp. 127-142.

Ellis, J., 1943: A tear fault in the Far East Rand; Trans. geol.Soc.S.Afr., 46, pp. 75-90.

Ellis, J., 1946: The simple dykes and sills of the Far East Rand; Trans. geol.Soc.S.Afr., 49, pp. 213-242.

Ferguson, H.F., 1967: Valley stress relief in the Allegheny Plateau; Eng. Geol., 4, pp. 63-71.

Ferguson, J., 1973: The Pilanesberg alkaline province, Southern Africa; Trans.geol.Soc.S.Afr., 73, pp. 249-270.

Fuller, A.O., 1958: A contribution to the petrology of the Witwatersrand System; Trans. geol.Soc.S.Afr., 61, pp. 19-45.

Fumerton, S.L., 1975: The Felsic Sills on the E.R.P.M., Boksburg. Unpubl. M.Sc. thesis, University of the Witwatersrand.

Friedman, M., 1964: Petrofabric techniques for the determination of principal stress directions in rocks. In Judd, W.R., ed., State of stress in the earth's crust; New York, Elsevier, pp. 451-552.

Gay, N.C., 1970: The failure of hollow sandstone cylinders subjected to hydrostatic compression - a preliminary report; Report number 46/70, Transvaal and Orange Free State Chamber of Mines Research Organisation, 15 pp.

Gay, N.C., 1972: Virgin rock stresses at Doornfontein Gold Mine, Carletonville, South Africa; J. Geol, 80, pp. 61-80

Gay, N.C., 1973: Fracture growth around openings in thick-walled cylinders of rock subjected to hydrostatic compression; Int. J. Rock.Mech.Min.Sci., 9, pp. 209-233.

Gay, N.C., 1975: In-situ stress measurements in Southern Africa; Tectonophysics (in press)

Gelletich, H., 1937: Über Magnetitführende Eruptive Gänge und Gangesysteme im Mittleren Teil des Südlichen Transvaals; Beitr. angew. Geophys. Bd. 6, Hf.4, s. 337-406.

Grey, C.J., 1931: Rockburst: The effect of crush burst movements or stope remnants and workings in their vicinity; J.Chem.Met.Min. Soc.S.Afr., 32, pp.226-240.

Grobbelaar, C., 1957: Some physical properties of strata of an East Rand mine - part 1. Unpubl. M.Ing.thesis, University of Stellenbosch. 82 pp.

Hallbauer, D.K., Wagner, H., an Cook, N.G.W., 1973: Some observations concerning the microsco[illegible] nd mechanical behaviour of quartzite specimens in [illegible], triaxial compression tests; Int.J.Rock Mech.Min.Sci., 10, pp. 713-726.

Hamilton, G.N.G., and Cooke, H.B.S., 1960: Geology for South African Students, 4th edn., Central News Agency Ltd. 441 pp.

Harker, A., 1964: Petrology for Students, 8th edn., Cambridge University Press. 283 pp.

Hatch, F.H., and Corstorphine, G.S., 1906: Geology of the Bezuidenhout Valley and the District East of Johannesburg; Trans.geol.Soc. S.Africa, 7, pp. 97-111.

Henderson, J.A.L., 1898: Petrographical and geological investigations of certain Transvaal norites gabbros and pyroxenites and other South African rocks; Dulau and Co., London, 55 pp.

Higgins, M.W., 1971: Cataclastic rocks; U.S. Geol.Surv.Prof.paper 687, 97 pp.

Hill, F.G., 1954: An investigation into the problem of rockbursts. An operational research project. Part 1. The approach to the problem and analysis of rockbursts that have occurred on the E.R.P.M. during the years 1948-53; J.Chem.Met.Min.Soc.S.Afr., 55, pp. 63-72.

Hoek, E., 1965: Rock fracture under static stress conditions; Report M.E.G. 383. C.S.I.R., Pretoria. 159 pp.

Horwood, C.B., 1910: Notes and analyses of typical Transvaal rocks; Trans.geol.Soc.S.Afr., 13, pp.29-55.

Irvine, T.N., and Baragar, W.R.A., 1971: A guide to the chemical classification of the common volcanic rocks; Can.J.Earth.Sci., 8, pp. 523-548.

Jaeger, J.C., and Cook, N.G.W., 1969: Fundamentals of Rock Mechanics; Chapman and Hall, London, 515 pp.

Johnson, A.M., 1970: Physical Processes in Geology; Freeman, Cooper and Co., San Francisco, 577 pp.

Kersten, R.W.O., 1964: Report on Chamber of Mines project 111/64/10108; Transvaal and Orange Free State Chamber of Mines Research Organisation, Johannesburg.

Komar, P.D., 1972: Mechanical interactions of phenocrysts and flow differentiation of igneous dykes and sill; Geol. Soc.Amer.Bull., 83, pp. 973-988.

Manton, W.I., 1968: The origin of associated basic and acid rocks in the Lebombo-Nuanetsi Igneous Province, Southern Africa, as implied by strontium isotopes; J. Petrology, 9, pp. 23-39.

McBirney, A.R., 1969: Andesitic and rhyolitic volcanism of orogenic belts; Amer. Geoph. Union Monograph 13, pp. 501-507.

McCarthy, T.S., 1975: In preparation

McDonald, M.A., 1911: The intrusive rocks of the Witwatersrand; Trans. geol Soc.S.Afr., 14, pp.89-98

McDougall, I., 1963: Potassium-argon age measurements on dolerites from Antarctica and South Africa; J. Geophys.Res., 68, pp. 1535-1546.

McGarr, A., 1971: Stable deformation of rock near deep-level tabular excavations; J. Geophy .Res., 76, pp. 7088-7106.

McGarr, A., Spottiswoode, S.M., and Gay, N.C., 1975: Relationship of tremors in a deep-level mine to induced stresses and to mechanical properties of rock in the focal region; (in press).

Mellor, E.T., 1910: Map of the Central Witwatersrand; Annual Report, S.Afr.Geol.Surv.,

Mellor, E.T., 1917: The geology of the Witwatersrand- explanation of the geological map of the Witwatersrand goldfield; S.Afr.Geol.Survey, Pretoria, 46 pp.

Mellor , E.T., 1921: The geology of the country surrounding Johannesburg- explanation of Sheet 52 (Johannesburg); S.Afr.Geol.Survey, Pretoria. 46 pp.

Nicolaysen, L.O., De Villiers, J.W.L., Burger, A.J., and Strelow, F.W.E., 1958: New age measurements relating to the absolute age of the Transvaal system and of the Bushveld Igneous Complex; Trans. geol.Soc.S.Afr., 61, pp. 137-163.

Nicolaysen, L.O., Burger, A.J., and Liebenberg, W.R., 1962: Evidence for the extreme age of certain minerals from the Dominion Reef conglomerates and the underlying granite in the Western Transvaal; Geochim. et Cosmochim. Acta, 26, pp. 15-23.

Nockolds, S.R., 1954: Average chemical compositions of some igneous rocks; Bull.geol.Soc.Am., 65, pp. 1007-1032

Norris, D.K., and Barron, K., 1968: Structural analysis of features on natural and artificial faults: In, Baer, A.J., and Norris, D.K., eds., Proceedings, Conference on Research in Tectonics (Kink Bands and Brittle Deformation). Geol. Surv.Can., Paper 68-52, pp.136-166.

Norrish, K., and Chappell, B.W., 1967: X-ray fluorescence spectrography. In Zussman, J., Physical Methods in Determinative Mineralogy; Academic Press, London, pp. 103-160.

Norrish, K., and Hutton, J.T., 1969: An accurate X-ray spectrographic method for the analysis of a wide range of geological samples; Geochim. et Cosmochim. Acta., 33, pp. 431-453.

Obert, L., and Duval, W.I., 1967: Rock Mechanics and the design of structures in rock: Wiley, New York. 650 pp.

Pallister, G.F., Gay, N.C., and Cook, N.G.W., 1971: Measurements of the virgin state of stress in rock at depth; Int. Soc. Rock Mech.Congr., 2d Belgrade 1970, Proc. v.1, paper 1-5.

Pollard, D.D., 1973: Derivation and evaluation of a mechanical model for sheet intrusions; Tectonophysics, 19, pp. 233-269.

Pretorius, D.A., 1964: The geology of the Central Rand Goldfield. In Haughton, S.M., Ed. The geology of some ore deposits in Southern Africa. I. Geol.Soc.S.Afr., 625 pp.

Pretorius, J.G.P., 1966: Seventh and final report on statistical analyses of practical data on rockbursts; statistical analyses of relations between rockbursts, seismic events and mining methods; Report ME/MR/94636. C.S.I.R., Pretoria, 43 pp.

Price, N.J., 1959: Mechanics of jointing in rocks; Geol. Mag., 96, pp. 149-167.

Price, N.J., 1966: Fault and joint development in brittle and semi-brittle rocks; Pergamon, 176 pp.

Ralston, I.T., 1953: The complex intrusives of the Far East Rand: Unpubl. M.Sc. Thesis, University of Pretoria.

Ramsay, J.G., 1967: Folding and fracturing of rocks; McGraw-Hill, New York, 568 pp.

Ramsay, J.G., and Graham, R.H., 1970: Strain variation in shear belts; Can. J. Earth Sc., 7, pp. 786-813.

Roberts, J.L., and Sanderson, D.J., 1971: The intrusive form of some basalt dykes showing flow lineation; Geol. Mag., 108, pp. 489-499.

Rock Mechanics Research Team, 1957: First report on the physical properties of rock - some properties of rock samples from the E.R.P.M. Ltd (with 23 appendices); Special Report. 15. C.S.I.R., Pretoria.

Rock Mechanics Research Team, 1959a: Second report on the physical properties of rock - some properties of hard rock from the East Rand Proprietary Mines; Special Report 28, C.S.I.R. Pretoria, 25 pp.

Rock Mechanics Research Team, 1959b: Fifth report on statistical analyses of practical data on rockbursts - an analysis of the influence of dykes, faults and raises on the incidence of rockbursts, Special Report, 31, C.S.I.R., Pretoria, 59 pp.

Rock Burst Committee, 1964: Recommendations of the rockburst committee, 1964; S.Afr. Dept.Mines., 12 pp.

Schafer, H.N.S., 1966: The determination of iron (II) oxide in silicates and refractory materials; The Analyst, 91, pp. 755-790.

Schreiner, G.D.L., and Van Niekerk, C.B., 1958: The age of a Pilanesberg dyke from the Central Witwatersrand; Trans.Geol.Soc.S.Afr., 61, pp.197-203.

Shipway, A.M., 1972: Some aspects of Witwatersrand geology with special reference to the Central Rand Area and E.R.P.M. Ltd; Unpubl. M.Sc. thesis, University of Leicester.

Sinclair, W.E., 1936: Rockbursts - their cause and prevention; J.Chem. Met. Min.Soc.S.Afr., 37, pp. 118-121 and 523-524.

Starkey, J., 1970: A computer programme to construct spherical projections. A computer programme to prepare orientation diagrams. In, Paulitsh, P., Experimental and Natural Rock Deformation; Springer-Verlag, Berlin, pp. 28-74.

Van der Berg, 1973: Personal communication

Van Niekerk, C.B., 1962: The age of the Gemspost Dyke from the Ventersposst Gold Mine; Trans.Geol.Soc.S.Afr., 65, pp. 105-111.

Van Niekerk, C.B., and Burger, A.J., 1964: The age of the Ventersdorp System. Ann. geol.Surv.S.Afr., 3, pp. 75-86.

Van Niekerk, C.B., 1969: Lead isotopic data relating to the age of the Dominion Reef lava; Trans.Geol.Soc.S.Afr., 72, pp. 37-45.

Van Zyl. J.P., 1970: The petrology of the Merensky Reef and the associated rocks on Swartklip 988, Rustenberg District. In Visser, D.J.L., and Von Gruenewaldt, G., eds., Symposium on the Bushveld Igneous Complex and other layered intrusives; Geol. Soc.S.Afr., Sp.Pub.1. pp. 80-107.

Waters, A., 1962: Basalt magma types and their tectonic association - Pacific northwest of the United States; Amer. geophys.Union Monograph, 6, pp. 158-170.

Wedepohl, K.H., 1969: Compositions and abundances of common igneous rocks. In Wedepohl, K.H., ed., Handbook of Geochemistry, Vol.1, Springer-Verlag, Berlin. pp

Whiteside, H.C.M., 1950: The geology of a part of the Far East Rand Basin with special reference to the economic horizons and the footwall beds; Unpubl. Ph.D. thesis, London University.

Wiebols, G.A., Jaeger, J.C. and Cook, N.G.W., 1968: Rock property tests in a stiff testing machine; In Gray, K.E., Tenth symposium on rock mechanics, Austin, Texas, 861 pp.

MAP 2
E.R.P.M.
STRUCTURAL
GEOLOGY
T N
COMET FAULT
SOUTH REEF FAULT
PHOENIX FAULT
SHEASBY FAULT
STRUTHERS FAULT
VAN DYK FAULT
GODIN FAULT
SIMMER DYKE
WITWATERSRAND DYKE
ROSE DEEP DYKE
C
D
F
G
H
K
L
SILL 192 IN FOOTWALL
Vertical shaft
Inclined shaft
Mine boundary
Dyke
Fault - downthrown side
- dip direction
5 4 3 2 1 0 500 1000 1500 2000
metres
(BASED ON PLANS MADE AVAILABLE BY ERPM)
S. L. FUMERTON & D. G. JEFFERY (1974)


E.R.P.M.
UNDERGROUND
WORKINGS
Projected onto surface
MAP 1
T N
2 NORTH
1 NORTH
ANGELO
DRIEFONTEIN
2 SOUTH
1 SOUTH
MAIN
AGNES MUNRO
COMET
1 SOUTH
BLUE SKY
CASON
SECONDARY
WIT DEEP EAST
ANGELO WEST
COMET
21 M.H.
22 station cross cut
27 M.H.
HERCULES
(22) 3000 M.H.
CINDERELLA
CINDERELLA EAST
VENTILATION
TERTIARY
SECONDARY
34 M.H.
SOUTH WEST VERTICAL
WEST 1
41 M.H.
42 M.H.
37 M.H.
CINDERELLA EAST
TERTIARY
45 M.H.
CENTRAL VERTICAL
45 M.H.
SOUTH WEST SUBVERTICAL
49 Main haulage
49 M.H.
58 M.H.
WEST 2
49 M.H.
CENTRAL SUBVERTICAL
TERTIARY
49 M.H.
58 M.H.
57 M.H.
68 M.H.
QUATERNARY
D
F
G
H
K
L
C
SOUTH EAST VERTICAL
58 M.H.
56 Main haulage
'D' pilot winze
'E' pilot winze
DRIEFONTEIN
SOUTH EAST SUBVERTICAL
68 M.H.
'F' pilot winze
WESTERN SECTION
K1
'M' pilot winze
'N' pilot winze
'O' pilot winze
FAR EAST SUBVERTICAL
FAR EAST VERTICAL
H1
77 level east stope
ANGELO
'H' pilot winze
80 level 3428m below surface
HERCULES
CENTRAL SECTION
EASTERN SECTION
Main Reef Road
Germiston
Boksburg
Heidelberg
500 4 3 2 1 0
500
1000
1500
2000
2500
metres